

SILK-ELASTINLIKE PROTEIN POLYMERS FOR  
ADENOVIRAL CANCER GENE THERAPY

by

Joshua Alexander Gustafson

A dissertation submitted to the faculty of  
The University of Utah  
in partial fulfillment of the requirements for the degree of

Doctor of Philosophy

Department of Bioengineering

The University of Utah

December 2012

Copyright © Joshua Alexander Gustafson 2012

All Rights Reserved

# The University of Utah Graduate School

## STATEMENT OF DISSERTATION APPROVAL

The dissertation of **Joshua Alexander Gustafson**

has been approved by the following supervisory committee members:

<b>Hamidreza Ghandehari</b>	, Chair	<b>3/22/12</b>
_____		_____
		Date Approved
<b>Joseph Cappello</b>	, Member	
_____		_____
		Date Approved
<b>David Grainger</b>	, Member	<b>3/22/12</b>
_____		_____
		Date Approved
<b>Jason Hunt</b>	, Member	
_____		_____
		Date Approved
<b>Jindrich Kopecek</b>	, Member	<b>3/22/12</b>
_____		_____
		Date Approved

and by **Patrick Tresco**, Chair of  
the Department of **Bioengineering**

and by Charles A. Wight, Dean of The Graduate School.

## ABSTRACT

The treatment of head and neck cancer is a complicated task which requires that many factors be considered before the best option can be chosen. The best treatment, providing the greatest efficacy with minimal side effects, is likely to be a localized nonsurgical treatment. Such a treatment would allow resolution of the primary tumor without the devastating systemic side effects associated with chemotherapy nor the social and psychological side effects associated with scarring and disfigurement resulting from surgical resection. Locally delivered gene therapy with viral vectors is a promising approach due to advances in delivery-enhancing materials. One such material is genetically engineered silk-elastinlike protein polymer (SELP), which due to its repeating structure and method of synthesis can be precisely modified to produce desired properties, such as pore size, swelling ratio, release rate, and mechanical strength. In this dissertation, it is shown that one particular analog of this polymer exhibits superior performance in the enhancement of adenoviral gene delivery, with enhancement of localization of gene expression of up to 55-fold, and reduction in acute immune response as measured by differential white blood cell count and hepatotoxicity due to viral administration. Further improvement of this material has been to include matrix-metalloproteinase (MMP)-sensitive sites in the polymer to provide it the capability to biodegrade more rapidly. Advantages to an MMP-responsive material include the ability

to respond to changes in the tumor environment, as increased MMP activity can correlate with increased invasiveness and, in many cases, metastasis. The insertion of the MMP-responsive sequence caused sensitivity to both MMP-2 and MMP-9, with 63% and 44% increases in protein loss from sensitive hydrogels exposed to MMP-2 and MMP-9, respectively, compared to unexposed control. Further, MMP-2 and MMP-9 exposure caused 41% and 24% reduction in compressive modulus, and 95% and 66% increased release of 100nm polystyrene nanoparticles, respectively. These results show the potential of SELPs in increasing the safety and efficacy of adenoviral gene therapy.

To Mom, Dad, Jake, Grandma, Grandpa, Grandma Sandy, and Grandpa Alex. Without your support, this would have been impossible. Really.

## CONTENTS

ABSTRACT.....	iii
LIST OF FIGURES .....	viii
LIST OF TABLES .....	xi
ABBREVIATIONS .....	xii
ACKNOWLEDGEMENTS .....	xviii
Chapter	
1 INTRODUCTION .....	1
1.1 Introduction.....	1
1.2 Aims and scope of this dissertation .....	3
1.3 References.....	10
2 LITERATURE BACKGROUND.....	13
2.1 Introduction.....	13
2.2 Cancer gene therapy.....	14
2.3 Head and neck squamous cell carcinoma: Disease and implications of matrix-metalloproteinases.....	43
2.4 Genetically engineered polymers: Overview .....	54
2.5 Silk-elastinlike protein polymers for controlled gene delivery.....	98
2.6 Conclusions.....	106
2.7 References.....	108
3 SILK-ELASTINLIKE RECOMBINANT POLYMERS FOR GENE THERAPY OF HEAD AND NECK CANCER: FROM MOLECULAR DEFINITION TO CONTROLLED GENE EXPRESSION .....	135
3.1 Introduction.....	135
3.2 Materials and methods .....	137
3.3 Results and discussion .....	141

3.4 Conclusions.....	159
3.5 References.....	160
<b>4 SILK-ELASTINLIKE HYDROGEL IMPROVES THE SAFETY OF ADENOVIRUS MEDIATED GENE-DIRECTED ENZYME-PRODRUG THERAPY .....</b>	<b>162</b>
4.1 Introduction.....	162
4.2 Materials and methods .....	164
4.3 Results and discussion .....	167
4.4 Conclusions.....	182
4.5 References.....	183
<b>5 MATRIX-METALLOPROTEINASE RESPONSIVE SILK-ELASTINLIKE PROTEIN POLYMERS .....</b>	<b>185</b>
5.1 Introduction.....	185
5.2 Materials and methods .....	186
5.3 Results.....	202
5.4 Discussion.....	218
5.5 Conclusions.....	225
5.6 References.....	227
<b>6 CONCLUSIONS AND FUTURE DIRECTIONS .....</b>	<b>229</b>
6.1 Conclusions.....	229
6.2 Future directions .....	232
6.3 References.....	235
<b>APPENDIX: EFFICACY OF SELP-MEDIATED GENE-DIRECTED ENZYME- PRODRUG THERAPY IN AN IMMUNOCOMPETENT MOUSE MODEL.....</b>	<b>236</b>



## LIST OF FIGURES

### Figure

1.1: Schematics of three SELP analogs used for viral gene delivery .....	5
2.1: Gene-directed enzyme-prodrug therapy .....	17
2.2: Types of matrix-mediated viral gene delivery .....	41
2.3: Random concatamerization.....	56
2.4: Recursive directional ligation .....	58
2.5: Open-ended rolling circle amplification .....	60
2.6: Synthetic strategy for SELP-815K .....	72
2.7: MALDI-TOF mass spectra of SELP-815K polymers .....	74
2.8: Amino acid analysis of SELP-815K.....	75
3.1: SELP-structure dependence of intratumoral beta-galactosidase expression .....	143
3.2: SELP-structure dependence of hepatic beta-galactosidase expression.....	144
3.3: Ratio of intratumoral to hepatic beta galactosidase expression.....	145
3.4: Histological analysis of beta galactosidase expression.....	148
3.5: Bioluminescent imaging for SELP-815K 4 wt%+Ad.CMV.Luc Day 4 .....	149
3.6: Bioluminescent imaging for SELP-815K 4 wt%+Ad.CMV.Luc Day 14 .....	150
3.7: Bioluminescent imaging for SELP-815K 4 wt%+Ad.CMV.Luc day 21 .....	151
3.8: Bioluminescent imaging for Ad.CMV.Luc day 4.....	152
3.9: Bioluminescent imaging for Ad.CMV.Luc day 14.....	153

3.10: Bioluminescent imaging for Ad.CMV.Luc day 21.....	154
3.11: Protein loss over time from SELPs degraded by human leukocyte elastase .....	156
3.12: Total protein loss due to elastase degradation as a function of SELP composition and elastase concentration.....	157
4.1: Animal weights from day 0-84 for SELP-mediated GDEPT toxicity.....	169
4.2: Animal weights from day 0-14 for SELP-mediated GDEPT toxicity.....	170
4.3: Differential white blood cell count at week 1 for SELP-mediated GDEPT toxicity .....	171
4.4: Liver enzyme levels at week 1 for SELP-mediated GDEPT toxicity.....	173
4.5: Differential white blood cell count at week 2 for SELP-mediated GDEPT toxicity .....	175
4.6: Liver enzyme levels at week 2 for SELP-mediated GDEPT toxicity.....	176
4.7: Differential white blood cell count at week 4 for SELP-mediated GDEPT study ...	178
4.8: Liver enzyme levels at week 4 for SELP-mediated GDEPT toxicity.....	180
4.9: Differential white blood cell count at week 12 for SELP-mediated GDEPT toxicity .....	181
5.1: Synthesis of SELP-815K-MMPRS monomer gene segment .....	188
5.2: Agarose gel showing SELP-815K-MMPRS colony screening for monomer gene segment .....	192
5.3: Multimerization of SELP-815K-MMPRS gene segments .....	193
5.4: Agarose gel showing SELP-815K-MMPRS polymer gene segments.....	194
5.5: SDS-PAGE gel showing small-scale SELP-815K-MMPRS production .....	197
5.6: SDS-PAGE analysis of 10 nM MMP-2 digest of SELP-815K over time .....	205
5.7: SDS-PAGE analysis of 10 nM MMP-2 digest of SELP-815K-MMPRS over time .....	206

5.8: SDS-PAGE analysis of 40 nM MMP-2 digest of SELP-815K over time .....	207
5.9: SDS-PAGE analysis of 40 nM MMP-2 digest of SELP-815K-MMPRS over time .....	208
5.10: SDS-PAGE analysis of 10 nM MMP-9 digest of SELP-815K over time .....	209
5.11: SDS-PAGE analysis of 10 nM MMP-9 digest of SELP-815K-MMPRS over time .....	210
5.12: SDS-PAGE analysis of 40 nM MMP-9 digest of SELP-815K over time .....	211
5.13: SDS-PAGE analysis of 40 nM MMP-9 digest of SELP-815K-MMPRS over time .....	212
5.14: Total degradation at 2 weeks for SELP-815K±MMPRS hydrogels.....	214
5.15: Protein loss over time for SELP-815K hydrogels .....	215
5.16: Protein loss over time for SELP-815K-MMPRS hydrogels.....	216
5.17: Compressive modulus of hydrogels in the presence and absence of MMPs.....	217
5.18: Total release of 100nm nanoparticles from SELP-815K±MMPRS hydrogels in the presence and absence of MMPs.....	219
5.19: Nanoparticle release over time for SELP-815K hydrogels .....	220
5.20: Nanoparticle release over time for SELP-815K-MMPRS hydrogels.....	221
A.1: Efficacy of SELP-mediated GDEPT in immunocompetent mice.....	241

## LIST OF TABLES

### Table

2.1: Known human MMP's and their biological substrates.....	48
2.2: SELP structures and properties.....	66
4.1: Animals per study group and end point for toxicity studies .....	166
5.1: Oligonucleotides for SELP-815K-MMPRS monomer gene synthesis.....	190

## ABBREVIATIONS

A/Ala	Alanine
AAV	Adeno-associated virus
Ad	Adenoviruses
Ad CMV LacZ	Adenovirus encoding for beta galactosidase, under the cytomegalovirus promoter
Ad CMV Luc	Adenovirus encoding for luciferase, under the cytomegalovirus promoter
AFM	Atomic force microscopy
ALT	Alanine aminotransferase
ANOVA	Analysis of variance
AST	Aspartate aminotransferase
$\beta$ -gal	Beta-galactosidase
BCA	Bicinchoninic acid
Bcl-2	B cell lymphoma 2
BONCAT	Bio-orthogonal noncanonical amino acid tagging
C/Cys	Cysteine
CAR	Coxsackievirus and adenovirus receptor
CBC	Complete blood count
CD28	Cluster of differentiation 28

CHAPS	3- ((3-Cholamidopropyl)dimethylammonio)-1-Propanesulfonic Acid
CHO-K1	Chinese hamster ovary cell line
CMV	Cytomegalovirus
CO <sub>2</sub>	Carbon dioxide
COMP	Cartilage oligomeric matrix protein
CPRG	Chlorophenol Red-β-D-Galactopyranoside
CV	Cloning vector
D/Asn	Aspartic acid
DEAE	Diethylaminoethyl cellulose
DI	Deionized water
DMA	Dynamic mechanical analysis
DNA	Deoxyribonucleic acid
DOPE	1,2-Dioleoyl-sn-Glycero-3-Phosphoethanolamine
DOSPA	2,3-dioleyloxy- <i>N</i> -[2(sperminecarboxamido)ethyl]- <i>N,N</i> -dimethyl-1-propanaminium trifluoroacetate
DOTAP	1,2-Dioleoyloxy-3-(trimethylammonio)-propane
DOTMA	<i>N</i> -[1-(2,3,-dioleyloxy)propyl]- <i>N,N,N</i> -trimethylammoniumchloride
E/Glu	Glutamic acid
ECM	Extracellular matrix
EGF	Epidermal growth factor
EGFR	Epidermal growth factor receptor
ELP	Elastin like peptide
Enz	Enzyme

EV	Expression vector
F/Phe	Phenylalanine
FGF-2	Fibroblast growth factor
FTIR	Fourier transform infrared spectroscopy
G/Gly	Glycine
G2-M	Gap 2- mitosis
G3	Generation 3
G4	Generation 4
GCV	Ganciclovir
GDEPT	Gene-directed enzyme prodrug therapy
GFP	Green fluorescent protein
GM-CSF	Granulocyte macrophage colony stimulating factor
GPI	Glycosylphosphatidylinositol
H/His	Histidine
HEPES	N-2-Hydroxyethylpiperazine-N'-2-Ethanesulfonic Acid
HIV	Human immunodeficiency virus
HNSCC	Head and neck squamous cell carcinoma
HPLC	High performance liquid chromatography
HPMA	Poly [ <i>N</i> -(2-hydroxypropyl)methacrylamide]
HPV	Human papilloma virus
HSVtk	Herpes simplex virus thymidine kinase
HUVEC	Human umbilical vein endothelial cell
I/Ile	Isoleucine

IACUC	Institutional Animal Care and Use Committee
IC <sub>50</sub>	Inhibitory concentration at 50%
IL-10	Interleukin 10
IMRT	Intensity modulated radiation therapy
K/Lys	Lysine
L/Leu	Leucine
LCST	Lower critical solution temperature
Luc	Luciferase
M/Met	Methionine
MALDI-TOF	Matrix assisted laser desorption ionization time of flight mass spectrometry
MCP	Membrane cofactor protein
MGS	Monomer gene segment
MMA	Methyl methacrylate
MMGD	Matrix-mediated gene delivery
MMP	Matrix metalloproteinase
MMPRS	Matrix-metalloproteinase responsive sequence
mRNA	Messenger RNA
N/Asn	Asparagine
NaCl	Sodium chloride
NCAA	Noncanonical amino acids
NVP	N-vinyl pyrrolidone
OD	Optical density



OERCA	Overlap extension rolling circle amplification
P/Pro	Proline
PAMAM	Poly(amido amine) dendrimers
PBS	Phosphate buffered saline
PCR	Polymerase chain reaction
PDMAEMA	Poly((2-dimethylamino)ethyl methacrylate)
pDNA	Plasmid DNA
PEG	Poly(ethylene glycol)
PEI	Poly(ethylenimine)
PFU	Plaque forming units
PLGA	Poly(lactic-co-glycolic acid)
PLL	Poly(l-lysine)
PUMP	Putative metalloproteinase
Q/Gln	Glutamine
R/Arg	Arginine
RB94	Retinoblastoma 94
RDL	Recursive directional ligation
RNA	Ribonucleic acid
RPM	Revolutions per minute
RT-PCR	Real-time polymerase chain reaction
S/Ser	Serine
SANS	Small angle neutron scattering
SAP	Shrimp Alkaline Phosphatase

SDS-PAGE	Sodium dodecyl sulfate polyacrylamide gel electrophoresis
SELP	Silk-elastinlike polymer
SLP	Silklike polymer
SPARC	Secreted protein acidic and rich in cysteine
ssDNA	Single-stranded DNA
T/Thr	Threonine
T-ALL	T cell acute lymphoblastic leukemia
TB	Terrific broth
TEM	Transmission electron microscopy
TGF- $\beta$ 1	Transforming growth factor beta 1
TIMP	Tissue inhibitors of metalloproteases
TNF-alpha	Tumor necrosis factor alpha
triEGMA	Ethoxytriethylene glycol methacrylate
tRNA	Transfer ribonucleic acid
V/Val	Valine
VEGF	Vascular endothelial growth factor
VSV	Vesicular stomatitis virus
W/Trp	Tryptophan
X-SCID	X-linked severe combined immune deficiency
Y/Tyr	Tyrosine

## ACKNOWLEDGEMENTS

I would first like to thank my research advisory committee for all of your input, discussion, and criticism of the following work.

Dr. Hunt's clinical perspective on the treatment of head and neck cancer has caused a shift in my views on this project and I will carry those lessons with me as I progress as a researcher. The ability to remain focused on the patient and the outcome is a valuable attribute and I appreciate the discussions we have had.

Dr. Joseph Cappello is another friend and collaborator with whom I have had many important and, at times, difficult conversations. Joe has been the person who has taught me most of all to acknowledge and abandon naïveté. Scientific research is a brutal place sometimes, and it can feel like hours and hours of research can mean so much, or so little. Joe has been the man who has given me the ability to temper both extremes, and put things in perspective. Further, his generosity with his time, information, and insight has proven invaluable to my career thus far as a scientist, and I look forward to future discussions and work together. Also, without his guidance in scaleup of silk-elastinlike polymers, my world for the last several years would have been sadly overrun by shaker flasks and nickel columns.

Dr. Kopecek has made sure that I have paid close attention to the drug delivery aspect of this work, and his experience and insight have been influential to my approach to research. I hope to eventually acquire his ability to find the small, intricate, but very

important questions and oversights which can turn a good idea into either a great idea or a forgotten page in a notebook.

Dr. Grainger has been another lasting influence on my development as an educator and researcher. Dr. Grainger has served as a role model for me of what an educator should be, and his involvement in his department and community, both academic and industrial, has been an important example for me of what one can accomplish with the right attitude and dedication.

The notion of performing a significant body of scientific work without the element of teamwork is, to be candid, absurd. With this in mind, I would like to individually thank Robert Price, a great friend and great labmate, for his countless hours of discussion, collaboration, and work together. The importance of Robert's input on my development as a researcher, scientist, and educator cannot be understated. Any time I had some off-the-wall theoretical calculation or needed to have someone take shots at a crazy idea, Robert was there. Also, when it came to doing a seemingly impossible quantity of work on a short deadline, Robert and I could move mountains (of mice).

Additionally, I would like to thank Dr. Khaled Greish. Dr. Greish has taught me more than probably any single person in my entire education, and the patience and understanding which he showed me even during trying times will serve as a model on which to build my own values in the future. And while we had our differences, working with Khaled always resulted in furthering my knowledge and overall awareness of research observations.

I would also be remiss if I did not acknowledge the contributions of Dr. Leonard Pease to my development as a scientist and person. Leonard is another collaborator with

whom I have had numerous 1-hour meetings which have extended well past the 2-hour mark, during which we have managed to touch on so many aspects of my project and others that it has made me feel as if I know nothing of what I am doing. Leonard has also shown me the value of tireless work, and its returns in both scientific and family life, and that it is possible to have both a strong career and a strong dedication to a family.

Another person whom I would like to acknowledge is coach Richard “Vick” Vickery, my freshman football coach at Somerset High School. Coach Vick taught me with football what I had never learned up to that point in my life, and has stuck with me and helped me through numerous difficult times, and that is to believe in myself and not accept personal failure. When these begin to falter, I can still hear his encouragement and unwillingness to give up, and this has been essential to my ability to press on even when it seems like I cannot go further.

Jason Read and Adam Gormley, my closest friends, have also been essential to enabling me to keep things in perspective, keep going, remember to have fun, and enjoy this part of my life through the high times and low ones.

I would also like to thank Heather Herd. There have been times when I have needed to be weak, and needed someone to understand me, accept me for who I am, and be there to support me, and she has been my rock.

Finally, I would like to thank my research advisor, Dr. Hamid Ghandehari. While his patience and willingness to allow my growth, sometimes at the cost of efficiency and results, has been of innumerable importance to my development as a scientist, it was his initial willingness to take a risk on me which has been germane to my success as a graduate student. Dr. Ghandehari has never doubted my overly optimistic timelines and

impossible research goals, but instead allowed me to push my limits and has remained unbelievably patient with my growth as a person and scientist over the last (almost) 5 years. His inability to tell anyone “no”, yet somehow miraculously manage to do everything he gets involved with, and do it well, will hopefully someday cease to be a mystery to me.

## INTRODUCTION

### 1.1 Introduction

Since the initial conceptualization of gene therapy, the problem of safe and efficient delivery of nucleic acids to target cells *in vivo* has continued to restrict the utility of this promising treatment approach.<sup>1-5</sup> Innate biological mechanisms, likely developed over the course of the evolution of our species to protect against virulent infection, have now become the enemy of a seemingly infinite number of possible treatments for human disease. Researchers have been attempting strategies which will allow the power of gene therapy to be unlocked, for countless hours of unraveling the intricacies of the human genome to come to some fruition. Yet as our understanding of how human disease develops, the questions remain: Why do our bodies turn on themselves? How can debilitating genetic errors remain uncorrected? What possible methods may be employed to intervene? Arguably the most theoretically effective strategy, direct repair of “incorrect” genetic code by specific transduction of external genetic material, has remained an elusive ideal. How much easier would treatment of disease be if clinicians could simply “reprogram” the body to not have the disease? Much effort has gone into the development of natural or man-made vectors to facilitate the expression of external genes in cells.<sup>4, 6</sup> However, even with successful identification of methods by which to introduce foreign genetic material, specificity of gene transduction to only specific cells remains an issue. Effective targeting of gene products is particularly important when the

gene of interest is used as a method to directly or indirectly initiate cell destruction, as in the case of cancer gene therapy. The expression of this type of gene in nontarget tissues has obvious ramifications, with the potential for organ damage or destruction along with many other undesirable side effects. There is a clear need to develop methods and strategies to increase the specificity of gene therapy for the treatment of cancer. However, while this remains fact, current clinical approaches to the treatment of cancer are faced with many similar challenges involving nonspecific exposure as well. Even with decades of research by thousands of investigators, there is still a drastic effect on quality of life as a result of many of the current state-of-the-art cancer treatments.<sup>7-14</sup> In some cases, the consequences of receiving treatment for a life-threatening cancer outweigh their ability to prolong life<sup>15-17</sup>; it is the classical balance between quality of life and quantity of life. Properly controlled cancer gene therapy has the potential to alleviate adverse effects and allow for the best possible treatment conditions in terms of patient compliance, happiness, and efficacy, which when combined have the potential to revolutionize modern cancer treatment.

One method by which gene transfer can be controlled is using matrix-mediated gene delivery (MMGD).<sup>18-20</sup> MMGD is the use of a biomaterial to control the delivery of a gene product in a spatiotemporal fashion. This may or may not occur by responding to stimuli present in the local environment, or stimuli provided externally. MMGD has advantages over other methods of gene delivery for many reasons. Most notably, MMGD systems can be designed to release their therapeutic gene products only in the presence of certain biological molecules, thereby giving these materials the ability to target their release to only certain sites of a tissue or only after an activating molecule or



enzyme has been released in the desired area. These materials could also potentially be designed to respond to environmental stimuli, such as temperature or pH, which would either restrict or enhance the release of therapeutic genes in a well-controlled manner. Another advantage to the use of MMGD is that instead of release being governed only by the diffusion of one molecule (the vector or naked DNA), the release rate is controlled by the diffusion of two molecules, the release stimulus and the vector, and the reaction kinetics between the stimulus and the tether. This allows the materials to be designed to precisely release at the rate desired by manipulating the sensitivity of the tether, the sensitivity of the material, or the material properties of the matrix governing the diffusion of solutes within the material. Further, administration of nucleic acids or nucleic acid delivery vehicles in matrices may potentially reduce the exposure of such constructs to the nuclease-rich extracellular environment. Such a protective effect would reduce the loss of gene expression activity due to degradation.

## **1.2 Aims and scope of this dissertation**

The necessity for an effective and safe gene delivery system can be addressed through a number of possible strategies. In this work, we investigate the utility of a genetically engineered protein polymer to accomplish this goal. Silk-elastinlike protein polymers (SELPs) are a class of genetically engineered polymers which have been investigated for use in several different applications, including viral gene delivery.<sup>18, 21, 22</sup> This material is composed of repeating units of silk (GAGAGS) and elastin (GVGVVP) units, which are arranged into blocks of several of each type of unit to form SELP monomers.<sup>23</sup> One major advantage to using these polymers is the ability to precisely

modify the length and arrangement to affect change in physicochemical properties.<sup>21, 24</sup> Three constructs of SELP have thus far been synthesized: SELP-47K, SELP-415K, and SELP-815K, so named for their arrangement of silk units and elastin units. Schematics of these three structures are shown in Figure 1.1. SELP-47K is composed of four silk units followed by eight elastin units per monomer, with one of these elastin units possessing a lysine substitution (GKGVP) denoted by “K”. SELP-415K has 4 silk and 16 elastin units per monomer, and SELP-815K has 8 silk and 16 elastin units. The number of monomers for each polymer is chosen such that the molecular weight of each polymer is approximately the same.

The central hypothesis of this dissertation is that by specifically manipulating the sequence and arrangement of the amino acid blocks comprising silk-elastinlike protein polymers in this way, a structure of this polymer can be identified and used as a material to enhance viral gene delivery. Increasing silk unit length and decreasing elastin unit length are hypothesized to decrease release rate, leading to more effective localization of viral gene transfection and consequently improved safety and efficacy of viral delivery when mediated by SELP. The ideal structure of SELP would show significant improvements in the physical distribution of adenoviral gene transfection and improve the safety of localized adenoviral gene therapy. The goal of this research is to take steps toward constructing such a material and using the highly specific modification capability of genetically engineered polymers. This hypothesis was tested through the completion of three Specific Aims.

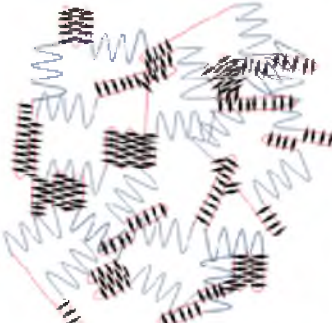
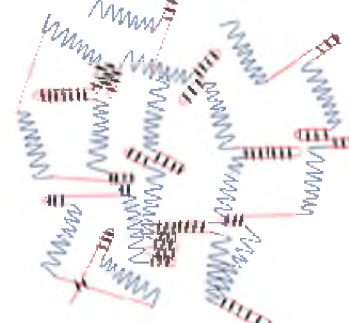
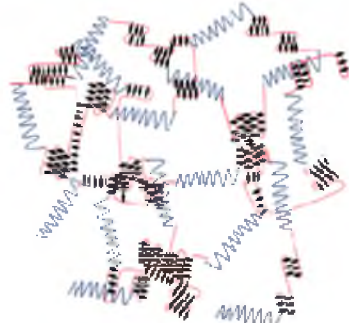
$[(GVGVVP)_4GKGVVP(GVGVVP)_3(GAGAGS)_4]_{12}(GVGVVP)_4GKGVVP(GVGVVP)_3(GAGAGS)_4$	$[(IGVGVVP)_7GKGVVP(GVGVVP)_{11}(GAGAGS)_4]_7(GVGVVP)_4GKGVVP(GVGVVP)_{11}(GAGAGS)_2$	$[GAGS(GAGAGS)_2(GVGVVP)_4GKGVVP(GVGVVP)_{11}(GAGAGS)_5GA]_6$
		
SELP-47K	SELP-415K	SELP-815K

Figure 1.1: Schematics of three SELP analogs used for viral gene delivery. Blue=elastin blocks, red=silk blocks, black=crosslinks between silk blocks.

1.2.1 Compare the structure-dependence of viral delivery from  
silk-elastinlike protein polymers for duration and extent  
of gene transfection *in vivo*

The three SELP structures in the context of viral delivery were compared for the distribution, magnitude, and longevity of viral gene expression in xenograft tumors grown in the flanks of athymic nude mice. Further, SELPs were compared in the context of degradation by elastase, a common protease found ubiquitously throughout the body. The hypothesis driving this research was that modifications to the structure of SELP would produce structure-dependent changes in adenoviral gene transfection and degradation of these polymers. Gene transfection was analyzed using two different assays, one an organ lysate colorimetric assay performed using a  $\beta$ -galactosidase reporter gene, and the other being a luciferin-luciferase reporter system for real-time gene expression detection. Tissue  $\beta$ -galactosidase expression was histologically analyzed to investigate the specific distribution of gene expression within tumor tissue. In addition to structure-dependence of gene expression, the relative degradability of these three constructs was assessed by incubation with human elastase, which revealed that degradability is dependent on hydrogel weight percentage, silk:elastin ratio, and silk unit length. This work revealed that SELP-815K and SELP-47K at 4 wt% offered the greatest enhancement in gene delivery efficiency, while degradability was highest in SELP-415K, followed by SELP-47K and SELP-815K. These studies set the stage for further assessment of SELPs-47K and-815K at 4 wt% in the improvement of efficacy and safety of viral gene delivery.

1.2.2 Assess the safety of silk-elastinlike protein polymer-mediated gene-directed enzyme-prodrug therapy using adenoviral vectors *in vivo*

This aim was intended to investigate the ability of SELP-815K at 4 wt% concentration to improve the safety of gene-directed enzyme-prodrug therapy (GDEPT). GDEPT is, in general, the use of a foreign gene introduced into cells to sensitize those cells to an ordinarily nontoxic or minimally toxic substance, the prodrug.<sup>25-28</sup> In this case, the enzyme-prodrug system applied was herpes simplex virus thymidine kinase (HSVtk) as the activating enzyme, and ganciclovir (GCV) as the prodrug.<sup>26-28</sup> The ability of SELP to improve the safety of this system was investigated by injecting adenovirus encoding for HSVtk suspended in 0.9% saline or SELP-815K at 4 wt% subcutaneously in an immunocompetent mouse model. Following viral injection, daily administration of GCV was performed and mouse weights were assessed daily to monitor overall well-being. At four selected time points (i.e., 1, 2, 4, and 12 weeks) animals were sacrificed and complete differential blood count and clinical chemistry panel were performed on all mice. The results revealed that delivery of adenovirus in SELP eliminated acute immune response observed at week 1 in the adenovirus + saline injection, as well as the apparent hepatotoxicity observed at week 4. Overall, the results of this study show that delivery of adenovirus in a SELP hydrogel eliminates many of the concerns which are associated with adenoviral delivery in this model. One unresolved issue which was observed in this study was an apparent limited biodegradability of SELPs, with almost the entire injected gel masses recoverable even at the 12 weeks postinjection time point.

### 1.2.3 Synthesize and characterize a novel, matrix-metalloproteinase responsive analog of SELP-815K

In this aim, a new analog of SELP containing a matrix-metalloproteinase (MMP)-degradable amino acid sequence, GPQGIFGQ (single amino acid abbreviations are used), was genetically engineered and the degradation, release, and mechanical properties of the resulting protein polymer and hydrogel were assessed. The degradable sequence was inserted immediately at the C-terminal side of the lysine substitution due to its location within the elastin units, as this was thought to have the least effect on gelation. The individual polymer chains were observed to be degradable by MMP-2 and MMP-9, as were hydrogels composed of these polymers. The release of fluorescent nanoparticles of 100nm was also affected by MMP-2 and MMP-9 treatment. These results indicate that the degradation of SELP can be controlled and optimized for viral delivery in response to MMPs present in the tumor microenvironment. The ability of these hydrogels to potentially respond to MMPs increases their utility as viral delivery materials for the treatment of cancer, as these enzymes are important to cancer survival, invasion, and propagation, and their expression level has been correlated with increased aggressiveness and propensity to metastasize.

This dissertation covers the work performed to accomplish these aims, as well as supplemental data which further aid in the understanding of how SELPs improve adenoviral gene delivery, and how these materials are constructed. Chapter 2 of this dissertation provides a broad review of literature applicable to this body of work, including gene delivery, head and neck cancer etiology and treatment, MMPs, genetically engineered protein polymers, and previous work on SELPs for viral delivery. Parts of this

chapter have been published elsewhere.<sup>18</sup> Chapters 3,<sup>29</sup> 4,<sup>30</sup> and 5,<sup>31</sup> discuss the experimental results acquired towards the completion of Specific Aims 1, 2, and 3, respectively, while Chapter 6 provides a conclusion and discussion of future directions for this project, silk-elastinlike protein polymers, and genetically engineered polymers in general. The Appendix discusses the results of a pilot efficacy study which was performed in immunocompetent mice in order to compare results with previously published work investigating efficacy in immunocompromised mice.<sup>32</sup>

### 1.3 References

1. Rapti, K.; Chaanine, A. H.; Hajjar, R. J., Targeted gene therapy for the treatment of heart failure. *Can J Cardiol* **2011**, *27*, (3), 265-283.
2. Evans, C., Gene therapy for the regeneration of bone. *Injury* **2011**, *42*, (6), 599-604.
3. Pack, D. W.; Hoffman, A. S.; Pun, S.; Stayton, P. S., Design and development of polymers for gene delivery. *Nat Rev Drug Discov* **2005**, *4*, (7), 581-593.
4. Elsabahy, M.; Nazarali, A.; Foldvari, M., Non-viral nucleic acid delivery: key challenges and future directions. *Curr Drug Deliv* **2011**, *8*, (3), 235-244.
5. Roth, J. A.; Cristiano, R. J., Gene therapy for cancer: what have we done and where are we going? *JNCI Journal of the National Cancer Institute* **1997**, *89*, (1), 21-39.
6. Young, L. S.; Searle, P. F.; Onion, D.; Mautner, V., Viral gene therapy strategies: from basic science to clinical application. *J Pathol* **2006**, *208*, (2), 299-318.
7. Shapiro, C. L.; Recht, A., Side effects of adjuvant treatment of breast cancer. *N Engl J Med* **2001**, *344*, (26), 1997-2008.
8. Meiorow, D.; Nugent, D., The effects of radiotherapy and chemotherapy on female reproduction. *Hum Reprod Update* **2001**, *7*, (6), 535-543.
9. Gelderblom, H.; Verweij, J.; Nooter, K.; Sparreboom, A., Cremophor EL: the drawbacks and advantages of vehicle selection for drug formulation. *Eur J Cancer* **2001**, *37*, (13), 1590-1598.
10. Eifel, P.; Axelson, J. A.; Costa, J.; Crowley, J.; Curran, W. J., Jr.; Deshler, A.; Fulton, S.; Hendricks, C. B.; Kemeny, M.; Kornblith, A. B.; Louis, T. A.; Markman, M.; Mayer, R.; Roter, D., National Institutes of Health Consensus Development Conference Statement: adjuvant therapy for breast cancer, November 1-3, 2000. *J Natl Cancer Inst* **2001**, *93*, (13), 979-989.
11. Cortes, J. E.; Pazdur, R., Docetaxel. *J Clin Oncol* **1995**, *13*, (10), 2643-2655.
12. Speth, P. A.; van Hoesel, Q. G.; Haanen, C., Clinical pharmacokinetics of doxorubicin. *Clin Pharmacokinet* **1988**, *15*, (1), 15-31.
13. Schein, P. S.; Winokur, S. H., Immunosuppressive and cytotoxic chemotherapy: long-term complications. *Ann Intern Med* **1975**, *82*, (1), 84-95.
14. Sonis, S. T., Mucositis as a biological process: a new hypothesis for the development of chemotherapy-induced stomatotoxicity. *Oral Oncol* **1998**, *34*, (1), 39-43.



15. Swetz, K. M.; Smith, T. J., Palliative chemotherapy: When is it worth it and when is it not? *Cancer J* **2010**, *16*, (5), 467-472.
16. Payne, S. A., A study of quality of life in cancer patients receiving palliative chemotherapy. *Soc Sci Med* **1992**, *35*, (12), 1505-1509.
17. Gunnars, B.; Nygren, P.; Glimelius, B., Assessment of quality of life during chemotherapy. *Acta Oncol* **2001**, *40*, (2-3), 175-184.
18. Gustafson, J. A.; Ghandehari, H., Silk-elastinlike protein polymers for matrix-mediated cancer gene therapy. *Adv Drug Deliv Rev* **2010**, *62*, (15), 1509-1523.
19. Mallapragada, S. K.; Agarwal, A., Synthetic sustained gene delivery systems. *Curr Topics Med Chem* **2008**, *8*, (4), 311-330.
20. Jin, X.; Liu, L.; Mei, L.; Leng, X.; Zhang, C.; Sun, H.; Song, C.; Levy, R. In *Antibody Modified Collagen Matrix for Site-Specific Gene Delivery*, 2008; ACS Publications: 2008; pp 243-261.
21. Cresce, A. W.; Dandu, R.; Burger, A.; Cappello, J.; Ghandehari, H., Characterization and real-time imaging of gene expression of adenovirus embedded silk-elastinlike protein polymer hydrogels. *Mol Pharm* **2008**, *5*, (5), 891-897.
22. Dandu, R.; Ghandehari, H.; Cappello, J., Characterization of structurally related adenovirus-laden silk-elastinlike hydrogels. *J Bioact Compat Pol* **2008**, *23*, (1), 5-19.
23. Cappello, J.; Crissman, J.; Dorman, M.; Mikolajczak, M.; Textor, G.; Marquet, M.; Ferrari, F., Genetic engineering of structural protein polymers. *Biotechnol Prog* **1990**, *6*, (3), 198-202.
24. Dandu, R.; Cresce, A. V.; Briber, R.; Dowell, P.; Cappello, J.; Ghandehari, H., Silk-elastinlike protein polymer hydrogels: Influence of monomer sequence on physicochemical properties. *Polymer* **2009**, *50*, (2), 366-374.
25. Altaner, C., Prodrug cancer gene therapy. *Cancer Lett* **2008**, *270*, (2), 191-201.
26. Moolten, F. L., Drug sensitivity ("suicide") genes for selective cancer chemotherapy. *Cancer Gene Ther* **1994**, *1*, (4), 279-287.
27. Hamel, W.; Magnelli, L.; Chiarugi, V. P.; Israel, M. A., Herpes simplex virus thymidine kinase/ganciclovir-mediated apoptotic death of bystander cells. *Cancer Res* **1996**, *56*, (12), 2697-2702.

28. Mesnil, M.; Yamasaki, H., Bystander effect in herpes simplex virus-thymidine kinase/ganciclovir cancer gene therapy: role of gap-junctional intercellular communication. *Cancer Res* **2000**, *60*, (15), 3989-3999.
29. Gustafson, J.; Greish, K.; Frandsen, J.; Cappello, J.; Ghandehari, H., Silk-elastinlike recombinant polymers for gene therapy of head and neck cancer: from molecular definition to controlled gene expression. *J Control Release* **2009**, *140*, (3), 256-261.
30. Gustafson, J. A.; Price, R. A.; Greish, K.; Cappello, J.; Ghandehari, H., Silk-elastin-like hydrogel improves the safety of adenovirus-mediated gene-directed enzyme-prodrug therapy. *Mol Pharm* **2010**, *7*, (4), 1050-1056.
31. Gustafson, J. A.; Price, R. A.; Frandsen, J.; Henak, C.; Cappello, J.; Ghandehari, H., Synthesis and characterization of a matrix-metalloproteinase responsive silk-elastinlike protein polymer. *Biomacromolecules* **2012**, *Submitted*.
32. Greish, K.; Frandsen, J.; Scharff, S.; Gustafson, J.; Cappello, J.; Li, D.; O'Malley, B. W., Jr.; Ghandehari, H., Silk-elastinlike protein polymers improve the efficacy of adenovirus thymidine kinase enzyme prodrug therapy of head and neck tumors. *J Gene Med* **2010**, *12*, (7), 572-579.

## CHAPTER 2

### LITERATURE BACKGROUND

#### **2.1 Introduction**

The enhancement of gene delivery with respect to both localization and magnitude is a key area of research with the potential to unlock a vast quantity of treatments for many diseases. Even with decades of research and significant funding, methods of delivering genetic material which result in effective treatment of disease are virtually nonexistent. This lack of success in the field as a whole calls for new materials, methods, and strategies for the enhancement of gene delivery. The careful use of adenoviral vectors, evolved over eons to be efficacious gene delivery machines, is a possible answer to the question of clinically useful gene delivery approaches. In order to enhance the capabilities and safety of adenoviral vectors, they must be protected from the body's natural defenses for as long as possible before they reach their target, and this goal can be accomplished by physically segregating them in a hydrogel. The development of an ideal material from which to deliver adenoviral vectors must have several characteristics:

1. **Highly controllable physicochemical properties:** The pore size, mechanical properties, state of matter, and interactions with the adenovirus must be tightly controllable.

2. High level of biocompatibility: In the context of cancer, the material must not enhance the progression of the disease, nor cause undesirable systemic effects due to its administration. Further, the material must be degradable, and the products resulting from that degradation must not cause unacceptable toxicity.
3. Bioresponsiveness: The ideal material will have the capability to respond to changes in the local environment. Enhanced delivery with progressing disease state and vice versa would increase the efficiency and efficacy of the treatment.

The combination of the right target and delivery system for a given application has great potential to be successful. A platform which allows rapid development of such systems would greatly enhance the research into what characteristics or properties would be considered to be ideal.

## **2.2 Cancer gene therapy**

Of all currently researched clinical targets for gene therapy, cancer is by far the most common, comprising 1107 out of 1714 (64.6%) total gene therapy clinical trials worldwide in 2011.<sup>1</sup> Gene therapy approaches are particularly attractive to cancer treatment for many reasons, such as the current insufficiency of very effective, reliable, and nonintrusive treatments, and the high prevalence of the general disease. Despite extensive effort in clinical research in this area, there still does not exist a single approved gene therapy treatment in the United States, and only two treatments have been approved worldwide, both in China.<sup>2, 3</sup> The concerns regarding gene therapy for the treatment of cancer have shifted from safety to efficacy. Thousands of clinical trials have successfully passed Phase I, but are stalling following Phase II, as evidenced by the fact that only

3.6% of such trials have reached Phases III or IV.<sup>1</sup> Currently, there are a wide range of strategies being employed to increase the efficacy of cancer gene therapy in hopes of producing a clinically viable, safe, and effective treatment.

### 2.2.1 Cancer gene therapy strategies and approaches

Cancer gene therapy has been attempted using a diverse selection of techniques in terms of treatment strategy, vector, and delivery. The main approaches for cancer gene therapy include use of suicide genes,<sup>4, 5</sup> oncolytic viruses,<sup>6, 7</sup> tumor suppressor genes,<sup>8</sup> antiangiogenesis targets,<sup>9, 10</sup> and immunotherapy.<sup>11, 12</sup> The genes of interest for these different approaches are packaged in a vector, which is broadly defined as a chemical or organism intended to enhance the ability of the therapeutic genetic material to enter the cell and be expressed. Vectors are broadly classified in two categories: viral vectors, in which viruses are genetically modified to carry specific genes of interest; and nonviral vectors, which cover a broad range of complexation or encapsulation methods intended to aid in the delivery of genes. It is now quite uncommon that “naked plasmid” be delivered as a stand-alone gene therapy method, as plasmid DNA is susceptible to degradation by nucleases and clearance *in vivo*, in addition to having inefficient cell entry and subsequent expression profiles. In addition to the aforementioned vectors, there are specific methods by which researchers have aimed to improve the delivery of these vectors, and are generally referred to as physical delivery methods.<sup>13</sup> When combined, the various options of biological targets, vectors, and delivery methods offer a powerful and highly diverse toolbox for the design and implementation of gene therapy for the treatment of cancer and other diseases.

### 2.2.1.1 Suicide gene therapy

Suicide gene therapy is considered to be the introduction of genetic material into a tumor which is intended to directly result in cell death via apoptosis. One type of suicide gene therapy is gene-directed enzyme-prodrug therapy (GDEPT), in which a gene is introduced encoding for a protein which is able to convert a prodrug into an active compound. An example of this type of therapy is the herpes simplex virus thymidine kinase (HSVtk)-ganciclovir (GCV) system, depicted in Figure 2.1.<sup>14</sup> In this approach, HSVtk is produced in target cells, imparting in them the ability to convert GCV into ganciclovir monophosphate. GCV monophosphate is further phosphorylated into diphosphate and triphosphate forms by normal cellular kinases. GCV triphosphate is a potent cytotoxic compound which competes with deoxyguanosine triphosphate during DNA synthesis, resulting in cell cycle interruption and cell death.<sup>15, 16</sup> Further, the GCV monophosphate has been shown to transport between cells via gap junctions, resulting in what is known as the “bystander effect”,<sup>4, 16, 17</sup> as these cells still produce the toxic GCV triphosphate and are killed as a result, but were not transfected with the therapeutic gene. Another common example of suicide gene therapy is the introduction of retinoblastoma 94 (RB94), a truncated version of a native weak tumor suppressor protein. RB94 was shown to potently induce G2-M cell cycle arrest by reduction in telomerase activity, telomere erosion, and chromosomal crisis in several *in vitro* and *in vivo* cancer models.<sup>5, 18, 19</sup> One disadvantage of this system compared to a bystander effect GDEPT approach is that each cell must be successfully infected by a virus in order to be killed, which is extremely difficult to induce.

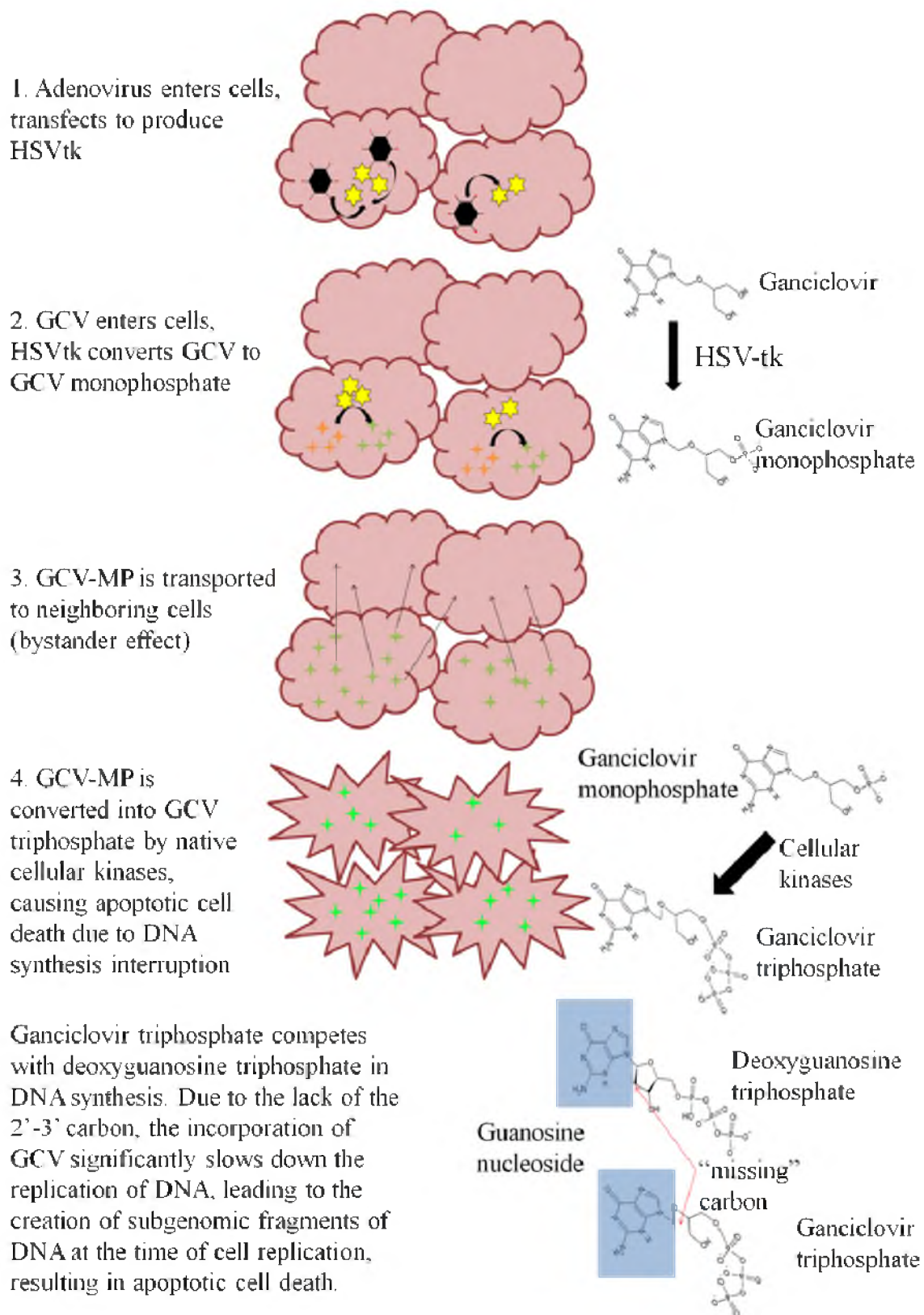


Figure 2.1: Gene-directed enzyme-prodrug therapy

### **2.2.1.2 Oncolytic viruses**

Broadly defined, oncolytic viruses selectively or preferentially transfect cancer cells, resulting in selective killing. Oncolytic viruses in the context of this work are those which destroy target cells by lytic viral replication, i.e., the tumor cells are killed by physical lysis due to viral replication or depletion of intracellular resources used to replicate the virus.<sup>20</sup> One example of this approach is the systemic administration of attenuated vesicular stomatitis virus (VSV), which is able to rapidly and selectively replicate in cancer cells while not affecting noncancerous cells.<sup>7, 21</sup> The mechanism for this activity is that this virus is very sensitive to interferon-mediated detection and clearance, but certain cancer cells do not possess the ability to respond to interferon signaling, resulting in their death by physical rupture due to viral replication. The biggest advantage to this system is that, due to the specificity of its effect, it can be administered systemically, thereby possibly infecting metastatic tumors along with a known primary tumor. However, and again due to its sensitivity, it may require physiologically toxic titers of virus to be administered in order for an effective initial dose of virus to reach the tumor. Further, VSV has been shown to cause a form of encephalitis in humans, causing the complete attenuation of VSV to be necessary for clinical translation.<sup>22</sup> Recent developments in oncolytic VSV development include increasing the efficacy of this treatment by adding the cancer specific suicide gene p53,<sup>6</sup> and by increasing the blockage of interferon pathways in target cells.<sup>23</sup>



### **2.2.1.3 Tumor suppressor genes**

Tumor suppressor gene therapy is typically intended to replace the function of a lost or mutated regulatory pathway protein which has resulted in the development of cancer. The classic example of tumor suppressor gene therapy is the introduction of a functional p53 gene into cancers which arose from a lack thereof.<sup>24</sup> In normally functioning cells, p53 serves as a quality control protein for genome mutations: it can activate DNA repair mechanisms by arresting the cell cycle and activating repair proteins, or it can induce apoptosis if the damage to the DNA is too extensive to allow complete repair.<sup>25, 26</sup> Mutations in the p53 gene resulting in ineffective or nontrafficked forms of p53 protein allow DNA damage to go unchecked, allowing errors in cell replication to occur, thereby resulting in cancer. Mutations in the p53 gene are observed in approximately 50% of all human tumors.<sup>8</sup> and delivery of p53 genes has no effect on off-target cells as p53 is a naturally expressed protein and it is the lack of expression of functional p53 which leads to tumorigenesis in these cases.

### **2.2.1.4 Antiangiogenesis gene therapy**

The classic 1971 publication by Dr. Judah Folkman revealing tumor angiogenesis as a potential target for the treatment of cancer<sup>27</sup> has led to many strategies and attempts to inhibit or eliminate the ability of tumors to recruit or grow new vasculature, thereby causing the tumor to stop growing or regress as a result of insufficient nutrients to sustain living cells. In general, antiangiogenic cancer gene therapy is divided into two approaches: the inhibition of pro-angiogenic factors, or the enhancement of anti-angiogenic factors.<sup>9</sup> The most common targets in inhibition type antiangiogenic gene

therapy are related to the vascular endothelial growth factor (VEGF) receptor and its related downstream intracellular machinery.<sup>10</sup> VEGF is very commonly implicated in the formation of neovasculature and there have already been approved antibody-based treatments which target the growth factor itself (Avastin).<sup>28</sup> A recent example of gene therapy for VEGF pathway knockdown has targeted VEGF itself by encoding for soluble VEGF receptor.<sup>29, 30</sup> A recent example of enhancement of an antiangiogenic factor is the delivery of endostatin-encoding, liposome-packaged adenovirus.<sup>31</sup> Antiangiogenic gene therapy approaches have unfortunately faced difficulties in the clinic for a number of reasons. The two most significant are the fact that angiogenesis is not regulated by a single pathway, i.e., complete eradication of one mechanism is not sufficient to completely stop angiogenesis from occurring, and that successful blockage of angiogenesis is typically only cytostatic. Cytostatic treatments temporarily stop the growth of the tumor but do not reduce its size, and may actually select for cells which can live in hypoxic and low nutrient environments.<sup>10</sup> There has also been some recent results suggesting that antiangiogenic therapy may actually increase invasiveness of the tumor and the likelihood of metastasis.<sup>32</sup>

### **2.2.1.5 Gene-mediated immunotherapy**

The overall goal of cancer immunotherapy is to use the patient's own immune system to attack an established tumor, typically done by administration of immunostimulatory factors<sup>33</sup> or administration of the patient's own immune cells with or without genetic modification.<sup>11, 12, 34-36</sup> Many current approaches to genetically enhanced cancer immunotherapy are centered around modifying the patient's own T-cells *ex-vivo*

to overcome difficulties faced by traditional unmodified autologous T-cell expansion and re-implantation. The three main challenges as laid out by Berry et al. are : 1. Difficulties in isolating and expanding endogenous, specific, tumor-reactive cells, 2. Poor survival of isolated and expanded cells following re-implantation, and 3. The immunosuppressive nature of the tumor microenvironment.<sup>36</sup> Gene therapy is used to overcome these challenges in several ways. Introduction of genes into T-cells encoding for specific receptors to attack specific tumor types has been attempted for many types of cancer,<sup>36</sup> and the efficacy of such approaches is greatly increased when the receptor is designed as a chimera with a T-cell co-stimulatory factor such as CD28.<sup>37, 38</sup> Survival of the newly implanted cells can be improved by several methods, for example, inducing overexpression of anti-apoptotic factors such as Bcl-2.<sup>39</sup> The immunosuppressive nature of the tumor environment has been addressed in a similar manner as the difficulty in specificity, with chimeric tumor-specific antigen receptors overcoming many of these issues.<sup>38</sup>

### 2.2.2 Delivery strategies for cancer gene therapy

The delivery and expression of genetic material in target cells has long been the most significant challenge in gene therapy.<sup>40-42</sup> To overcome these significant challenges, researchers have employed many different methods and designs for gene delivery systems. The design of gene delivery systems encompasses many levels, from vectors which interface directly with the therapeutic genetic material, to strategies for delivering either vector protected or “naked” DNA, and many combinations thereof. The vector which is selected for a particular application has drastic effects on the efficacy and safety

of the gene delivery system as a whole. These carriers can be divided into two basic classes: viral vectors and nonviral vectors. Viral vectors are generally much more efficient and effective at delivering gene products to the nucleus and inducing expression of the desired protein. However, there are safety concerns revolving around this type of gene delivery. On the other hand, nonviral vectors generally are safe to administer and most of them are not known to elicit immune response to the same extent as viral vectors, but they exhibit greatly reduced transfection efficiency when compared to viral vectors.

### **2.2.2.1 Nonviral vectors**

The basic strategy behind nonviral vector design is to engineer chemically synthesized carriers to both mask the DNA from the body's response, thus increasing circulation time and safety, and additionally to aid in the trafficking of the genetic material into the cell for expression.<sup>43, 44</sup> Nonviral vectors are faced with many challenges, as they must have mechanisms built in to overcome the biological barriers associated with gene transfer while maintaining the ability to transfer the genes of interest such that they will be expressed. This is to be done without compromising toxicity, and in the case of anticancer gene therapy, the complex would ideally be specifically targeted to cancer cells to avoid collateral transfection and potential cell death or organ destruction. The basic types of nonviral vectors from a materials standpoint are polymers,<sup>45, 46</sup> lipids,<sup>47</sup> polypeptides,<sup>48</sup> and nanoparticles.<sup>43, 49</sup>

#### 2.2.2.1.1 Polymers for gene delivery

**2.2.2.1.1.1 Poly L-lysine (PLL).** Pioneering work was performed investigating the DNA complexation capabilities of poly L-lysine (PLL) in 1975.<sup>50</sup> PLL condenses DNA, and its ability to affect the expression of complexed nucleic acids was demonstrated both *in vitro*<sup>51</sup> and *in vivo*.<sup>52</sup> PLL has been shown to exhibit relatively high cytotoxicity and can be unstable and aggregate depending on salt concentration. Attempts have been made to circumvent both of these issues with some success, and targeting of PLL complexes has been employed to overcome the typical nonspecific gene transduction associated with polymeric carriers. Recent applications of PLL for gene delivery involve modifications to the architecture of the polymer complexes intended to increase the gene delivery efficiency while reducing the cytotoxicity, for example, forming dendritic structures of PLL with grafted poly(ethylene glycol) (PEG).<sup>53</sup> These complexes showed significantly increased transfection efficiency while displaying negligible cytotoxicity *in vitro*.

**2.2.2.1.1.2 Poly(ethylenimine) (PEI).** PEI is by far the most extensively investigated cationic polymer for gene delivery, and the initial demonstration of PEI's nucleic acid transfer capabilities was performed in 1995 by Behr et al.<sup>54</sup> PEI is particularly attractive as a gene delivery agent due to its very high positive charge density, allowing it to complex with a large amount of DNA, and its ability to be easily derivatized to impart specific properties. Early studies on gene delivery with PEI revealed that in general, increasing molecular weight of linear PEI causes greater transfection efficiency and cytotoxicity,<sup>55, 56</sup> and it has been determined that in general, the optimal molecular weight of PEI for gene transfer ranges from 5kDa to 25kDa,<sup>57</sup> More recent

developments of PEI as a gene delivery agent have been largely focused on reducing the toxicity *in vivo*, which has been shown to be significant,<sup>58</sup> with the strong positive charge density of the polymer being implicated<sup>59</sup> as well as PEI-DNA complexes' ability to activate complement.<sup>60</sup> PEGylation of PEI-DNA complexes has been employed as a strategy to reduce this toxicity with some success.<sup>61</sup> However, it has been demonstrated that the addition of PEG reduces cellular uptake and consequently gene expression.<sup>62</sup> The development of a biodegradable, acid-labile PEI was a significant breakthrough in improving PEI-mediated delivery and was shown to have comparable transfection efficiency to 25kDa PEI while demonstrating greatly reduced cytotoxicity.<sup>63</sup>

**2.2.2.1.1.3 Poly(methacrylate).** Polymethacrylates represent another extensively studied category of cationic polymers for gene delivery. The initial use of these polymers for gene delivery was demonstrated using poly((2-dimethylamino)ethyl methacrylate) (PDMAEMA) complexed with plasmid DNA.<sup>64</sup> These initial studies on PDMAEMA demonstrated a strong ability to transfect COS-7 cells *in vitro*. However, they also demonstrated very strong toxicity, with an IC<sub>50</sub> of only 30µg/ml. The reason for this toxicity, like that of many cationic polymer-based gene delivery systems, was likely the highly positive zeta potential, measured at +30mV. Further developments in the use of polymethacrylates for gene delivery involve copolymerization of DMAEMA with methyl methacrylate (MMA), ethoxytriethylene glycol methacrylate (triEGMA), or N-vinyl pyrrolidone (NVP).<sup>65</sup> These results showed that in the case of copolymerization with MMA, the cytotoxicity was significantly increased, accompanied by a decrease in transfection efficiency. In the case of polymerization with triEGMA, cytotoxicity and transfection efficiency both decreased, and copolymerization with NVP resulted in

decreased cytotoxicity and increased transfection efficiency.<sup>65</sup> More recent developments in the use of polymethacrylates for gene delivery involve the formation of nanoparticles from poly(lactide-co-glycolide) and poly(methacrylate) blends, which were shown to be safe and efficient in *in vivo* delivery of plasmid DNA encoding for IL-10.<sup>66</sup>

**2.2.2.1.1.4 Cyclodextrins.** Cyclodextrins are polysaccharides composed of glucose which have been joined via  $\alpha(1,4)$  linkages.<sup>67</sup> The attachment of glucose in this way forms a cyclic polymer which forms a shape similar to a truncated hollow cone, as steric effects due to the distribution of hydroxyls in relation to linkage points cause the glucose molecules to tilt inward. These materials have been used as copolymers in either an embedded configuration, in which the cyclodextrin is part of the polymer backbone, or in a pendant configuration, in which the cyclodextrin is grafted as a side chain.<sup>67</sup> The initial work performed investigating the use of cyclodextrin-containing polymers evaluated the embedded configuration. Specifically, a cyclodextrin derivative 6A,6D-dideoxy-6A,6D-di(2-aminoethanethio)- $\beta$ -cyclodextrin copolymerized with dimethylsuberimidate in an AABBAABB architecture showed improved transfection efficiency and significantly reduced cytotoxicity compared to PEI in BHK-21 cells and CHO-K1 cells. Recently, more complex architectures incorporating cyclodextrins have been used to improve the transfection efficiency and reduce the toxicity of gene delivery. An example of this is the formation of PEGylated supramolecular chitosan-graft-(PEI- $\beta$ -cyclodextrin) copolymers.<sup>68</sup> These constructs are formed by first forming a PEI-modified cyclodextrin, and then grafting it to a chitosan polymer. The cytotoxicity and transfection efficiency of this construct has been compared to 25kDa PEI, which was shown to be

much less cytotoxic with comparable transfection efficiencies.<sup>68</sup> PEGylation of these polymers reduced their transfection efficiency.

#### 2.2.2.1.2 Liposomal gene delivery systems

The application of liposomes as gene delivery mediators was first demonstrated in 1982,<sup>69</sup> and since then, much work has been performed on the improvement and application of these vectors for gene delivery.<sup>70-72</sup> The lipoplexes themselves are formed first by producing liposomes of cationic lipids, followed by their complexation with DNA to be delivered. Once the complexes are endocytosed, they escape the endosome by a proposed “flip flop reorganization of phospholipids”,<sup>43, 73</sup> resulting in release of the complexed DNA into the cytoplasm and gene expression.

**2.2.2.1.2.1 N-[1-(2,3,-dioleyloxy)propyl]-N,N,N-trimethylammoniumchloride (DOTMA).** DOTMA was one of the earliest and commonly used cationic lipids for DNA complexation and delivery. Results from experiments investigating its transfection efficiency show that it performs better than DEAE-dextran and calcium chloride precipitation methods. However, cytotoxicity became an issue with increasing lipid concentration.<sup>74</sup> Modifications have been made to DOTMA to try to mitigate this toxicity while maintaining or improving its gene delivery capabilities. In one case, a hydroxyethyl derivative of DOTMA in a 1:1 blend with 1,2-Dioleoyl-sn-Glycero-3-Phosphoethanolamine (DOPE) was shown to have increased *in vitro* transfection efficiency in addition to positive *in vivo* results, although the studies lacked a control by which to normalize and compare the results to standard DOTMA or other known transfection reagents.<sup>75</sup>



**2.2.2.1.2.2 LipofectAMINE®.** LipofectAMINE is the trade name for a cationic liposome gene delivery system composed of a 3:1 ratio of 2,3-dioleoyloxy-*N*-[2(sperminecarboxamido)ethyl]-*N,N*-dimethyl-1-propanaminium trifluoroacetate (DOSPA) to DOPE.<sup>76, 77</sup> LipofectAMINE exhibits efficient gene delivery *in vitro*; however, it also exhibits significant cytotoxicity,<sup>78</sup> as is observed with many cationic DNA complexes. Further, studies have investigated the *in vivo* utility of LipofectAMINE, and the results have shown that delivery is very inefficient and in many cases nonexistent.<sup>79</sup> Lipofectamine has been mostly used as an *in vitro* tool to investigate the effects of transfer of particular genes for experimental purposes, as it is commercially available, reliable, and easy to use.<sup>80, 81</sup> Also, due to its status as one of the first widely available and most familiar transfection reagents, it is commonly used as a positive control for transfection in studies examining the efficiency of new gene delivery complexes.<sup>79, 82</sup>

**2.2.2.1.2.3 Other lipoplexes.** Issues with gene delivery with lipid-based systems are mostly related to efficiency of gene transduction, cytotoxicity, and the stability of the gene delivery complexes.<sup>83, 84</sup> Recent attempts to overcome these issues have included the addition of PEG to the surface of DNA-carrying liposomes with specific targeting moieties also added for increased specificity,<sup>85</sup> and the development of more “biomimetic” lipids for use in liposomes, such as phospholipids.<sup>83</sup> Other attempts at improving the performance of lipoplexes include the functionalization of cholesterol with amino acids, producing increased transfection efficiency compared to 1,2-Dioleoyloxy-3-(trimethylammonio)-propane (DOTAP), another common commercially available liposomal transfection reagent.<sup>86</sup>

### 2.2.2.1.3 Peptide-based gene delivery systems

The use of lipophilic or cationic polypeptides is another method by which DNA has been complexed for delivery to cells. The most common polypeptide for gene delivery is poly(L-lysine), as discussed previously, where its main mechanism of action is to serve as a polycationic DNA condensing agent. Much work has been done in the area of biointeractive peptides which allow targeting or specific activation of peptide-DNA complexes in specific locations, with some constructs combining these two approaches.<sup>87</sup> This ability to incorporate specifically activatable or targetable motifs into nonviral gene delivery constructs has made peptide-based gene delivery systems an exciting and attractive field of research.

**2.2.2.1.3.1 Self-condensing systems.** The ability to utilize precise synthetic techniques with a broad array of available chemistries allows interesting properties to be designed into peptide gene delivery systems. One example of this approach is the creation of a polypeptide Cys<sub>n</sub>-Trp-Lys<sub>18</sub>, where n=1-4.<sup>88</sup> The polylysine portion of this peptide serves to complex with DNA, and the cysteines spontaneously form disulfide bonds, thereby providing interpeptide crosslinks resulting in greater stability and smaller size. This system was investigated *in vitro* and resulted in significantly increased transfection compared to a noncrosslinking variety of the peptide, particularly for the peptide Cys-Trp-Lys<sub>17</sub>-Cys. An interesting aspect of these results is that this increased transfection was observed with no increased amount of reporter DNA entering the cell, suggesting that the peptides themselves had the ability to increase the efficiency of gene transfer inside the cell.<sup>88</sup> This work was later built upon by using shorter polymers containing His residues (Cys-His-Lys<sub>6</sub>-His-Cys) in order to facilitate endosomal escape.<sup>88</sup>

**2.2.2.1.3.2 Cell-penetrating systems.** Several cell-penetrating peptides have been used in fusion or complexes with cationic DNA-binding peptides to form cell-penetrating gene delivery systems. In general, cell-penetrating peptides are predominantly composed of cationic amino acids, which are thought to promote binding to the cell surface and aid in the complexation of DNA.<sup>89</sup> Many of these systems are derived from viruses, such as INF derived from influenza<sup>90, 91</sup> and the *tat* peptide derived from HIV.<sup>92, 93</sup> The INF peptide was first reported as a gene delivery mediator in 1992 as a fusion peptide with polylysine and polylysine-transferrin with positive results.<sup>91</sup> The *tat* peptide derived from HIV has been used as a gene delivery enhancing peptide on its own and in combination with other vectors and showed clear transfection advantages.<sup>93</sup> Another example of a cell-penetrating peptide is the KALA peptide, which was specifically designed for gene delivery and not derived from nature.<sup>94</sup> The KALA peptide exhibits a random coil structure at low pH, and as pH is increased to physiological, it assembles into a  $\alpha$ -helical structure. This  $\alpha$ -helical structure was used to complex DNA and showed the ability to destabilize model liposomes of anionic and neutral charge, and mediate reporter gene transfer into several cell types.<sup>94</sup>

**2.2.2.1.3.3 Targeted systems.** The concept of specific cellular targeting has been applied to gene delivery in several ways. Examples of targeted gene delivery include using the Arg-Gly-Asp (RGD) ligand as part of a DNA-complexing fusogenic peptide system<sup>95</sup> and as part of targeted polyplex systems.<sup>96, 97</sup> RGD is a commonly used ligand in drug delivery which targets  $\alpha_v\beta_3$  integrins among several others, and is generally used to target sites of angiogenesis, as these integrins are overexpressed on endothelial cells in these situations.<sup>98</sup> Another example of a targeted peptide-based system is targetable Lys-

His polypeptides, which have been functionalized with fibroblast growth factor 2 (FGF-2)<sup>99</sup> to target cells overexpressing fibroblast growth factor receptor, which is common among certain types of cancer cells.<sup>100</sup>

### **2.2.2.2 Viral vectors for gene delivery**

Studies have found that even with advances in nonviral gene delivery systems, viral vectors exhibit higher transfection efficiency with virtually no cytotoxicity.<sup>101</sup> Additionally, studies comparing many nonviral systems have shown that all of those which have good transfection efficiency also are very cytotoxic.<sup>102</sup> This trade-off in efficiency and toxicity is due to the high positive charge density required by nonviral systems to form complexes with DNA. Viral vectors take advantage of millennia of evolution to very efficiently transfect cells while keeping them alive, and with advances in genetic engineering techniques, viruses can be reprogrammed to transfect cells with genes of interest. Even with this distinct advantage of purpose-built machinery for getting foreign genetic material into cells, the application of viruses for gene therapy has resulted in disappointing few successes. These issues are primarily related to the efficacy of such treatments *in vivo*, which is attributed to several factors, including lack of long-term gene expression, low level of transfection in target cell populations, and immune clearance by the host prior to transfection.<sup>103</sup>

#### **2.2.2.2.1 Early problems with viral gene delivery**

Viral vectors have been shown to possess very high transfection efficiency *in vitro*, and are by far the most common gene delivery vectors in worldwide clinical trials;

nearly 75% of the 1714 gene therapy clinical trials underway as of March 2011 use one of many types of viral vectors to aid in gene transfer.<sup>1</sup> While viral vector-assisted delivery is the most efficient and effective method for gene delivery, the safety and immunogenicity of these vectors are concerns. The stigma surrounding gene therapy treatments, particularly those employing viral vectors, is due to a combination of unfortunate adverse events in gene therapy clinical trials and a lack of accurate reporting on these events to the general and scientific public. The first event which is commonly referenced by opponents of viral gene delivery occurred at the University of Pennsylvania, where an 18-year-old patient suffering from ornithine transcarbamylase deficiency suffered a fatal acute systemic immune response following administration of adenoviral gene therapy.<sup>104</sup> It was later revealed that the investigators committed several transgressions of protocol and procedure which led to this event, including the administration of an extremely high titer of virus on multiple occasions, and the inclusion of the patient in the trial in spite of the fact that several of his preprocedure biomarker levels should have excluded him from the study.<sup>105</sup>

Another event which caused the safety of viral vectors to be initially questioned occurred during a clinical trial for the retroviral treatment of X-linked Severe Combined Immune Deficiency (X-SCID).<sup>106, 107</sup> Initially, results were reported in the New England Journal of Medicine indicating that the gene therapy successfully treated X-SCID in the majority of patients by employing an *ex-vivo* bone marrow treatment procedure.<sup>106</sup> However, in the months following treatment, four of nine initially treated patients developed leukemia due to insertional mutagenesis caused by the retroviral treatment.<sup>107</sup> Later, the same treatment would be used in another trial for X-SCID, in which similar

events were observed and the cause of leukemia was determined to be the result of insertional mutagenesis in combination with several other genetic mutations which were required to develop the secondary disease.<sup>108</sup> The reasoning behind performing the second trial is unclear. However, the motivation could possibly have been that the specific form of leukemia which developed in the initial trial, T-cell acute lymphoblastic leukemia (T-ALL) has a cure rate of 80%. X-SCID renders the patient defenseless against all infection, and requires isolation from the external environment as protection from potential infection if bone marrow transplantation is not successful.

The 2007 passing of a patient undergoing adeno-associated virus (AAV)-mediated treatment for rheumatoid arthritis<sup>109</sup> is another event which is commonly and incorrectly referenced as a viral gene therapy adverse event. The patient had received two intra-articular injections of AAV encoding for a TNF- $\alpha$  antagonist, which are commonly given as injections of the purified antagonist (i.e., etanercept). In the weeks following the second injection, the patient experienced several systemic symptoms and passed away 3 weeks following the second administration. After extensive investigation into the cause of death in this trial, it was determined that disseminated histoplasmosis, a fungal infection, was responsible for the fatality.<sup>109</sup> While it is uncommon that this type of infection is fatal, the patient had been on immunosuppressive therapy for several years leading up to her death, and it was determined that this allowed the infection to grow to unmanageable size, resulting in “bleeding complications and multiple organ failure”.<sup>109</sup> The misrepresentation of these results as having emanated from the use of viruses to deliver gene therapy has led to misperceptions for viral gene delivery. However, the actual pathogenesis in these cases was not caused by the vectors themselves.

#### 2.2.2.2.2 Adenoviral vectors

The most common viral vector currently in gene therapy clinical trials is adenovirus, comprising 24.2% of all gene therapy clinical trials as of March 2011.<sup>1</sup> Structurally, adenoviruses are nonenveloped, with capsids composed of 240 hexon bases and 12 penton bases, and a dsDNA carrying capacity of 36-40kb.<sup>110</sup> Attached to each penton base there is a fiber protein, the knob domain of which interacts with the Coxsackievirus and Adenovirus Receptor (CAR). Additionally, there is a specialized motif in the penton base which interacts with integrin as a coreceptor, most commonly  $\alpha_v\beta_3$ .<sup>111</sup> The virus is endocytosed via clathrin-coated pits, stimulated by the integrin binding event. Following endocytosis, the decreasing pH of the endosome causes dissociation of fiber proteins from the surface of the virus, thus exposing the penton bases. The penton bases facilitate endosomal escape via a conformational change resulting in an increased exposure of hydrophobic residues,<sup>112</sup> thus allowing escape of the virus from the endosome. Endosomal escape of the virus is followed by trafficking of the viral genome via traversing microtubules and entry into the nucleus via nuclear pores, allowing gene expression.<sup>110</sup> Due to the episomal nature of the genetic material following nuclear transport, the gene expression of adenovirus is transient, and is typically gone after 1-2 weeks following initial infection.

There are many important considerations in the delivery of adenovirus-mediated gene therapy, possibly the most important of which is that there is a high prevalence of immunity to adenoviruses in the human population.<sup>110, 113</sup> This causes systemically delivered adenoviruses to be rapidly cleared or in some cases can cause a severe immune response, both of which are detrimental to the efficacy of the treatment and the latter of

which can be extremely dangerous to the patient's health. Another limitation to the use of adenoviruses in gene delivery is that adenoviruses infect nonspecifically; any cell expressing Coxsackievirus and Adenovirus Receptor (CAR) on its surface can potentially be infected by the virus and thus subject to its therapeutic effect, whatever it may be. Additionally, there are significant differences in CAR receptor density among the tissues of the body, and even among cancers of the same tissue type.<sup>114</sup> This complicates the determination of the necessary dose for therapeutic effect, along with potentially causing unforeseen consequences in nontarget tissues if they happen to express a high density of CAR receptors.

The most significant advances in cancer gene therapy have been made with adenoviral vectors, with the only two approvals worldwide being for adenovirus-mediated cancer gene therapy in China.<sup>2,3</sup> These two approved treatments both work with the p53 tumor suppressor gene, which was discussed previously.

#### 2.2.2.2.3 Retroviral vectors

Retroviral vectors, including lentiviruses, are the next most common vector for gene therapy clinical trials as of March 2011, representing 23% of trials.<sup>1</sup> Retroviruses are distinctly different from adenoviruses in that they integrate their own genome into that of the host cell, resulting in permanent expression of the viral genes. Retroviruses are enveloped viruses, meaning that the capsid is contained within a lipid vesicle which is obtained from the host during budding/cellular exit. The retroviral genome is 7-10kb single-stranded RNA, with two identical copies per virus particle. Retroviral vectors have been used to deliver the HSV-tk gene for the treatment of malignant brain tumors.<sup>115</sup>



However, the efficacy results were disappointing, with only five of fifteen patients responding, and the responders having small average tumor size when compared to the rest of the group. Further work examined the retroviral administration of a hepatoma-specific version of thymidine kinase, and was demonstrated *in vitro* to specifically sensitize hepatoma cell lines to a prodrug.<sup>116</sup> Retroviruses were also used in the X-SCID clinical trial conducted in France, which as previously discussed cured the patients of X-SCID but caused a type of curable leukemia in a significant percentage of patients.<sup>106, 107</sup>

#### 2.2.2.2.4 Adeno-associated virus vectors

Adeno-associated viruses, or AAVs, represent another heavily researched type of viral vector. AAVs are physically much smaller than most other viruses, with the virion having a typical diameter of 25 nm, and a single-stranded DNA genome of only 4.7 kb.<sup>117</sup> AAVs are also unique in that they are a helper-dependent virus, meaning that in order to effectively reproduce and infect a tissue, there must be a residing adenovirus or herpes simplex virus infection.<sup>117</sup> One major advantage to AAVs as gene delivery vectors is that in spite of high incidences of pre-existing immunity to many AAV serotypes,<sup>118</sup> cytotoxic T-cell responses to AAVs are not common following administration.<sup>110</sup> Early work on AAVs as gene delivery vectors showed high levels of prolonged gene expression in muscle tissue, with no humoral immune response to the reporter protein being expressed and only a low-level humoral response to the vector itself, allowing re-administration.<sup>119</sup> A recent example of gene therapy using AAV is the long-term expression of neuropeptide Y via AAV-mediated gene therapy.<sup>120</sup> This treatment has been shown to effectively knock down kainic acid-induced epileptic seizures in rats which have had a

viral administration to the hippocampus, and the long duration of gene expression of AAVs allows this effect to continue over long periods of time.<sup>120</sup> Another interesting application of AAVs in gene delivery is ocular delivery of AAVs for the treatment of congenital childhood blinding disorders.<sup>121</sup>

#### 2.2.2.2.5 Other viral vectors

There are many other classes of viral vectors being researched for gene delivery applications, including vaccinia virus, poxvirus, and herpes simplex virus.<sup>1</sup> These vectors have been used for very diverse applications and combined, make up almost 17% of gene therapy clinical trials.<sup>1</sup> Vaccinia virus in particular has gained a lot of recent attention as an oncolytic viral vector, with several clinical trials underway, including a recombinant vaccinia virus encoding for GM-CSF.<sup>122</sup> Exciting efficacy data were gathered from several Phase I and Phase II trials, with response rates up to 75% observed particularly in melanoma,<sup>122</sup> and a large Phase II study of this treatment for first-line treatment of refractory hepatocellular carcinoma is currently recruiting.<sup>123</sup>

#### 2.2.2.3 Delivery of vectors and naked DNA

There is a diverse selection of tools available for the delivery and expression of genetic material in cells and tissues. These range from directly mechanical methods which physically force new genetic material into target cells, biological approaches which employ microorganisms or cellular receptors to deliver gene products into cells, and chemical methods designed to mask or target the gene products from the body's defenses. In addition to these types of systems, there are numerous cross-over or hybrid

methods using two or more of these basic types of approaches to generate a more efficacious gene delivery device.

#### 2.2.2.3.1 Physical methods

**2.2.2.3.1.1 Gene gun.** Developed in the 1980s, the gene gun represents an example of using direct mechanical force to introduce foreign gene products into a population of target cells.<sup>124</sup> The earliest designs of the gene gun employed 1-4 $\mu$ m tungsten pellets coated with the DNA of interest, which were loaded into an air pistol and projected at a colony of cells in a petri dish. Following designs used a .22 caliber charge to shoot quite literally a bullet, with the microparticles deposited on the end of the bullet and thus launched with high velocity at the target.<sup>125, 126</sup> The bullet would be stopped by a disk of Lexan placed at the end of the barrel, and the particles would be projected towards the cells of interest at 1000-2000 feet per second. Since that initial design, the gene gun has evolved into a more refined tool, however still based on the forcible projection of heavy metal particles coated with plasmid DNA into target cells. Current versions of the gene gun are distributed by Biorad and use a helium pulse to project gold microparticles coated with genetic material.<sup>127, 128</sup>

The gene gun has shown good efficacy in transfecting plant cells<sup>129</sup> and has been a very common method for this purpose since the 1990s.<sup>130-134</sup> Predictably, however, the gene gun's hopes for use as a therapeutic delivery device in animals are jeopardized by the tendency of a certain population of cells within the target area to be immediately destroyed by the impact of the metallic particles, and the limited depth to which the DNA

will be delivered by the gun. It is, however, useful for research purposes when applied to animals as it provides rapid and localized gene expression.<sup>135, 136</sup>

**2.2.2.3.1.2 Electroporation.** Electroporation for gene transfer, first reported in 1982 by Neumann, et al.,<sup>137</sup> uses pulsed electric fields to temporarily and nonlethally disrupt the membranes of cells to allow the passage of materials into the interior of the cells. This method works on the principle that, by charging a cell to the point where its capacitance is exceeded, the cell membrane will open pores and thereby allow the electrophoretic delivery of DNA, which will move in a predictable manner in the electric field. The extent, duration, and location of the permeabilization can be controlled precisely by changing the orientation and amplitude of the electrical current, and by using a pulsed electric field as opposed to a constant one.<sup>138</sup> One example of this type of control is that small structures, i.e., organelles, require higher amplitudes of electrical field to cause permeabilization. Unfortunately, the levels of applied electric field required to electroporate organelles would cause damaging or lethal levels of poration to occur in the cell membrane. This problem was solved using nanosecond pulses of amplitude sufficient to open the membranes of the organelles, but due to the considerably higher charging time required to open the cell membrane than the organelles, the nanosecond pulses do not disrupt the cell as a whole.<sup>139</sup>

Electroporation is a highly efficient method of delivering material into cells, particularly DNA, as it moves in electric field and therefore can be delivered much more rapidly than materials requiring diffusion to enter the cells. This short time required to deliver the genes of interest reduces the risk of damage to the cells by the applied electric

field. Current and historical clinical progress in the use of electroporation to aid in the delivery of tumor chemotherapy is reviewed extensively elsewhere.<sup>140</sup>

**2.2.2.3.1.3 Hydrostatic pressure-driven gene delivery.** Another physical method used to assist in the delivery of gene therapy is to simply cause an increase in the local hydrostatic pressure in the area of interest, which essentially forces small molecules into cells and the interstitium. There are several methods by which this increase in hydrostatic pressure has been achieved, including the delivery of an extremely large volume dose of pDNA (approximately equal to blood volume) by tail vein injection in mice,<sup>141</sup> and the clamping of blood vessels to cause the necessary increase in pressure to increase transfection.<sup>142</sup> There are obvious limitations to this method's utility in humans, particularly the large-dose method, as an increase in blood volume of that magnitude would likely cause rupture of any number of blood vessels throughout the body, in addition to heavily straining the kidneys.

#### 2.2.2.3.2 Depot release methods

In order to minimize potentially harmful effects and to make gene delivery a more viable clinical option, there has been a large quantity of research into how to make the administration of viral and nonviral vectors safer and more effective. Each of these approaches has specific advantages and limitations, and for each individual application, there is likely one approach which will produce the best results. The main advantage to these methods is that, with proper design considerations, these materials can very precisely control the release of a wide range of materials to a highly localized area with minimal escape of the therapeutic agent, and thus a reduced chance of treatment-

associated side effects. This makes these methods an attractive option for situations in which highly localized delivery is desired, such as the treatment of solid tumors or single-organ diseases.

**2.2.2.3.2.1 Matrix-mediated gene delivery.** Matrix-mediated gene delivery (MMGD) is the use of a depot which interacts directly with the gene carrier, be it a virus, polyplex, liposome, etc., with the goal of control over spatial and temporal gene delivery. A general schematic of various approaches to MMGD is shown in Figure 2.2. The most common approaches for this purpose are to either tether the carriers to a material for localized expression,<sup>143-146</sup> complex the carriers with a secondary material,<sup>147-149</sup> or place the carrier in a matrix to control spatial and temporal release.<sup>150-157</sup> Materials designed for matrix-mediated gene delivery are most commonly either entirely synthetic or natural polymers which have been modified in some way to interact with the pDNA complex or viral vector being delivered. One example of this approach is the use of poly(amido amine) (PAMAM) dendrimers complexed with DNA, delivered from a collagen scaffold, for *in vitro* transfection.<sup>158</sup> Other materials which have been used include collagen modified with avidin,<sup>145</sup> polylysine-biotin and poly(ethylenimine)-biotin complexes,<sup>159</sup> hyaluronic acid-collagen hydrogels,<sup>160</sup> and functionally terminated self-assembled monolayers.<sup>144</sup> Antivirus antibodies are also commonly used to tether viral vector particles to biomaterial surfaces for enhanced control of gene expression.<sup>143, 146</sup>

**2.2.2.3.2.2 Polymers for matrix-mediated gene delivery.** Far more common and widely used are the polymeric gene delivery scaffolds, which usually employ simple diffusion sometimes in combination with enzymatic degradation to release either naked DNA, viral vectors, or nonviral complexes with nucleic acids. Natural polymers are

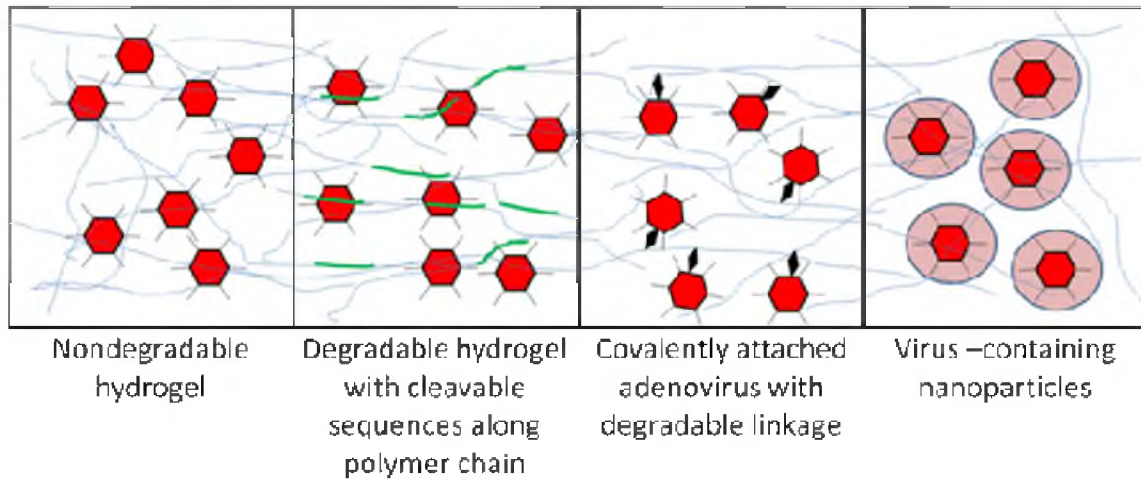


Figure 2.2: Types of matrix-mediated viral gene delivery

widely used in this type of application, as they tend to limit the immune response to the material *in vivo*. One common natural material is collagen that has been used for delivery of viral vectors,<sup>153, 161</sup> naked plasmid,<sup>162-166</sup> and nonviral vectors.<sup>167</sup> Modifications of collagen are also used for delivery of various vectors and plasmid DNA.<sup>168-170</sup> Fibrin is also used for matrix-mediated gene delivery<sup>150, 152, 171, 172</sup> and is especially useful for wound healing applications as it is a natural component of the clotting cascade in addition to having a pore structure conducive to controlled-release.

Several different synthetic polymers are also used for polymeric gene delivery. One example is PLGA microspheres<sup>151, 173</sup> designed as a potential delivery system for the treatment of brain tumors. By encapsulating the adenoviral vectors in PLGA, the viral vector was less recognizable by the local immune cells, thus allowing for more than one administration of the treatment and greater efficiency. PLGA has also been used as a stationary depot for plasmid DNA release.<sup>174</sup> Another example of synthetic polymers in polymeric gene delivery is a thermosensitive triblock copolymer of PEG-PLGA-PEG<sup>175,</sup><sup>176</sup> which was used to deliver a TGF- $\beta$ 1 encoding gene directly to a wound site. Photocrosslinked PEG hydrogels have also been used to encapsulate and release DNA in a controlled manner,<sup>156, 177</sup> as have PLGA scaffolds.<sup>178</sup>

Polymeric delivery systems possess the ability to relatively easily control release of gene products because there are a limited number of factors influencing release from this type of material. The types of materials used to make these matrices are not limited to only those which DNA or vectors can be attached to, widening the range of matrices which can be designed. This reduces the risk of unforeseen interactions and side effects and increases the chances of an effective treatment. Polymeric delivery systems can also



be designed to be mechanically and environmentally sensitive, enabling a release trigger to be incorporated which is independent of chemical reaction or enzyme activity and their associated design constraints. By simplifying the design in this way, release can be controlled tightly via many parameters, for example degradation, temperature-dependent self-assembly/disassembly, and porosity among many other possibilities, without the need for specific biological conditions to be present.

## **2.3 Head and neck squamous cell carcinoma: Disease and implications of matrix-metalloproteases (MMPs)**

### 2.3.1 Introduction

Head and neck cancer is described as any epithelial cancer which occurs in the sinuses, nose, mouth, pharynx, or larynx, most of which are head and neck squamous cell carcinomas (HNSCCs).<sup>179</sup> There are an estimated 350,000 new cases of HNSCC (including laryngeal cancer) diagnosed worldwide, comprising about 3% of all new cancer cases.<sup>180</sup> In the United States, it is estimated to be the sixth most common new cancer diagnosis in 2011 with 52,140 new cases, and resulting in 11,460 deaths.<sup>181</sup> The primary risk factors for HNSCC are alcohol and tobacco consumption,<sup>182-185</sup> which have a multiplicative combined effect, in addition to family history<sup>186, 187</sup> and environmental factors. A relatively recently discovered and significant risk factor for HNSCC has been identified as human papilloma virus (HPV) infection, specifically with HPV type 16,<sup>188-190</sup> the same HPV type which is commonly implicated in cervical cancer<sup>191-193</sup> and the vaccine for which is considered a great success and is now commonly administered.<sup>191, 194, 195</sup> While the incidence and fatality rates of HNSCC are not as significant as more

common cancers, HNSCC presents a challenging problem for clinicians, with many factors to consider before a treatment is decided upon. Much of this complication is due to the site of the disease, as the clinician must consider factors beyond just the elimination of the cancer, including preservation of the patient's ability to swallow, breathe, and speak normally. Further, the location of these cancers is a socially sensitive area: it has been shown that permanent scarring or disfigurement to a patient's face significantly increases their risk for depression and anxiety disorders.<sup>196</sup>

### 2.3.2 Current treatment options for HNSCC

#### **2.3.2.1 Surgery**

Cases of HNSCC in which the tumor is considered resectable are most commonly treated surgically. The resectability of a tumor is determined by the surgeon performing the procedure. However, in general, a tumor is considered unresectable if it involves invasion of the carotid artery, the base of the skull, or the prevertebral musculature.<sup>179</sup> While surgery is the current standard of care, it is common for some tumors which would normally be considered resectable to be treated with other approaches if they involve an organ which is particularly sensitive to surgical intervention. Examples of this would be disease significantly involving the larynx (voice loss) or pharynx (swallowing loss).<sup>197</sup>

#### **2.3.2.2 Radiation therapy**

Radiation therapy is a very common postsurgical adjuvant treatment option as well as a primary treatment option in patients in which surgery is not possible or not the best option due to side effects and organ preservation concerns.<sup>179</sup> Standard radiotherapy

techniques for the management of HNSCC involve once daily dosing in a 5 day on, 2 day off arrangement. However, research and meta-analysis has shown that there is significant benefit to altered fractionation approaches, which are given 7 days per week either once daily in the normal daily dose or twice daily in half-doses<sup>179, 197-199</sup> with the general trend being that administering more frequently results in greater management and survival outcomes. It is likely that this is due to recovery of the cancer cells during the rest periods, allowing establishment of greater populations of cells which are less sensitive to the radiotherapy. Another improved form of radiotherapy is called intensity modulated radiation therapy (IMRT), and is essentially a more focused and localized approach to radiotherapy which involves image-guided administration of radiation to improve efficacy and reduce damage to surrounding tissue structures.<sup>179, 197</sup>

### **2.3.2.3 Chemoradiotherapy**

The combination of chemotherapy and radiation therapy has proven to be an effective treatment modality for HNSCC patients, and concomitant chemoradiotherapy has emerged as the most preferred treatment in patients with unresectable tumors. Concomitant chemo and radiation therapy exhibits significant survival and localized control benefit over radiotherapy alone, chemotherapy alone, or induction chemotherapy, in which chemo is administered prior to radiation.<sup>179, 200-202</sup> Cisplatin and derivatives are the most common chemotherapeutic agents to be delivered with radiotherapy, and have been successfully used in combination with radiotherapy for other types of cancer.<sup>203-205</sup>

#### **2.3.2.4 Other approaches**

In addition to traditional treatment approaches for HNSCC such as surgery, radiotherapy, chemotherapy, and combinations thereof, there has been significant research into advanced therapies which specifically target the tumor. One common target for HNSCC is the epithelial growth factor receptor, which has been shown to be overexpressed in many cases of HNSCC.<sup>206, 207</sup> Examples of drugs which have been developed to target EGFR are Cetuximab, Gefitinib, Erlotinib, and Lapatinib.<sup>197</sup> Another notable advance in the management of HNSCC was the approval of two adenovirus-mediated therapies for HNSCC, both of which target the p53 gene and were discussed previously.<sup>2,3</sup>

### 2.3.3 MMPs and their role in HNSCC

#### **2.3.3.1 Overview of MMPs**

Matrix metalloproteases, or MMPs, are a family of structurally related endopeptidases, which exist in a dynamic balance with tissue inhibitors of metalloproteases (TIMPs) to control myriad biological functions requiring ECM degradation. Proper function and regulation of MMPs is responsible for diverse biological functions such as angiogenesis, embryonic development, and wound healing. The major structural features of MMPs include the signal domain, the propeptide, the catalytic domain, and the hemopexin domain. The propeptide domain is characterized by the highly conserved “cysteine switch” motif, PRCGXPD, which is responsible for the suppression of the activity of the MMP proenzyme, while the catalytic domain has a characteristic HEXGHXXGXXH motif, which binds a  $Zn^{2+}$  ion and serves as the active

site for protein cleavage.<sup>208, 209</sup> There are over 20 known specific MMPs, divided into subgroups based on their additional domains and known biological functions. The main classes of MMPs are collagenases, gelatinases, stromelysins, matrilysins, membrane-type MMPs, and other unclassified MMPs.<sup>210</sup> Table 2.1 shows a summary of the known functions of MMPs of each type.<sup>210</sup> Collagenases (MMP-1, -8, -13, and -18) are generally known to cleave interstitial collagen types I, II, and III, and structurally are composed of the four basic domains: signal, propeptide, catalytic, and hemopexin, with no further modifications. The gelatinases, MMP-2 and MMP-9, are unique from other MMPs in that they have three fibronectin type II repeats in their catalytic domain structure which mediate binding to various ECM proteins including gelatin, collagen, and laminin.<sup>208, 210</sup> MMPs -2 and -9 are important for various normal biological functions, but are also commonly implicated in the escape and formation of metastases in many tumor types, including HNSCC.<sup>202, 208, 211</sup> Stromelysins, the third class of MMPs, have similar structures to the collagenases and perform standard ECM-degradative processes, but are additionally involved in the activation of the proenzymes for other MMPs.<sup>208, 210</sup> The stromelysins are composed of MMPs -3, -10, and -11. The matrilysins are a unique group of MMPs (MMP-7 and MMP-26) which lack the hemopexin domain. MMP-7 digests a variety of ECM molecules. However, it is also responsible for interaction and activation of several cell-surface proteins.<sup>208, 210</sup> MMP-26 is expressed at the highest levels in endometrial tissue with particularly high expression in endometrial cancer and other epithelial cancer cell lines. However, its exact function has yet to be elucidated.<sup>208, 212</sup> The membrane-type MMPs are further subclassified based on their attachment to the cell surface, with four being transmembrane proteins (MMP-14, -15, -16, and -24), and two

Table 2.1

Known human MMPs and their biological substrates<sup>210</sup>

Enzyme	MMP	ECM Substrates	Other Substrates
Interstitial collagenase; Collagenase 1	MMP-1	Collagens (type I, II, III, VII, VIII, X, and XI), gelatin, fibronectin, vitronectin, laminin, entactin, tenascin, aggrecan, link protein, myelin basic protein, versican	Autolytic, C1q, $\alpha$ 2-Macroglobulin, ovostatin, $\alpha$ 1-PI, $\alpha$ 1-antichymotrypsin, IL1- $\beta$ , proTNF $\alpha$ , IGFBP-2, IGFBP-3, casein, serum amyloid A, proMMP-1, proMMP-2, proMMP-9
Neutrophil collagenase; Collagenase 2	MMP-8	Collagens (type I, II, and III), aggrecan	Autolytic, C1q, $\alpha$ 2-Macroglobulin, ovostatin, $\alpha$ 1-PI, substance P, fibrinogen, angiotensin I, angiotensin II, bradykinin, plasmin C1-inhibitor
Collagenase 3	MMP-13	Collagens (type I, II, III, IV, VI, IX, X, and XIV), collagen telopeptides, gelatin, fibronectin, SPARC, aggrecan, perlecan, large tenascin-C	Autolytic, C1q, $\alpha$ 2-Macroglobulin, casein, fibrinogen, factor XII, $\alpha$ 1-antichymotrypsin, proMMP-9
Gelatinase A	MMP-2	Collagens (type I, II, III, IV, V, VII, X, and XI), gelatin, elastin, fibronectin, vitronectin, laminin, entactin, tenascin, SPARC, aggrecan, link protein, galectin-3, versican, decorin, myelin basic protein	Autolytic, $\alpha$ 1-PI, $\alpha$ 2-Macroglobulin, $\alpha$ 1-antichymotrypsin, IL1- $\beta$ , proTNF $\alpha$ , IGFBP-3, IGFBP-5, substance P, serum amyloid A, proMMP-1, proMMP-2, proMMP-9, proMMP-13, latent TGF $\beta$ , MCP-3 (monocyte chemoattractant protein-3), FGFR1 (fibroblast growth factor receptor 1), big endothelin-1, plasminogen
Gelatinase B	MMP-9	Collagens (type IV, V, XI, and XIV), gelatin, elastin, vitronectin, laminin, SPARC, aggrecan, link protein, galectin-, versican, decorin, myelin basic protein	Autolytic, $\alpha$ 2-Macroglobulin, ovostatin, $\alpha$ 1-PI, IL1- $\beta$ , proTNF $\alpha$ , substance P, casein, carboxymethylated transferrin, angiotensin I, angiotensin II, plasminogen, proTGF $\beta$ 29, IL-2R $\alpha$ 13, release of VEGF

Table 2.1 (Continued)

Enzyme	MMP	ECM Substrates	Other Substrates
Stromelysin-1	MMP-3	Collagens (type III, IV, V, VII, IX, X, and XI), collagen telopeptides, gelatin, elastin, fibronectin, vitronectin, laminin, entactin, tenascin, SPARC, aggrecan, link protein, decorin, myelin basic protein, perlecan, versican, fibulin	Autolytic, $\alpha$ 2-Macroglobulin, ovostatin, $\alpha$ 1-PI, $\alpha$ 2antiplasmin, $\alpha$ 1-antichymotrypsin, IL1- $\beta$ , proTNF $\alpha$ , IGFBP-3, substance P, T-kininogen, casein, carboxymethylated transferrin, antithrombin-III, serum amyloid A, fibrinogen, plasminogen, osteopontin, proMMP-1, proMMP-3, proMMP-7, proMMP-8, proMMP-9, proMMP-13, IGFBP-3, E-cadherin, pro-HB-EGF, u-PA, fibrin, PAI-1
Stromelysin-2	MMP-10	Collagens (type III, IV, and V), gelatin, elastin, fibronectin, aggrecan, link protein,	Autolytic, casein, proMMP-1, proMMP-7, proMMP-8, proMMP-9
Stromelysin-3	MMP-11	gelatin, fibronectin, collagen type IV, laminin	$\alpha$ 1-PI, $\alpha$ 2-Macroglobulin, ovostatin, IGFBP-1, casein, $\alpha$ 2-antiplasmin, plasminogen activator inhibitor-2, casein, carboxymethylated-transferrin
Matrilysin-1, PUMP-1	MMP-7	Collagens (type I, and IV), gelatin, elastin, fibronectin, vitronectin, laminin, entactin, tenascin, SPARC, aggrecan, link protein, decorin, myelin basic protein, fibulin, versican,	Autolytic, $\alpha$ 1-PI, $\alpha$ 2-Macroglobulin, proTNF $\alpha$ , casein, carboxymethylated transferrin, osteopontin18, proMMP-1, proMMP-2, pro-MMP-7 proMMP-9, plasminogen,
Matrilysin-2	MMP-26	Collagen type IV $\pm$ , gelatin, fibronectin, vitronectin	$\alpha$ 1-PI, $\alpha$ 2-Macroglobulin, fibrinogen, proMMP-9
MT-1MMP	MMP-14	Collagens (type I, II, and III), gelatin, fibronectin, tenascin, vitronectin, laminin, entactin, aggrecan, perlecan	$\alpha$ 2-Macroglobulin, ovostatin, $\alpha$ 1-PI, proTNF- $\alpha$ fibrinogen, factor XI, fibrin, CD44, tissue transglutaminase, proMMP-2, proMMP-13

Table 2.1 (Continued)

Enzyme	MMP	ECM Substrates	Other Substrates
MT2-MMP	MMP-15	Fibronectin, tenascin, entactin, laminin, aggrecan, perlecan	ProTNF $\alpha$ , tissue transglutaminase, proMMP-2
MT3-MMP	MMP-16	Collagen type III, gelatin, fibronectin, vitronectin, laminin	$\alpha$ 1-PI, $\alpha$ 2-Macroglobulin, casein, proMMP-2, tissue transglutaminase
MT5-MMP	MMP-24	Fibronectin, gelatin, chondroitin sulphate proteoglycan, dermatan sulphate proteoglycan	ProMMP-2, tissue transglutaminase
MT4-MMP	MMP-17	gelatin	Fibrinogen, fibrin, proTNF $\alpha$ , proMMP-2 $\pm$
MT6-MMP	MMP-25	Collagen type IV, gelatin, fibronectin, chondroitin sulphate proteoglycan, dermatan sulphate proteoglycan	Fibrinogen, fibrin, $\alpha$ 1-PI, proMMP-2
Macrophage Elastase	MMP-12	Collagens (type I, V, and IV), gelatin, elastin, fibronectin, vitronectin, laminin, entactin, osteonectin <sup>46</sup> , aggrecan, myelin basic protein	$\alpha$ 2-Macroglobulin, $\alpha$ 1-PI, proTNF $\alpha$ , fibrinogen, factor XI, casein, plasminogen
	MMP-19	Collagen type IV, gelatin, laminin, entactin, Ig tenascin-C, fibronectin, aggrecan, COMP	Autolysis, fibrinogen, fibrin
Enamelysin	MMP-20	Amelogenin, aggrecan, COMP	Autolysis
CA-MMP	MMP-23	gelatin	Autolysis, casein
Epilysin	MMP-28		Casein



being attached via glycosylphosphatidylinositol (GPI) (MMPs -17 and -25).<sup>210</sup> All membrane-type MMPs except MMP-17 can activate pro-MMP2, and all membrane type MMPs can act on ECM proteins. Structurally, the membrane-type MMPs differ from the other soluble MMP groups due to their transmembrane domain or GPI anchor domains, but still have the highly conserved catalytic site, propeptide, and hemopexin region.<sup>208, 210</sup>

### **2.3.3.2 MMP-2 and MMP-9: Function in cancer**

MMPs -2 and -9 are known as gelatinase type A and B, respectively, due to their known ability to degrade gelatin (denatured collagen). MMP-2 is also known as 72-kDa type IV collagenase, and MMP-9 as 92-kDa type IV collagenase, due to their expression as 72-kDa and 92-kDa pro-enzymes, respectively. Structurally, MMPs -2 and -9 are composed of the standard conserved MMP-domains: signal, propeptide, catalytic domain, and hemopexin domain, but differ from other MMPs in that their catalytic domains contain three repeats of the fibronectin type II domain, which is implicated in collagen binding.<sup>213</sup>

Activation of proMMP-2 can occur by several different mechanisms, but most commonly, proMMP-2 is activated by other surface bound MMPs.<sup>210</sup> MT1-MMP, also known as MMP-14, is often implicated in the activation of proMMP-2 via a well-studied and characterized mechanism requiring the binding of TIMP-2 to proMMP-2, followed by the activation of proMMP-2 by MMP-14 which has not bound TIMP-2.<sup>214</sup> Interestingly, it has also been shown that if MMP-14 is bound to TIMP-2, this complex can bind proMMP-2 which is subsequently activated by a nearby MMP-14 which has not bound TIMP-2.<sup>215</sup> The functional activation of MMP-2 by MMP-14 is important to the

role of MMP-14 in cancer and has led to research investigating the inhibition of MMP-14 as a potential therapeutic approach.<sup>202</sup> ProMMP-9 has been shown to be activated by MMP-3<sup>216</sup> or by bacterial proteases.<sup>217</sup> Interestingly, proMMP-9 can also be activated by active MMP-2, and this activation is inhibited by TIMP-1 and TIMP-2.<sup>218</sup>

In normal situations, MMPs -2 and -9 contribute to many processes involving cell migration and signaling, for example, angiogenesis<sup>219, 220</sup> and inflammation/innate immunity.<sup>221, 222</sup> In the context of cancer, the role of MMP-2 and MMP-9 are primarily implicated in angiogenesis, with many of the *in vitro* studies suggesting a link between MMP-2, MMP-9, and cellular invasion not holding up *in vivo*.<sup>223</sup> MMP-9 contributes to cancer angiogenesis by liberation of VEGF from the extracellular matrix,<sup>224</sup> and by processing of the VEGF-A isoform, removing the domains responsible for ECM association and therefore increasing bioavailability.<sup>225</sup> Further, MMP-9 has been shown to be involved in the maturation of neovasculature by a mechanism related to pericyte recruitment.<sup>226</sup> MMP-9 is also involved in the liberation of hematopoietic cells from the stem cell niche and incorporation of these bone marrow derived cells into the tumor vasculature.<sup>227, 228</sup> MMP-2 has been shown to have a strong effect on angiogenesis by its interaction with intratumoral  $\alpha_v\beta_3$  integrin, enabling endothelial cell migration.<sup>229</sup> This effect has been further shown in a study which specifically disrupted the  $\alpha_v\beta_3$ -MMP-2 interaction, in which angiogenesis was significantly diminished.<sup>230</sup> Overall, studies which genetically or chemically inhibit the activities of MMP-2 and MMP-9 show significantly reduced angiogenesis, highlighting their importance in this vital cancer development process.

These results are additionally supported by the work of Stokes et al., who carefully and extensively mapped MMP-2 and MMP-9 levels, along with all other known MMPs and many other proteases, in excised HNSCC tissue and subsequently correlated these findings with disease state.<sup>231</sup> Specifically, MMP expression levels for inside the tumor, at the tumor margin, and in adjacent healthy tissues were compared, with expression levels in healthy nonadjacent tissues serving as a control. This study revealed many important findings: 1) both MMP-2 and MMP-9 are significantly overexpressed in and around primary HNSCC tumors compared to normal healthy tissues; 2) MMP-3 (an activator of MMP-9), MMP-14 (an activator of MMP-2), and TIMP-2 (a necessary cofactor for MMP-14-mediated activation of proMMP-2) were additionally found at high levels in and around tumors; 3) MMP-2 mRNA levels decreased with increasing tumor grade; and 4) MMP-9 levels decreased significantly in the primary tumor with the appearance of lymph node metastasis.<sup>231</sup> There are several important conclusions which can be drawn from these findings. First of all, the increased presence of MMP-2 and MMP-9 in primary tumors justifies the use of these proteases as activating enzymes for a therapeutic treatment. The increase in MMP-3, MMP-14, and TIMP-2 levels further supports this strategy, as this increases the likelihood of proMMP-9 and proMMP-2 activation. The decrease in MMP-2 and MMP-9 expression as the tumor progresses does diminish their utility as an activator for treatment of advancing disease; however, the expression levels do not return to normal as long as the tumor is present.

## 2.4 Genetically engineered protein polymers: Overview

### 2.4.1 Introduction

Genetically engineered polymers are materials which are encoded by DNA, synthesized in living microorganisms or cells, and are composed of block repeats. Original descriptions of genetically engineered polymers were first published in 1990.<sup>232, 233</sup> Since these initial works, several researchers have explored the benefits of programming microorganisms to produce polymers.<sup>234-237</sup> The most significant benefit to this method is the high degree of control over the polymer sequence, block arrangement, and length which are determined by the DNA sequence. With further advances in the area of noncanonical amino acids, it has become possible to genetically synthesize polymers with functional groups not found on natural amino acids, opening the field up to creating materials which were never before possible.<sup>238</sup> Further, upon completion of the DNA encoding for the desired material, it can be produced at any scale starting with a single clone of the original DNA. Advances in purification and bioprocessing procedures have streamlined the production of these materials. With the promise of this field of research, novel approaches of delivering bioactive agents employing genetically engineered polymers are emerging and have been reviewed extensively.<sup>48, 234, 235, 239-245</sup>

### 2.4.2 Cloning and synthetic strategies for genetically engineered polymers

Broadly, the creation of the necessary genetic material to produce a genetically engineered protein-based polymer requires the following progression: The creation of a monomer gene, encoding for a single repeat of the desired material, followed by the “polymerization” of this monomer gene to produce a large piece of DNA encoding for

the entire polymer. Depending on the synthetic strategy, the polymerization occurs in an expression vector,<sup>232</sup> or the “polymer gene” is digested out of a cloning vector and ligated into an expression vector,<sup>246</sup> which is transformed into a production organism and grown to high density. Protein production is induced during this growth. Purification of the newly synthesized protein can occur by various methods, but commonly by affinity chromatography or specific phase transitioning at a small laboratory scale. The culture expansion and protein purification procedures are usually system-specific, but the polymer gene synthesis is done by one of three methods: random concatamerization,<sup>232</sup> recursive directional ligation,<sup>246</sup> or overlap extension rolling circle amplification (OERCA).<sup>247</sup>

#### **2.4.2.1 Random concatamerization**

The synthesis of polymer genes by random concatamerization is the earliest synthesis method reported,<sup>248</sup> and is outlined in Figure 2.3. The design of a synthetic strategy for this type of approach involves the insertion of complimentary, nonpalindromic restriction sites at each end of the desired monomer, typically designed into the original oligonucleotide synthesis. This monomer is then inserted into a high-copy cloning vector, scaled up in *E.coli*, purified at high concentration, and digested out of the cloning vector using a single restriction enzyme. The resulting monomer genes are purified from the vector DNA via preparative agarose gel electrophoresis followed by gel extraction of the monomer gene fragment. The monomer gene population is then ligated in a high ratio with purified expression vector which has been linearized with a restriction

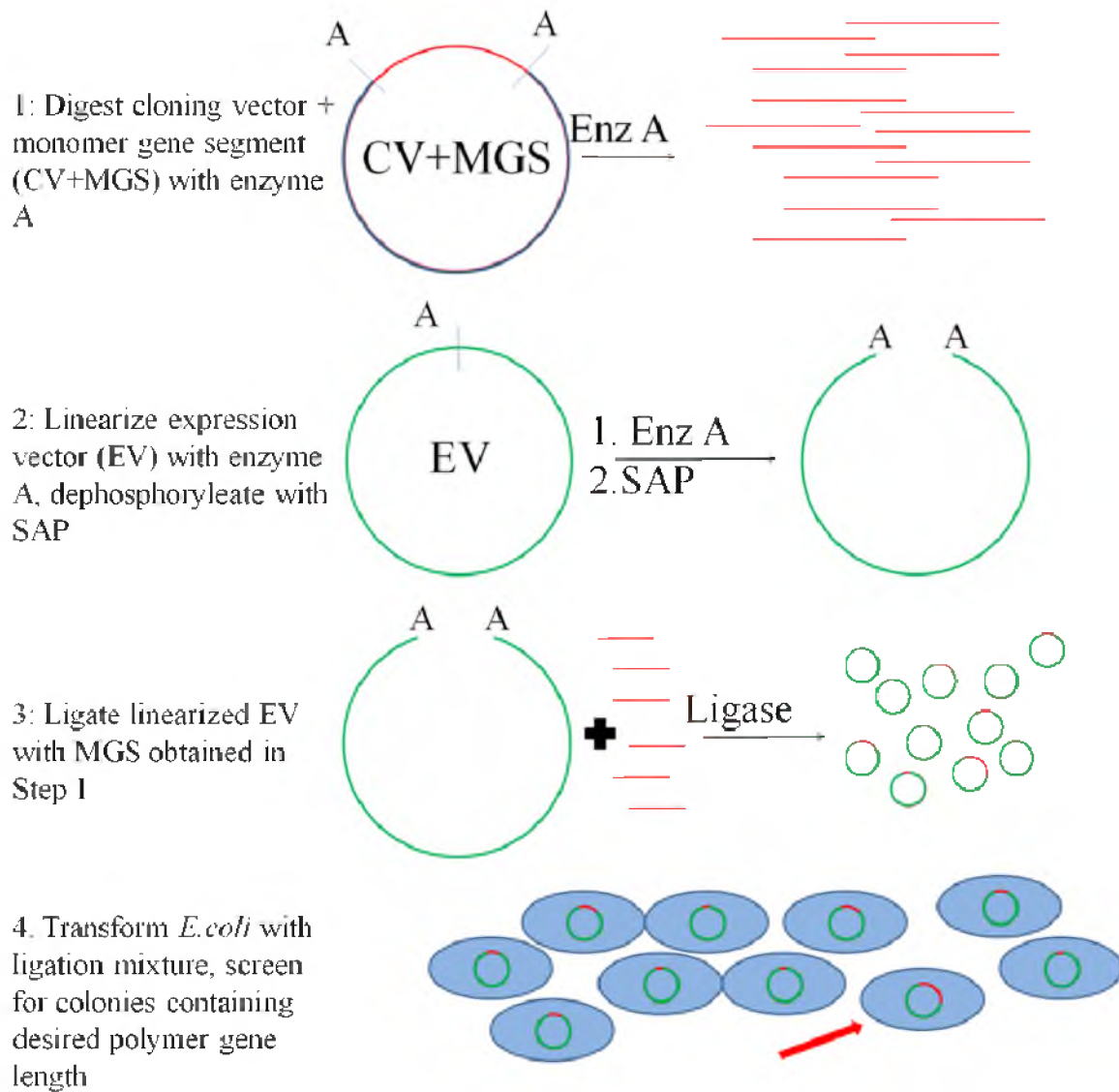


Figure 2.3: Random concatamerization (adapted from<sup>248</sup>)

enzyme which produces ends compatible with the monomers, and has been dephosphorylated to eliminate autoligation and recircularization. The ligation reaction is used to transform *E.coli* and the transformed bacteria are plated on selective medium. Following ample time for growth, single colonies are selected and must be screened for the length of polymer which they contain. This method is advantageous in that it is not difficult to design and implement, and may produce the desired polymer length rapidly. The disadvantages of this method become evident when large monomers are used to form large polymers, as the probability of the desired polymer lengths forming is quite low and can require months of colony screening to obtain the desired polymer.

#### **2.4.2.2 Recursive directional ligation**

Recursive directional ligation (RDL) is a process which was developed to produce an entire library of polymer lengths for a given system and employs a stepwise approach, adding one monomer at a time.<sup>246</sup> A schematic of this approach is shown in Figure 2.4. In this approach, oligonucleotides are designed with two different enzyme specificities at their sticky ends, but with the two sticky ends compatible. The monomer is ligated into a cloning vector and expanded as in random concatamerization. For multimerization, the monomer is digested out of the cloning vector with a double digest, for example, Enzyme A and Enzyme B. A separate population of vector containing monomer is digested by Enzyme A only, dephosphorylated, and the monomer population from the double digest is ligated to the Enzyme A-linearized vector. This yields a dimer at this step, which is then used at subsequent steps to add one more monomer per step until a polymer of desired length is reached. Appropriate selection of enzymes and recognition sites is

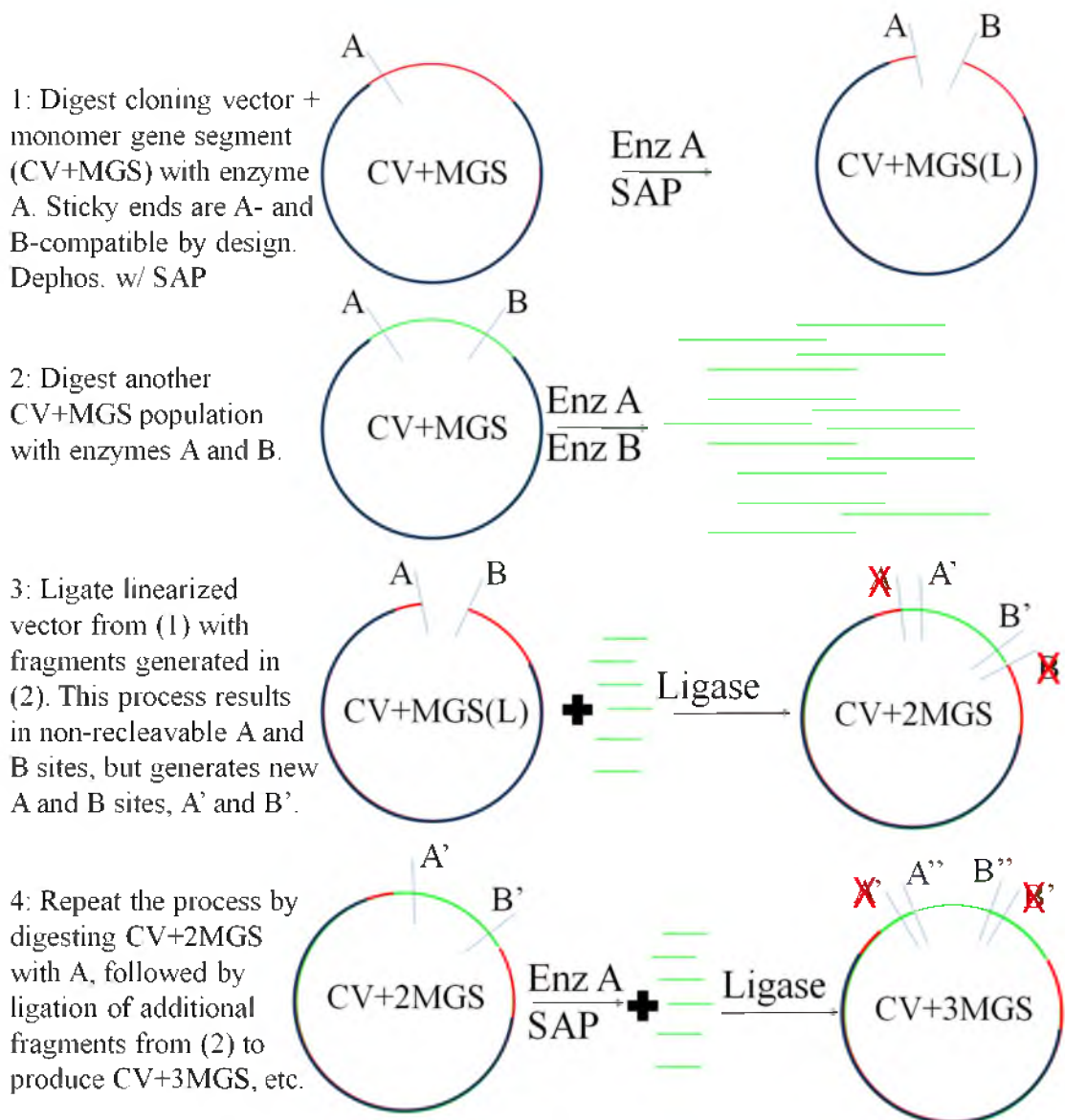


Figure 2.4: Recursive directional ligation (adapted from<sup>246</sup>)



essential to the success of this approach. The specific strategy published previously employed a creative approach in which two enzymes were used that recognize distant sequences, and cut degenerate bases downstream.<sup>246</sup> Specifically, BglI and PflMI were used. BglI has a recognition and cut sequence of GCCNNNN<sup>^</sup>NGGC, where the underlined portion represents the recognition site, ^ represents the top strand cut site, N can represent any nucleotide, and PflMI has a recognition/cut sequence of CCANNNN<sup>^</sup>NTGG. By designing the degenerate sites to be compatible with one another, it allows specific cutting of only one end of the monomer, with the same sticky end resulting. The overhang was “GGC” for the top strand (5’-3’) and “CCG” for the bottom strand (3’-5’). One monomer insert per step is encouraged statistically by ligating the monomers and vectors in a low molar ratio (1:1-1:5). Once the desired polymer length is achieved, the polymer gene is transferred to an appropriate expression plasmid, transformed into an expression cell line, and scaled up. Purification and downstream processing following RDL is protein and expression system specific.

#### **2.4.2.3 Overlap Extension Rolling Circle Amplification (OERCA)**

OERCA represents a new approach to the one-step synthesis of an entire library of polymer gene lengths, which combines the precision of RDL with the convenience and speed of random concatamerization.<sup>247</sup> This method is depicted in Figure 2.5. The general approach of OERCA is that the initial template is a single-stranded circular DNA, which encodes for the desired monomer gene. Primers directed at the 3’ and 5’ ends of the monomer are reacted with the template circle in PCR. During the first step of this reaction, the polymerase synthesizes several different lengths of the polymer by rolling

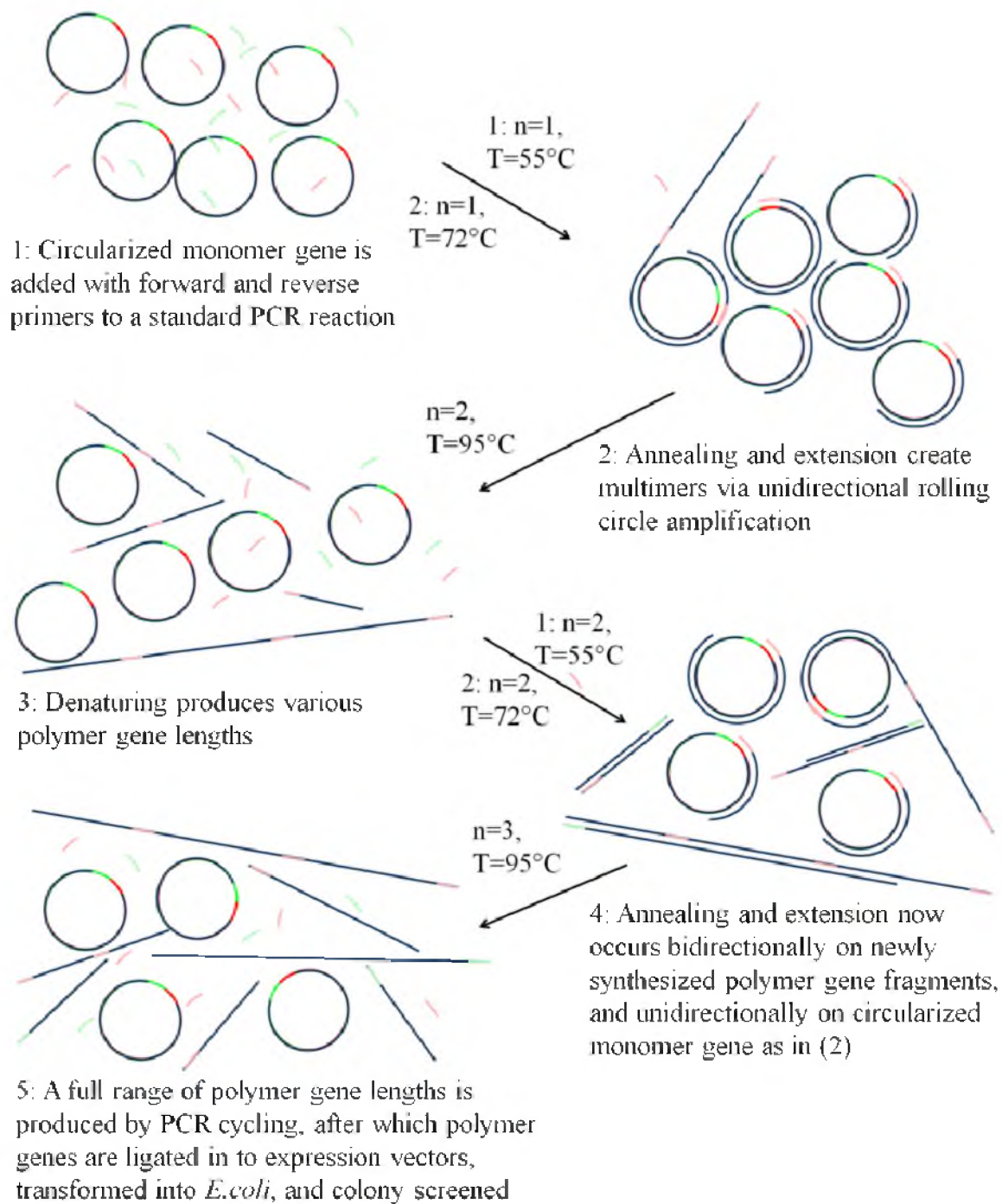


Figure 2.5: Open-ended rolling circle amplification (adapted from<sup>247</sup>)

circle amplification. Subsequently, these polymer genes are able to hybridize with one another by their ends, producing longer gene segments. While this lengthening is occurring, the original circular ssDNA template is being amplified repeatedly, resulting in shorter lengths of polymer gene. This process has been shown to be controllable by several different process parameters.<sup>247</sup> Decreasing primer concentration while keeping cycle number constant increases the average length of the synthesized gene products. Increasing cycle number while keeping primer concentration constant increases the average length of gene products. The addition of further primer during the reaction serves to “fill in” lower polymer lengths which were expanded to high molecular weight with increasing cycle number. Following this reaction, the desired polymer genes can be inserted into any expression vector as a blunt fragment, and downstream protein production/purification can be initiated. OERCA is a very powerful tool for producing a large quantity of varying gene lengths, and while it does require colony screening to determine the length of each polymer gene, the ability to tune a process to produce a large fraction of the desired polymer length presents a distinct advantage over random concatamerization. Further, the one-step gene polymerization approach makes OERCA much faster than RDL, and again by tuning the reaction to the desired size ranges, a complete library of a range of polymer lengths can be obtained.

#### 2.4.3 Classes of genetically engineered protein polymers

Much of the work done in genetically engineered protein polymers has been in the areas of elastinlike polypeptides (ELPs<sup>235, 242</sup>), silklike protein polymers of both silkworm<sup>232, 237</sup> and spider dragline<sup>249-251</sup> silks, collagen,<sup>252, 253</sup> and silk- elastinlike

protein polymers (SELPs).<sup>232, 234, 237</sup> Other notable advances in the field include the advent of noncanonical amino acids and their incorporation into protein polymers, as these open the field of protein polymers to chemistry which has never before been available,<sup>238</sup> as well as alanine-rich helical polypeptides,<sup>245</sup> and cationic recombinant polymers for systemic gene delivery, as previously discussed in Section 2.2.2.1.3.3.<sup>48, 99</sup>

#### **2.4.3.1 Elastinlike protein polymers (ELPs)**

Elastinlike protein polymers are generally defined by a repeating sequence of VGVXP, where X is referred to as the “guest residue” and can be any amino acid other than proline.<sup>235, 254, 255</sup> Extensive work has been done on the characterization of structure dependence of properties in these materials and the physical chemistry behind these properties.<sup>235, 255</sup> The base sequence of ELP is derived from a common repeating unit in mammalian elastin.<sup>256</sup> The main property of ELPs which has made them an attractive protein polymer for both basic and applied sciences is their ability to undergo a phase transition with changing temperature. ELPs are water-soluble below their lower critical solution temperature (LCST), and rapidly respond to temperatures exceeding their LCST by losing solubility, aggregating, and falling out of solution.<sup>255</sup> The temperature at which this transition occurs can be tuned by modification of the guest residue: more hydrophobic guest residues result in lower LCSTs.<sup>255</sup> This effect is observable for homopolymers of ELP as well as block copolymers, where systems have been created which have different regions of temperature sensitivity and hydrophobicity.

The ability to reliably produce highly specific stimuli-responsive materials has garnered an active field of research into the design of stimuli-sensitive nanoparticulate

systems using ELPs as a base polymer. One example is taking advantage of this tunable temperature dependence to produce thermally responsive drug delivery systems.<sup>257-259</sup> In these systems, an ELP was designed which had an LCST of approximately 40°C, which allowed it to remain soluble in circulation at physiological temperature. By heating the target site, in this case a tumor, to 42°C, the ELP undergoes a phase transition preferentially in the tumor, causing accumulation.<sup>257-259</sup> Another drug delivery system developed using ELPs has taken advantage of the ability to produce specific changes to the polymers to impart desired properties. For example, chimeric ELPs primarily composed of Val-Ala-Gly guest residue compositions at a ratio of 1:8:7 with a (Gly-Gly-Cys)<sub>8</sub> motif at one end were produced.<sup>260</sup> This motif was used to attach the cytotoxic chemotherapeutic drug doxorubicin, and to impart a hydrophobic character to that end of the polymer such that it self-assembled into a nanoparticle. These nanoparticles were used to treat a subcutaneous colon cancer model in BALB/c mice, and showed a greatly improved survival benefit and was able to reduce the size of the established tumors over the entire course of the study, with no observable tumor recovery. This work has further expanded into encoding specific modifications to polymers used for nanoparticle formation intended to improve their effect, specifically adenovirus knob domain.<sup>261</sup>

#### **2.4.3.2 Silk-based polymers**

Another natural polymer which has attracted attention in the area of genetically engineered protein polymer design is silk. In nature, there are two distinct forms of silk, coming from spider dragline or the common silkworm, *b. mori*. The silk produced by *b. mori* is produced as a very strong, thin fiber coated in a glue-like protein called sericin,

which allows it to adhere to itself and form a tight cocoon during metamorphosis from worm to moth.<sup>262</sup> This fine thread is valued in the textile industry but has also been used in medical applications, most commonly as nondegradable suture. The primary structure of silkworm silk is dominated by repeats of the hexapeptide GAGAGS, which self-assemble into  $\beta$ -sheet type structures when produced as a linear polymer.<sup>232</sup> Use of genetically engineered silkworm silk-based materials has been limited. One example of genetic engineering of silkworm silk is the genetic engineering of a silkworm which was modified to produce cocoon silk containing the fibronectin-derived RGD cell adhesion sequence.<sup>263</sup>

Spider dragline silk most commonly used in research applications is derived from *Nephila clavipes*, an orb weaver spider.<sup>244</sup> *N. clavipes* dragline is composed of two different but structurally similar proteins, which are both used to form the natural dragline. The first successful cloning and expression of these two proteins as a genetically engineered protein polymer was published in 1995,<sup>250</sup> based on a consensus repeat sequence derived from the amino acid sequences of each of the proteins. These two consensus sequences were determined to be GQGGYGGLGGQGAGRGLGGQ GAGA(A<sub>n</sub>)GGA for the first discovered, termed NCMAG1 or Spidroin 1,<sup>251</sup> and GPGGYGPGQQGPGGYGPGQQGPSGPS(A<sub>n</sub>) for NCMAG2, or Spidroin 2.<sup>249</sup> Current research employing these structural motifs for the production of protein polymers includes gene delivery vehicles,<sup>264</sup> burn dressings,<sup>265</sup> and bone tissue engineering scaffolds.<sup>266</sup>

### 2.4.3.3 Silk-elastinlike protein polymers

Cappello et al. first reported the design and synthesis of recombinant silk-elastinlike protein polymers in 1990.<sup>232</sup> Silk-elastinlike polymers are made up of repeating “blocks” of amino acids, referred to as “silk blocks” (Gly-Ala-Gly-Ala-Gly-Ser) and “elastin blocks”(Gly-Val-Gly-Val-Pro). The silk blocks consist of the sequence GAGAGS, and are based on the naturally occurring fibrillar silk of *b. mori*, the common silkworm.<sup>232, 267</sup> The design of the elastin blocks is based on mammalian elastin, a very common connective tissue in the body which gives skin its elasticity.<sup>232, 256</sup> A significant body of research has been focused on manipulating the “guest residue” position of the elastin blocks, and changing the silk:elastin ratio, to observe how modifications to the structure of SELP affect its properties. Table 2.2 summarizes all versions of SELPs which have been publicly disclosed, and briefly summarizes known properties, where such information is available. Additionally, this table provides structural information and nomenclature to serve as a reference for the coming section.

#### 2.4.3.3.1 Original SELP structures: Valine guest residue

Studies performed on these early SELPs were focused on the changes in crystallinity of the polymers as peptides were inserted into the sequences of SLPs which were composed entirely of GAGAGS repeats. It was found that pure SLP, which was composed of 168 repeats of GAGAGS (~76kDa), had a very crystalline structure, characterized by X-ray diffraction and FTIR-dichroism.<sup>232</sup> In order to observe structure-dependent effects on the  $\beta$ -sheet structure, either elastin groups (GVGVP) or tyrosine-containing motifs were inserted into the sequence. The elastin groups provide a periodic

Table 2.2: SELP Structures and Properties

Descriptive Name	Literature Name	Sequence	Mw (kDa)	Guest Residue	Hydrogel Forming	Thermally Responsive	Applications
SELP-28	SELP0 <sup>237</sup>	[(E) <sub>8</sub> (S) <sub>2</sub> ] <sub>18</sub>	80.5	Val	No	NR	NR
SELP-94	SELP1 <sup>237</sup>	[(E) <sub>4</sub> (S) <sub>9</sub> ] <sub>13</sub>	89.0	Val	Yes, Ins.	NR	NR
SELP-88	SELP3 <sup>237</sup>	[(E) <sub>8</sub> (S) <sub>8</sub> ] <sub>11</sub>	84.2	Val	Yes	NR	NR
SELP-812	SELP4 <sup>237</sup>	[(E) <sub>12</sub> (S) <sub>8</sub> ] <sub>8</sub>	79.5	Val	NR	NR	NR
SELP-816	SELP5 <sup>237, 268</sup>	[(E) <sub>16</sub> (S) <sub>8</sub> ] <sub>7</sub>	84.5	Val	Yes	Yes	Controlled drug delivery <sup>268</sup>
SELP-68	SELP7 <sup>237</sup>	[(E) <sub>8</sub> (S) <sub>6</sub> ] <sub>12</sub>	80.3	Val	NR	NR	NR
SELP-48	SELP8 <sup>237, 268</sup>	[(E) <sub>8</sub> (S) <sub>4</sub> ] <sub>12</sub>	69.9	Val	Yes	Yes	Controlled drug delivery <sup>268</sup>
SELP-18	V11 <sup>269</sup>	[(E) <sub>8</sub> (S)] <sub>11</sub>	47.6	Val	No	Yes	NR
SELP-17E-16	E16 <sup>270</sup>	[(E) <sub>4</sub> (EE)(E) <sub>3</sub> (S)] <sub>16</sub>	66.1	Glu	No	Yes	NR
SELP-17E-11	E11 <sup>269</sup>	[(E) <sub>4</sub> (EE)(E) <sub>3</sub> (S)] <sub>11</sub>	47.6	Glu	No	Yes	NR



Table 2.2 Continued

Descriptive Name	Literature Name	Sequence	Mw (kDa)	Guest Residue	Hydrogel Forming	Thermally Responsive	Applications
SELP-27K	SELP0K <sup>268</sup>	[(S) <sub>2</sub> (E) <sub>4</sub> (EK)(E) <sub>3</sub> ] <sub>18</sub>	80.7	Lys	No	Yes	Vascular grafts, spinal column regeneration, critical wound closure <sup>271,271</sup> [271][271][271][271][271][271][271][271][271][271][271][271][271]
SELP-37K	SELP9K <sup>268</sup>	[(S) <sub>3</sub> (E) <sub>4</sub> (EK)(E) <sub>3</sub> ] <sub>12</sub>	60.1	Lys	No	Yes	Vascular grafts
SELP-47K	SELP8K/ SELP47K <sup>268</sup>	[(S) <sub>4</sub> (E) <sub>4</sub> (EK)(E) <sub>3</sub> ] <sub>13</sub>	69.8	Lys	Yes	Yes	Urethral bulking agent, dermal augmentation agent, vascular grafts, controlled drug delivery <sup>268, 272-279</sup> 280, 281, tissue engineering <sup>280</sup>
SELP-415K	SELP415K <sup>275</sup>	[(S) <sub>4</sub> (E) <sub>4</sub> (EK)(E) <sub>11</sub> ] <sub>8</sub>	71.5	Lys	Yes	Yes	Controlled drug delivery <sup>275-278, 282</sup>
SELP-815K	SELP815K <sup>282</sup>	[(S) <sub>8</sub> (E) <sub>4</sub> (EK)(E) <sub>11</sub> ] <sub>6</sub>	65.3	Lys	Yes	Yes	Controlled drug delivery <sup>282</sup>
SELP-17Y	SE8Y <sup>283</sup>	[(E) <sub>4</sub> (EY)(E) <sub>3</sub> (S)] <sub>14</sub>	55.6	Tyr	NR	Yes	NR
SELP-27Y	S2E8Y <sup>283</sup>	[(E) <sub>4</sub> (EY)(E) <sub>3</sub> (S <sub>2</sub> )] <sub>12</sub>	53.0	Tyr	NR	Yes	NR
SELP-47Y	S4E8Y <sup>283</sup>	[(E) <sub>4</sub> (EY)(E) <sub>3</sub> (S <sub>4</sub> )] <sub>9</sub>	47.8	Tyr	NR	No	NR

interruption by forming kinked coil structures, while the tyrosines provide a bulky side chain which is capable of interrupting the  $\beta$ -sheet stabilizing hydrogen bonding between neighboring peptide backbones. The structures produced were called SLP4 [(GAGAGS<sub>6</sub>)]<sub>28</sub>, SLP3 [(GAGAGS)<sub>9</sub>GAAGY]<sub>19</sub>, SELP1 [(GAGAGS)<sub>9</sub>GAA(VPGVG)<sub>4</sub>VAAGY]<sub>14</sub>, and SELP3 [(GAGAGS)<sub>8</sub>(GVGVVP)<sub>8</sub>]<sub>12</sub>. It was observed that SLP4, the unmodified silk-only polymer, was the most crystalline. The next most crystalline structure was that of SELP1, which contained both the elastin motifs and a tyrosine residue in close proximity to the silk repeats. The least crystalline structures were those of SLP3 and SELP3, which contained a tyrosine residue near the silk repeat and elastin repeats, respectively. This result was confirmed by both X-ray crystallography and circular dichroism. It was expected that the SELP1, which contained both the steric,  $\beta$ -sheet interrupting modification and the long elastin motif interruption would have been the least crystalline, and the reason for these results is unclear. Macroscopically, the SLP4 and SLP3 powders appeared to be of similar crystallinity, with the SELP1 and SELP3 powders appearing more amorphous and fluffy.

#### 2.4.3.3.2 Synthesis and characterization of lysine-containing SELPs

While the earlier work with comparing protein polymer structure with varying valine-containing SELPs provided insight into how modifications of primary structure affected downstream network formation, uses for these polymers were primarily as research tools. Later versions of SELP investigated the effects of adding a charged residue, lysine, in the guest residue position of the elastin-like sequence. For example SELP-47K is a structure in which instead of four silk units to eight elastin units per

monomer repeat, contained four silk units to seven elastin units in the monomer, with one elastin unit having the sequence GKGVP.<sup>268</sup> The amino acid sequence for this polymer was MDPVVLQRRDWENPGVTQLVRLAAHPPFASDPMGAGSGAGS [(GVGVP)<sub>4</sub> GKGV P (GVGVP)<sub>3</sub>(GAGAGS)<sub>4</sub>]<sub>12</sub> [(GVGVP)<sub>4</sub> GKGVP (GVGVP)<sub>3</sub>(GAGAGS)<sub>2</sub> GAGAMPGRYQDLRSHHHHHH, depicted in Figure 1.1. This polymer formed a stable hydrogel network, and did so at a much more rapid rate than did the standard valine guest SELP of the same silk:elastin ratio (see Table 2.2 SELP-48, [(GVGVP)<sub>8</sub>(GAGAGS)<sub>4</sub>]<sub>13</sub>). With the only modification of this sequence being the addition of a single lysine per monomer repeat (13 per polymer chain in this case), it is apparent that the lysine groups were responsible for this increased gelation rate and extent. The precise mechanism of this change has not been investigated, however there are several possible reasons. One possible reason is a hydrogen bonding interaction between the primary amine group on the lysine, and the oxygen atom in the peptide backbone of adjacent polymer strands. This interaction would stabilize the normally mobile elastin group and anchor it to any peptide chain that may be nearby, holding the structure together until more permanent and stable  $\beta$ -sheet structures could form. Another potential explanation of this stabilization is the formation of salt bridges between the lysine and any of the three aspartic acids or one glutamic acid in the head sequence, or the two aspartic acid residues in the tail sequence. This is a strong interaction which would be capable of anchoring the individual peptide chains together, thereby bringing the  $\beta$ -sheet forming silk units in closer contact and encouraging rapid self-assembly. This polymer forms a stable hydrogel network at concentrations equal to or greater than 4 wt%, with the rate of hydrogel formation increasing with increasing temperature.

Gelation properties of SELP-47K are also concentration and time dependent, and the polymer showed release properties which depended on polymer concentration and molecular weight of the drug.<sup>268</sup> Further physicochemical characterization of these hydrogels was performed to evaluate their swelling ratio and its dependence on factors such as pH, temperature, media ionic strength and cure time.<sup>272, 284</sup> As a result of the rheological properties of these polymers and their temperature-induced gelation, experiments were performed to evaluate the ability of SELP-47K to control the release of plasmid DNA,<sup>273, 274</sup> adenovirus,<sup>276, 277</sup> and drugs ranging from low molecular weights up to 500kDa dextran conjugates,<sup>268, 279</sup> which will be discussed later.

Based on initial physicochemical characteristics and release profiles of SELP-47K, two new analogs, namely SELP-415K (four silk units and fifteen elastin units with an additional elastin unit containing a lysine residue)<sup>275</sup> and SELP-815K (eight silk units and fifteen elastin units with an additional elastin unit containing a lysine residue)<sup>282</sup> were synthesized by genetic engineering techniques. The rationale is that by controlling the sequence and length of silk and elastin blocks while keeping the molecular weight of the polymer constant, it is possible to tailor gelation, mechanical strength, release and transfection efficiency. The three constructs varied in sequence of silk and elastin blocks while keeping their molecular weights consistent. It was found through physical characterization that increased silk block content in SELPs rendered a hydrogel with greater crosslinking density, and increased elastin block content resulted in a softer gel with lower mechanical strength.<sup>282</sup> For the purposes of gene delivery with adenoviral carriers, this translates to faster and more complete release as silk block content decreases and elastin block content increases.

As an example of the overall synthetic strategy of SELPs the biosynthesis of SELP-815K is outlined in Figure 2.6.<sup>282</sup> Synthesis is performed via random concatamerization, as discussed in Section 2.4.2.1. In brief, the monomer gene segment (DNA encoding for a single 8-silk, 15-elastin, 1-Lys-modified elastin monomer) was produced by digesting plasmid pPT340, encoding for SELP-415K, with BanII restriction enzyme to produce a plasmid encoding for SELP-215K. Plasmid pSY1378, encoding for six silk units, was then linearized using BanII, purified, and treated with shrimp alkaline phosphatase (SAP). Following removal of SAP, pPT340 and pSY1378 were ligated at a 1:1 molar ratio using T4 ligase. The resulting mixture was then used to transform Dh5 $\alpha$  chemically-competent *E.coli*, which were plated with chloramphenicol. Following formation of colonies, they were isolated, propagated, and plasmid DNA was purified. Restriction digestion was followed by agarose gel electrophoresis to visualize a fragment of 384bp, representing the SELP-815K monomer gene segment. Following production of the SELP-815K monomer gene segment, they were excised from their parental plasmids as BanI fragments and self-ligated using T4 DNA ligase, forming SELP-815K multimers. The expression vector, pPT317, was digested with BanI and treated with SAP, then randomly multimerized with the SELP-815K insert using T4 DNA ligase. This ligation mixture was used to transform Dh5 $\alpha$  chemically-competent *E.coli*, which were plated with kanamycin. The 6-mer was isolated via colony PCR and restriction digestion procedures, and plasmids encoding for the 1-, 2-, 3-, 4-, and 5-mer were also isolated. The 6-mer was chosen because this number of 815K repeats yields a polymer with the most similar molecular weight (65,374 Da)<sup>282</sup> to the previous analogs (SELP-47K 13-mer, 69,814 Da,<sup>284</sup> SELP-415K 8-mer, 71,500 Da<sup>275</sup>). The “polymerization” for

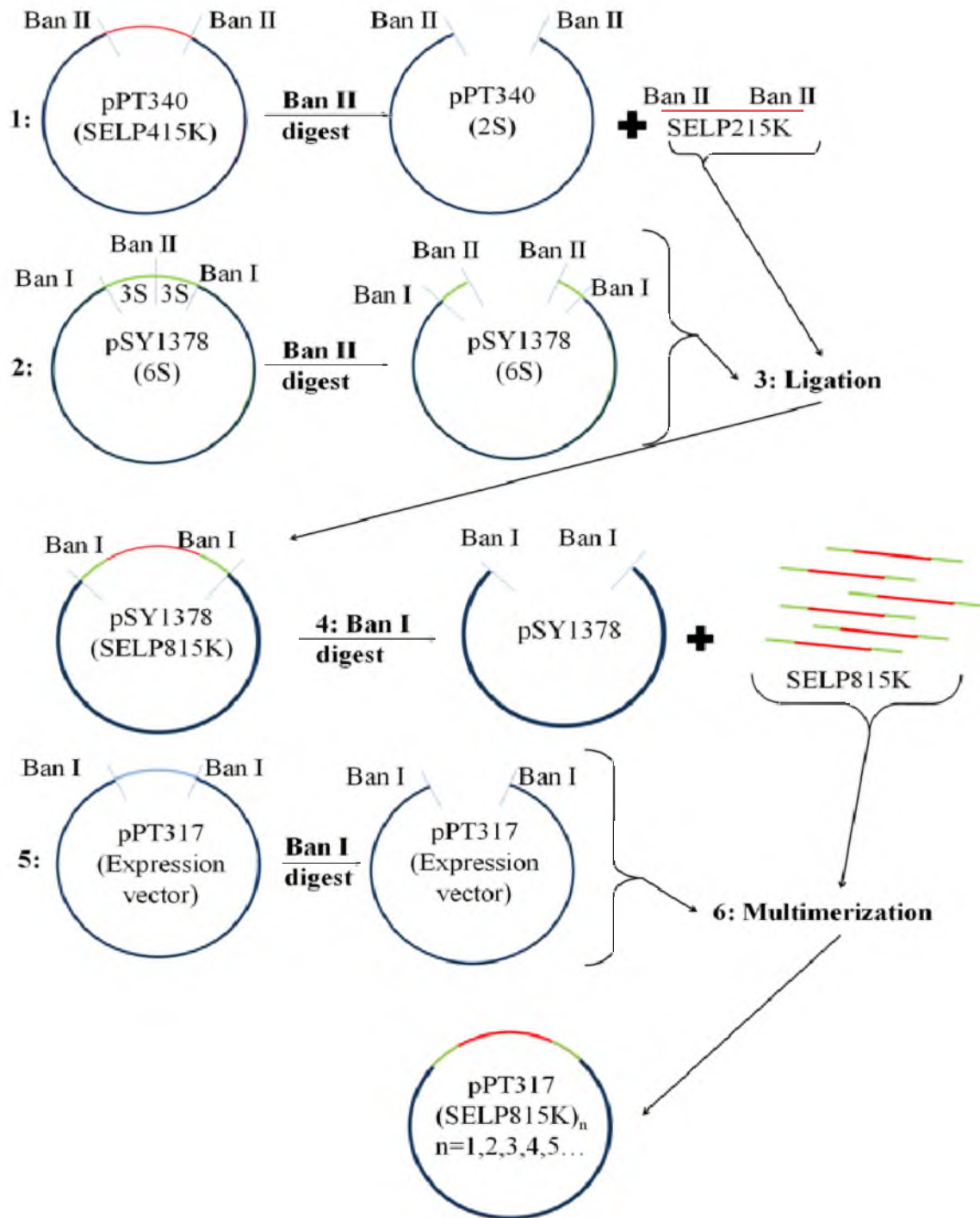


Figure 2.6: Synthetic strategy for SELP-815K (adapted from<sup>282</sup>)

recombinant polymers takes place at the genetic level, and can therefore be closely evaluated before large-scale protein production. Large-scale production is performed using only specific plasmids encoding for the polymer of desired length, thus largely eliminating polydispersity of the resulting polymer population and maintaining precise control over the polymer's amino acid sequence.

**2.4.3.3.2.1 Molecular methods.** SELPs have been well-characterized in terms of structure and composition, using common protein analysis methods. The molecular weights of hydrogel-forming SELPs used for gene delivery studies<sup>275, 282</sup> were confirmed by sodium dodecyl sulfate-polyacrylamide gel electrophoresis (SDS-PAGE), amino acid analysis, and matrix-assisted laser desorption-ionization-time-of-flight (MALDI-TOF) mass spectrometry. Typical mass spectrometry and amino acid analysis data for SELP-815K are shown in Figures 2.7 and 2.8, respectively. As observed, distinct molecular weights of the polymer can be obtained using recombinant techniques. The analyses of each structure of SELP showed that their molecular weights were within reasonable margin of error based on expected amino acid sequence. Amino acid analysis was also performed on SELP-815K, and the results agreed with the projected values based on the expected amino acid sequence and gene sequencing data for the monomer and polymer gene segments.<sup>282</sup>

**2.4.3.3.2.2 Atomic force microscopy (AFM) of SELP self-assembly.** In order to investigate the self-assembly properties of SELPs at the molecular level, AFM was performed on low polymer concentrations, well below hydrogel-forming values.<sup>285</sup> The initial studies were only performed on SELP-415K as among the analogs under investigation this was the SELP with the longest incubation time before gelation. Self-

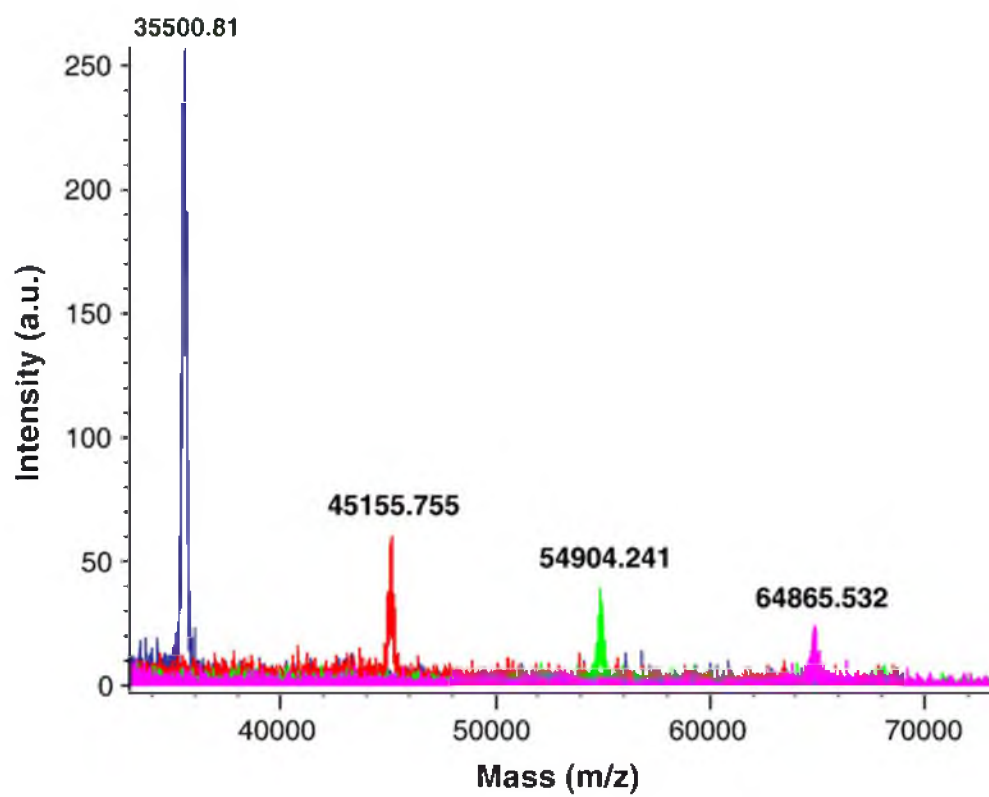


Figure 2.7: MALDI-TOF mass spectra of SELP-815K polymers<sup>282</sup>



Amino Acids	SELP-815K-6mer	
	Res/Mol Th <sup>a</sup>	Res/Mol Ob <sup>a,b</sup>
Gly	344	333.30
Val	189	192.48
Ala	105	101.66
Pro	102	118.58
Ser	50	45.59
As(x)	7	7.37
His	7	5.45
Arg	5	3.93
Gl(x)	4	4.54
Leu	4	3.62
Met	3	1.70
Lys	6	5.31
Thr	1	1.25
Tyr	1	1.12
Trp	1	0.00
Phe	1	1.52

Figure 2.8: Amino acid analysis of SELP-815K<sup>282</sup>

assembly was concentration-dependent and tended towards the formation of nanofibers as concentration was increased. Additionally, these results showed that the size of the nanofibers was not affected by SELP concentration. However increasing concentration yielded increased density of fibers. Further, AFM studies indicated the strong dependence of fiber formation on ionic strength. A known fiber-forming concentration (1 $\mu$ g/ml) of SELP-415K was incubated in NaCl concentrations ranging from 5 mM to 100 mM and imaged using AFM. Lower ionic strength solutions supported more robust fiber formation, and the effect of ionic strength on fiber formation was concentration dependent as opposed to a rapid transition to an absence of fibers with increasing ionic strength. Further studies were performed to investigate the kinetics of SELP nanofiber formation. These studies revealed rapid formation of fibers at low ionic strength on a mica surface, while higher ionic strength conditions caused slower fiber formation with a more typical lag, burst, plateau type of kinetics as observed for other proteinaceous fibers.<sup>286-288</sup> This suggests that fiber formation on the mica surface is driven by electrostatic interactions between the surface and the SELP chains, and increasing salt concentration provides shielding of these interactions, thereby reducing formation of fibers on the surface.

A more recent analysis of SELP by AFM revealed a very interesting behavior of SELP adsorbed to mica surfaces.<sup>289</sup> SELP-815K was adsorbed to a mica surface for 30 minutes at a concentration of 5 $\mu$ g/ml, after which the SELP solution was removed and the surface was washed three times with DI water. Following washing, the surface was probed with an AFM in tapping mode, and a sparse network of nanofibers was observed. Following the initial scan, the surface was scanned at several later time intervals, and it

was observed that over time, many more nanofibers were forming. In order to examine whether or not this was due to the nanomechanical stimulus of the AFM tip, a stimulus intensity study was performed, as well as a condition in which a field of view was stimulated with the AFM, allowed to incubate for 30 minutes, and then zoomed out and re-scanned. It was shown that increasing the magnitude of the stimulus correlated directly with increased surface coverage by the nanofibers, and in the field-of-view experiment it could easily be observed that the additional formation of fibers was confined just to the areas which were physically stimulated with the AFM tip. These results correlate with observations that in order to form stable hydrogels reliably and quickly, SELP must be exposed to a significant shearing event, with increasing shear resulting in more rapid gelation.

**2.4.3.3.2.3 Gelation properties of SELPs.** The rate, mechanism, concentration, and required environment for gelation were studied at length for the hydrogel-forming structures of SELP. Early studies of these properties revealed that the gelation of SELPs is a mildly exothermic reaction, the properties of which are characteristic of a “nonreversible crystallization event”.<sup>268</sup> The gelation of SELP was also confirmed by viscometry, which showed an increase in viscosity of the polymer solution with time,<sup>268</sup> suggesting that the individual SELP polymers were associating with one another. One very important property revealed by the viscometry experiments is that the time for gelation is strongly dependent on the number of silk units per monomer repeat. Under isothermal conditions at 37°C and at identical protein concentrations, it was observed that SELP-816 reached the upper maximal limit of the viscometer after approximately 57 minutes, while SELP-47K took approximately 108 minutes and SELP-27K did not show

a significant increase in viscosity during the 125 minute measurement time.<sup>268</sup> The structural arrangement of these polymers is described in Table 2.2. While it has since been established that the addition of a lysine guest residue greatly reduces gelation times in static gelation conditions, the shear applied to the SELP-816 sample by the rheometer overcame this property and induced more rapid gelation correlated with silk unit content. This result combined with the AFM results<sup>289</sup> suggest that the physical stimulation of these polymers induces self-assembly of the GAGAGS silk unit repeats, resulting in nanofiber (2-D) or hydrogel formation (3-D). In later experiments, where the SELP-47K was allowed to gel in a mechanical stimulus-free environment, it was observed that gelation began to occur as early as 5 minutes after being placed in a 37°C environment.

Included in these rheological gelation studies was an investigation into the temperature dependence of SELP gelation. In addition to the 37 degree condition, SELP-47K and SELP-816 were measured at 23°C and 4°C.<sup>268</sup> As expected, it was observed that the gelation time was temperature dependent, with significant increases in gelation time as the temperature was decreased. The effect was so profound that at 4°C, SELP-47K first showed signs of gelation at approximately 24 hours after the start of the experiment.<sup>268</sup> Another characteristic of SELP gelation examined whether or not solutes expected to aid or inhibit crystallization had an effect on SELP gelation. To answer this question, SELP-47K gelation was measured in the presence of 6M urea, precrystallized SELP-47K, and PBS only (control). It was hypothesized that the urea would disrupt the ability of SELP to form gels by preventing hydrogen-bond formation, while the precrystallized SELP-47K in solution would serve as attractive nucleation sites and therefore accelerate gelation. This hypothesis was shown to be correct, as SELP in the

presence of SELP seed crystals gelled approximately 30 minutes faster than the control condition (110 minutes), and the SELP in the presence of urea had not shown signs of gelling up to 6 hours from the start of the experiment.<sup>268</sup>

The critical gelation concentration (CGC) of each of the hydrogel-forming, lysine-substituted SELP compositions has not been experimentally determined, but can be estimated. The use of SELP-47K and SELP-815K at concentrations as low as 4 wt% and SELP-415K as low as 10.8% has been published.<sup>282, 290</sup> In unpublished experiments, SELP-415K has been observed to gel at concentrations as low as 8 wt%, and SELPs -47K and -815K are considered likely to be able to gel at concentrations lower than 4 wt% although this has not been used for any experiments. These differences are attributable to the density of silk units per monomer repeat, as they are responsible for crosslinking events in SELP gelation. An increase in silk units therefore increases the theoretical concentration of crosslinks and decreases the amount of polymer necessary to form a fully crosslinked network.

Previous experiments demonstrated the strong dependence of physical properties on the molecular sequence of the linear SELPs. Extending this to three-dimensional networks, studies were performed to investigate the specific effects that each modification of SELP has on the physical properties of resulting hydrogels.

**2.4.3.3.2.4 Factors influencing swelling of SELP hydrogels.** Hydrogel swelling ratio ( $q$ ) is a measure of the weight of a hydrated hydrogel divided by its dry weight that has been measured for SELPs.<sup>278, 282, 284</sup> This parameter is useful in predicting the ability of a hydrogel to ‘soak up’ potentially useful solutions, delivery via diffusion, pore size, and mechanical properties. Extensive studies have been performed to evaluate swelling

ratio of SELP hydrogels over a range of polymer concentrations and compositions along with the effects of pH, temperature, ionic strength of media, solutes, and gelation time of the sample. It was found that changes in pH had little or no effect on the swelling ratio between pH 2 and pH 12.<sup>275, 282, 284</sup> Studies on SELP-415K at 12 wt% showed that there is temperature dependence, with an observed swelling ratio of approximately 16 at 4°C with a steady decrease in swelling ratio to less than 10 at 47°C.<sup>275</sup> This is contrary to findings with SELP-47K and SELP-815K, which showed no appreciable temperature dependence over the range of 4°C to 47°C and had swelling ratios of approximately 10 for 12 wt% gel in both cases. The reason behind this is most likely due to the fact that SELP-415K has a higher elastin:silk ratio than SELP-47K and SELP-815K and long elastin blocks, which allow the temperature-dependent self-assembly of the elastin blocks to occur, as they are not as rigidly confined as they would be in the case of the higher silk content SELPs. Similar effects were seen with other SELP structures.<sup>283</sup>

The largest factor for swelling ratio in the same SELP structure was, not surprisingly, hydrogel cure time. All three polymers showed cure time dependence at 12 wt%, with SELP-415K showing stronger cure time dependence than SELP-47K<sup>275</sup> and SELP-815K.<sup>282</sup> In another study, SELP-47K was shown to have stronger cure time dependence at 8 wt% than at 12 wt%.<sup>284</sup> This can be explained by the changes in overall concentration of the crosslinking beta-sheet forming silk blocks. Because all of the polymers are synthesized to have approximately the same molecular weight, the overall concentration of silk blocks in a solution of SELP-415K at 12 wt% is much lower than that of SELP-47K. The number of silk blocks in SELP-815K is also significantly higher than in SELP-415K, therefore explaining the intermediate swelling ratios in all

conditions. The reduced number of silk blocks in SELP-415K causes the beta-sheets to form more slowly in this polymer than both SELP-47K and SELP-815K, thus producing a much looser network during a short cure time. Over an extended period of time, more beta sheets are given time to form, and therefore, the relative reduction in swelling ratio becomes higher for SELP-415K than for SELP-47K and SELP-815K. The reduction of weight percentage from 12 wt% to 8 wt% also reduces this silk block concentration, therefore similarly increasing the amount of time required for an equivalent number of crosslinks at 12 wt%.

Another factor which was shown to influence swelling ratio of SELP-47K gels at low weight percentages was the incorporation of adenoviruses.<sup>277</sup> The changes in swelling ratio in general were not extreme. However, there is a trend suggesting that swelling ratio of 4 wt% hydrogels of SELP-47K decreases as adenovirus count increases.<sup>277</sup> This implies that there is some interaction between the viruses and SELPs, likely occurring at a high enough frequency to create simulated crosslinks in the polymer which are not a result of the interaction of silk blocks on different polymer chains. While this phenomenon is true of low weight percentage SELPs, similar studies performed on 11.7 wt% SELP-47K and SELP-415K hydrogels did not show the same trend.<sup>277</sup>

**2.4.3.3.2.5 Soluble fraction of SELPs.** Due to the proposed application of SELP hydrogels *in vivo*, it was necessary to assess the amount of polymer soluble fraction generated with each formulation in order to draw conclusions about possible side effects based on the amount of free polymer chains released. This property of SELP was assessed in several different experiments. Hydrogels of SELP-47K (4, 8, and 11.7 wt%) and SELP-415K (11.7 wt% only) were produced by drawing liquid polymer solutions

into a 1cc syringe, followed by gelation for particular lengths of time.<sup>277</sup> Following gelation time, the gel cylinders were cut into 50 $\mu$ l disks, placed into release media (1X Dulbecco's phosphate buffered saline with 0.01% sodium azide) and agitated at 120RPM in a shaking incubator at 37°C. Solubilized protein was assessed by removing all release media and performing a bicinchoninic acid (BCA) protein assay to determine soluble polymer weight.<sup>277</sup> It was shown that after a 4-hour cure time, the soluble fraction of SELP-47K hydrogel at 11.7 wt% was approximately 15%, meaning that at least 15% of the protein in the original sample did not participate in the crosslinking and formation of the hydrogel network.

Due to the adjustment of the number of monomer repeats, it is true that the total silk content per polymer strand will be similar between the two; however, the longer contiguous silk units are statistically more likely to leave "open" crosslinking sites than are the shorter units found in SELP-47K structure, increasing the likelihood that completely noncrosslinked polymer can randomly associate with another strand. SELP-415K at 12 wt% was also investigated in this study<sup>277</sup> and it showed nearly identical soluble fraction amounts to SELP-47K over the time of the study, with a slightly slower release rate in the beginning. This observation is likely related to the mechanism of gelation of these polymers. Crosslinks are formed due to association of silk units into beta-sheets, which requires the polymer strands to be within close proximity of one another in order for the hydrogen bonds to form between the adjoining silk units. In the case of SELPs -47K and -415K, the short silk blocks, while allowing some crosslinks to form in high density, it is likely that the adjoining elastin units could sterically hinder attachment of a large number of chains. In the case of SELP-815K however, the longer



silk units are likely to allow more polymer strands to attach to each other. While it is true that the elastin units will theoretically hinder some of the silk units, the 100% longer silk unit of SELP-815K is likely to compensate for this effect. It was shown that after 24 hours of gelation, the soluble fraction was much lower, with approximately 8 wt% soluble fraction for the same polymer at the same concentration.<sup>284</sup> These results give information regarding the time-dependence of the physical interactions which cause the crosslinks to form, as the same polymer conditions gave 25% soluble fraction after a 1-hour gelation time.<sup>284</sup> It would appear that there is a fast initial crosslinking which occurs shortly after the temperature of liquid solution is raised, followed by a leveling off of the rate of crosslink formation most likely due to steric hindrance of the crosslinking sites actually being able to locate one another.

Another study on the soluble fraction of SELP hydrogels was an investigation into the effects of adenovirus incorporation into the liquid polymer solution on the amount of soluble fraction.<sup>277</sup> This is particularly applicable as SELPs are currently being investigated as a possible delivery device for adenovirus-mediated anticancer gene therapy. These studies showed that there is little to no effect on the amount of protein soluble fraction released from the hydrogel by incorporating adenoviruses into the liquid polymer before gelation.<sup>277</sup> Results are encouraging as they imply that SELPs can be applied *in vivo* as an adenovirus delivery device with no added material-related side effects due to the inclusion of the viruses. These results also suggest that there is minimal chemical interaction between the monomers and adenoviruses, as it would be expected that interaction between the virus and monomer would cause an increase in soluble fraction. It is thought that this complex would be more likely to be sterically hindered

and thus blocked from forming crosslinks, which would likely interfere with the pore network formed by the polymerization of the SELPs.

**2.4.3.3.2.6 Thermal analysis of water in SELPs.** Using differential scanning calorimetry, SELP hydrogels were characterized for their nonfreezable water content, heat capacity, and temperature dependence of both.<sup>291</sup> This information is very important to the application of SELP as a polymeric delivery depot, as the nonfreezable water has been hypothesized to be partially bound to the polymer chains by hydrogen bonding, which would have implications in diffusive release of solutes from the hydrogel if the solutes were contained in this area of the fluid. It was found in these studies that up to 27% of the water in SELP-47K hydrogels is nonfreezable, and is approximately in a 1:1 ratio by weight with the polymer.<sup>291</sup> These studies also revealed some interesting information regarding the freezable water contained within the hydrogels. It was revealed that the melting of water entrapped in SELP hydrogels occurred over a 25 degree range, which is highly atypical of bulk water. It was stated that this very broad melting curve was possibly a result of either segregation of small water clusters which melted at different rates, or that the heat energy put into the system was shared between the melting of the freezable water and the mixing of the polymer chains and liquid water.<sup>291</sup>

This study also investigated the overall effects of hydration of the hydrogels on the melting of frozen entrapped water, and the effect on heat capacity of the entrapped water. For the heat capacity measurements, it was shown that there is little or no dependence of heat capacity on hydration of the polymer for temperatures below 0°C, while there is a linear dependence for temperatures above 0°C. The heat capacity values were also compared based on temperature, and a similar trend was observed, with very

little dependence observed for freezing temperatures and a linear dependence observed for higher temperatures. These values mostly agreed with accepted literature values, indicating that the nonfreezable water in SELP-47K hydrogels is not likely to be completely bound to the polymer strands.

**2.4.3.3.2.7 Mechanical properties of SELP hydrogels.** In order to be successfully applied as localized gene delivery systems, it is desirable that SELPs be injected directly into a tumor, and therefore be liquid in their initial form. Following gelation, the material cannot be mechanically weak, as this will make it susceptible to flow which will affect release rate of the therapeutics from the hydrogel. Also, a material which is very pliable or soft will allow the gel to migrate from the injection site, which is likely to reduce its utility as a localized delivery system. As an initial assessment of the material properties of SELP hydrogels, cone and plate rheology was used to measure the shear modulus of SELP-47K and SELP-415K hydrogels, both at 12 wt%.<sup>275</sup> Shear modulus is a parameter describing the ability of a material to resist shear strain under exposure to shear stress. This information is useful for the application of SELP hydrogels *in vivo* because it provides some insight into their ability to resist deformation and migration from the injection site, which could have negative consequences for the delivery of bioactive agents. Using cone and plate rheology, the shear modulus of SELP-47K hydrogel was found to be 1.3 MPa, while the same value for SELP-415K hydrogel was 0.37 MPa.<sup>275</sup> This large difference in modulus can be explained by the fact that SELP-47K has a significantly higher density of beta sheet and crosslink-forming silk units than does SELP-415K, and therefore is expected to exhibit increased mechanical strength in this assessment. This is another example of the tunable property of SELP

hydrogels which can be controlled precisely at the molecular level to make these materials suitable for matrix-mediated gene delivery.

In order to assess the mechanical strength of SELP hydrogels, studies were performed using dynamic mechanical analysis (DMA).<sup>282</sup> A sinusoidal compression of the sample at controlled frequency was used to assess the storage and loss moduli of SELP hydrogels. The storage modulus is related to the stiffness of the material and is typically associated with the elastic properties, while the loss modulus is related to the dampening and energy dissipation of the material due to its viscous properties. A direct comparison between SELP-47K, -415K, and -815K at 12 wt% was performed in order to assess the structure-dependent differences in mechanical properties among these three polymers.<sup>282</sup> In this study, gels were subject to a strain range of 0.2-2%, and all samples were tested at 1Hz. The results showed that of the three gels tested, SELP-47K had the highest storage modulus, followed by SELP-815K and SELP-415K, respectively. These results suggest that mechanical properties are primarily determined by the number of elastin blocks per monomer repeat, and the length of the silk blocks also contribute to some extent. The results of this study also illustrate the fact that the contribution of silk blocks to the mechanical properties is mostly stiff, noncompliant regions of the gel, as the SELPs with higher silk fractions (SELP-47K and SELP-815K) fractured at strains greater than 1.5%, while SELP-415K, with about 30% fewer silk blocks per monomer, was able to resist fracture throughout the tested range of 0.2-2%.

In a separate study, DMA was performed on hydrogels formed from SELP-47K at 4 wt%, 8 wt%, and 12 wt%, and SELP-415K at 12 wt%,<sup>276</sup> to examine the concentration-dependence of mechanical properties of these polymers. In this study, a frequency sweep

was used to examine the differences in the properties of the hydrogels at various strain rates. It was shown that there is very little frequency-dependence and a very strong concentration-dependence for the storage modulus in SELP hydrogels, with 12 wt% SELP-47K having a storage modulus of 1.6 MPa, compared to 8 wt% and 4 wt% gels which had moduli of 0.5 MPa and 0.075 MPa, respectively. The result was expected as there is a much higher density of crosslinking silk units at higher concentration, and therefore, it is very likely that there is a higher density of crosslinks, leading to an increase in mechanical strength. This trend is also observed when the modulus for SELP-415K at 12 wt% is compared to these figures. 12 wt% SELP-415K hydrogel yielded a value of 0.07 MPa, very similar to 4 wt% SELP-47K. This is likely due to the significantly shorter elastin blocks found in SELP-47K, which allow more rapid and frequent self-assembly of silk units to occur than in the case of SELP-415K. The reduced silk block composition does not, however, have a direct 1:1 relationship with decreases in storage modulus, suggesting that there are other factors which contribute to the properties of SELP hydrogels aside from the density of crosslinking units. Among possibilities for such differences are the specific arrangement of the crosslinking units with one another, i.e., doubling crosslinking units does not necessarily mean doubling the number of crosslinks. In this case, this reduction in crosslinking density would be caused by elastin's interruption of the silk's crystallization. Further, the self-assembly characteristics of the elastin blocks could be responsible for the decrease in mechanical properties as the elastin does not form stiff beta sheet structures as silk does.

#### **2.4.3.3.2.8 Transmission Electron Microscopy (TEM) of SELP hydrogels.**

TEM was employed to provide a picture of what the microstructure of SELP hydrogels

looks like as a function of SELP composition (SELP-47K vs. SELP-415K) and concentration (SELP-47K at 4%, 8%, and 12%). TEM studies were particularly useful in determining the crystal structure of SELPs along with the interfibril spacing in a SELP hydrogel.<sup>277</sup> The TEM images show that interfibril spacing has an obvious dependence on SELP composition, with higher concentrations exhibiting lower interfibril distances, although for all concentrations, the interfibril distances were highly variable. Another interesting piece of information given by the TEM images was an image of an adenovirus virion, which showed that the interfiber spacing is significantly larger (~93nm) than the diameter of the virion (~22nm).<sup>277</sup> This suggests that viruses inside the hydrogel network should not be completely immobilized by the SELP material; however, completely unimpeded diffusion should not occur either. This makes SELP a strong candidate for the controlled release of virus particles over an extended period of time.

**2.4.3.3.2.9 Small-Angle Neutron Scattering (SANS) of SELP hydrogels.** To gain further insight into the hydrogel pore structure, network properties were examined as a function of polymer sequence by small angle neutron scattering (SANS) techniques. SANS allows the examination of microstructures in the range 1-100nm through the analysis of elastic neutron scattering.<sup>292</sup> SANS analysis was used to examine the correlation between the observed macroscopic properties of SELPs such as equilibrium swelling and mechanical modulus with the underlying network structure. The data were fit using a combined Debye-Bueche power law model which revealed trends in the SELP fibril correlation length that confirm observations about structural effects.<sup>293</sup> SELP hydrogels conformed closely with a modified gel model of the general form  $I(Q) = A Q^b + (B Q^2 \epsilon^2)^2 + C$ , which uses a power-law fit for the high  $q$  scattering combined with the Debye-Bueche model at low to intermediate  $Q$

(above  $Q = 0.02 \text{ \AA}^{-1}$ ). The combined Debye-Bueche/power law model provided a nearly complete fit over the full  $q$ -range of collected data. This analysis of SELP-47K, -415K, and -815K revealed scattering profiles that, while similar in form, showed a characteristic trend in low  $q$  power-law scattering and Debye-Bueche correlation length  $((4\pi K\epsilon^2 \text{corr}L^2)/(1 + Q^2 \text{corr}L^2)^2)$ . The calculated correlation length depicts a trend in the observation that is in the order SELP-415K > SELP-815K > SELP-47K. This is consistent with the dynamic mechanical analysis (DMA) data showing that SELP-47K had the highest storage modulus. Presence of shorter elastin blocks separating the crystallized silk blocks of the SELP-47K compared with the other analogs (-415K and -815K) resulted in a stiffer hydrogel with smaller spacing of the crystalline silk units. In contrast, SELP-415K had the longest correlation length and the lowest storage modulus. The silk blocks of SELP-415K are separated by elastin blocks twice the length as SELP-47K, and as these cross-linking blocks move further apart, the elastinlike nature of the SELP becomes more pronounced and the storage modulus decreases. SELP-815K presents an interesting case where the silk blocks are doubled in length over SELP-47K while also having a long elastin block as in SELP-415K. While the larger silk blocks provide improved cross-linking when combined with a 15-unit elastin block, the correlation length and storage modulus falls between those of SELP-47K and -415K. The combination of SANS and DMA data together suggest that the elastin block of the SELPs predominantly influence the effective pore size.

**2.4.3.3.2.10 Release properties of SELP hydrogels.** In order to assess the ability of SELP hydrogels to deliver therapeutic agents in a spatial- and temporally controlled manner, a series of *in vitro* release experiments were performed. These studies were a prelude to extensive *in vivo* studies which assessed the delivery, localization, and efficacy

of bioactive agents from SELPs. Several investigations have been performed on the ability of SELP hydrogels to control the release of many simulated traditional therapeutic agents, ranging in molecular weight from 180 Da (theophylline)<sup>272</sup> to 500kDa (fluorescein-dextran).<sup>268</sup> In general, all of the solutes tested showed size-dependent release from SELP-47K. The rates of release from the hydrogels as a function of solute size yield some important information regarding the applicability of SELP as a controlled release system for molecular therapeutics. The molecules released from SELP-47K 12 wt% (theophylline, MW180, Vitamin B12, MW1355, and cytochrome c, MW 12384) were all completely recovered by 4 hours after the start of the release study.<sup>272</sup> A similar study, however, revealed that 20 wt% SELP-47K was able to release 85% of the originally loaded amount of 500 kDa fluorescein-dextran in a controlled manner over the course of 10 days, suggesting that this size range of therapeutics would be a good candidate for long-term controlled release from SELP-47K hydrogels.<sup>268</sup> This study also showed that a 40 kDa conjugate dansyl-dextran was released steadily over approximately 3 days, which could also be a useful time period of release for some applications.

Further studies performed by Dinerman et al. investigated the release properties of small molecule species based on charge.<sup>279</sup> Specifically, the fluorescent dyes fluorescein (negative charge), rhodamine B (amphoteric), and rhodamine 6G (positive charge) were used as model molecules of approximately identical molecular weight but differing charge. It was shown that the positively charged dye, rhodamine 6G, had the slowest release rate, while the negatively charged dye released fastest. This is likely due to hydrophobic interactions between the dye and the hydrophobic amino acids in the polymer chain. This was supported by visual observations of the diffusion front



characteristics in the gels containing each of the dyes, as the most hydrophilic dye exhibited a visually distinct diffusion front, while this was absent in the other, more hydrophobic dyes.

These studies additionally encompassed the release of poly(amido amine) (PAMAM) dendrimers of differing generation and functionality. Dendrimers of G3 and G4 were compared directly and exhibited almost no difference in release properties, as their hydrodynamic radii differed only by 0.26nm.<sup>294</sup> Surface functionality was shown to play an important role in the rate and extent of release of dendrimers however, with amine terminated G3 dendrimers being released at a rate of nearly 100% by 6 hours, and carboxyl terminated G3 dendrimers only reaching about 70% release in the same time period. The difference between the two types of surface functionalization was narrower for G4 dendrimers, with carboxyl terminated systems reaching about 85% release and amine-terminated G4 reaching the same level as for G3. These observations, coupled with a large increase in release rate and extent of carboxyl-terminated dendrimers following addition of salt to the system, suggests that amine terminated dendrimers do not interact with the SELPs, while carboxyl terminated dendrimers interact with the positive charges (likely the lysine groups), slowing their release.

The *in vitro* bioactivity of therapeutic molecules released from SELPs was also evaluated, to examine the impact of interaction with the polymer on the efficacy of the released molecules. Pantarin, a genetically engineered mitotoxin,<sup>268</sup> was used for the bioactivity studies. To conduct the experiments, radioactively labeled Pantarin was added to the SELP-47K solution, and allowed the liquid to form a gel. After gelation, the polymer was placed in an elution tube and the remaining Pantarin in the hydrogel was

measured using a gamma counter. The bioactivity of the released Pantarin was assessed by analyzing the Pantarin content in the elution sample, and exposing cells to the sample or fresh Pantarin. Using these methods, it was shown that Pantarin was stable and retained nearly 100% of its bioactivity after release from the SELP hydrogel. These results are encouraging as they suggest that delivery via a SELP hydrogel would not require an increased dose of therapeutic molecule to compensate for inactivation via interaction with the gel.

**2.4.3.3.2.11 Biodegradability of SELP hydrogels.** It is essential to characterize the degradation properties of SELPs if they are to be used as gene and drug delivery systems. Degradation of SELP hydrogels *in vivo* could have significant effects on release properties of bioactive agents, as the decreasing gel density will cause further and faster release over time. Biodegradation analysis also allows further insight into the potential for long-term effects of using the material.

Another aspect of SELP degradability examined the effects of elastase-dependent degradation on the release of plasmid DNA from the hydrogels. To assess these effects, SELP hydrogels containing plasmid DNA were produced and incubated in the presence and absence of elastase, with DNA content periodically measured in the release media.<sup>278</sup> A substantial effect on DNA release was observed when hydrogels were incubated in the presence of elastase compared to an elastase-free control, likely owing to degradation of the SELP over time. The effect for SELP-47K was a nearly 30% increase in DNA release, while the increase in DNA release from SELP-415K was almost 40%.<sup>278</sup> This information combined with the structure-dependent degradability data reveal another

variable which can be manipulated on the molecular level to produce SELPs with desired properties.

Swelling ratio is another property of SELP hydrogels which is influenced by biodegradation.<sup>278</sup> It was shown that after only 24 hours of exposure to elastase, significant increase in swelling ratio was observed, and this effect was more profound in higher elastin-containing polymers. This suggests that for applications in which degradation is favorable, control over elastin content will allow control over degradation properties.

**2.4.3.3.2.12 Biocompatibility of injected SELPs.** The biocompatibility of SELP-47K has been investigated by direct injection of liquid polymer to guinea pigs subcutaneously and intradermally.<sup>268</sup> After rapid gelation, the guinea pigs were closely monitored for signs of an immune response, material migration, or excessive irritation. Histology was performed on the tissue around and including the injection site to look for signs of toxicity, allergy, or inflammation, of which none were found to be significantly present. The histology also allowed observations of the nature of the gel mass after injection, which showed that the gel tends to either interpenetrate dermal collagen, or remain isolated in subcutaneous pockets.<sup>268</sup> The only signs of response to the material after injection were observed at day 28, when there was some cellular infiltration into the outside edges of the gel along with occasional clusters of foreign body giant cells which appeared to be associated with SELPs. Notably, even at 28 days postinjection, there were no signs of significant, harmful immunological reaction or inflammation.

#### 2.4.3.3.3 Synthesis and characterization of tyrosine-containing SELPs

Recently, a series of three SELPs with similar molecular weights were synthesized with a tyrosine in the guest residue position of one elastin unit per polymer repeat.<sup>283</sup> These polymers were intended to be used to study the self-assembly properties of SELPs. The sequences of the three new SELPs were:

SE8Y: [(GAGAGS)(GVGVP)<sub>4</sub>(GYGVP)(GVGVP)<sub>3</sub>]<sub>14</sub>

S2E8Y: [(GAGAGS)<sub>2</sub>(GVGVP)<sub>4</sub>(GYGVP)(GVGVP)<sub>3</sub>]<sub>12</sub>

S4E8Y: [(GAGAGS)<sub>4</sub>(GVGVP)<sub>4</sub>(GYGVP)(GVGVP)<sub>3</sub>]<sub>9</sub>

Tyrosine was chosen for the guest residue in this case because it caused the transition temperature of the elastin block portion of this polymer to be in the physiological range and allowed temperature-dependent properties to be investigated, although the tyrosine SELPs did not actually demonstrate physiological temperature transitions. For initial studies, the polymers were diluted to a concentration of 0.2 mg/ml, then dried on a silicon substrate and analyzed under SEM. It was found that the polymers formed globular structures which were assumed to be micelles, which had similar sizes between the three polymers (60nm, 55nm, and 70nm average radius for polymers SE8Y, S2E8Y, and S4E8Y, respectively). The likelihood of micelle formation in this case is rather low, as the radii of the formed particles were disproportionately large as compared to their molecular weights and therefore their likely single-particle hydrodynamic radii. Further, DLS measurements estimated the  $R_H$  of the polymers to be 4.5nm for SE8Y, about 38nm for S2E8Y, and about 68nm for S4E8Y. Based on these results, it is much more likely that the observed particles were random agglomerates of many protein strands, the assembly of which are structure-dependent. In cases of low silk content, these

interactions were likely mediated by random hydrophobically-driven self-assembly for the elastin units, while increasing silk unit composition shifts to the formation of small  $\beta$ -sheet structures randomly associated with neighboring  $\beta$ -sheets or elastin units via hydrophobic interactions. The initial application of a low concentration of protein to the substrate may have resulted in a single molecule suspension; however, by drying the solution, the concentration of the protein increased, thereby resulting in the forced interaction of several polymer chains. The fact that this interaction occurred at a temperature at which silk blocks are likely to assemble into  $\beta$ -sheet structures supports the conclusion that these were random agglomerates. Further experiments presented on these polymers showed that two of the polymers possessed a fully reversible temperature transition, which began at a temperature of 41°C and completed at about 60°C. These two polymers were the SE8Y and the S2E8Y polymers, with the S4E8Y polymer showing negligible temperature response even up to 100°C. These results agree with results from lysine-containing SELPs (to be discussed) which show temperature dependence of hydrogel properties for high elastin:silk ratios, with this effect disappearing as the silk content is increased.

#### **2.4.3.4 Noncanonical amino acids**

The field of genetically engineered polymers has often taken cues from nature to aid in the design of polymer systems, which have led to significant advances in the understanding of self-assembly, protein folding, and other structural insights. Unfortunately, working exclusively with the 20 naturally occurring amino acids leaves the bioengineer with somewhat of a limited toolbox. The availability of chemistries and

substitutions on amino acid side chains has been expanded in part due to the advent of noncanonical amino acids (NCAAs). NCAAs are introduced by modification of transfer RNAs (tRNAs), which are used to assemble proteins based on an mRNA template, in addition to selective depletion of tRNAs which are desired to be replaced.<sup>238</sup>

NCAAs have proven to be very useful to many fields of research. One notable example is referred to as bio-orthogonal noncanonical amino acid tagging (BONCAT).<sup>295</sup> This method uses the inducible incorporation of the noncanonical azidohomoalanine that provide azide chemistry to proteins following induction, allowing easy separation and identification by alkyne affinity chromatography followed by tandem mass spectrometry. In the initial publication of this method, 192 proteins synthesized in a 2-hour window by HEK293 were tagged and identified.<sup>295</sup> This is a very powerful method for studying biological processes, as it allows the spatial and temporal identification of protein expression in response to environmental stimuli to be studied. Another research tool developed using NCAAs is the creation of epidermal growth factor (EGF) with p-azidophenylalanine substitution.<sup>296</sup> By incorporating this NCAA into EGF, it became photoreactive and was bound to glass slides by UV irradiation. The mechanisms of cell adhesion for an epidermoid carcinoma cell line were then studied by comparing the adhesion of these cells to the EGF-immobilized surface before and after pretreatment with soluble EGF.<sup>296</sup> Also it was shown that in hepatocytes, the EGF-immobilized surface was able to maintain hepatocyte function for 3 days, while soluble EGF incubation resulted in no hepatocyte function.<sup>296</sup>

#### 2.4.3.5 Other genetically engineered polymers

Aside from the previously discussed materials, several specifically designed and multifunctional recombinant polymers have been reported. One example of this type of material is the alanine-rich helical polypeptides, which are composed of repeating sequences of alanine, glutamine, and glutamic acid.<sup>245, 297</sup> The spacing of the glutamine and glutamic acid residues causes these peptides to self-assemble into folded  $\beta$ -sheet structures, which associate with one another head-to-head, tail-to-tail causing the histidine tags by which the peptides are purified to be adjacent to one another.<sup>298</sup> This arrangement of peptide chains causes this material to have very interesting properties related to their ability to associate with gold nanoparticles specifically at these histidine-rich regions, allowing the possibility of creating highly ordered gold nanoparticle arrays.<sup>298</sup>

Other interesting materials have been developed by incorporating specific cell binding motifs from nature into existing recombinant polymers. One example of this is the incorporation of the CS5 binding motif from fibronectin into the sequence of an elastinlike polymer.<sup>299-301</sup> It was found in these studies that the incorporation of the CS5 domain promoted HUVEC cell adhesion, spreading, and soluble factor release comparable to culture on fibronectin surfaces,<sup>299</sup> although when compared to RGD-modified polymers, the RGD sequence appeared to perform better.<sup>301</sup>

## 2.5 Silk-elastinlike protein polymers for controlled gene delivery

Due to the favorable release properties of macromolecules from SELP hydrogels, these controlled release systems were investigated as potential gene delivery depots. Early studies focused on the delivery of naked plasmid DNA from these hydrogels *in vitro* and *in vivo*, while later studies investigated the release of adenovirus *in vitro* and *in vivo*.

### 2.5.1 *In vitro* gene delivery from SELPs

#### 2.5.1.1 Release of plasmid DNA from SELP hydrogels

As an initial assessment of the utility of SELP hydrogels for gene therapy, the ability of these copolymers to deliver plasmid DNA was evaluated, as were the effects of DNA size, configuration, concentration, polymer cure time, and ionic strength of the release media. Influence of DNA configuration on release was examined for three forms of DNA: open circular, supercoiled, and linear. The experiments were performed by loading 12 wt% SELP-47K with a known concentration of DNA of a particular form, creating gels from the DNA-laden polymer, and incubating in release media of 1X PBS with 0.01% sodium azide.<sup>274</sup> DNA detection was performed using the PicoGreen reagent. It was shown that the linear DNA was most readily released with 30% release after 28 days, followed by supercoiled (24%) and open circular (~2%). The reasoning behind this dramatic decrease in DNA release from linear and supercoiled to open circular is thought to be impalement of the ring-shaped DNA on the fibers of the SELP hydrogel, which is supported by studies which have shown a similar phenomenon during gel electrophoresis of open circular plasmid DNA.<sup>274, 302, 303</sup>



The effect of the size of plasmids on the rate and extent of release was also examined by evaluating release of DNA in the range of 2.6 kbp to 11 kbp from SELP-47K hydrogels.<sup>274</sup> It was shown that release rate and extent are both highly dependent on the size of the DNA, with the 2.6 kbp molecule giving over 30% release over 1 month, while the largest molecule, 11 kbp, was less than 5% recovered after a month.<sup>274</sup> This is to be expected as all of the DNA molecules theoretically would have similar charge and therefore similar types of interaction with the SELPs, leaving size as the only determining factor for release rate. Larger sizes of DNA would be more impeded in their movement through the hydrogel for several reasons, including increased frequency of physical interaction with the polymer and the decreased diffusivity of larger molecules compared to smaller ones of similar composition and structure.

Another aspect of DNA release studied was the physical environment to which the DNA-laden hydrogels were subject. This includes investigation into the effects of hydrogel cure time, DNA concentration, and ionic strength of the release medium.<sup>273</sup> It was shown that the release of pDNA is highly dependent on ionic strength, with nearly zero release of DNA from hydrogels in ionic strength 0.10 M or lower, and greatly increased (~75%) release from hydrogels in ionic strength of 0.17 M or higher. This is explained by an increased incidence of interaction between the DNA and SELP hydrogel at ionic strengths which do not provide adequate counterions for shielding interactions between protonated primary amine groups on the SELP chain and negatively charged phosphate groups on the DNA.<sup>273</sup>

Other experiments investigated the effects of hydrogel cure time on the release of pDNA from SELP-47K. It was observed that for 8 wt% SELP-47K, there was very little

difference between release rate after 4 hours of cure time vs. 1 hour of cure time, with both of the samples reaching approximately 75-80 wt% release after the 1 month incubation. This was not the case with the 12 wt% hydrogels, which showed a stronger dependence on hydrogel cure time. The 12 wt% gel which was cured for 1 hour had both a faster rate and higher quantity of overall release (70%) than did the 12 wt% gel which was cured for 4 hours (50% release).<sup>273</sup> This is likely due to the decrease in swelling ratio and thus pore size observed as a function of cure time in previous studies,<sup>284</sup> which is likely to impede the release of the large DNA molecules. Along with this experiment, the effect of DNA concentration on release was investigated. These studies showed that in the range studied, there was no dependence of release rate or extent on the concentration of DNA loaded into the hydrogel.<sup>273</sup> The bioactivity of pDNA released from SELP-47K hydrogel was also examined using an *in vitro* cell transfection assay.<sup>274</sup> It was shown that there is little or no effect on the bioactivity of released pDNA from the hydrogels, as the expression levels for the SELP release samples were very close to those observed for DNA incubated in PBS over 1 month.<sup>274</sup>

### **2.5.1.2 Release of adenoviruses from SELP hydrogels**

A promising application of SELP hydrogels is for controlled spatial and temporal delivery of viral carriers for gene therapy. Initial studies on the release of viruses from SELP investigated the release of a green fluorescent protein (GFP)-carrying adenovirus from SELP-47K hydrogels.<sup>274</sup> This experiment was performed by loading virus into liquid SELP solution at 4 wt%, 8 wt%, or 12 wt% to a concentration of  $6 \times 10^5$  plaque forming units (PFU)/50 $\mu$ l. SELP-47K was allowed to cure for 4 hours at 37°C, then cut

into cylindrical disks of 50 $\mu$ l each. Gels were placed into 1ml of release media (PBS) and agitated for 29 days in a shaking incubator. At days 1, 8, 15, 22, and 29, the release media was removed and an aliquot was used to transfect HEK-293 cells. The results of this study showed a very strong dependence of release on polymer concentration, with 4 wt% polymer showing release for 22 days, 8 wt% releasing over 15 days, and 11.3 wt% polymer showing virtually no release. While these studies were not quantitative, they illustrated the importance of polymer concentration on controlled viral release from SELP hydrogels.

Another study on the release of adenoviruses from SELPs was performed in a similar manner, but used a much higher concentration of virus ( $1 \times 10^9$  PFU) and RT-PCR to quantify release.<sup>157</sup> Controlled release was observed over 28 days from SELP-47K at 4 wt% for the standard 50  $\mu$ l gel, and steady linear release for 4 wt% SELP as a 100  $\mu$ l gel. These results indicated that SELP-47K can effectively control the location and duration of transfection when used as a delivery system for adenoviruses. This study also investigated the bioactivity of the released viruses. It was shown that, while the number of released viruses could be controlled using SELP matrices, there appeared to be a 30-40% reduction in virus infectivity after incubation in SELPs.<sup>157</sup> It was hypothesized that this reduction in infectivity was due to inactivation of the virus by media components, specifically fetal bovine serum.

A study was performed to compare the characteristics of adenovirus release from SELP-47K and SELP-415K.<sup>277</sup> As expected, SELP-415K showed much higher rates of release than did an equivalent concentration of SELP-47K, most likely due to the increase in the length of the elastin blocks of SELP-415K compared to SELP-47K. The results of

this study indicate a structure dependence for release of adenovirus particles which shows that either higher lengths of the elastin blocks or a lower silk:elastin ratio in SELPs contribute to higher release rates and more complete release of viral load from the hydrogels. It is the manipulation of these two parameters which allows the release characteristics of SELPs to be fine-tuned for the delivery of specific therapeutic agents, including adenoviruses.

### 2.5.2 Silk-elastinlike polymers for gene delivery *in vivo*

The *in vitro* characterizations performed on SELPs and their ability to control the release of therapeutic agents yielded important information regarding not only the characteristics of the polymer itself, but also the changes in these characteristics resulting from manipulations of the polymer. It is also extremely important to evaluate the safety and biocompatibility of these polymers, as failure in this area can hamper their clinical translation for gene delivery. Finally, the efficacy of the polymer-virus approach needs to be evaluated in a disease state to clarify whether or not the level of control exercised on bioactive agent release is sufficient to give therapeutic effect with minimal adverse effects.

#### **2.5.2.1 Release of luciferase – encoding pDNA from SELP hydrogels**

In order to evaluate the ability of SELP polymer to effectively control the release of plasmid DNA, a study was performed using a reporter gene (*renilla* luciferase) to attempt to locally transfect a MDA-MB-435 tumor xenograft in athymic nude mice.<sup>274</sup> The studies were performed by first injecting the mice with a concentrated cell solution

containing  $1 \times 10^6$  cells in  $100 \mu\text{l}$  of Hank's Balanced Salt Solution. Tumors were allowed to grow until they reached a size of  $\sim 8\text{mm}$ , after which they were injected with  $100 \mu\text{l}$  of polymer 47K with pDNA encoding for *r. luciferase*. At days 3, 7, 14, 21, and 28, animals were euthanized and the tumors were resected along with the area of skin immediately surrounding the tumor for analysis of luciferase expression. It was found that in the earlier time points, there was a large difference between the luciferase expression in the tumor vs. the skin for the hydrogel-mediated delivery cohort, while there was very little difference between transfection in the tumor and transfection in the skin around the tumor. As the study moved further along, however, this difference diminished and the hydrogel showed reduced benefit beyond 7 days postinjection for most formulations. These results show that SELP is able to localize the release of pDNA over the period of approximately 1 week, after which point the intratumoral expression levels become more similar to the expression levels in the skin. While a longer period of localized transfection would be desirable, these results are positive in that localized, controlled delivery was observed. For pDNA delivery applications, it would be desirable to manipulate the polymer formulation to control the location of the transfection for longer than 1 week.

#### **2.5.2.2 Biodistribution of released adenoviral particles**

The main motivation behind delivering adenoviruses using SELPs is twofold. First, controlled delivery of therapeutics inside a tumor will likely improve efficacy, as more drug is likely to reach the target cells than systemic administration and uncontrolled intratumoral injection. Second, by controlling distribution, some of the major toxicological concerns with viral delivery can be reduced, as high titers of adenovirus

throughout the body can cause massive immunological problems and possibly death.<sup>104</sup> Off-target distribution of virus also is likely to cause hepatotoxicity due to both the high concentration of coxsackie and adenovirus receptors (CAR) and the high level of vascularization in the liver. A series of experiments were performed in order to compare the ability of SELPs to free viral injection in terms of increased transfection in a xenograft tumor and reduced distribution of virus to the liver. The initial transfection study was performed using tumor xenografts of MB-435 and FaDu cells.<sup>157</sup> The reporter gene used for these studies was GFP. Ad-GFP was injected into the tumors in 50 $\mu$ l of SELP-47K at a concentration of  $5 \times 10^8$  PFU. The results showed that there was, in fact, GFP expression in both types of tumors, although the MDA-MB-435 tumor showed more even distribution of transfection than did the FaDu tumors, due to preexisting barriers within the FaDu tumors. It was also shown that the expression of GFP lasted for approximately 11 days at a high level, after which expression depleted in the bulk of the tumor tissue and was localized around the injection site. It was hypothesized that this reduction in expression level was due to either entrapment of virus particles, release of particles into the bloodstream and eventual degradation by the liver, or virus inactivation by the mouse's humoral immune system.

### **2.5.2.3 Efficacy of SELP-mediated adenoviral gene therapy**

SELP's application as a gene delivery system for the treatment of cancer faces several challenges. While the structure and physicochemical properties of the polymer will influence its release characteristics, a perhaps more important aspect of this treatment's efficacy is the choice of therapeutic virus. The least traumatic and lowest-risk

application of SELP would be in a cancer which is readily accessible by needle without having to surgically open the patient to access the affected site. Additionally, the cancerous cells would be most vulnerable to the type of treatment being proposed if they expressed high levels of CAR receptor, as this would encourage rapid uptake of the viruses, leading to higher cell death. HNSCC is located in a very accessible area of the body, allowing simple injection of SELP directly into the tumor mass. Additionally, HNSCC cells have high CAR receptor density,<sup>114</sup> making them vulnerable to this type of treatment. For these reasons, combined with the significantly high incidence and low 5-year survival rate of this cancer, HNSCC was determined to be a viable and worthwhile target for SELP-mediated gene therapy. For *in vivo* studies on the efficacy of this treatment, a variety of different approaches were necessary due to the lack of a long-term immunocompetent HNSCC model which does not violate standards for animal treatment. In order to develop a comprehensive assessment of the efficacy of SELP-mediated gene therapy in the treatment of HNSCC, an initial efficacy study was performed using human xenograft tumors in nude mice, followed by mouse fibrosarcoma S-180 tumors grown in immunocompetent CD-1 mice.

Several cell lines were evaluated for the human xenograft study due to concerns about the effects of CAR receptor density on the ability of the adenoviruses to gain entrance into the target cells.<sup>114</sup> Two primary HNSCC cell lines, JHU-012 and JHU-022, which are isolated from the oral cavity and larynx, respectively, and a third cell line FaDu sourced from the pharynx of an HNSCC patient were used. It was shown that CAR density increases in the order of FaDu, JHU-012, JHU-022, and preliminary studies were performed on xenografts of each of these tumors. JHU-022 xenografts were chosen due

to their growth rate and ease to scale up in culture, in addition to their high CAR density. However, in experiments investigating the distribution and intensity of gene expression, it was observed that JHU-012 and JHU-022 showed very comparable intratumoral transfection levels. The reasons for this are currently under investigation; however, results are indicating that the density of the tumor's extracellular matrix has an important effect on the susceptibility of the tumor to high transfection levels.

## **2.6 Conclusions**

The use of recombinant polymers for gene therapy is at very early stages. The high degree of control over polymer sequence and length enables precise correlation of polymer structure with function. This has profound implications in both systemic and matrix-mediated gene therapy. In the context of matrix-mediated gene therapy, function of the polymeric network relates to gelation, mechanical properties, release, transfection, efficacy, degradation, elimination, and biocompatibility of the polymers. As discussed above, it has been shown that recombinant SELPs can be precisely tailor-made to control gelation time, mechanical strength, adenoviral and plasmid DNA release, temporal and spatial transfection, degradation, and efficacy in murine tumor models. In order for matrix-mediated viral gene therapy to become a viable treatment option however, it is essential that the safety and efficacy of such systems be further improved. It is imperative that a delivery strategy be found which can fully take advantage of the high transfection efficiency of viruses; however, this must be done in a manner which does not cause unreasonably high toxicity or inflammatory response to the viral vector. The role of the



immune response to the SELP/adenoviral system as related to antitumor efficacy and safety will need further detailed examination in animal models with intact immune functions.

Although SELPs show promise in improving both the safety and efficacy of adenoviral gene delivery, the hydrogels that were studied to-date were not completely degraded over the desired period of time. Hence, incorporation of additional motifs in the polymer backbone that further facilitate degradation of the hydrogels in the tumor environment is essential. Engineering degradable sequences or sequences which will increase the effective pore size of SELP hydrogels can improve release and allow more rapid degradation and elimination of the polymers following treatment.

## 2.7 References

1. Edelstein, M. Gene Therapy Clinical Trials Worldwide. <http://www.wiley.com/legacy/wileychi/genmed/clinical/> (10/18),
2. Garber, K., China approves world's first oncolytic virus therapy for cancer treatment. *J Natl Cancer Inst* **2006**, *98*, (5), 298-300.
3. Zhang, S.-w.; Xiao, S.-w.; Liu, C.-q.; Sun, Y.; Su, X.; Li, D.-m.; Xu, G.; Zhu, G.-y.; Xu, B., Recombinant adenovirus-p53 gene therapy combined with radiotherapy for head and neck squamous-cell carcinoma. *Zhonghua Zhongliu Zazhi* **2005**, *27*, (7), 426-428.
4. Hamel, W.; Magnelli, L.; Chiarugi, V. P.; Israel, M. A., Herpes simplex virus thymidine kinase/ganciclovir-mediated apoptotic death of bystander cells. *Cancer Res* **1996**, *56*, (12), 2697-2702.
5. Li, D.; Day, K. V.; Yu, S.; Shi, G.; Liu, S.; Guo, M.; Xu, Y.; Sreedharan, S.; O'Malley, B. W., Jr., The role of adenovirus-mediated retinoblastoma 94 in the treatment of head and neck cancer. *Cancer Res* **2002**, *62*, (16), 4637-4644.
6. Heiber, J. F.; Barber, G. N., Vesicular stomatitis virus expressing tumor suppressor p53 Is a highly attenuated, potent oncolytic agent. *J Virol* **2011**, *85*, (20), 10440-10450.
7. Stojdl, D. F.; Lichty, B. D.; tenOever, B. R.; Paterson, J. M.; Power, A. T.; Knowles, S.; Marius, R.; Reynard, J.; Poliquin, L.; Atkins, H.; Brown, E. G.; Durbin, R. K.; Durbin, J. E.; Hiscott, J.; Bell, J. C., VSV strains with defects in their ability to shutdown innate immunity are potent systemic anti-cancer agents. *Cancer Cell* **2003**, *4*, (4), 263-275.
8. Bischoff, J. R.; Kirn, D. H.; Williams, A.; Heise, C.; Horn, S.; Muna, M.; Ng, L.; Nye, J. A.; Sampson-Johannes, A.; Fattaey, A.; McCormick, F., An adenovirus mutant that replicates selectively in p53-deficient human tumor cells. *Science* **1996**, *274*, (5286), 373-376.
9. Chen, Q. R.; Zhang, L.; Gasper, W.; Mixson, A. J., Targeting tumor angiogenesis with gene therapy. *Mol Genet Metab* **2001**, *74*, (1-2), 120-127.
10. Samaranayake, H.; Maatta, A. M.; Pikkarainen, J.; Yla-Herttuala, S., Future prospects and challenges of antiangiogenic cancer gene therapy. *Hum Gene Ther* **2010**, *21*, (4), 381-396.
11. Ngo, M. C.; Rooney, C. M.; Howard, J. M.; Heslop, H. E., Ex vivo gene transfer for improved adoptive immunotherapy of cancer. *Hum Mol Genet* **2011**, *20*, (R1), R93-99.

12. Schmitt, T. M.; Ragnarsson, G. B.; Greenberg, P. D., T cell receptor gene therapy for cancer. *Hum Gene Ther* **2009**, *20*, (11), 1240-1248.
13. Mehier-Humbert, S.; Guy, R. H., Physical methods for gene transfer: improving the kinetics of gene delivery into cells. *Adv Drug Deliv Rev* **2005**, *57*, (5), 733-753.
14. Culver, K. W.; Ram, Z.; Wallbridge, S.; Ishii, H.; Oldfield, E. H.; Blaese, R. M., In vivo gene transfer with retroviral vector-producer cells for treatment of experimental brain tumors. *Science* **1992**, *256*, (5063), 1550-1552.
15. Cheng, Y. C.; Grill, S. P.; Dutschman, G. E.; Nakayama, K.; Bastow, K. F., Metabolism of 9-(1,3-dihydroxy-2-propoxymethyl)guanine, a new anti-herpes virus compound, in herpes simplex virus-infected cells. *J Biol Chem* **1983**, *258*, (20), 12460-12464.
16. Touraine, R. L.; Ishii-Morita, H.; Ramsey, W. J.; Blaese, R. M., The bystander effect in the HSVtk/ganciclovir system and its relationship to gap junctional communication. *Gene Ther* **1998**, *5*, (12), 1705-1711.
17. Mesnil, M.; Yamasaki, H., Bystander effect in herpes simplex virus-thymidine kinase/ganciclovir cancer gene therapy: role of gap-junctional intercellular communication. *Cancer Res* **2000**, *60*, (15), 3989-3999.
18. Zhang, X.; Multani, A. S.; Zhou, J. H.; Shay, J. W.; McConkey, D.; Dong, L.; Kim, C. S.; Rosser, C. J.; Pathak, S.; Benedict, W. F., Adenoviral-mediated retinoblastoma 94 produces rapid telomere erosion, chromosomal crisis, and caspase-dependent apoptosis in bladder cancer and immortalized human urothelial cells but not in normal urothelial cells. *Cancer Res* **2003**, *63*, (4), 760-765.
19. Roig, J. M.; Molina, M. A.; Cascante, A.; Calbo, J.; Carbo, N.; Wirtz, U.; Sreedharan, S.; Fillat, C.; Mazo, A., Adenovirus-mediated retinoblastoma 94 gene transfer induces human pancreatic tumor regression in a mouse xenograft model. *Clin Cancer Res* **2004**, *10*, (4), 1454-1462.
20. Kuruppu, D.; Tanabe, K. K., Viral oncolysis by herpes simplex virus and other viruses. *Cancer Biol Ther* **2005**, *4*, (5), 524-531.
21. Stojdl, D. F.; Lichty, B.; Knowles, S.; Marius, R.; Atkins, H.; Sonenberg, N.; Bell, J. C., Exploiting tumor-specific defects in the interferon pathway with a previously unknown oncolytic virus. *Nat Med* **2000**, *6*, (7), 821-825.
22. Kelly, E. J.; Nace, R.; Barber, G. N.; Russell, S. J., Attenuation of vesicular stomatitis virus encephalitis through microRNA targeting. *J Virol* **2010**, *84*, (3), 1550-1562.

23. Paglino, J. C.; van den Pol, A. N., Vesicular stomatitis virus has wide oncolytic activity against human sarcomas; rare resistance is overcome by blocking interferon pathways. *J Virol* **2011**, JVI. 00723-00711v00721.
24. Greenblatt, M. S.; Bennett, W. P.; Hollstein, M.; Harris, C. C., Mutations in the p53 tumor suppressor gene: clues to cancer etiology and molecular pathogenesis. *Cancer Res* **1994**, *54*, (18), 4855-4878.
25. Levine, A. J., p53, the cellular gatekeeper for growth and division. *Cell* **1997**, *88*, (3), 323-331.
26. May, P.; May, E., Twenty years of p53 research: structural and functional aspects of the p53 protein. *Oncogene* **1999**, *18*, (53), 7621-7636.
27. Folkman, J., Tumor angiogenesis: therapeutic implications. *N Engl J Med* **1971**, *285*, (21), 1182-1186.
28. Los, M.; Roodhart, J. M.; Voest, E. E., Target practice: lessons from phase III trials with bevacizumab and vatalanib in the treatment of advanced colorectal cancer. *Oncologist* **2007**, *12*, (4), 443-450.
29. Sallinen, H.; Anttila, M.; Narvainen, J.; Koponen, J.; Hamalainen, K.; Kholova, I.; Heikura, T.; Toivanen, P.; Kosma, V. M.; Heinonen, S.; Alitalo, K.; Yla-Herttuala, S., Antiangiogenic gene therapy with soluble VEGFR-1, -2, and -3 reduces the growth of solid human ovarian carcinoma in mice. *Mol Ther* **2009**, *17*, (2), 278-284.
30. Verrax, J.; Defresne, F.; Lair, F.; Vandermeulen, G.; Rath, G.; Dessy, C.; Preat, V.; Feron, O., Delivery of soluble VEGF receptor 1 (sFlt1) by gene electrotransfer as a new anti-angiogenic cancer therapy. *Mol Pharm* **2011**, *8*, 701-708.
31. Wang, L.; Yao, B.; Li, Q.; Mei, K.; Xu, J. R.; Li, H. X.; Wang, Y. S.; Wen, Y. J.; Wang, X. D.; Yang, H. S.; Li, Y. H.; Luo, F.; Wu, Y.; Liu, Y. Y.; Yang, L., Gene therapy with recombinant adenovirus encoding endostatin encapsulated in cationic liposome in coxsackievirus and adenovirus receptor-deficient colon carcinoma murine models. *Hum Gene Ther* **2011**, *22*, (9), 1061-1069.
32. Perez-Ribes, M.; Allen, E.; Hudock, J.; Takeda, T.; Okuyama, H.; Vials, F.; Inoue, M.; Bergers, G.; Hanahan, D.; Casanovas, O., Antiangiogenic therapy elicits malignant progression of tumors to increased local invasion and distant metastasis. *Cancer Cell* **2009**, *15*, (3), 220-231.
33. Keating, M.; Cazin, B.; Coutre, S.; Bhiriray, R.; Kovacs, T.; Langer, W.; Leber, B.; Maughan, T.; Rai, K.; Tjønnfjord, G., Campath-1H treatment of T-cell prolymphocytic leukemia in patients for whom at least one prior chemotherapy regimen has failed. *J Clin Oncol* **2002**, *20*, (1), 205-213.

34. Hunder, N. N.; Wallen, H.; Cao, J.; Hendricks, D. W.; Reilly, J. Z.; Rodmyre, R.; Jungbluth, A.; Gnjatic, S.; Thompson, J. A.; Yee, C., Treatment of metastatic melanoma with autologous CD4+ T cells against NY-ESO-1. *N Engl J Med* **2008**, *358*, (25), 2698-2703.
35. Turtle, C. J.; Riddell, S. R., Genetically retargeting CD8+ lymphocyte subsets for cancer immunotherapy. *Curr Opin Immunol* **2011**, *23*, (2), 299-305.
36. Berry, L. J.; Moeller, M.; Darcy, P. K., Adoptive immunotherapy for cancer: the next generation of gene-engineered immune cells. *Tissue Antigens* **2009**, *74*, (4), 277-289.
37. Haynes, N. M.; Trapani, J. A.; Teng, M. W.; Jackson, J. T.; Cerruti, L.; Jane, S. M.; Kershaw, M. H.; Smyth, M. J.; Darcy, P. K., Rejection of syngeneic colon carcinoma by CTLs expressing single-chain antibody receptors codelivering CD28 costimulation. *J Immunol* **2002**, *169*, (10), 5780-5786.
38. Jena, B.; Dotti, G.; Cooper, L. J., Redirecting T-cell specificity by introducing a tumor-specific chimeric antigen receptor. *Blood* **2010**, *116*, (7), 1035-1044.
39. Charo, J.; Finkelstein, S. E.; Grewal, N.; Restifo, N. P.; Robbins, P. F.; Rosenberg, S. A., Bcl-2 overexpression enhances tumor-specific T-cell survival. *Cancer Res* **2005**, *65*, (5), 2001-2008.
40. Scanlon, K. J., Cancer gene therapy: challenges and opportunities. *Anticancer Res* **2004**, *24*, (2A), 501-504.
41. Li, S.; Huang, L., Nonviral gene therapy: promises and challenges. *Gene Ther* **2000**, *7*, (1), 31-34.
42. Greco, O.; Scott, S. D.; Marples, B.; Dachs, G. U., Cancer gene therapy: 'delivery, delivery, delivery'. *Front Biosci* **2002**, *7*, d1516-1524.
43. Mintzer, M. A.; Simanek, E. E., Nonviral vectors for gene delivery. *Chem Rev* **2009**, *109*, (2), 259-302.
44. Segura, T.; Shea, L. D., Materials for nonviral gene delivery. *Ann Rev Mat Res* **2001**, *31*, (1), 22.
45. Pack, D. W.; Hoffman, A. S.; Pun, S.; Stayton, P. S., Design and development of polymers for gene delivery. *Nat Rev Drug Discov* **2005**, *4*, (7), 581-593.
46. Yu, H.; Wagner, E., Bioresponsive polymers for nonviral gene delivery. *Curr Opin Mol Ther* **2009**, *11*, (2), 165-178.

47. Donkuru, M. D.; Badea, I.; Wettig, S.; Verrall, R.; Elsbahy, M.; Foldvari, M., Advancing nonviral gene delivery: lipid-and surfactant-based nanoparticle design strategies. *Nanomedicine* **2010**, *5*, (7), 1103-1127.
48. Canine, B. F.; Hatefi, A., Development of recombinant cationic polymers for gene therapy research. *Adv Drug Deliv Rev* **2010**, *62*, (15), 1524-1529.
49. Petkar, K. C.; Chavhan, S. S.; Agatonovik-Kustrin, S.; Sawant, K. K., Nanostructured materials in drug and gene delivery: a review of the state of the art. *Crit Rev Ther Drug Carrier Syst* **2011**, *28*, (2), 101-164.
50. Laemmli, U. K., Characterization of DNA condensates induced by poly(ethylene oxide) and polylysine. *Proc Natl Acad Sci U S A* **1975**, *72*, (11), 4288-4292.
51. Wu, G. Y.; Wu, C. H., Receptor-mediated in vitro gene transformation by a soluble DNA carrier system. *J Biol Chem* **1987**, *262*, (10), 4429-4432.
52. Wu, G. Y.; Wu, C. H., Receptor-mediated gene delivery and expression in vivo. *J Biol Chem* **1988**, *263*, (29), 14621-14624.
53. Huang, R.; Liu, S.; Shao, K.; Han, L.; Ke, W.; Liu, Y.; Li, J.; Huang, S.; Jiang, C., Evaluation and mechanism studies of PEGylated dendrigraft poly-L-lysines as novel gene delivery vectors. *Nanotechnology* **2010**, *21*, 265101.
54. Boussif, O.; Lezoualc'h, F.; Zanta, M. A.; Mergny, M. D.; Scherman, D.; Demeneix, B.; Behr, J. P., A versatile vector for gene and oligonucleotide transfer into cells in culture and in vivo: polyethylenimine. *Proc Natl Acad Sci U S A* **1995**, *92*, (16), 7297-7301.
55. Godbey, W. T.; Wu, K. K.; Mikos, A. G., Size matters: molecular weight affects the efficiency of poly(ethylenimine) as a gene delivery vehicle. *J Biomed Mater Res* **1999**, *45*, (3), 268-275.
56. Fischer, D.; Li, Y.; Ahlemeyer, B.; Krieglstein, J.; Kissel, T., In vitro cytotoxicity testing of polycations: influence of polymer structure on cell viability and hemolysis. *Biomaterials* **2003**, *24*, (7), 1121-1131.
57. Neu, M.; Fischer, D.; Kissel, T., Recent advances in rational gene transfer vector design based on poly(ethylene imine) and its derivatives. *J Gene Med* **2005**, *7*, (8), 992-1009.
58. Thomas, M.; Lu, J. J.; Ge, Q.; Zhang, C.; Chen, J.; Klibanov, A. M., Full deacylation of polyethylenimine dramatically boosts its gene delivery efficiency and specificity to mouse lung. *Proc Natl Acad Sci U S A* **2005**, *102*, (16), 5679-5684.

59. Godbey, W. T.; Wu, K. K.; Mikos, A. G., Poly(ethylenimine)-mediated gene delivery affects endothelial cell function and viability. *Biomaterials* **2001**, *22*, (5), 471-480.
60. Plank, C.; Mechtler, K.; Szoka, F. C., Jr.; Wagner, E., Activation of the complement system by synthetic DNA complexes: a potential barrier for intravenous gene delivery. *Hum Gene Ther* **1996**, *7*, (12), 1437-1446.
61. Ogris, M.; Brunner, S.; Schuller, S.; Kircheis, R.; Wagner, E., PEGylated DNA/transferrin-PEI complexes: reduced interaction with blood components, extended circulation in blood and potential for systemic gene delivery. *Gene Ther* **1999**, *6*, (4), 595-605.
62. Merdan, T.; Kunath, K.; Petersen, H.; Bakowsky, U.; Voigt, K. H.; Kopecek, J.; Kissel, T., PEGylation of poly(ethylene imine) affects stability of complexes with plasmid DNA under in vivo conditions in a dose-dependent manner after intravenous injection into mice. *Bioconjug Chem* **2005**, *16*, (4), 785-792.
63. Kim, Y. H.; Park, J. H.; Lee, M.; Park, T. G.; Kim, S. W., Polyethylenimine with acid-labile linkages as a biodegradable gene carrier. *J Control Release* **2005**, *103*, (1), 209-219.
64. Cherng, J. Y.; van de Wetering, P.; Talsma, H.; Crommelin, D. J.; Hennink, W. E., Effect of size and serum proteins on transfection efficiency of poly ((2-dimethylamino)ethyl methacrylate)-plasmid nanoparticles. *Pharm Res* **1996**, *13*, (7), 1038-1042.
65. van de Wetering, P.; Cherng, J. Y.; Talsma, H.; Crommelin, D. J.; Hennink, W. E., 2-(Dimethylamino)ethyl methacrylate based (co)polymers as gene transfer agents. *J Control Release* **1998**, *53*, (1-3), 145-153.
66. Basarkar, A.; Singh, J., Poly (lactide-co-glycolide)-polymethacrylate nanoparticles for intramuscular delivery of plasmid encoding interleukin-10 to prevent autoimmune diabetes in mice. *Pharm Res* **2009**, *26*, (1), 72-81.
67. Mellet, C. O.; Fernández, J. M. G.; Benito, J. M., Cyclodextrin-based gene delivery systems. *Chem. Soc. Rev.* **2010**, *40*, (3), 1586-1608.
68. Ping, Y.; Liu, C.; Zhang, Z.; Liu, K. L.; Chen, J.; Li, J., Chitosan-graft-(PEI-beta-cyclodextrin) copolymers and their supramolecular PEGylation for DNA and siRNA delivery. *Biomaterials* **2011**, *32*, (32), 8328-8341.
69. Schaefer-Ridder, M.; Wang, Y.; Hofschneider, P. H., Liposomes as gene carriers: efficient transformation of mouse L cells by thymidine kinase gene. *Science* **1982**, *215*, (4529), 166-168.

70. Felgner, J. H.; Kumar, R.; Sridhar, C. N.; Wheeler, C. J.; Tsai, Y. J.; Border, R.; Ramsey, P.; Martin, M.; Felgner, P. L., Enhanced gene delivery and mechanism studies with a novel series of cationic lipid formulations. *J Biol Chem* **1994**, *269*, (4), 2550-2561.
71. Gao, X.; Huang, L., Cationic liposome-mediated gene transfer. *Gene Ther* **1995**, *2*, (10), 710-722.
72. Templeton, N. S.; Lasic, D. D.; Frederik, P. M.; Strey, H. H.; Roberts, D. D.; Pavlakis, G. N., Improved DNA: liposome complexes for increased systemic delivery and gene expression. *Nat Biotechnol* **1997**, *15*, (7), 647-652.
73. Xu, Y.; Szoka, F. C., Jr., Mechanism of DNA release from cationic liposome/DNA complexes used in cell transfection. *Biochemistry* **1996**, *35*, (18), 5616-5623.
74. Felgner, P. L.; Gadek, T. R.; Holm, M.; Roman, R.; Chan, H. W.; Wenz, M.; Northrop, J. P.; Ringold, G. M.; Danielsen, M., Lipofection: a highly efficient, lipid-mediated DNA-transfection procedure. *Proc Natl Acad Sci U S A* **1987**, *84*, (21), 7413-7417.
75. Bennett, M. J.; Aberle, A. M.; Balasubramaniam, R. P.; Malone, J. G.; Malone, R. W.; Nantz, M. H., Cationic lipid-mediated gene delivery to murine lung: correlation of lipid hydration with in vivo transfection activity. *J Med Chem* **1997**, *40*, (25), 4069-4078.
76. Gebeyehu, G.; Jessee, J. A.; Ciccarone, V. C.; Hawley-Nelson, P.; Chytil, A. Cationic lipids. 5337416, 1994.
77. Vierling, P.; Santaella, C.; Greiner, J., Highly fluorinated amphiphiles as drug and gene carrier and delivery systems. *J Fluor Chem* **2001**, *107*, (2), 337-354.
78. Dodds, E.; Dunckley, M. G.; Naujoks, K.; Michaelis, U.; Dickson, G., Lipofection of cultured mouse muscle cells: a direct comparison of Lipofectamine and DOSPER. *Gene Ther* **1998**, *5*, (4), 542-551.
79. MacLaughlin, F. C.; Mumper, R. J.; Wang, J.; Tagliaferri, J. M.; Gill, I.; Hinchcliffe, M.; Rolland, A. P., Chitosan and depolymerized chitosan oligomers as condensing carriers for in vivo plasmid delivery. *J Control Release* **1998**, *56*, (1-3), 259-272.
80. Kohama, T.; Olivera, A.; Edsall, L.; Nagiec, M. M.; Dickson, R.; Spiegel, S., Molecular cloning and functional characterization of murine sphingosine kinase. *J Biol Chem* **1998**, *273*, (37), 23722-23728.
81. Dalby, B.; Cates, S.; Harris, A.; Ohki, E. C.; Tilkins, M. L.; Price, P. J.; Ciccarone, V. C., Advanced transfection with Lipofectamine 2000 reagent: primary neurons, siRNA, and high-throughput applications. *Methods* **2004**, *33*, (2), 95-103.



82. Clements, B. A.; Incani, V.; Kucharski, C.; Lavasanifar, A.; Ritchie, B.; Uludag, H., A comparative evaluation of poly-L-lysine-palmitic acid and Lipofectamine (TM) 2000 for plasmid delivery to bone marrow stromal cells. *Biomaterials* **2007**, *28*, (31), 4693-4704.
83. Montier, T.; Benvegna, T.; Jaffres, P. A.; Yaouanc, J. J.; Lehn, P., Progress in cationic lipid-mediated gene transfection: a series of bio-inspired lipids as an example. *Curr Gene Ther* **2008**, *8*, (5), 296-312.
84. Lv, H.; Zhang, S.; Wang, B.; Cui, S.; Yan, J., Toxicity of cationic lipids and cationic polymers in gene delivery. *J Control Release* **2006**, *114*, (1), 100-109.
85. Laine, C.; Mornet, E.; Lemiegre, L.; Montier, T.; Cammas-Marion, S.; Neveu, C.; Carmoy, N.; Lehn, P.; Benvegna, T., Folate-equipped pegylated archaeal lipid derivatives: synthesis and transfection properties. *Chemistry* **2008**, *14*, (27), 8330-8340.
86. Li, L.; Song, H.; Luo, K.; He, B.; Nie, Y.; Yang, Y.; Wu, Y.; Gu, Z., Gene transfer efficacies of serum-resistant amino acids-based cationic lipids: dependence on headgroup, lipoplex stability and cellular uptake. *Int J Pharm* **2011**, *408*, (1-2), 183-190.
87. Martin, M. E.; Rice, K. G., Peptide-guided gene delivery. *AAPS J* **2007**, *9*, (1), E18-29.
88. McKenzie, D. L.; Smiley, E.; Kwok, K. Y.; Rice, K. G., Low molecular weight disulfide cross-linking peptides as nonviral gene delivery carriers. *Bioconjug Chem* **2000**, *11*, (6), 901-909.
89. Bolhassani, A., Potential efficacy of cell-penetrating peptides for nucleic acid and drug delivery in cancer. *Biochim Biophys Acta* **2011**, *1816*, (2), 232-246.
90. Wiley, D. C.; Skehel, J. J., The structure and function of the hemagglutinin membrane glycoprotein of influenza virus. *Annu Rev Biochem* **1987**, *56*, 365-394.
91. Wagner, E.; Plank, C.; Zatloukal, K.; Cotten, M.; Birnstiel, M. L., Influenza virus hemagglutinin HA-2 N-terminal fusogenic peptides augment gene transfer by transferrin-polylysine-DNA complexes: toward a synthetic virus-like gene-transfer vehicle. *Proc Natl Acad Sci U S A* **1992**, *89*, (17), 7934-7938.
92. Ruben, S.; Perkins, A.; Purcell, R.; Joung, K.; Sia, R.; Burghoff, R.; Haseltine, W. A.; Rosen, C. A., Structural and functional characterization of human immunodeficiency virus tat protein. *J Virol* **1989**, *63*, (1), 1-8.
93. Rudolph, C.; Plank, C.; Lausier, J.; Schillinger, U.; Muller, R. H.; Rosenecker, J., Oligomers of the arginine-rich motif of the HIV-1 TAT protein are capable of transferring plasmid DNA into cells. *J Biol Chem* **2003**, *278*, (13), 11411-11418.

94. Wyman, T. B.; Nicol, F.; Zelphati, O.; Scaria, P. V.; Plank, C.; Szoka, F. C., Jr., Design, synthesis, and characterization of a cationic peptide that binds to nucleic acids and permeabilizes bilayers. *Biochemistry* **1997**, *36*, (10), 3008-3017.
95. Collins, L.; Fabre, J. W., A synthetic peptide vector system for optimal gene delivery to corneal endothelium. *J Gene Med* **2004**, *6*, (2), 185-194.
96. Nie, Y.; Schaffert, D.; Rodl, W.; Ogris, M.; Wagner, E.; Gunther, M., Dual-targeted polyplexes: one step towards a synthetic virus for cancer gene therapy. *J Control Release* **2011**, *152*, (1), 127-134.
97. Tian, H.; Lin, L.; Chen, J.; Chen, X.; Park, T. G.; Maruyama, A., RGD targeting hyaluronic acid coating system for PEI-PBLG polycation gene carriers. *J Control Release* **2011**, *155*, (1), 47-53.
98. Haubner, R.; Wester, H. J.; Burkhart, F.; Senekowitsch-Schmidtke, R.; Weber, W.; Goodman, S. L.; Kessler, H.; Schwaiger, M., Glycosylated RGD-containing peptides: tracer for tumor targeting and angiogenesis imaging with improved biokinetics. *J Nucl Med* **2001**, *42*, (2), 326-336.
99. Hatefi, A.; Megeed, Z.; Ghandehari, H., Recombinant polymer-protein fusion: a promising approach towards efficient and targeted gene delivery. *J Gene Med* **2006**, *8*, (4), 468-476.
100. Sosnowski, B. A.; Gonzalez, A. M.; Chandler, L. A.; Buechler, Y. J.; Pierce, G. F.; Baird, A., Targeting DNA to cells with basic fibroblast growth factor (FGF2). *J Biol Chem* **1996**, *271*, (52), 33647-33653.
101. Lozier, J. N.; Yankaskas, J. R.; Ramsey, W. J.; Chen, L.; Berschneider, H.; Morgan, R. A., Gut epithelial cells as targets for gene therapy of hemophilia. *Hum Gene Ther* **1997**, *8*, (12), 1481-1490.
102. Huh, S. H.; Do, H. J.; Lim, H. Y.; Kim, D. K.; Choi, S. J.; Song, H.; Kim, N. H.; Park, J. K.; Chang, W. K.; Chung, H. M.; Kim, J. H., Optimization of 25 kDa linear polyethylenimine for efficient gene delivery. *Biologicals* **2007**, *35*, (3), 165-171.
103. Young, L. S.; Searle, P. F.; Onion, D.; Mautner, V., Viral gene therapy strategies: from basic science to clinical application. *J Pathol* **2006**, *208*, (2), 299-318.
104. Raper, S. E.; Chirmule, N.; Lee, F. S.; Wivel, N. A.; Bagg, A.; Gao, G. P.; Wilson, J. M.; Batshaw, M. L., Fatal systemic inflammatory response syndrome in a ornithine transcarbamylase deficient patient following adenoviral gene transfer. *Mol Genet Metab* **2003**, *80*, (1-2), 148-158.

105. Minutes of Symposium and Meeting, December 8-10, 1999. In Recombinant DNA Advisory Committee, U.S. Department of Health and Human Services, Public Health Service, National Institutes of Health, Bethesda, MD, 1999.
106. Hacein-Bey-Abina, S.; Le Deist, F.; Carlier, F.; Bouneaud, C.; Hue, C.; De Villartay, J. P.; Thrasher, A. J.; Wulffraat, N.; Sorensen, R.; Dupuis-Girod, S.; Fischer, A.; Davies, E. G.; Kuis, W.; Leiva, L.; Cavazzana-Calvo, M., Sustained correction of X-linked severe combined immunodeficiency by ex vivo gene therapy. *N Engl J Med* **2002**, *346*, (16), 1185-1193.
107. Hacein-Bey-Abina, S.; von Kalle, C.; Schmidt, M.; Le Deist, F.; Wulffraat, N.; McIntyre, E.; Radford, I.; Villeval, J. L.; Fraser, C. C.; Cavazzana-Calvo, M.; Fischer, A., A serious adverse event after successful gene therapy for X-linked severe combined immunodeficiency. *N Engl J Med* **2003**, *348*, (3), 255-256.
108. Howe, S. J.; Mansour, M. R.; Schwarzwaelder, K.; Bartholomae, C.; Hubank, M.; Kempfski, H.; Brugman, M. H.; Pike-Overzet, K.; Chatters, S. J.; de Ridder, D.; Gilmour, K. C.; Adams, S.; Thornhill, S. I.; Parsley, K. L.; Staal, F. J.; Gale, R. E.; Linch, D. C.; Bayford, J.; Brown, L.; Quaye, M.; Kinnon, C.; Ancliff, P.; Webb, D. K.; Schmidt, M.; von Kalle, C.; Gaspar, H. B.; Thrasher, A. J., Insertional mutagenesis combined with acquired somatic mutations causes leukemogenesis following gene therapy of SCID-X1 patients. *J Clin Invest* **2008**, *118*, (9), 3143-3150.
109. Frank, K. M.; Hogarth, D. K.; Miller, J. L.; Mandal, S.; Mease, P. J.; Samulski, R. J.; Weisgerber, G. A.; Hart, J., Investigation of the cause of death in a gene-therapy trial. *N Engl J Med* **2009**, *361*, (2), 161-169.
110. Jooss, K.; Chirmule, N., Immunity to adenovirus and adeno-associated viral vectors: implications for gene therapy. *Gene Ther* **2003**, *10*, (11), 955-963.
111. Nemerow, G. R.; Stewart, P. L., Role of alpha(v) integrins in adenovirus cell entry and gene delivery. *Microbiol Mol Biol Rev* **1999**, *63*, (3), 725-734.
112. Medina-Kauwe, L. K., Endocytosis of adenovirus and adenovirus capsid proteins. *Adv Drug Deliv Rev* **2003**, *55*, (11), 1485-1496.
113. Routes, J. M., Role of Natural Killer (NK) Cells in Immunity to Adenoviruses. *Adenovirus Methods and Protocols* **1998**, *1*, 129-141.
114. Li, D.; Duan, L.; Freimuth, P.; O'Malley, B. W., Jr., Variability of adenovirus receptor density influences gene transfer efficiency and therapeutic response in head and neck cancer. *Clin Cancer Res* **1999**, *5*, (12), 4175-4181.
115. Ram, Z.; Culver, K. W.; Oshiro, E. M.; Viola, J. J.; DeVroom, H. L.; Otto, E.; Long, Z.; Chiang, Y.; McGarrity, G. J.; Muul, L. M.; Katz, D.; Blaese, R. M.; Oldfield,

E. H., Therapy of malignant brain tumors by intratumoral implantation of retroviral vector-producing cells. *Nat Med* **1997**, *3*, (12), 1354-1361.

116. Huber, B. E.; Richards, C. A.; Krenitsky, T. A., Retroviral-mediated gene therapy for the treatment of hepatocellular carcinoma: an innovative approach for cancer therapy. *Proc Natl Acad Sci U S A* **1991**, *88*, (18), 8039-8043.

117. Wu, Z.; Asokan, A.; Samulski, R. J., Adeno-associated virus serotypes: vector toolkit for human gene therapy. *Mol Ther* **2006**, *14*, (3), 316-327.

118. Boutin, S.; Monteilhet, V.; Veron, P.; Leborgne, C.; Benveniste, O.; Montus, M. F.; Masurier, C., Prevalence of serum IgG and neutralizing factors against adeno-associated virus (AAV) types 1, 2, 5, 6, 8, and 9 in the healthy population: implications for gene therapy using AAV vectors. *Hum Gene Ther* **2010**, *21*, (6), 704-712.

119. Fisher, K. J.; Jooss, K.; Alston, J.; Yang, Y.; Haecker, S. E.; High, K.; Pathak, R.; Raper, S. E.; Wilson, J. M., Recombinant adeno-associated virus for muscle directed gene therapy. *Nat Med* **1997**, *3*, (3), 306-312.

120. Noe, F. M.; Sørensen, A. T.; Kokaia, M.; Vezzani, A., Gene therapy of focal-onset epilepsy by adeno-associated virus vector-mediated overexpression of neuropeptide Y. *Epilepsia* **2010**, *51*, 96.

121. Vandenberghe, L. H.; Auricchio, A., Novel adeno-associated viral vectors for retinal gene therapy. *Gene Ther* **2012**, *19*, (2), 162-168.

122. Guse, K.; Cerullo, V.; Hemminki, A., Oncolytic vaccinia virus for the treatment of cancer. *Expert Opin Biol Ther* **2011**, *11*, (5), 595-608.

123. Lukashev, M. E.; Werb, Z., ECM signalling: orchestrating cell behaviour and misbehaviour. *Trends Cell Biol* **1998**, *8*, (11), 437-441.

124. Sanford, J. C.; Klein, T. M.; Wolf, E. D.; Allen, N., Delivery of substances into cells and tissues using a particle bombardment process. *Particulate Sci Tech* **1987**, *5*, (1), 27-37.

125. Klein, T. M.; Arentzen, R.; Lewis, P. A.; Fitzpatrick-McElligott, S., Transformation of microbes, plants and animals by particle bombardment. *Biotechnology (N Y)* **1992**, *10*, (3), 286-291.

126. Klein, T. M.; Wolf, E. D.; Wu, R.; Sanford, J. C., High-velocity microprojectiles for delivering nucleic acids into living cells. *Nature* **1987**, *327*, (6117), 70-73.

127. Williams, R. S.; Johnston, S. A.; Riedy, M.; DeVit, M. J.; McElligott, S. G.; Sanford, J. C., Introduction of foreign genes into tissues of living mice by DNA-coated microprojectiles. *PNAS* **1991**, *88*, (7), 2726-2730.

128. Voiland M, M. L., Development of the "Gene Gun" at Cornell. *New York State Agricultural Experiment Station News Release* 1999.
129. Daniel, H., *Transformation and Foreign Gene Expression in Plants Mediated by Microprojectile Bombardment*. 1997; Vol. 62.
130. Becker, D.; Brettschneider, R.; Lorz, H., Fertile transgenic wheat from microprojectile bombardment of scutellar tissue. *Plant J* **1994**, 5, (2), 299-307.
131. Iida, A.; Seki, M.; Kamada, M.; Yamada, Y.; Morikawa, H., Gene delivery into cultured plant cells by DNA-coated gold particles accelerated by a pneumatic particle gun. *TAG Theoretical and Applied Genetics* **1990**, 80, (6), 813-816.
132. Sawahel, W.; Onde, S.; Knight, C.; Cove, D., Transfer of foreign DNA into *Physcomitrella patens* protonemal tissue by using the gene gun. *Plant Mol Biol Rep* **1992**, 10, (4), 314-315.
133. Chung, B. Y.; Miller, W. A.; Atkins, J. F.; Firth, A. E., An overlapping essential gene in the Potyviridae. *Proc Natl Acad Sci U S A* **2008**, 105, (15), 5897-5902.
134. Curin, M.; Ojangu, E. L.; Trutnyeva, K.; Ilau, B.; Truve, E.; Waigmann, E., MPB2C, a microtubule-associated plant factor, is required for microtubular accumulation of tobacco mosaic virus movement protein in plants. *Plant Phys* **2007**, 143, (2), 801-811.
135. Cheng, L.; Ziegelhoffer, P. R.; Yang, N. S., In vivo promoter activity and transgene expression in mammalian somatic tissues evaluated by using particle bombardment. *Proc Natl Acad Sci US A* **1993**, 90, (10), 4455-4459.
136. Shiraishi, A.; Converse, R. L.; Liu, C. Y.; Zhou, F.; Kao, C. W.; Kao, W. W., Identification of the cornea-specific keratin 12 promoter by in vivo particle-mediated gene transfer. *Invest Ophthalmol Vis Sci* **1998**, 39, (13), 2554-2561.
137. Neumann, E.; Schaefer-Ridder, M.; Wang, Y.; Hofschneider, P. H., Gene transfer into mouse lymphoma cells by electroporation in high electric fields. *EMBO J* **1982**, 1, (7), 841.
138. Gehl, J., Electroporation: theory and methods, perspectives for drug delivery, gene therapy and research. *Acta Physiol Scand* **2003**, 177, (4), 437-447.
139. Schoenbach, K. H.; Beebe, S. J.; Buescher, E. S., Intracellular effect of ultrashort electrical pulses. *Bioelectromagnetics* **2001**, 22, (6), 440-448.
140. Sersa, G.; Miklavcic, D.; Cemazar, M.; Rudolf, Z.; Pucihar, G.; Snoj, M., Electrochemotherapy in treatment of tumours. *Eur J Surg Oncol* **2008**, 34, (2), 232-240.

141. Zhang, G.; Gao, X.; Song, Y. K.; Vollmer, R.; Stolz, D. B.; Gasiorowski, J. Z.; Dean, D. A.; Liu, D., Hydroporation as the mechanism of hydrodynamic delivery. *Gene Ther* **2004**, *11*, (8), 675-682.
142. Liang, K. W.; Nishikawa, M.; Liu, F.; Sun, B.; Ye, Q.; Huang, L., Restoration of dystrophin expression in mdx mice by intravascular injection of naked DNA containing full-length dystrophin cDNA. *Gene Ther* **2004**, *11*, (11), 901-908.
143. Abrahams, J. M.; Song, C.; DeFelice, S.; Grady, M. S.; Diamond, S. L.; Levy, R. J., Endovascular microcoil gene delivery using immobilized anti-adenovirus antibody for vector tethering. *Stroke* **2002**, *33*, (5), 1376-1382.
144. Gersbach, C. A.; Coyer, S. R.; Le Doux, J. M.; Garcia, A. J., Biomaterial-mediated retroviral gene transfer using self-assembled monolayers. *Biomaterials* **2007**, *28*, (34), 5121-5127.
145. Levy, R. J.; Song, C.; Tallapragada, S.; DeFelice, S.; Hinson, J. T.; Vyavahare, N.; Connolly, J.; Ryan, K.; Li, Q., Localized adenovirus gene delivery using antiviral IgG complexation. *Gene Ther* **2001**, *8*, (9), 659-667.
146. Stachelek, S. J.; Song, C.; Alferiev, I.; Defelice, S.; Cui, X.; Connolly, J. M.; Bianco, R. W.; Levy, R. J., Localized gene delivery using antibody tethered adenovirus from polyurethane heart valve cusps and intra-aortic implants. *Gene Ther* **2004**, *11*, (1), 15-24.
147. Kalyanasundaram, S.; Feinstein, S.; Nicholson, J. P.; Leong, K. W.; Garver, R. L., Coacervate microspheres as carriers of recombinant adenoviruses. *Cancer Gene Ther* **1999**, *6*, (2), 107-112.
148. Pandori, M.; Hobson, D.; Sano, T., Adenovirus-microbead conjugates possess enhanced infectivity: a new strategy for localized gene delivery. *Virology* **2002**, *299*, (2), 204-212.
149. Sailaja, G.; HogenEsch, H.; North, A.; Hays, J.; Mittal, S. K., Encapsulation of recombinant adenovirus into alginate microspheres circumvents vector-specific immune response. *Gene Ther* **2002**, *9*, (24), 1722-1729.
150. Andree, C.; Voigt, M.; Wenger, A.; Erichsen, T.; Bittner, K.; Schaefer, D.; Walgenbach, K. J.; Borges, J.; Horch, R. E.; Eriksson, E.; Stark, G. B., Plasmid gene delivery to human keratinocytes through a fibrin-mediated transfection system. *Tissue Eng* **2001**, *7*, (6), 757-766.
151. Beer, S. J.; Matthews, C. B.; Stein, C. S.; Ross, B. D.; Hilfinger, J. M.; Davidson, B. L., Poly (lactic-glycolic) acid copolymer encapsulation of recombinant adenovirus reduces immunogenicity in vivo. *Gene Ther* **1998**, *5*, (6), 740-746.

152. Breen, A.; Strappe, P.; Kumar, A.; O'Brien, T.; Pandit, A., Optimization of a fibrin scaffold for sustained release of an adenoviral gene vector. *J Biomed Mater Res A* **2006**, *78*, (4), 702-708.
153. Gu, D. L.; Nguyen, T.; Gonzalez, A. M.; Printz, M. A.; Pierce, G. F.; Sosnowski, B. A.; Phillips, M. L.; Chandler, L. A., Adenovirus encoding human platelet-derived growth factor-B delivered in collagen exhibits safety, biodistribution, and immunogenicity profiles favorable for clinical use. *Mol Ther* **2004**, *9*, (5), 699-711.
154. Nof, M.; Shea, L. D., Drug-releasing scaffolds fabricated from drug-loaded microspheres. *J Biomed Mater Res* **2002**, *59*, (2), 349-356.
155. Pascher, A.; Palmer, G. D.; Steinert, A.; Oligino, T.; Gouze, E.; Gouze, J. N.; Betz, O.; Spector, M.; Robbins, P. D.; Evans, C. H.; Ghivizzani, S. C., Gene delivery to cartilage defects using coagulated bone marrow aspirate. *Gene Ther* **2004**, *11*, (2), 133-141.
156. Quick, D. J.; Anseth, K. S., Gene delivery in tissue engineering: a photopolymer platform to coencapsulate cells and plasmid DNA. *Pharm Res* **2003**, *20*, (11), 1730-1737.
157. Hatefi, A.; Cappello, J.; Ghandehari, H., Adenoviral gene delivery to solid tumors by recombinant silk-elastinlike protein polymers. *Pharm Res* **2007**, *24*, (4), 773-779.
158. Bielinska, A. U.; Yen, A.; Wu, H. L.; Zahos, K. M.; Sun, R.; Weiner, N. D.; Baker, J. R., Jr.; Roessler, B. J., Application of membrane-based dendrimer/DNA complexes for solid phase transfection in vitro and in vivo. *Biomaterials* **2000**, *21*, (9), 877-887.
159. Segura, T.; Volk, M. J.; Shea, L. D., Substrate-mediated DNA delivery: role of the cationic polymer structure and extent of modification. *J Control Release* **2003**, *93*, (1), 69-84.
160. Segura, T.; Chung, P. H.; Shea, L. D., DNA delivery from hyaluronic acid-collagen hydrogels via a substrate-mediated approach. *Biomaterials* **2005**, *26*, (13), 1575-1584.
161. Doukas, J.; Chandler, L. A.; Gonzalez, A. M.; Gu, D.; Hoganson, D. K.; Ma, C.; Nguyen, T.; Printz, M. A.; Nesbit, M.; Herlyn, M.; Crombleholme, T. M.; Aukerman, S. L.; Sosnowski, B. A.; Pierce, G. F., Matrix immobilization enhances the tissue repair activity of growth factor gene therapy vectors. *Hum Gene Ther* **2001**, *12*, (7), 783-798.
162. Ochiya, T.; Nagahara, S.; Sano, A.; Itoh, H.; Terada, M., Biomaterials for gene delivery: atelocollagen-mediated controlled release of molecular medicines. *Curr Gene Ther* **2001**, *1*, (1), 31-52.

163. Fang, J.; Zhu, Y. Y.; Smiley, E.; Bonadio, J.; Rouleau, J. P.; Goldstein, S. A.; McCauley, L. K.; Davidson, B. L.; Roessler, B. J., Stimulation of new bone formation by direct transfer of osteogenic plasmid genes. *Proc Natl Acad Sci U S A* **1996**, *93*, (12), 5753-5758.
164. Tyrone, J. W.; Mogford, J. E.; Chandler, L. A.; Ma, C.; Xia, Y.; Pierce, G. F.; Mustoe, T. A., Collagen-embedded platelet-derived growth factor DNA plasmid promotes wound healing in a dermal ulcer model. *J Surg Res* **2000**, *93*, (2), 230-236.
165. Bonadio, J.; Smiley, E.; Patil, P.; Goldstein, S., Localized, direct plasmid gene delivery in vivo: prolonged therapy results in reproducible tissue regeneration. *Nat Med* **1999**, *5*, (7), 753-759.
166. Ochiya, T.; Takahama, Y.; Nagahara, S.; Sumita, Y.; Hisada, A.; Itoh, H.; Nagai, Y.; Terada, M., New delivery system for plasmid DNA in vivo using atelocollagen as a carrier material: the Minipellet. *Nat Med* **1999**, *5*, (6), 707-710.
167. Cohen-Sacks, H.; Elazar, V.; Gao, J.; Golomb, A.; Adwan, H.; Korchov, N.; Levy, R. J.; Berger, M. R.; Golomb, G., Delivery and expression of pDNA embedded in collagen matrices. *J Control Release* **2004**, *95*, (2), 309-320.
168. Chandler, L. A.; Gu, D. L.; Ma, C.; Gonzalez, A. M.; Doukas, J.; Nguyen, T.; Pierce, G. F.; Phillips, M. L., Matrix-enabled gene transfer for cutaneous wound repair. *Wound Repair Regen* **2000**, *8*, (6), 473-479.
169. Chandler, L. A.; Doukas, J.; Gonzalez, A. M.; Hoganson, D. K.; Gu, D. L.; Ma, C.; Nesbit, M.; Crombleholme, T. M.; Herlyn, M.; Sosnowski, B. A.; Pierce, G. F., FGF2-Targeted adenovirus encoding platelet-derived growth factor-B enhances de novo tissue formation. *Mol Ther* **2000**, *2*, (2), 153-160.
170. Hijjawi, J.; Mogford, J. E.; Chandler, L. A.; Cross, K. J.; Said, H.; Sosnowski, B. A.; Mustoe, T. A., Platelet-derived growth factor B, but not fibroblast growth factor 2, plasmid DNA improves survival of ischemic myocutaneous flaps. *Arch Surg* **2004**, *139*, (2), 142-147.
171. Breen, A. M.; Dockery, P.; O'Brien, T.; Pandit, A. S., The use of therapeutic gene eNOS delivered via a fibrin scaffold enhances wound healing in a compromised wound model. *Biomaterials* **2008**, *29*, (21), 3143-3151.
172. Schek, R. M.; Hollister, S. J.; Krebsbach, P. H., Delivery and protection of adenoviruses using biocompatible hydrogels for localized gene therapy. *Mol Ther* **2004**, *9*, (1), 130-138.
173. Beer, S. J.; Hilfinger, J. M.; Davidson, B. L., Extended release of adenovirus from polymer microspheres: potential use in gene therapy for brain tumors. *Adv Drug Deliv Rev* **1997**, *27*, (1), 59-66.



174. Eliaz, R. E.; Szoka, F. C., Jr., Robust and prolonged gene expression from injectable polymeric implants. *Gene Ther* **2002**, *9*, (18), 1230-1237.
175. Lee, P. Y.; Li, Z.; Huang, L., Thermosensitive hydrogel as a Tgf-beta1 gene delivery vehicle enhances diabetic wound healing. *Pharm Res* **2003**, *20*, (12), 1995-2000.
176. Li, Z.; Ning, W.; Wang, J.; Choi, A.; Lee, P. Y.; Tyagi, P.; Huang, L., Controlled gene delivery system based on thermosensitive biodegradable hydrogel. *Pharm Res* **2003**, *20*, (6), 884-888.
177. Quick, D. J.; Anseth, K. S., DNA delivery from photocrosslinked PEG hydrogels: encapsulation efficiency, release profiles, and DNA quality. *J Control Release* **2004**, *96*, (2), 341-351.
178. Shea, L. D.; Smiley, E.; Bonadio, J.; Mooney, D. J., DNA delivery from polymer matrices for tissue engineering. *Nat Biotechnol* **1999**, *17*, (6), 551-554.
179. Argiris, A.; Karamouzis, M. V.; Raben, D.; Ferris, R. L., Head and neck cancer. *Lancet* **2008**, *371*, (9625), 1695-1709.
180. Jemal, A.; Bray, F.; Center, M. M.; Ferlay, J.; Ward, E.; Forman, D., Global cancer statistics. *CA Cancer J Clin* **2011**, *61*, (2), 69-90.
181. *American Cancer Society. Cancer Facts & Figures 2011.*; American Cancer Society: Atlanta, 2011.
182. Vineis, P.; Alavanja, M.; Buffler, P.; Fontham, E.; Franceschi, S.; Gao, Y. T.; Gupta, P. C.; Hackshaw, A.; Matos, E.; Samet, J.; Sitas, F.; Smith, J.; Stayner, L.; Straif, K.; Thun, M. J.; Wichmann, H. E.; Wu, A. H.; Zaridze, D.; Peto, R.; Doll, R., Tobacco and cancer: recent epidemiological evidence. *J Natl Cancer Inst* **2004**, *96*, (2), 99-106.
183. Lopez, R. V.; Zago, M. A.; Eluf-Neto, J.; Curado, M. P.; Daudt, A. W.; da Silva-Junior, W. A.; Zanette, D. L.; Levi, J. E.; de Carvalho, M. B.; Kowalski, L. P.; Abrahao, M.; de Gois-Filho, J. F.; Boffetta, P.; Wunsch-Filho, V., Education, tobacco smoking, alcohol consumption, and IL-2 and IL-6 gene polymorphisms in the survival of head and neck cancer. *Braz J Med Biol Res* **2011**, *44*, (10), 1006-1012.
184. Lubin, J. H.; Muscat, J.; Gaudet, M. M.; Olshan, A. F.; Curado, M. P.; Dal Maso, L.; Wunsch-Filho, V.; Sturgis, E. M.; Szeszenia-Dabrowska, N.; Castellsague, X.; Zhang, Z. F.; Smith, E.; Fernandez, L.; Matos, E.; Franceschi, S.; Fabianova, E.; Rudnai, P.; Purdue, M. P.; Mates, D.; Wei, Q.; Herrero, R.; Kelsey, K.; Morgenstern, H.; Shangina, O.; Koifman, S.; Lissowska, J.; Levi, F.; Daudt, A. W.; Neto, J. E.; Chen, C.; Lazarus, P.; Winn, D. M.; Schwartz, S. M.; Boffetta, P.; Brennan, P.; Menezes, A.; La Vecchia, C.; McClean, M.; Talamini, R.; Rajkumar, T.; Hayes, R. B.; Hashibe, M., An examination of male and female odds ratios by BMI, cigarette smoking, and alcohol consumption for

cancers of the oral cavity, pharynx, and larynx in pooled data from 15 case-control studies. *Cancer Causes Control* **2011**, *22*, (9), 1217-1231.

185. Pelucchi, C.; Tramacere, I.; Boffetta, P.; Negri, E.; La Vecchia, C., Alcohol consumption and cancer risk. *Nutr Cancer* **2011**, *63*, (7), 983-990.

186. Burgaz, S.; Coskun, E.; Demircigil, G. C.; Kocabas, N. A.; Cetindag, F.; Sunter, O.; Edinsel, H., Micronucleus frequencies in lymphocytes and buccal epithelial cells from patients having head and neck cancer and their first-degree relatives. *Mutagenesis* **2011**, *26*, (2), 351-356.

187. Negri, E.; Boffetta, P.; Berthiller, J.; Castellsague, X.; Curado, M. P.; Dal Maso, L.; Daudt, A. W.; Fabianova, E.; Fernandez, L.; Wunsch-Filho, V.; Franceschi, S.; Hayes, R. B.; Herrero, R.; Koifman, S.; Lazarus, P.; Lence, J. J.; Levi, F.; Mates, D.; Matos, E.; Menezes, A.; Muscat, J.; Eluf-Neto, J.; Olshan, A. F.; Rudnai, P.; Shangina, O.; Sturgis, E. M.; Szeszenia-Dabrowska, N.; Talamini, R.; Wei, Q.; Winn, D. M.; Zaridze, D.; Lissowska, J.; Zhang, Z. F.; Ferro, G.; Brennan, P.; La Vecchia, C.; Hashibe, M., Family history of cancer: pooled analysis in the International Head and Neck Cancer Epidemiology Consortium. *Int J Cancer* **2009**, *124*, (2), 394-401.

188. Bishop, J. A.; Westra, W. H., Human papillomavirus-related small cell carcinoma of the oropharynx. *Am J Surg Pathol* **2011**, *35*, (11), 1679-1684.

189. Sudhoff, H. H.; Schwarze, H. P.; Winder, D.; Steinstraesser, L.; Gorner, M.; Stanley, M.; Goon, P. K., Evidence for a causal association for HPV in head and neck cancers. *Eur Arch Otorhinolaryngol* **2011**, *268*, (11), 1541-1547.

190. Gillison, M. L.; Koch, W. M.; Capone, R. B.; Spafford, M.; Westra, W. H.; Wu, L.; Zahurak, M. L.; Daniel, R. W.; Viglione, M.; Symer, D. E.; Shah, K. V.; Sidransky, D., Evidence for a causal association between human papillomavirus and a subset of head and neck cancers. *J Natl Cancer Inst* **2000**, *92*, (9), 709-720.

191. Koutsky, L. A.; Ault, K. A.; Wheeler, C. M.; Brown, D. R.; Barr, E.; Alvarez, F. B.; Chiacchierini, L. M.; Jansen, K. U., A controlled trial of a human papillomavirus type 16 vaccine. *N Engl J Med* **2002**, *347*, (21), 1645-1651.

192. Munoz, N.; Bosch, F. X.; de Sanjose, S.; Herrero, R.; Castellsague, X.; Shah, K. V.; Snijders, P. J.; Meijer, C. J., Epidemiologic classification of human papillomavirus types associated with cervical cancer. *N Engl J Med* **2003**, *348*, (6), 518-527.

193. Walboomers, J. M. M.; Jacobs, M. V.; Manos, M. M.; Bosch, F. X.; Kummer, J. A.; Shah, K. V.; Snijders, P. J. F.; Peto, J.; Meijer, C. J. L. M.; Munoz, N., Human papillomavirus is a necessary cause of invasive cervical cancer worldwide. *J Pathol* **1999**, *189*, (1), 12-19.

194. Bosch, F. X.; Manos, M. M.; Munoz, N.; Sherman, M.; Jansen, A. M.; Peto, J.; Schiffman, M. H.; Moreno, V.; Kurman, R.; Shah, K. V., Prevalence of human papillomavirus in cervical cancer: a worldwide perspective. International biological study on cervical cancer (IBSCC) Study Group. *J Natl Cancer Inst* **1995**, *87*, (11), 796-802.
195. Villa, L. L., Quadrivalent vaccine against human papillomavirus to prevent high-grade cervical lesions. *N Engl J Med* **2007**, *356*, (19), 1915-1927.
196. Islam, S.; Ahmed, M.; Walton, G. M.; Dinan, T. G.; Hoffman, G. R., The association between depression and anxiety disorders following facial trauma--a comparative study. *Injury* **2010**, *41*, (1), 92-96.
197. Raza, S.; Kornblum, N.; Kancharla, V. P.; Baig, M. A.; Singh, A. B.; Kalavar, M., Emerging therapies in the treatment of locally advanced squamous cell cancers of head and neck. *Recent Pat Anticancer Drug Discov* **2011**, *6*, (2), 246-257.
198. Bourhis, J.; Overgaard, J.; Audry, H.; Ang, K. K.; Saunders, M.; Bernier, J.; Horiot, J. C.; Le Maitre, A.; Pajak, T. F.; Poulsen, M. G.; O'Sullivan, B.; Dobrowsky, W.; Hliniak, A.; Skladowski, K.; Hay, J. H.; Pinto, L. H.; Fallai, C.; Fu, K. K.; Sylvester, R.; Pignon, J. P., Hyperfractionated or accelerated radiotherapy in head and neck cancer: a meta-analysis. *Lancet* **2006**, *368*, (9538), 843-854.
199. Parsons, J. T.; Mendenhall, W. M.; Cassisi, N. J.; Isaacs, J. H., Jr.; Million, R. R., Hyperfractionation for head and neck cancer. *Int J Radiat Oncol Biol Phys* **1988**, *14*, (4), 649-658.
200. Pignon, J. P.; Bourhis, J.; Domenge, C.; Designe, L., Chemotherapy added to locoregional treatment for head and neck squamous-cell carcinoma: three meta-analyses of updated individual data. MACH-NC Collaborative Group. Meta-Analysis of Chemotherapy on Head and Neck Cancer. *Lancet* **2000**, *355*, (9208), 949-955.
201. Pignon, J. P.; le Maitre, A.; Maillard, E.; Bourhis, J., Meta-analysis of chemotherapy in head and neck cancer (MACH-NC): an update on 93 randomised trials and 17,346 patients. *Radiother Oncol* **2009**, *92*, (1), 4-14.
202. Rosenthal, E. L.; Matrisian, L. M., Matrix metalloproteases in head and neck cancer. *Head Neck* **2006**, *28*, (7), 639-648.
203. Rose, P. G.; Bundy, B. N.; Watkins, E. B.; Thigpen, J. T.; Deppe, G.; Maiman, M. A.; Clarke-Pearson, D. L.; Insalaco, S., Concurrent cisplatin-based radiotherapy and chemotherapy for locally advanced cervical cancer. *N Engl J Med* **1999**, *340*, (15), 1144-1153.
204. Schaake-Koning, C.; van den Bogaert, W.; Dalesio, O.; Festen, J.; Hoogenhout, J.; van Houtte, P.; Kirkpatrick, A.; Koolen, M.; Maat, B.; Nijs, A.; et al., Effects of

concomitant cisplatin and radiotherapy on inoperable non-small-cell lung cancer. *N Engl J Med* **1992**, *326*, (8), 524-530.

205. Walsh, T. N.; Noonan, N.; Hollywood, D.; Kelly, A.; Keeling, N.; Hennessy, T. P., A comparison of multimodal therapy and surgery for esophageal adenocarcinoma. *N Engl J Med* **1996**, *335*, (7), 462-467.

206. Santini, J.; Formento, J. L.; Francoual, M.; Milano, G.; Schneider, M.; Dassonville, O.; Demard, F., Characterization, quantification, and potential clinical value of the epidermal growth factor receptor in head and neck squamous cell carcinomas. *Head Neck* **1991**, *13*, (2), 132-139.

207. Weichselbaum, R. R.; Dunphy, E. J.; Beckett, M. A.; Tybor, A. G.; Moran, W. J.; Goldman, M. E.; Vokes, E. E.; Panje, W. R., Epidermal growth factor receptor gene amplification and expression in head and neck cancer cell lines. *Head Neck* **1989**, *11*, (5), 437-442.

208. Klein, T.; Bischoff, R., Physiology and pathophysiology of matrix metalloproteinases. *Amino Acids* **2011**, *41*, (2), 271-290.

209. Nagase, H.; Woessner, J. F., Jr., Matrix metalloproteinases. *J Biol Chem* **1999**, *274*, (31), 21491-21494.

210. Visse, R.; Nagase, H., Matrix metalloproteinases and tissue inhibitors of metalloproteinases: structure, function, and biochemistry. *Circ Res* **2003**, *92*, (8), 827-839.

211. John, A.; Tuszynski, G., The role of matrix metalloproteinases in tumor angiogenesis and tumor metastasis. *Pathol Oncol Res* **2001**, *7*, (1), 14-23.

212. Marchenko, G. N.; Ratnikov, B. I.; Rozanov, D. V.; Godzik, A.; Deryugina, E. I.; Strongin, A. Y., Characterization of matrix metalloproteinase-26, a novel metalloproteinase widely expressed in cancer cells of epithelial origin. *Biochem J* **2001**, *356*, (Pt 3), 705-718.

213. Steffensen, B.; Wallon, U. M.; Overall, C. M., Extracellular matrix binding properties of recombinant fibronectin type II-like modules of human 72-kDa gelatinase/type IV collagenase. High affinity binding to native type I collagen but not native type IV collagen. *J Biol Chem* **1995**, *270*, (19), 11555-11566.

214. Wang, Z.; Juttermann, R.; Soloway, P. D., TIMP-2 is required for efficient activation of proMMP-2 in vivo. *J Biol Chem* **2000**, *275*, (34), 26411-26415.

215. Butler, G. S.; Butler, M. J.; Atkinson, S. J.; Will, H.; Tamura, T.; Schade van Westrum, S.; Crabbe, T.; Clements, J.; d'Ortho, M. P.; Murphy, G., The TIMP2

membrane type 1 metalloproteinase "receptor" regulates the concentration and efficient activation of progelatinase A. A kinetic study. *J Biol Chem* **1998**, *273*, (2), 871-880.

216. Ogata, Y.; Enghild, J. J.; Nagase, H., Matrix metalloproteinase 3 (stromelysin) activates the precursor for the human matrix metalloproteinase 9. *J Biol Chem* **1992**, *267*, (6), 3581-3584.

217. Maeda, H.; Okamoto, T.; Akaike, T., Human matrix metalloprotease activation by insults of bacterial infection involving proteases and free radicals. *Biol Chem* **1998**, *379*, (2), 193-200.

218. Fridman, R.; Toth, M.; Pena, D.; Mobashery, S., Activation of progelatinase B (MMP-9) by gelatinase A (MMP-2). *Cancer Res* **1995**, *55*, (12), 2548-2555.

219. Zucker, S.; Mirza, H.; Conner, C. E.; Lorenz, A. F.; Drews, M. H.; Bahou, W. F.; Jesty, J., Vascular endothelial growth factor induces tissue factor and matrix metalloproteinase production in endothelial cells: Conversion of prothrombin to thrombin results in progelatinase a activation and cell proliferation. *Int J Cancer* **1998**, *75*, (5), 780-786.

220. van Hinsbergh, V. W.; Engelse, M. A.; Quax, P. H., Pericellular proteases in angiogenesis and vasculogenesis. *Arterioscler Thromb Vasc Biol* **2006**, *26*, (4), 716-728.

221. Lemjabbar, H.; Gosset, P.; Lamblin, C.; Tillie, I.; Hartmann, D.; Wallaert, B.; Tonnel, A. B.; Lafuma, C., Contribution of 92 kDa gelatinase/type IV collagenase in bronchial inflammation during status asthmaticus. *Am J Respir Crit Care Med* **1999**, *159*, (4 Pt 1), 1298-1307.

222. Parks, W. C.; Wilson, C. L.; Lopez-Boado, Y. S., Matrix metalloproteinases as modulators of inflammation and innate immunity. *Nat Rev Immunol* **2004**, *4*, (8), 617-629.

223. Fingleton, B., Matrix metalloproteinases: roles in cancer and metastasis. *Front Biosci* **2006**, *11*, 479-491.

224. Bergers, G.; Brekken, R.; McMahon, G.; Vu, T. H.; Itoh, T.; Tamaki, K.; Tanzawa, K.; Thorpe, P.; Itohara, S.; Werb, Z.; Hanahan, D., Matrix metalloproteinase-9 triggers the angiogenic switch during carcinogenesis. *Nat Cell Biol* **2000**, *2*, (10), 737-744.

225. Lee, S.; Jilani, S. M.; Nikolova, G. V.; Carpizo, D.; Iruela-Arispe, M. L., Processing of VEGF-A by matrix metalloproteinases regulates bioavailability and vascular patterning in tumors. *J Cell Biol* **2005**, *169*, (4), 681-691.

226. Chantrain, C. F.; Shimada, H.; Jodele, S.; Groshen, S.; Ye, W.; Shalinsky, D. R.; Werb, Z.; Coussens, L. M.; DeClerck, Y. A., Stromal matrix metalloproteinase-9

regulates the vascular architecture in neuroblastoma by promoting pericyte recruitment. *Cancer Res* **2004**, *64*, (5), 1675-1686.

227. Jodele, S.; Chantrain, C. F.; Blavier, L.; Lutzko, C.; Crooks, G. M.; Shimada, H.; Coussens, L. M.; Declerck, Y. A., The contribution of bone marrow-derived cells to the tumor vasculature in neuroblastoma is matrix metalloproteinase-9 dependent. *Cancer Res* **2005**, *65*, (8), 3200-3208.

228. Heissig, B.; Hattori, K.; Dias, S.; Friedrich, M.; Ferris, B.; Hackett, N. R.; Crystal, R. G.; Besmer, P.; Lyden, D.; Moore, M. A.; Werb, Z.; Rafii, S., Recruitment of stem and progenitor cells from the bone marrow niche requires MMP-9 mediated release of kit-ligand. *Cell* **2002**, *109*, (5), 625-637.

229. Brooks, P. C.; Stromblad, S.; Sanders, L. C.; von Schalscha, T. L.; Aimes, R. T.; Stetler-Stevenson, W. G.; Quigley, J. P.; Cheresch, D. A., Localization of matrix metalloproteinase MMP-2 to the surface of invasive cells by interaction with integrin alpha v beta 3. *Cell* **1996**, *85*, (5), 683-693.

230. Silletti, S.; Kessler, T.; Goldberg, J.; Boger, D. L.; Cheresch, D. A., Disruption of matrix metalloproteinase 2 binding to integrin alpha v beta 3 by an organic molecule inhibits angiogenesis and tumor growth in vivo. *Proc Natl Acad Sci U S A* **2001**, *98*, (1), 119-124.

231. Stokes, A.; Joutsa, J.; Ala-Aho, R.; Pitchers, M.; Pennington, C. J.; Martin, C.; Premachandra, D. J.; Okada, Y.; Peltonen, J.; Grenman, R.; James, H. A.; Edwards, D. R.; Kahari, V. M., Expression profiles and clinical correlations of degradome components in the tumor microenvironment of head and neck squamous cell carcinoma. *Clin Cancer Res* **2010**, *16*, (7), 2022-2035.

232. Cappello, J.; Crissman, J.; Dorman, M.; Mikolajczak, M.; Textor, G.; Marquet, M.; Ferrari, F., Genetic engineering of structural protein polymers. *Biotechnol Prog* **1990**, *6*, (3), 198-202.

233. McGrath, K. P.; Tirrell, D. A.; Kawai, M.; Mason, T. L.; Fournier, M. J., Chemical and biosynthetic approaches to the production of novel polypeptide materials. *Biotechnol Prog* **1990**, *6*, (3), 188-192.

234. Gustafson, J. A.; Ghandehari, H., Silk-elastinlike protein polymers for matrix-mediated cancer gene therapy. *Adv Drug Deliv Rev* **2010**, *62*, (15), 1509-1523.

235. Urry, D. W.; Urry, K. D.; Szaflarski, W.; Nowicki, M., Elastic-contractile model proteins: Physical chemistry, protein function and drug design and delivery. *Adv Drug Deliv Rev* **2010**, *62*, (15), 1404-1455.

236. Kopecek, J., Smart and genetically engineered biomaterials and drug delivery systems. *Eur J Pharm Sci* **2003**, *20*, (1), 1-16.

237. Cappello, J., Genetically engineered protein polymers. In *Handbook of Biodegradable Polymers*, Domb, A.; Kost, J.; Wiseman, D., Eds. Harwood Academic Publishers: Amsterdam, 1997; pp 387-416.
238. Connor, R. E.; Tirrell, D. A., Non-canonical amino acids in protein polymer design. *J Macromol Sci, Part C: Pol Rev* **2007**, *47*, (1), 9-28.
239. Bidwell, G. L., 3rd; Raucher, D., Cell penetrating elastin-like polypeptides for therapeutic peptide delivery. *Adv Drug Deliv Rev* **2010**, *62*, (15), 1486-1496.
240. Ghandehari, H.; Hatefi, A., Advances in recombinant polymers for delivery of bioactive agents. *Adv Drug Deliv Rev* **2010**, *62*, (15), 1403.
241. Kim, W.; Chaikof, E. L., Recombinant elastin-mimetic biomaterials: Emerging applications in medicine. *Adv Drug Deliv Rev* **2010**, *62*, (15), 1468-1478.
242. McDaniel, J. R.; Callahan, D. J.; Chilkoti, A., Drug delivery to solid tumors by elastin-like polypeptides. *Adv Drug Deliv Rev* **2010**, *62*, (15), 1456-1467.
243. Nettles, D. L.; Chilkoti, A.; Setton, L. A., Applications of elastin-like polypeptides in tissue engineering. *Adv Drug Deliv Rev* **2010**, *62*, (15), 1479-1485.
244. Numata, K.; Kaplan, D. L., Silk-based delivery systems of bioactive molecules. *Adv Drug Deliv Rev* **2010**, *62*, (15), 1497-1508.
245. Top, A.; Kiick, K. L., Multivalent protein polymers with controlled chemical and physical properties. *Adv Drug Deliv Rev* **2010**, *62*, (15), 1530-1540.
246. Meyer, D. E.; Chilkoti, A., Genetically encoded synthesis of protein-based polymers with precisely specified molecular weight and sequence by recursive directional ligation: examples from the elastin-like polypeptide system. *Biomacromolecules* **2002**, *3*, (2), 357-367.
247. Amiram, M.; Quiroz, F. G.; Callahan, D. J.; Chilkoti, A., A highly parallel method for synthesizing DNA repeats enables the discovery of 'smart' protein polymers. *Nat Mater* **2011**, *10*, (2), 141-148.
248. Ferrari, F. A.; Richardson, C.; Chambers, J.; Causey, S. C.; Pollock, T. J.; Cappello, J.; Crissman, J. W. Construction of synthetic DNA and its use in large polypeptide synthesis. 5243038, 1987.
249. Hinman, M. B.; Lewis, R. V., Isolation of a clone encoding a second dragline silk fibroin. *Nephila clavipes* dragline silk is a two-protein fiber. *J Biol Chem* **1992**, *267*, (27), 19320-19324.

250. Prince, J. T.; McGrath, K. P.; DiGirolamo, C. M.; Kaplan, D. L., Construction, cloning, and expression of synthetic genes encoding spider dragline silk. *Biochemistry* **1995**, *34*, (34), 10879-10885.
251. Xu, M.; Lewis, R. V., Structure of a protein superfiber: spider dragline silk. *Proc Natl Acad Sci U S A* **1990**, *87*, (18), 7120-7124.
252. Olsen, D.; Yang, C.; Bodo, M.; Chang, R.; Leigh, S.; Baez, J.; Carmichael, D.; Perala, M.; Hamalainen, E. R.; Jarvinen, M.; Polarek, J., Recombinant collagen and gelatin for drug delivery. *Adv Drug Deliv Rev* **2003**, *55*, (12), 1547-1567.
253. Tomita, M.; Munetsuna, H.; Sato, T.; Adachi, T.; Hino, R.; Hayashi, M.; Shimizu, K.; Nakamura, N.; Tamura, T.; Yoshizato, K., Transgenic silkworms produce recombinant human type III procollagen in cocoons. *Nat Biotechnol* **2003**, *21*, (1), 52-56.
254. Urry, D. W.; Okamoto, K.; Harris, R. D.; Hendrix, C. F.; Long, M. M., Synthetic, crosslinked polypentapeptide of tropoelastin: an anisotropic, fibrillar elastomer. *Biochemistry* **1976**, *15*, (18), 4083-4089.
255. Urry, D. W., Physical chemistry of biological free energy transduction as demonstrated by elastic protein-based polymers. *J Phys Chem B* **1997**, *101*, (51), 11007-11028.
256. Sandberg, L. B.; Soskel, N. T.; Leslie, J. G., Elastin structure, biosynthesis, and relation to disease states. *N Engl J Med* **1981**, *304*, (10), 566-579.
257. Meyer, D. E.; Shin, B. C.; Kong, G. A.; Dewhirst, M. W.; Chilkoti, A., Drug targeting using thermally responsive polymers and local hyperthermia. *J Control Release* **2001**, *74*, (1-3), 213-224.
258. Meyer, D. E.; Kong, G. A.; Dewhirst, M. W.; Zalutsky, M. R.; Chilkoti, A., Targeting a genetically engineered elastin-like polypeptide to solid tumors by local hyperthermia. *Cancer Res* **2001**, *61*, (4), 1548-1554.
259. Liu, W.; Dreher, M. R.; Furgeson, D. Y.; Peixoto, K. V.; Yuan, H.; Zalutsky, M. R.; Chilkoti, A., Tumor accumulation, degradation and pharmacokinetics of elastin-like polypeptides in nude mice. *J Control Release* **2006**, *116*, (2), 170-178.
260. MacKay, J. A.; Chen, M.; McDaniel, J. R.; Liu, W.; Simnick, A. J.; Chilkoti, A., Self-assembling chimeric polypeptide-doxorubicin conjugate nanoparticles that abolish tumours after a single injection. *Nat Mater* **2009**, *8*, (12), 993-999.
261. Sun, G.; Hsueh, P. Y.; Janib, S. M.; Hamm-Alvarez, S.; Andrew MacKay, J., Design and cellular internalization of genetically engineered polypeptide nanoparticles displaying adenovirus knob domain. *J Control Release* **2011**, *155*, (2), 218-226.



262. Meinel, L.; Hofmann, S.; Karageorgiou, V.; Kirker-Head, C.; McCool, J.; Gronowicz, G.; Zichner, L.; Langer, R.; Vunjak-Novakovic, G.; Kaplan, D. L., The inflammatory responses to silk films in vitro and in vivo. *Biomaterials* **2005**, *26*, (2), 147-155.
263. Yanagisawa, S.; Zhu, Z.; Kobayashi, I.; Uchino, K.; Tamada, Y.; Tamura, T.; Asakura, T., Improving cell-adhesive properties of recombinant Bombyx mori silk by incorporation of collagen or fibronectin derived peptides produced by transgenic silkworms. *Biomacromolecules* **2007**, *8*, (11), 3487-3492.
264. Numata, K.; Reagan, M. R.; Goldstein, R. H.; Rosenblatt, M.; Kaplan, D. L., Spider silk-based gene carriers for tumor cell-specific delivery. *Bioconjug Chem* **2011**, *22*, (8), 1605-1610.
265. Baoyong, L.; Jian, Z.; Denglong, C.; Min, L., Evaluation of a new type of wound dressing made from recombinant spider silk protein using rat models. *Burns* **2010**, *36*, (6), 891-896.
266. Gomes, S.; Leonor, I. B.; Mano, J. F.; Reis, R. L.; Kaplan, D. L., Spider silk-bone sialoprotein fusion proteins for bone tissue engineering. *Soft Matter* **2011**, *7*, (10), 4964-4973.
267. Lucas, F.; Shaw, J. T.; Smith, S. G., The amino acid sequence in a fraction of the fibroin of Bombyx mori. *Biochem J* **1957**, *66*, (3), 468-479.
268. Cappello, J.; Crissman, J. W.; Crissman, M.; Ferrari, F. A.; Textor, G.; Wallis, O.; Whitley, J. R.; Zhou, X.; Burman, D.; Aukerman, L.; Stedronsky, E. R., In-situ self-assembling protein polymer gel systems for administration, delivery, and release of drugs. *J Control Release* **1998**, *53*, (1-3), 105-117.
269. Nagarsekar, A.; Crissman, J.; Crissman, M.; Ferrari, F.; Cappello, J.; Ghandehari, H., Genetic engineering of stimuli-sensitive silk-elastin-like protein block copolymers. *Biomacromolecules* **2003**, *4*, (3), 602-607.
270. Nagarsekar, A.; Crissman, J.; Crissman, M.; Ferrari, F.; Cappello, J.; Ghandehari, H., Genetic synthesis and characterization of pH- and temperature-sensitive silk-elastinlike protein block copolymers. *J Biomed Mater Res* **2002**, *62*, (2), 195-203.
271. Girton, T. S.; Barocas, V. H.; Tranquillo, R. T., Confined compression of a tissue-equivalent: collagen fibril and cell alignment in response to anisotropic strain. *Journal of biomechanical engineering* **2002**, *124*, (5), 568.
272. Dinerman, A. A.; Cappello, J.; Ghandehari, H.; Hoag, S. W., Solute diffusion in genetically engineered silk-elastinlike protein polymer hydrogels. *J Control Release* **2002**, *82*, (2-3), 277-287.

273. Megeed, Z.; Cappello, J.; Ghandehari, H., Controlled release of plasmid DNA from a genetically engineered silk-elastinlike hydrogel. *Pharm Res* **2002**, *19*, (7), 954-959.
274. Megeed, Z.; Haider, M.; Li, D.; O'Malley, B. W., Jr.; Cappello, J.; Ghandehari, H., In vitro and in vivo evaluation of recombinant silk-elastinlike hydrogels for cancer gene therapy. *J Control Release* **2004**, *94*, (2-3), 433-445.
275. Haider, M.; Leung, V.; Ferrari, F.; Crissman, J.; Powell, J.; Cappello, J.; Ghandehari, H., Molecular engineering of silk-elastinlike polymers for matrix-mediated gene delivery: biosynthesis and characterization. *Mol Pharm* **2005**, *2*, (2), 139-150.
276. Cresce, A. W.; Dandu, R.; Burger, A.; Cappello, J.; Ghandehari, H., Characterization and real-time imaging of gene expression of adenovirus embedded silk-elastinlike protein polymer hydrogels. *Mol Pharm* **2008**, *5*, (5), 891-897.
277. Dandu, R.; Ghandehari, H.; Cappello, J., Characterization of structurally related adenovirus-laden silk-elastinlike hydrogels. *J Bioact Compat Pol* **2008**, *23*, (1), 5-19.
278. Hwang, D.; Moolchandani, V.; Dandu, R.; Haider, M.; Cappello, J.; Ghandehari, H., Influence of polymer structure and biodegradation on DNA release from silk-elastinlike protein polymer hydrogels. *Int J Pharm* **2009**, *368*, (1-2), 215-219.
279. Dinerman, A. A.; Cappello, J.; El-Sayed, M.; Hoag, S. W.; Ghandehari, H., Influence of solute charge and hydrophobicity on partitioning and diffusion in a genetically engineered silk-elastin-like protein polymer hydrogel. *Macromol Biosci* **2010**, *10*, (10), 1235-1247.
280. Haider, M.; Cappello, J.; Ghandehari, H.; Leong, K. W., In vitro chondrogenesis of mesenchymal stem cells in recombinant silk-elastinlike hydrogels. *Pharm Res* **2008**, *25*, (3), 692-699.
281. Qiu, W.; Huang, Y.; Teng, W.; Cohn, C. M.; Cappello, J.; Wu, X., Complete recombinant silk-elastinlike protein-based tissue scaffold. *Biomacromolecules* **2010**, *11*, (12), 3219-3227.
282. Dandu, R.; Cresce, A. V.; Briber, R.; Dowell, P.; Cappello, J.; Ghandehari, H., Silk-elastinlike protein polymer hydrogels: Influence of monomer sequence on physicochemical properties. *Polymer* **2009**, *50*, (2), 366-374.
283. Xia, X. X.; Xu, Q.; Hu, X.; Qin, G.; Kaplan, D. L., Tunable self-assembly of genetically engineered silk-elastin-like protein polymers. *Biomacromolecules* **2011**, *12*, (11), 3844-3850.

284. Dinerman, A. A.; Cappello, J.; Ghandehari, H.; Hoag, S. W., Swelling behavior of a genetically engineered silk-elastinlike protein polymer hydrogel. *Biomaterials* **2002**, *23*, (21), 4203-4210.
285. Hwang, W.; Kim, B. H.; Dandu, R.; Cappello, J.; Ghandehari, H.; Seog, J., Surface induced nanofiber growth by self-assembly of a silk-elastin-like protein polymer. *Langmuir* **2009**, *25*, (21), 12682-12686.
286. Kad, N. M.; Myers, S. L.; Smith, D. P.; Smith, D. A.; Radford, S. E.; Thomson, N. H., Hierarchical assembly of beta2-microglobulin amyloid in vitro revealed by atomic force microscopy. *J Mol Biol* **2003**, *330*, (4), 785-797.
287. Hortschansky, P.; Schroeckh, V.; Christopeit, T.; Zandomenighi, G.; Fandrich, M., The aggregation kinetics of Alzheimer's beta-amyloid peptide is controlled by stochastic nucleation. *Protein Sci* **2005**, *14*, (7), 1753-1759.
288. Fezoui, Y.; Teplow, D. B., Kinetic studies of amyloid beta-protein fibril assembly. Differential effects of alpha-helix stabilization. *J Biol Chem* **2002**, *277*, (40), 36948-36954.
289. Chang, J.; Peng, X. F.; Hijji, K.; Cappello, J.; Ghandehari, H.; Solares, S. D.; Seog, J., Nanomechanical stimulus accelerates and directs the self-assembly of silk-elastin-like nanofibers. *J Am Chem Soc* **2011**, *133*, (6), 1745-1747.
290. Gustafson, J.; Greish, K.; Frandsen, J.; Cappello, J.; Ghandehari, H., Silk-elastinlike recombinant polymers for gene therapy of head and neck cancer: from molecular definition to controlled gene expression. *J Control Release* **2009**, *140*, (3), 256-261.
291. Megeed, Z.; Cappello, J.; Ghandehari, H., Thermal analysis of water in silk-elastinlike hydrogels by differential scanning calorimetry. *Biomacromolecules* **2004**, *5*, (3), 793-797.
292. Ilavsky, J.; Jemian, P. R., Irena: tool suite for modeling and analysis of small-angle scattering. *J. Appl. Cryst.* **2009**, *42*, (2), 347-353.
293. Debye, P., Light scattering in soap solutions. *J Phys Colloid Chem* **1949**, *53*, (1), 1-8.
294. Fritzing, B.; Scheler, U., Scaling behaviour of PAMAM dendrimers determined by diffusion NMR. *Macromol Chem Phys* **2005**, *206*, (13), 1288-1291.
295. Dieterich, D. C.; Link, A. J.; Graumann, J.; Tirrell, D. A.; Schuman, E. M., Selective identification of newly synthesized proteins in mammalian cells using bioorthogonal noncanonical amino acid tagging (BONCAT). *Proc Natl Acad Sci U S A* **2006**, *103*, (25), 9482-9487.

296. Ogiwara, K.; Nagaoka, M.; Cho, C. S.; Akaike, T., Effect of photo-immobilization of epidermal growth factor on the cellular behaviors. *Biochem Biophys Res Commun* **2006**, *345*, (1), 255-259.
297. Farmer, R. S.; Top, A.; Argust, L. M.; Liu, S.; Kiick, K. L., Evaluation of conformation and association behavior of multivalent alanine-rich polypeptides. *Pharm Res* **2008**, *25*, (3), 700-708.
298. Sharma, N.; Top, A.; Kiick, K. L.; Pochan, D. J., One-dimensional gold nanoparticle arrays by electrostatically directed organization using polypeptide self-assembly. *Angew Chem* **2009**, *121*, (38), 7212-7216.
299. Heilshorn, S. C.; DiZio, K. A.; Welsh, E. R.; Tirrell, D. A., Endothelial cell adhesion to the fibronectin CS5 domain in artificial extracellular matrix proteins. *Biomaterials* **2003**, *24*, (23), 4245-4252.
300. Panitch, A.; Yamaoka, T.; Fournier, M. J.; Mason, T. L.; Tirrell, D. A., Design and biosynthesis of elastin-like artificial extracellular matrix proteins containing periodically spaced fibronectin CS5 domains. *Macromolecules* **1999**, *32*, (5), 1701-1703.
301. Liu, J. C.; Heilshorn, S. C.; Tirrell, D. A., Comparative cell response to artificial extracellular matrix proteins containing the RGD and CS5 cell-binding domains. *Biomacromolecules* **2004**, *5*, (2), 497-504.
302. Akerman, B., Effects of supercoiling in electrophoretic trapping of circular DNA in polyacrylamide gels. *Biophys J* **1998**, *74*, (6), 3140-3151.
303. Mickel, S.; Arena, V., Jr.; Bauer, W., Physical properties and gel electrophoresis behavior of R12-derived plasmid DNAs. *Nucleic Acids Res* **1977**, *4*, (5), 1465-1482.

## CHAPTER 3

### SILK-ELASTINLIKE RECOMBINANT POLYMERS FOR GENE THERAPY OF HEAD AND NECK CANCER: FROM MOLECULAR DEFINITION TO CONTROLLED GENE EXPRESSION

#### 3.1 Introduction

The analysis of the performance of SELP hydrogels as adenoviral delivery materials *in vivo* is a necessary next step towards the evaluation of this gene delivery system as a clinically viable treatment for HNSCC. The systemic variation of structure in SELPs allows their evaluation as a highly tunable matrix in the context of gene delivery, and will additionally allow the identification of which construct of SELP is best suited for intratumoral delivery of adenoviral vectors. Further, in order to investigate the ability of SELP to protect nontarget tissues from adenoviral transfection, hepatic expression levels of reporter adenovirus needs to be evaluated. The liver is specifically targeted as it is the most common site of off-target adenoviral infection.<sup>1</sup> This is due primarily to interaction with coagulation factor IX and complement factor C4 binding protein,<sup>2</sup> and interaction with CAR, although the lack of correlation between CAR expression and tissue tropism *in vivo*<sup>3</sup> combined with similar *in vivo* expression patterns between CAR-binding and

nonbinding adenovirus<sup>4, 5</sup> suggests that CAR plays a more diminished role than previously thought when adenovirus is administered *in vivo*.<sup>2</sup>

Based on the *in vitro* and *in vivo* results for adenoviral release from SELP hydrogels, studies were designed to investigate the structure-dependence of adenoviral delivery from SELPs. Adenovirus carrying the reporter gene LacZ, encoding for  $\beta$ -galactosidase, was injected into JHU-022 tumors growing on the flanks of nude mice. The viruses were suspended in either 0.9% injection saline or SELP solution, which was either SELP-47K, SELP-415K, or SELP-815K, and was additionally diluted to varying concentrations. Upon completion of each time point (1, 2, or 3 weeks) the animals were sacrificed, and the tumors and livers were removed and assayed for  $\beta$ -gal content. Further, histological staining for  $\beta$ -gal was performed on some tumor tissue from each time point. In order to support these studies, a parallel study was performed using a luciferase reporter adenovirus. Virus was injected into induced JHU-022 tumors in the flanks of nude mice, but instead of evaluating  $\beta$ -gal colorimetrically, luciferase expression was evaluated by luminescent imaging, which was performed every 3-4 days. Further work performed in this study investigated the degradability of SELP-815K by human leukocyte elastase, which was incubated with SELP hydrogels of different structure and concentration. Degradation was evaluated by bicinchoninic acid (BCA) assay performed on the 0.9% saline release medium, allowing quantification of released protein.

## 3.2 Materials and methods

### 3.2.1 Materials

SELP-47K was obtained from Protein Polymer Technologies, Inc. (San Diego, CA, USA). Linear SELP-415K<sup>6</sup> and -815K<sup>7</sup> were biosynthesized and characterized as described previously. Replication defective human adenoviruses (Ad) Type 5 with E1/E3 deletion, under the control of the CMV promoter, encoding for either  $\beta$ -galactosidase ( $\beta$ -gal) or firefly luciferase (Luc) reporter genes were purchased from Vector Biolabs (Philadelphia, PA, USA). JHU-022 oral cavity cancer cell line was a kind gift from Professor David Sidransky of Johns Hopkins University (Baltimore, MD, USA). Human Leukocyte Elastase was purchased from Elastin Products Company (Owensville, MO) and solubilized in Phosphate Buffered Saline (Sigma Aldrich, St. Louis, MO). Bicinchoninic acid protein assay was purchased from Thermo Scientific (Waltham, MA, USA) and the optical density (OD) measurements were performed using the SpectraMax M2 micro plate reader from Molecular Devices (Sunny Vale, CA, USA) coupled with a Softmax analytic software package. For bioluminescent imaging studies, luciferin was obtained from Gold Biotech (St. Louis, MO, USA). Animals were evaluated for luciferase expression using a Xenogen IVIS100 bioluminescent imaging system from Caliper Life Sciences (Hopkinton, MA, USA) coupled with analytical software, Igor PRO v.2.2.0, Wavemetrics Inc. (Lake Oswego, OR, USA). For establishing xenografts JHU-022 cells were cultured in Advanced Roswell Park Memorial Institute (RPMI 1640) medium containing 2mM L-Glutamine and 10% fetal calf serum (Gibco, Carlsbad, CA, USA). Chlorophenol Red- $\beta$ -D-Galactopyranoside (CPRG)  $\beta$ -gal quantitative kit was purchased from Imgenex (San Diego, CA, USA).  $\beta$ -

Galactosidase Reporter Gene Staining Kit was purchased from Sigma-Aldrich, Inc. (St. Louis, MO, USA ). Luciferase assay system was purchased from Promega (Madison, WI, USA). Six-week-old female athymic (*nu/nu*) mice were purchased from Charles River Laboratories (Davis, CA, USA) and were used for the animal studies in accordance with the Institutional Animal Care and Use Committee (IACUC) protocol of the University of Utah.

### 3.2.2 Quantitative evaluation of viral gene expression *in vivo*

Head and neck cancer xenografts were established by subcutaneously injecting  $2 \times 10^6$  JHU-022 cells suspended in 200  $\mu$ l Phosphate Buffer Saline (PBS) bilaterally in the flank of athymic nude (*nu/nu*) mice. Tumors were allowed to grow for 2 weeks to reach an average diameter of 7 mm. A dose of  $5 \times 10^8$  PFU of Ad-CMV-LacZ was administered to mice with SELP-415K (10.8 wt%), SELP-47K (8 wt% and 10.8 wt%), SELP-815K (4 wt%, 8 wt%, and 10.8 wt%), or physiological saline. Virus-polymer solutions were prepared by thawing SELP and virus stocks and mixing them gently with physiological saline. Mice were anesthetized using 4 wt% isofluorane mixed with oxygen, and intratumorally injected with 25  $\mu$ l of the polymer-virus solutions using a Hamilton syringe. On day 7, 14, and 21, mice were euthanized and tumor and liver tissue were isolated. CPRG  $\beta$ -gal colorimetric assay was performed as described previously.<sup>8</sup> Briefly, fresh tissue samples from the tumor and liver of animals were collected, snap-frozen in liquid nitrogen, ground with mortar and pestle, resuspended in 1 mL lysis buffer (50 mM HEPES, 5 mM CHAPS, pH 7.4) followed by sonication on ice in 10-15 second bursts for a total of 1 minute. Recovered tissue lysates were then



centrifuged for 45 minutes at 14,000 rpm and subsequently, upper aqueous layers were used for  $\beta$ -gal quantification. Colorimetric assays were then performed as outlined in the protocol provided with the kit. The optical density (OD) dynamic study was performed to assay the enzyme substrate kinetics, and time point of measurements were set at 40 minutes for tumor  $\beta$ -gal expression and 110 minutes for liver expression which represent the time points of peak interactions, respectively.

### 3.2.3 Tumor histology

For spatial distribution of  $\beta$ -gal in tumors, tissues were cryo-sectioned at 5  $\mu$ m and stained with a  $\beta$ -gal reporter gene staining kit. Kit manufacturer instructions were modified as follows: tissue sections were fixed for 3 minutes in fixation buffer, and then rinsed twice with PBS. Fixed sections were then stained with staining solution for 24 hours at 37° C, rinsed with PBS, and observed under light microscope. X-Gal stains  $\beta$ -galactosidase expressing cells and tissue areas dark blue.

### 3.2.4 Bioluminescence imaging of gene expression *in vivo*

Bioluminescent imaging was used as a secondary method of assessment of spatial control over gene expression in JHU-022 tumor-bearing athymic nu/nu mice as established above. Tumors were then injected with 25  $\mu$ l of SELP-415K (10.8 wt%), SELP-47K (4 wt%, 8 wt%, and 10.8 wt%), SELP-815K (4 wt%, 8 wt%, and 10.8 wt%) or physiological saline containing  $5 \times 10^8$  PFU of Ad.CMV.Luc. Imaging was performed on days 4, 7, 10, 14, and 21 by injection with 200  $\mu$ l of 15 mg/ml luciferin

intraperitoneally. Luminescence was imaged after 30 minutes, using Xenogen IVIS100, and images were analyzed using IgorPRO v.2.2.0.

### 3.2.5 *In vitro* assessment of hydrogel degradation

50 $\mu$ l SELP hydrogels were made by drawing 250 $\mu$ l of 12 wt% SELP-47K, SELP-415K, and SELP-815K, and 8 wt% SELP-815K solutions into separate 1 ml syringes. Syringes were placed in a 37°C incubator and allowed to gel for 24 hours. After incubation, the end was cut off of each syringe and 50  $\mu$ l gel disks were cut from the 250  $\mu$ l cylinder. These gels were placed in the inner wells of a 48-well plate containing 800  $\mu$ l of PBS + elastase, with a 1:6 dilution curve of elastase starting at 1000 ng/ml. The empty wells of the plate were filled with 1.5 ml PBS to control evaporation, and then the plates were sealed with self-adhesive sealing foil and agitated at 120 RPM. At each time point (1, 3, 7, 10, 14, 17, 21, 24, and 28 days) the full sample volume of 800  $\mu$ l was removed from each well, placed in a separate 1.5 ml microcentrifuge tube, and stored at -80°C. In order to assess the degradation of the SELPs, the micro BCA protein assay was used according to manufacturer's instructions to measure the soluble protein for each sample, followed by measuring absorbance at 561 nm.

### 3.2.6 Statistical analysis

The results of the quantitative evaluation of viral gene expression *in vivo* and comparative degradation rate *in vitro* are expressed as the mean  $\pm$  SE. Student's T test was used to analyze the significance of difference in reporter gene expression in different SELP treatment groups compared to plain Ad-LacZ treatment, and to analyze

the significance of SELP structure's influence on degradation rate. P values of  $< 0.05$  were indicative of statistically significant differences.

### 3.3 Results and discussion

#### 3.3.1 Spatio-temporal control of gene expression as a function of polymer structure

Selective delivery of a sufficient number of therapeutic gene copies to cancer cells remains a challenge in gene therapy. Current data from clinical trials using adenoviral vectors for gene delivery show that acute liver toxicity and immunogenicity are the major adverse effects limiting the dose of adenovirus that can be given to the patients.<sup>2,9</sup> These challenges indicate the need for tailor-making polymeric systems that can limit delivery of adenoviruses to solid tumors, prolong gene expression, and that are degraded and eliminated from the body over a specified period of time. In this study, we compared the duration and extent of gene expression in head and neck tumors when adenoviruses were delivered from hydrogels made from three SELP analogs. These polymers (Figure 1.1) were produced by recombinant techniques such that molecular weight of each linear chain remained constant while the sequence of silk and elastin repeats within each chain varied.<sup>6, 7, 10</sup> SELP-47K has 8 elastin units less in each monomer repeat than SELP-415K (Figure 1.1). As the temperature is raised, silk units hydrogen bond and elastin units self-assemble, forming hydrogels. At equivalent polymer concentrations, SELP-47K forms more robust hydrogels than SELP-415K, as evidenced previously by a lower degree of swelling and higher mechanical strength.<sup>7</sup> SELP-815K has a higher number of silk units per monomer repeat compared to SELP-

415K (Figure 1.1). At equivalent polymer concentrations, we had previously observed that hydrogels made from SELP-815K have intermediate degrees of swelling and storage moduli between SELP-47K and SELP-415K.<sup>7</sup> This is despite the fact that SELP-815K has a similar ratio of silk to elastin units compared to SELP-47K, providing evidence that in addition to the *ratio* of silk and elastin units, the *sequence* of these units in the polymer chain influences the physicochemical properties of the resulting hydrogels. We had also observed previously that polymer concentration influences the network properties of SELP hydrogels where a lower polymer concentration resulted in increased degree of swelling and release of bioactive agents.<sup>6, 7, 11-13</sup> Based on these observations, we hypothesized that by controlling both polymer structure and concentration, the location and duration of gene expression can be controlled when adenoviruses are delivered by SELPs to head and neck tumors.

Lac Z gene expression after co-injection of adenoviral vectors with each SELP structure and as a function of polymer concentration was evaluated in tumor and liver tissues of mice. Strong dependence of structure and concentration effect on gene expression was evident in terms of transfection levels and duration of gene expression (Figures 3.1-3.3). The results of the enzymatic assay in tumor lysates (Figure 3.1) show that SELP-815K at 4 wt% exhibits the highest transfection levels at all time points, with a greater than 10-fold increase of transfection over free virus after 1 week and 6-fold increase at 2 weeks. As the concentration of SELP-815K increased from 4 wt% to 8 wt% and 10.8 wt%, transfection levels decreased for the duration of study. The increased concentration leads to increased crosslinking density of hydrogel network, resulting in decreased release of the viruses and transfection. Matrix-

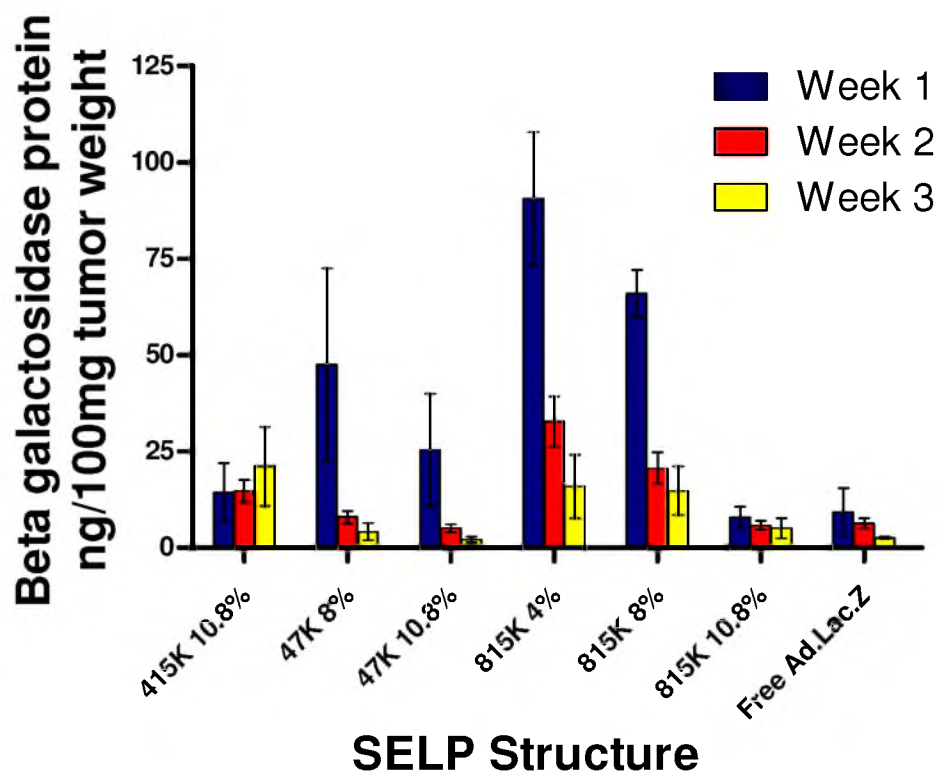


Figure 3.1: SELP-structure dependence of intratumoral beta-galactosidase expression.

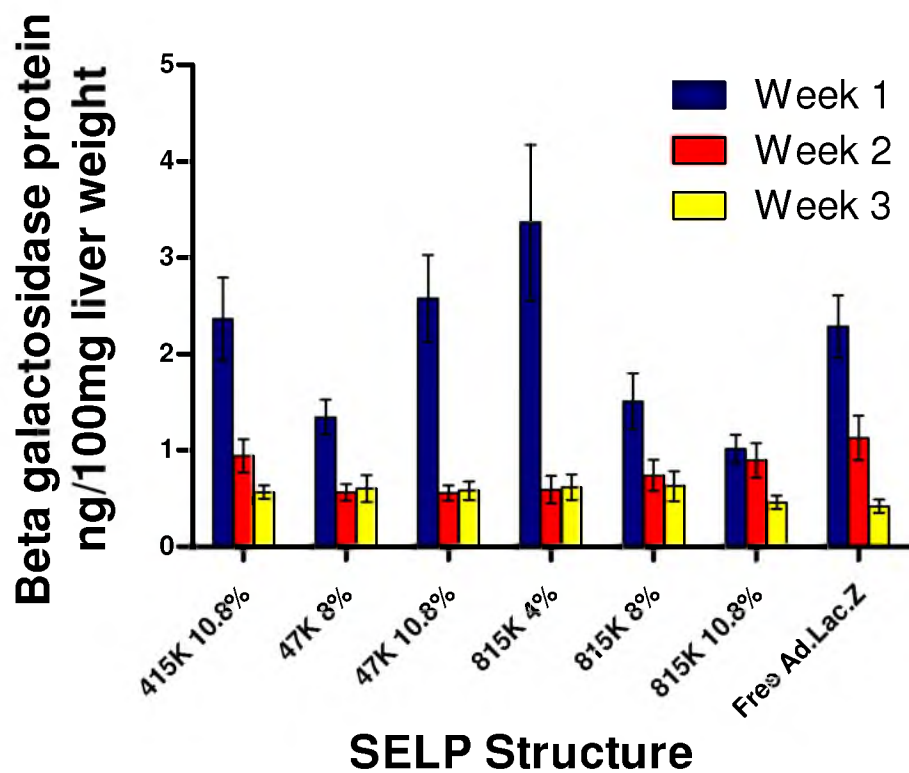


Figure 3.2: SELP-structure dependence of hepatic beta-galactosidase expression

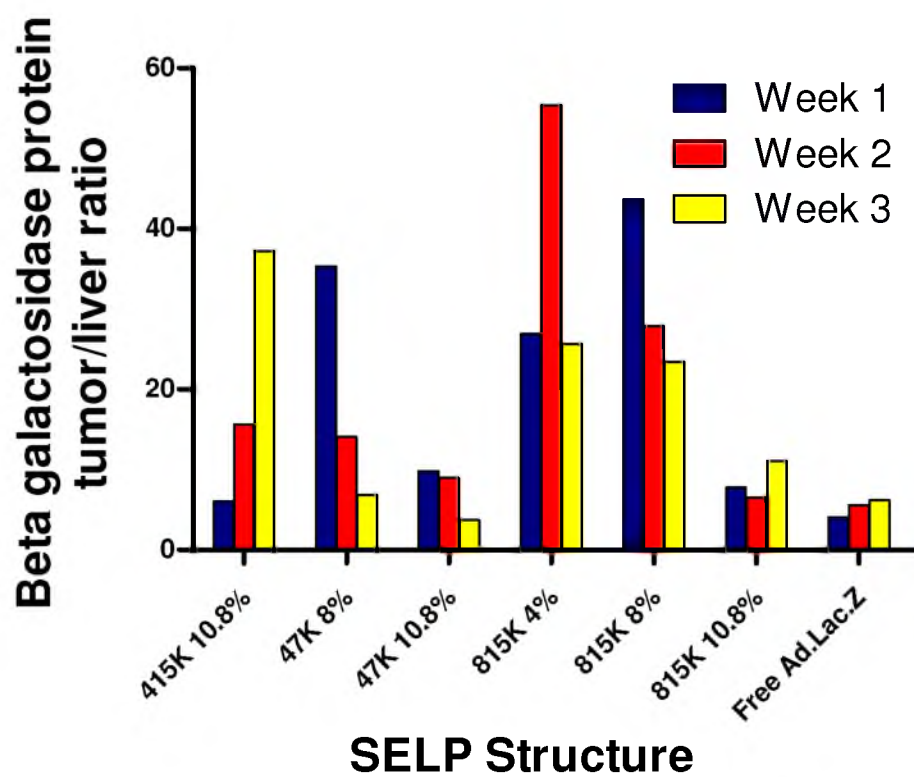


Figure 3.3: Ratio of intratumoral to hepatic beta galactosidase expression

mediated adenoviral delivery from SELP-47K hydrogels resulted in a lower transfection efficiency than delivery with SELP-815K polymers at equivalent polymer concentrations. Compared to SELP-815K, SELP-47K has shorter elastin segments between the silk crosslink points, leading to lower pore size and virus release.

Due to longer elastin units, the loose network of SELP-415K can only form stable hydrogels at the higher concentration of 10.8 wt%.<sup>6, 14</sup> At this concentration, higher transfection levels were observed compared to the virus-only group, demonstrating that some virus was trapped in the hydrogel network that influenced release. However, lower transfection was observed compared to other polymeric analogs, demonstrating that increased silk units in more robust gels made from SELP-47K and -815K prolong release of adenoviruses *in vivo*. In the case of plain Ad-LacZ injection, burst-release out of the tumor tissue is the most plausible explanation in which the bulk of the virus was released over the first week following injection, and was cleared before significant transfection could take place at week 1 and beyond.

The utility of SELP matrices in limiting virus distribution into the liver was evaluated at various polymer structures and concentrations. No significant differences in liver expression were observed for SELP polymers compared to free virus (Figure 3.2). However, when considering the tumor / liver ratio of gene expression, SELP-815K at 4 wt% exhibited 55-fold higher tumor expression than liver (Figure 3.3). In the case of plain viral injection, the highest tumor / liver expression ratio was only 5-fold. Clearly, SELP hydrogels localize gene expression to tumors and can augment the dose of adenoviruses that can be delivered up to 11 times for the same liver distribution as that of free viral injection. The spatial and temporal patterns of  $\beta$ -galactosidase expression in



SELP-415K, -815K, and plain virus treatment groups were evaluated by staining with X-gal of both tumor and liver tissues (Figure 3.4A-F). The observed patterns of gene expression in these tissues were in good agreement with the transfection data. In the SELP-415K group (Figure 3.4A,B), expression was apparent throughout the tissue, although in a lighter intensity than in the more localized and intense SELP-815K group (Figure 3.4C,D). The virus only group also had a high area of expression with a less dense staining (Figure 3.4E,F). Expression patterns in the SELP-415K and SELP-815K tumors showed prolonged expression through week 3 (Figure 3.4B,D), whereas expression in the virus only group was undetectable by week 3 (Figure 3.4F).

### 3.3.2 Bioluminescent imaging of SELP-mediated gene expression

Bioluminescent imaging of live tumor-bearing animals allows gene expression to be monitored in the same animal over the study period without the need to sacrifice the mouse for analysis. Unfortunately, issues with light attenuation, scattering, and reflection reduce the value of this technique for quantitative measurement. In this study, both methods were used to provide a more comprehensive assessment of gene expression by SELP-mediated delivery of adenoviruses to head and neck tumors. Representative images are shown in Figures 3.5-3.10. Figure 3.5-3.7 show postinjection 4, 14, and 21 days, respectively, of the SELP-815K 4 wt%+Ad.CMV.Luc group. Each animal expresses luciferase in the tumor at day 4, and that expression continues for all animals up to day 14. The two patches of expression anterior to the tumor in Figure 3.6 and 3.7 are due to liver expression, which appeared in only one animal in each group over the course of the study. In the virus only condition, only three animals expressed

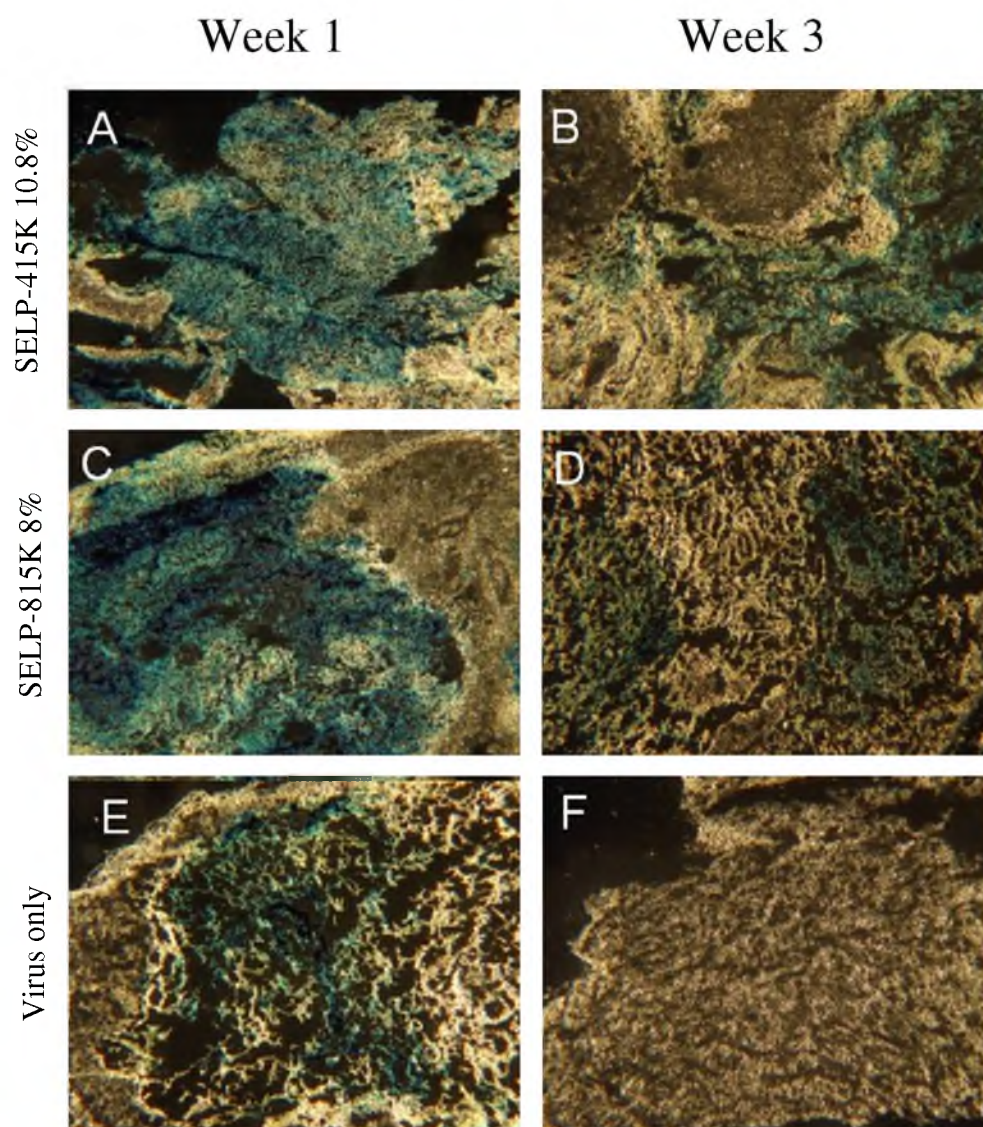


Figure 3.4: Histological analysis of beta galactosidase expression.

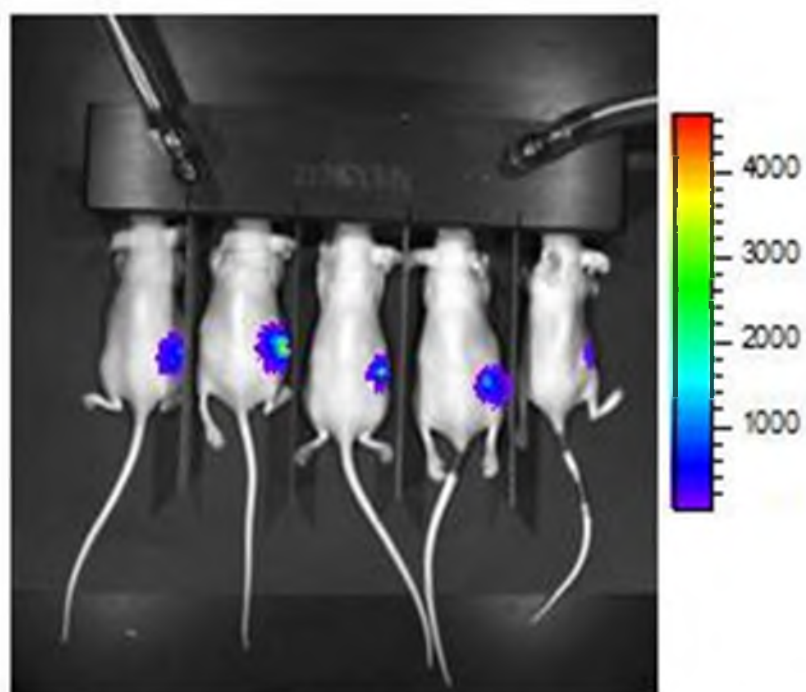


Figure 3.5: Bioluminescent imaging for SELP-815K 4 wt%+Ad.CMV.Luc Day 4

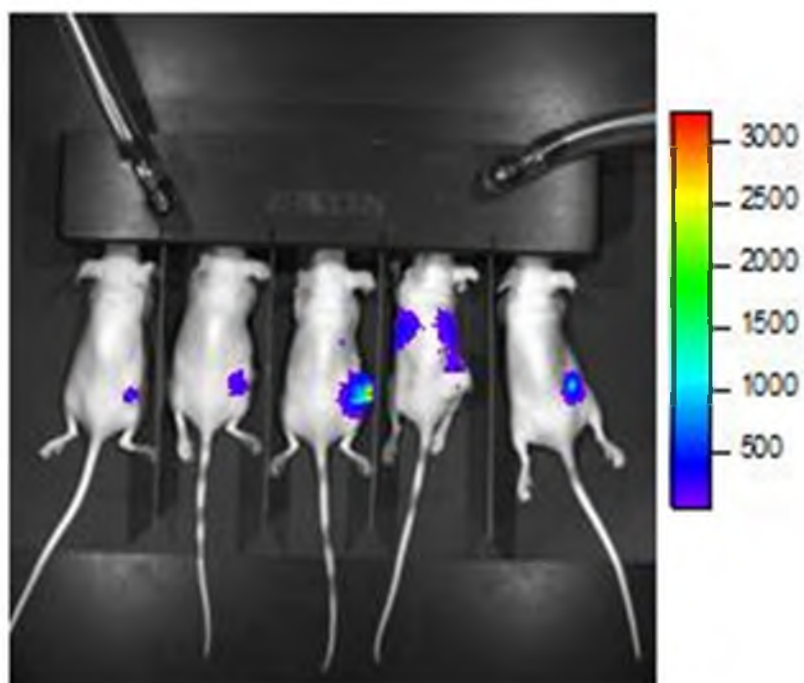


Figure 3.6: Bioluminescent imaging for SELP-815K 4 wt%+Ad.CMV.Luc Day 14

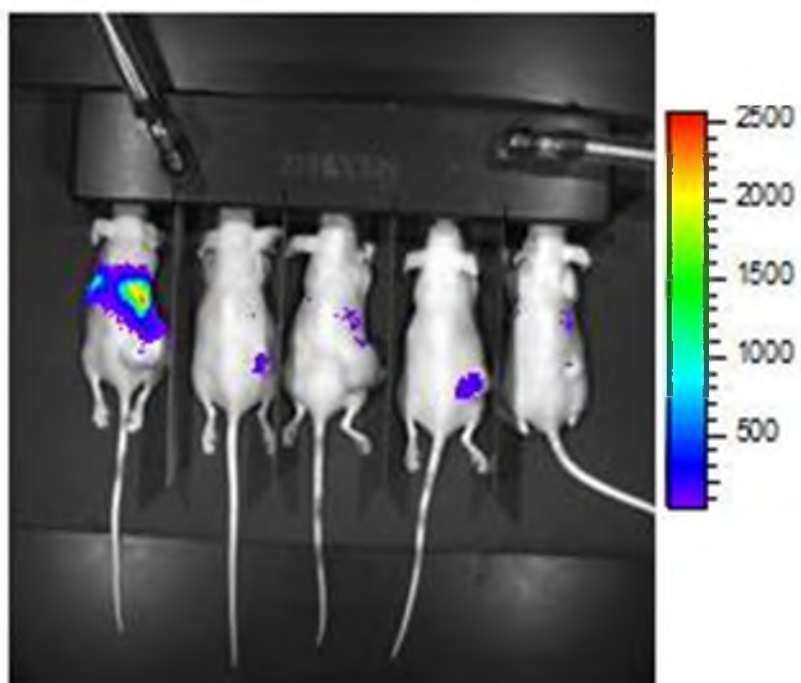


Figure 3.7: Bioluminescent imaging for SELP-815K 4 wt%+Ad.CMV.Luc day 21

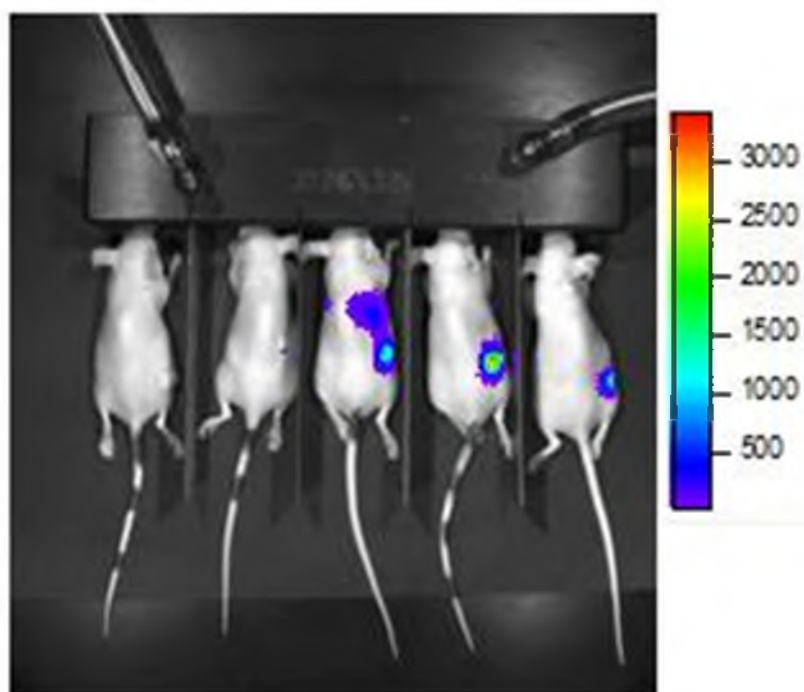


Figure 3.8: Bioluminescent imaging for Ad.CMV.Luc day 4

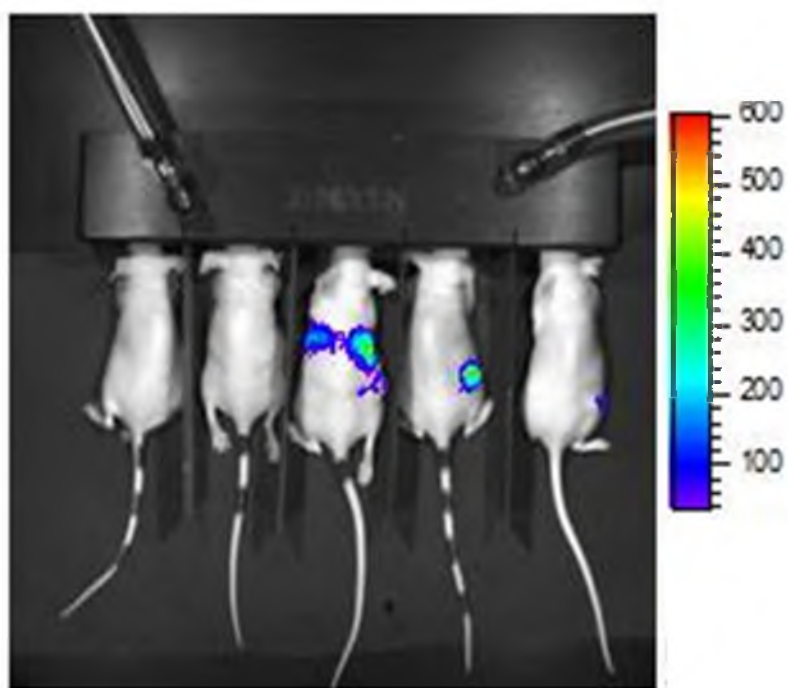


Figure 3.9: Bioluminescent imaging for Ad.CMV.Luc Day 14

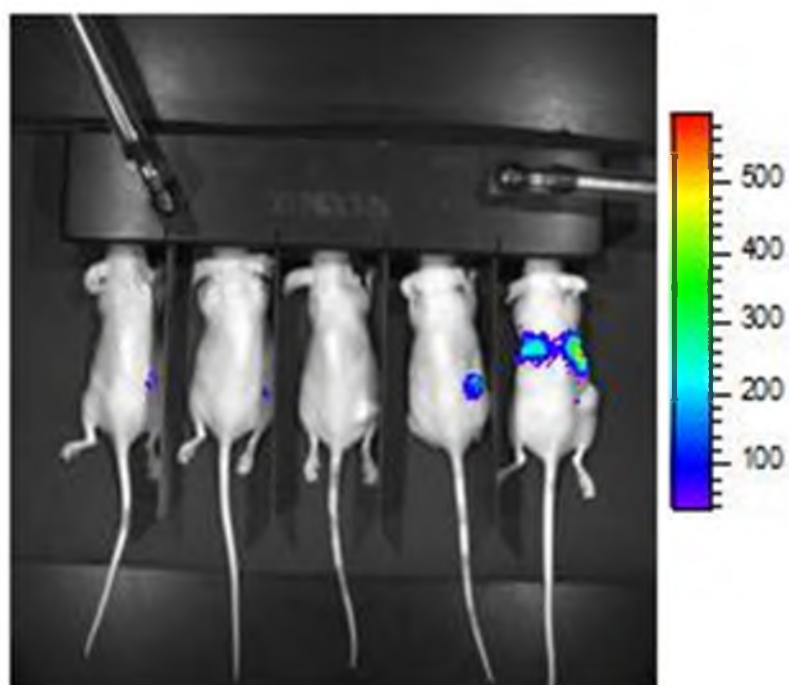


Figure 3.10: Bioluminescent imaging for Ad.CMV.Luc day 21



luciferase at day 4 (Figure 3.8). At day 21 (Figure 3.7), there is still tumor expression in all but one animal in the SELP-mediated group, illustrating the ability of SELP to prolong gene expression compared to free virus injection at the same time point, which shows only one animal with appreciable expression starting on day 14 (Figure 3.9). The bioluminescent images of gene expression correlate with the data acquired through enzyme assay and confirm the influence of SELP on controlling gene expression, which would likely improve the efficacy of treatment of head and neck cancer with a virus/prodrug system. Additionally, based on these results, SELP could improve the safety of this treatment, as SELP causes lower cumulative transfection in the liver, the primary organ affected by adenovirus toxicity.<sup>2,9</sup>

### 3.3.3 *In vitro* enzymatic degradation of SELP hydrogels

To successfully develop SELPs for matrix-mediated delivery, the biodegradation of these polymers needs to be studied. An ideal matrix is one that prolongs gene expression and degrades to amino acids for elimination from the body after gene delivery. The structure of the linear SELPs influences their degradation rate. We evaluated *in vitro* the influence of elastase concentration, polymer structure, and polymer concentration on degradation of the hydrogels. Degradation was measured as percent protein loss from the hydrogels. Protein loss is a function of release of soluble proteins that do not participate in the polymer network. An increase in degradation results in increased protein release. Figure 3.11 shows the time-dependent protein release of SELP hydrogels in a solution of human leukocyte elastase. Figure 3.12 shows

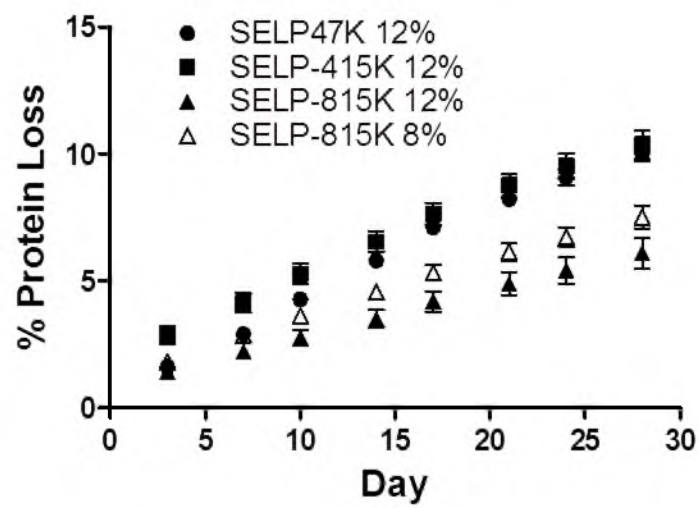


Figure 3.11: Protein loss over time from SELPs degraded by human leukocyte elastase

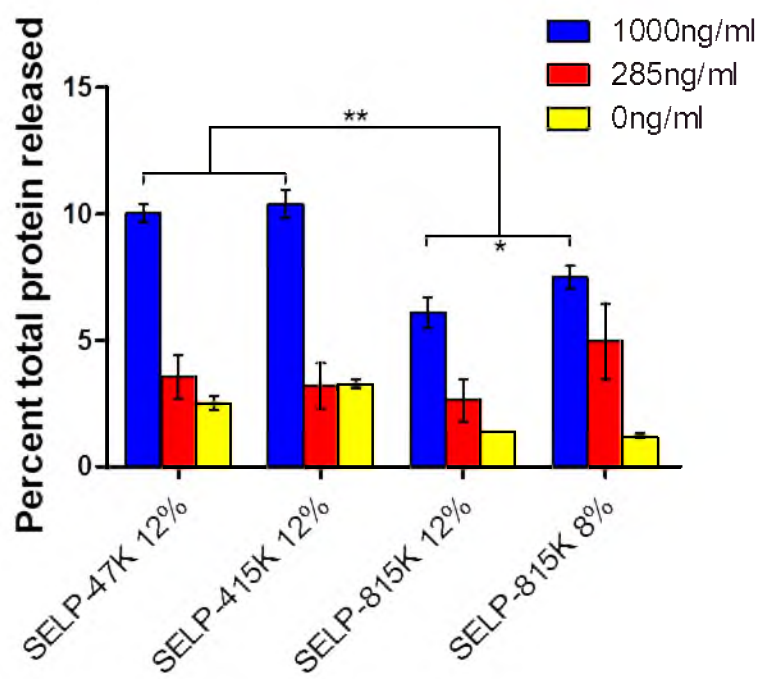


Figure 3.12: Total protein loss due to elastase degradation as a function of SELP composition and elastase concentration

a concentration-dependence of degradation with degradation increasing with increasing elastase concentration. After 1 month of incubation, SELP-47K 12 wt% and SELP-415K 12 wt% each lost more than 10% of their total weight, while SELP-815K at 12 wt% lost 6.1% of its weight and SELP-815K 8 wt % lost 7.5% of its weight in 1  $\mu\text{g/ml}$  elastase. In 285 ng/ml elastase, SELP-47K 12 wt% lost only 3.6%, SELP-415K 12 wt% lost 3.2%, and SELP-815 12% and 8 wt % lost 2.6% and 3.5%, respectively. These results show that, in general, SELPs with lower numbers of silk units degrade faster than SELPs with higher numbers of silk units. This is likely due to a combination of two factors: presence of less elastin units causes less degradation, and hydrogels with more silk units have a higher crosslinking density, leading to potentially less diffusion of the enzyme in the matrix and subsequent degradation. Pore size of the hydrogels is likely to influence the diffusion of elastase molecules which are around 25kDa. The differences in protein mass loss are due to differences in the three-dimensional network of the hydrogels. The longer silk units potentially form a more extensive network which can contribute to steric hindrance and hence physically shield the more degradation-susceptible elastin units, causing SELP-815K to degrade more slowly than both SELP-47K and SELP-415K. Similarly, the higher crosslinking of SELP-815K at 12 wt% results in a lower degradation rate.

In assessing the elastase-driven degradation of SELP hydrogels, another important parameter is the concentration of the enzyme in the media. An increase in concentration of elastase led to increased degradation of the hydrogels. This effect was more pronounced for hydrogels SELP-47K and SELP-415K where at the lower concentrations of 285 ng/ml, protein loss was minimal and similar or equal to the base

line loss of soluble fraction of the hydrogels. The differences in degradation and protein release from SELP hydrogels play an important role in the selection of appropriate structures for matrix-mediated gene delivery. The next logical step is to investigate the degradation of SELP hydrogels *in vivo* to help further understand the rate of SELP degradation in solid tumors and correlate polymer structure with *in vivo* degradation, gene release, transfection efficiency, and therapeutic efficacy.

### 3.4 Conclusions

The studies in this chapter demonstrate the utility of silk-elastinlike protein polymers in matrix-mediated gene delivery to head and neck solid tumors. By using genetic engineering techniques it is possible to tailor-make the structure of the hydrogels to control gel formation, mechanical properties, release, *in vivo* transfection, and degradation. In the series studied, viruses released from SELP-815K at 4 wt% polymer concentration showed the highest transfection efficiency and prolonged gene expression up to day 21. These hydrogels also minimized dissemination of the viruses to the liver. Future studies will be focused on investigating how the enhanced localization of adenoviral transfection offered by SELP-815K 4 wt% translates to reduced toxicity of therapeutic adenovirus.

The degradation of SELP was shown to be structurally dependent. At equivalent concentrations of polymers and elastase, degradation rate of SELP-815K was lower than SELP-415K and SELP-47K. Further work on the degradative properties of SELP will focus on other HNSCC-relevant enzymes, such as MMP-2 and MMP-9 which are commonly found in HNSCC and used as prognostic biomarkers.<sup>15, 16</sup>

### 3.5 References

1. Vrancken Peeters, M. J.; Perkins, A. L.; Kay, M. A., Method for multiple portal vein infusions in mice: quantitation of adenovirus-mediated hepatic gene transfer. *Biotechniques* **1996**, *20*, (2), 278-285.
2. Shayakhmetov, D. M.; Gaggar, A.; Ni, S.; Li, Z. Y.; Lieber, A., Adenovirus binding to blood factors results in liver cell infection and hepatotoxicity. *J Virol* **2005**, *79*, (12), 7478-7491.
3. Fechner, H.; Haack, A.; Wang, H.; Wang, X.; Eizema, K.; Pauschinger, M.; Schoemaker, R.; Veghel, R.; Houtsmuller, A.; Schultheiss, H. P.; Lamers, J.; Poller, W., Expression of coxsackie adenovirus receptor and alphav-integrin does not correlate with adenovector targeting in vivo indicating anatomical vector barriers. *Gene Ther* **1999**, *6*, (9), 1520-1535.
4. Alemany, R.; Curiel, D. T., CAR-binding ablation does not change biodistribution and toxicity of adenoviral vectors. *Gene Ther* **2001**, *8*, (17), 1347-1353.
5. Einfeld, D. A.; Schroeder, R.; Roelvink, P. W.; Lizonova, A.; King, C. R.; Kovesdi, I.; Wickham, T. J., Reducing the native tropism of adenovirus vectors requires removal of both CAR and integrin interactions. *J Virol* **2001**, *75*, (23), 11284-11291.
6. Haider, M.; Leung, V.; Ferrari, F.; Crissman, J.; Powell, J.; Cappello, J.; Ghandehari, H., Molecular engineering of silk-elastinlike polymers for matrix-mediated gene delivery: biosynthesis and characterization. *Mol Pharm* **2005**, *2*, (2), 139-150.
7. Dandu, R.; Cresce, A. V.; Briber, R.; Dowell, P.; Cappello, J.; Ghandehari, H., Silk-elastinlike protein polymer hydrogels: Influence of monomer sequence on physicochemical properties. *Polymer* **2009**, *50*, (2), 366-374.
8. Yang, Y.; Li, Q.; Ertl, H. C.; Wilson, J. M., Cellular and humoral immune responses to viral antigens create barriers to lung-directed gene therapy with recombinant adenoviruses. *J Virol* **1995**, *69*, (4), 2004-2015.
9. Mahasreshti, P. J.; Kataram, M.; Wang, M. H.; Stockard, C. R.; Grizzle, W. E.; Carey, D.; Siegal, G. P.; Haisma, H. J.; Alvarez, R. D.; Curiel, D. T., Intravenous delivery of adenovirus-mediated soluble FLT-1 results in liver toxicity. *Clin Cancer Res* **2003**, *9*, (7), 2701-2710.
10. Cappello, J.; Crissman, J. W.; Crissman, M.; Ferrari, F. A.; Textor, G.; Wallis, O.; Whitley, J. R.; Zhou, X.; Burman, D.; Aukerman, L.; Stedronsky, E. R., In-situ self-assembling protein polymer gel systems for administration, delivery, and release of drugs. *J Control Release* **1998**, *53*, (1-3), 105-117.

11. Dinerman, A. A.; Cappello, J.; Ghandehari, H.; Hoag, S. W., Swelling behavior of a genetically engineered silk-elastinlike protein polymer hydrogel. *Biomaterials* **2002**, *23*, (21), 4203-4210.
12. Dinerman, A. A.; Cappello, J.; Ghandehari, H.; Hoag, S. W., Solute diffusion in genetically engineered silk-elastinlike protein polymer hydrogels. *J Control Release* **2002**, *82*, (2-3), 277-287.
13. Megeed, Z.; Cappello, J.; Ghandehari, H., Controlled release of plasmid DNA from a genetically engineered silk-elastinlike hydrogel. *Pharm Res* **2002**, *19*, (7), 954-959.
14. Dandu, R.; Ghandehari, H.; Cappello, J., Characterization of structurally related adenovirus-laden silk-elastinlike hydrogels. *J Bioact Compat Pol* **2008**, *23*, (1), 5-19.
15. Klein, T.; Bischoff, R., Physiology and pathophysiology of matrix metalloproteases. *Amino Acids* **2011**, *41*, (2), 271-290.
16. Rosenthal, E. L.; Matrisian, L. M., Matrix metalloproteases in head and neck cancer. *Head Neck* **2006**, *28*, (7), 639-648.

## CHAPTER 4

# SILK-ELASTINLIKE HYDROGEL IMPROVES THE SAFETY OF ADENOVIRUS-MEDIATED GENE-DIRECTED ENZYME-PRODRUG THERAPY

### **4.1 Introduction**

In spite of its superior transfection efficiency, the application of adenoviruses as gene delivery vectors has been plagued with problems of toxicity which have delayed their advancement to clinical use, as previously mentioned in Section 2.2.2.2.1. Based on the results discussed in Chapter 3, delivery of adenoviruses in SELP hydrogel significantly improves the distribution profile of gene transfection; however, it is also necessary for a successful adenoviral delivery material to improve the safety of this treatment.

One way of achieving this goal would be to surface-modify or package the viruses such that they do not activate the immune system, which would require surface antigen molecules to be modified or covered to avoid detection. This approach has previously been attempted by conjugation of HPMA copolymers<sup>1</sup> or poly(ethylene glycol) (PEG)<sup>2, 3</sup> for disguising of adenovirus from detection and neutralization by host immune system. These approaches do accomplish the goal of reducing neutralization of the viral particles by various mechanisms, and in the case of HPMA copolymers actually affect an increase



in uptake by cells.<sup>1</sup> However, reduced immunogenicity comes at a cost of reduced efficacy of gene transduction. PEG showed similar results *in vitro*, almost completely eliminating transfection of cells in a coxsackie and adenovirus receptor (CAR)-dependent manner.<sup>3</sup> It is important to note that some organ-specific gene transduction is unaffected or even aided by surface functionalization of the viruses.<sup>2, 3</sup> However, this will not be appropriate for most applications of gene therapy, as it is a result of interactions with the surface hexon proteins with specific blood components (primarily clotting factors), leading to increased uptake by the liver.<sup>4, 5</sup> In terms of CAR-dependent transfection, surface functionalization thus far appears to completely ablate transfection.

Delivery of the viruses in a noninterfering depot such as SELP hydrogel may share the benefits of these systems by reducing the off-target distribution of adenovirus and thereby reducing its toxicity. The experiments described in this chapter investigate the ability of SELP hydrogel to perform this function. The specific enzyme-prodrug model therapeutic system under investigation is the herpes simplex virus thymidine kinase (HSVtk) – ganciclovir (GCV) system, discussed in Section 2.2.1.1 (Figure 2.1). In this enzyme-prodrug system, cells are transfected to produce HSVtk, which enables the cell to metabolize GCV to produce GCV-monophosphate.<sup>6-9</sup> GCV otherwise has a very low affinity for nonviral thymidine kinases, and therefore causes little to no conversion in cells not expressing HSVtk.<sup>7-9</sup> GCV-monophosphate can freely pass between cells via cell-cell junctions, and additionally can be further phosphorylated by native cellular kinases to produce GCV-triphosphate.<sup>7-9</sup> GCV-triphosphate is a potent inhibitor of DNA elongation by competing with guanosine for incorporation while significantly slowing the elongation of DNA, resulting in apoptotic cell death.

## 4.2 Materials and methods

### 4.2.1 Adenoviruses

Human adenovirus serotype 5 encoding for herpes simplex virus thymidine kinase (Ad.HSVtk) was purchased from Vector Biolabs (Philadelphia, PA) and used at a viral titer of  $1.5 \times 10^{11}$  PFU/ml. Viruses were stored at  $-80^{\circ}\text{C}$  and used immediately following defrosting to avoid unnecessary freeze-thaw cycles.

### 4.2.2 Animals

All animal studies were carried out with the permission and under the rules and guidelines of the University of Utah Institutional Animal Care and Use Committee. All mice used in this study were 4-6-week-old female standard CD-1 mice, purchased from Charles River Laboratories (Boston, MA). CD-1 mice have an intact immune system, which was anticipated to show adverse reactions to the viral vectors comparable to those observed in human trials. Mouse cages and bedding were changed weekly and food and water was checked and replenished daily as needed.

### 4.2.3 Injection of therapeutic Ad.HSVtk

For the toxicity studies, Ad.HSVtk was prepared by dilution in either sterile 0.9% physiological saline for injection (Baxter, Deerfield, IL) or SELP-815K which was previously synthesized<sup>10</sup> to a final concentration of  $1.5 \times 10^{11}$  PFU of virus per ml of solution. SELP-815K was used at a final concentration of 4 wt%, determined to be the leading candidate, as described in Chapter 3<sup>11</sup> and for improvement of virus-mediated GDEPT described in previous studies.<sup>12</sup> Mice were anesthetized and maintained in

anesthesia with 3% isoflurane in oxygen. After shaving and cleaning the injection site with 60% isopropanol, mice were subcutaneously injected with 50 $\mu$ l of solution in the right flank via a 26G needle on a 250 $\mu$ l Hamilton syringe. This resulted in an actual viral titer of  $\sim 7.6 \times 10^9$  PFU administered per mouse. The injection site was gently clamped for 10 seconds to prevent leakage, after which mice were returned to their cages. For consistency, the day of viral injection was considered day 0. The exact conditions administered are shown in Table 4.1.

#### 4.2.4 Injection of ganciclovir (GCV)

For treatment groups, a suspension of 1mg GCV (Sigma Aldrich, St. Louis, MO) per milliliter of 0.9% physiological saline was prepared and sterilized through a 0.22  $\mu$ m filter. Each day, animal weights were recorded, injection sites cleaned with 60% isopropanol, and mice injected i.p. with 1mg/ml GCV suspension through a 26G needle sufficient for a total dose of 25 mg/kg. Average dosing volume for these studies was approximately 0.6 ml. Mice were injected daily for the first 4 weeks of the 12 week recovery study, and for the entirety of the 1-, 2-, and 4-week studies.

#### 4.2.5 Necropsy and data collection

Upon completion of each study, mice were individually euthanized using 70% CO<sub>2</sub> in oxygen, with euthanasia confirmed by lack of breathing for 10s. Blood was taken via inferior vena cava stick, and drawn into a heparinized syringe through a 25G needle and deposited into a heparinized plastic blood tube. Minimal evidence of hemolysis was observed in blood samples. Injection sites were dissected for visual observation of local

Table 4.1

Animals per study group and end points for toxicity studies

<b>Group</b>	<b>1 week</b>	<b>2 weeks</b>	<b>4 weeks</b>	<b>12 weeks</b>
Control (saline only)	3	9	9	3
Ad.HSVtk+GCV	4	9	9	4
SELP-815K 4% + Ad.HSVtk + GCV	4	9	9	4

inflammation. Complete blood counts (CBCs) were performed within 2 hours of blood sample collection using a CBC-DIFF (Heska, Loveland, CO) blood count analyzer. Following CBC, samples were centrifuged at 10,000 rpm for 2.5 minutes and rapidly frozen at -80°C for future analysis. A blood chemistry panel consisting of blood urea nitrogen, creatinine, aspartate aminotransferase (AST), alanine aminotransferase (ALT), total bilirubin, total protein, and albumin was used as indicators of both kidney and liver toxicity. Additionally, globulin was calculated by subtracting albumin from total protein, and albumin/globulin ratio was calculated. Blood chemistry assessments were made using a DRI-CHEM (Heska, Loveland, CO) veterinary blood chemistry analyzer.

#### 4.2.6 Data interpretation

Mouse weight data were used to compare with values on day 0. The percentage weight gain was calculated for each mouse and used as a general indicator of animal health. Animal weight, blood count, and chemistry data were compared using two-tailed Student's t-tests, with results considered significant if p-values of <0.05 were obtained. Only data reflecting significant changes compared to control are included here. Specifically, animal weight, differential white blood cell count, and ALT/AST values are reported.

### 4.3 Results and discussion

Virus mediated GDEPT administered in SELP hydrogels for the treatment of cancer has been shown to be an effective treatment in a xenograft model of human head and neck cancer.<sup>12</sup> Due to legitimate concerns in the presence of a fully intact immune

system, it becomes necessary to carefully assess the ability of the delivery system to improve the safety of this treatment in an immunocompetent model. The toxicity of SELP-controlled, virus-mediated GDEPT was examined in the acute (1 week) phase, and a 12-week recovery study was performed to investigate the ability of the mice to return to normal weight and blood count after treatment had been stopped. Two additional time points were selected, 2 weeks and 4 weeks, corresponding to the apparent peak and resolution of toxicity based on mouse weight data gathered in the recovery study. It was considered that examination of the specific indicators of toxicity and organ inflammation/damage at these time points would allow diagnosis of the mechanism of toxicity, or at the very least the specific organs affected. This information could potentially be useful in the design of future systems and strategies for controlled delivery of viral gene therapy to localized diseases.

#### 4.3.1 Acute toxicity

Figures 4.1 and 4.2 show animal weight data for the toxicity studies. Acute toxicity was assessed with an endpoint of 7 days, at which time a lower weight gain was observed for the free viral delivery group compared to control. SELP-mediated delivery did not show statistically significant weight loss at any point during the first 7 days compared to both free viral delivery and control, although the mean values were less than control. It is noteworthy that virus injected without the hydrogels stopped gaining weight for 24 hours after injection, while this effect appeared at day 3 in the SELP-mediated group. White blood cell counts, shown in Figure 4.3, indicated a significant increase in total white blood cell count in the free virus group compared to both the SELP-mediated

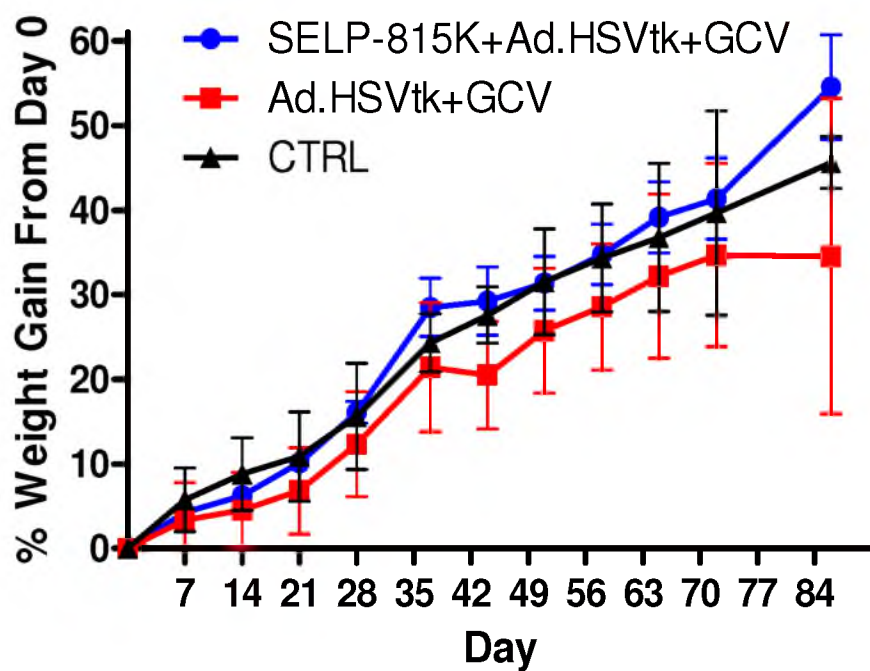


Figure 4.1: Animal weights from day 0-84 for SELP-mediated GDEPT toxicity study.  
Control: Saline only injection

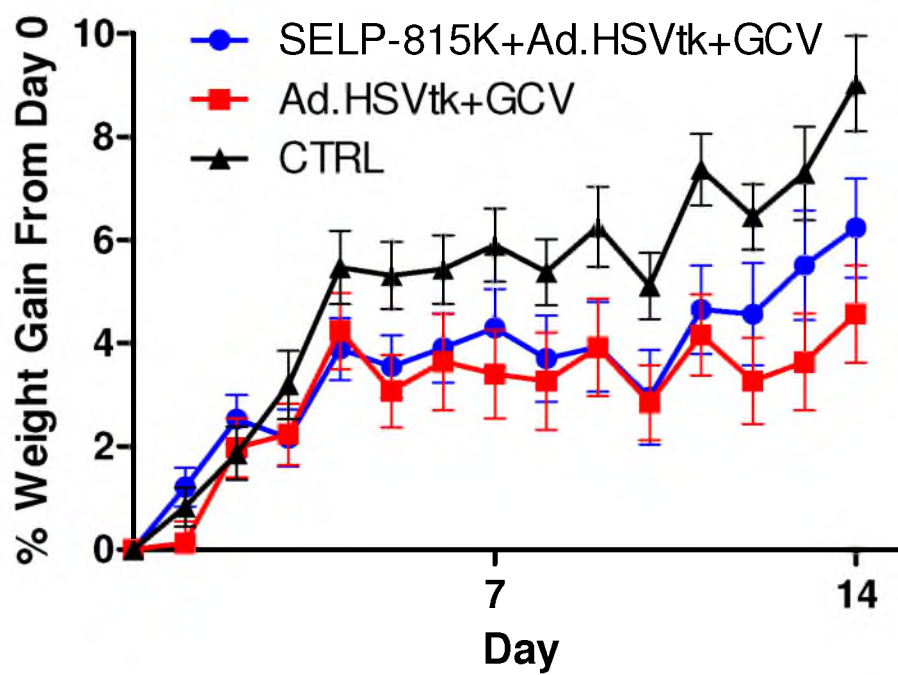


Figure 4.2: Animal weights from day 0-14 for SELP-mediated GDEPT toxicity study.  
Control: Saline only injection



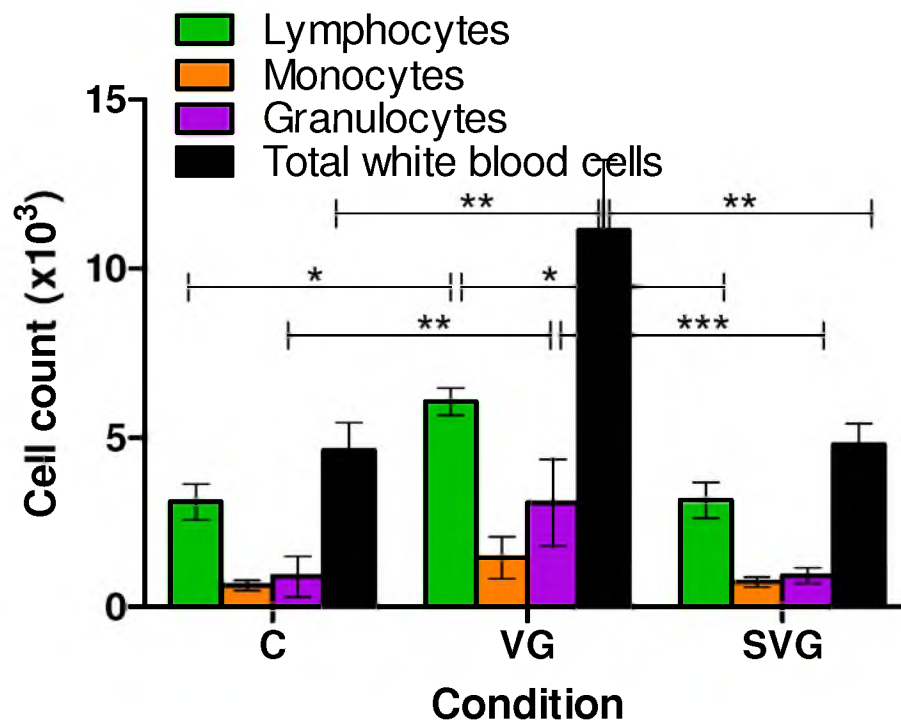


Figure 4.3: Differential white blood cell count at week 1 for SELP-mediated GDEPT toxicity study. C: Control (saline only injection), VG: Ad.HSVtk administered in saline with daily GCV injections, SVG: Ad.HSVtk administered in SELP-815K 4% with daily GCV injections

condition and the control. This overall increase is primarily due to elevated granulocyte and lymphocyte counts in the virus group, suggesting an acute immune response to the administered virus. The absence of this increase in total white blood cell count and differentials in the SELP-mediated group could potentially indicate that locally controlling viral gene delivery using SELP-815K hydrogel reduces or eliminates the systemic immune response to the adenoviral vectors.

Blood chemistry results for the acute toxicity study indicated the beginnings of hepatotoxicity (Figure 4.4) with elevated AST levels appearing in some mice in the free virus group. It is possible that this increase in AST is a result of damage to liver cells, which would likely be attributed to the therapeutic activity as opposed to immune mechanisms. This is because adenoviruses are known to be removed from circulation by the liver, increasing the probability of gene transfection in this organ. This phenomenon is consistent with our observations discussed in Chapter 3.<sup>11</sup> Statistical analysis did not yield any significant differences between groups in either ALT or AST, however. At this early stage, substantial liver toxicity is unexpected. It has been shown that adenoviral gene expression *in vivo* peaks at 6 days following exposure to the virus<sup>13</sup>; however, as the therapeutic gene itself does not cause cytotoxicity in our system,<sup>9</sup> it requires additional time for sufficient quantities of converted prodrug to accumulate and cause toxicity. SELP matrix appears to reduce the overall acute systemic toxicity of the treatment. Its apparent ability to reduce the magnitude of the acute systemic immune response to the adenoviral vector, as evidenced by reduced leukocytes (Figure 4.3), highlights the utility of this polymer for localized viral delivery.

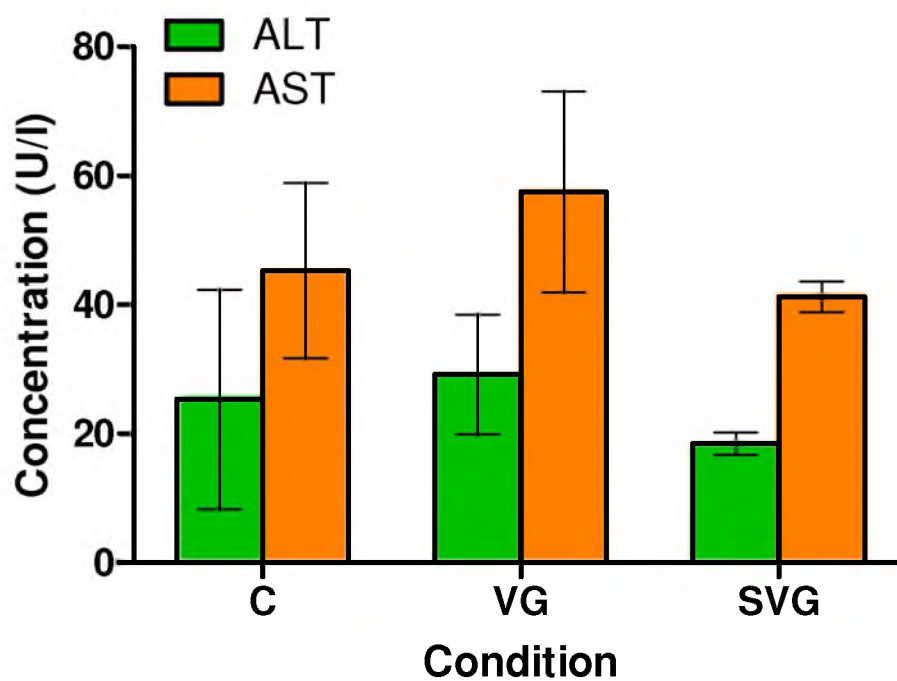


Figure 4.4: Liver enzyme levels at week 1 for SELP-mediated GDEPT toxicity study. C: Control (saline only injection), VG: Ad.HSVtk administered in saline with daily GCV injections, SVG: Ad.HSVtk administered in SELP-815K 4% with daily GCV injections

#### 4.3.2 Subacute toxicity – 2-week time point

A 2-week time point was selected in order to monitor the progression of toxicity of this system, as only initial phases appeared to occur in the 1-week study. Animal weight data over the first 2-weeks of study (Figure 4.2) showed the difference in the progression of toxicity between the SELP-mediated release and free virus conditions. Weight gains were significantly reduced for the free virus group compared to the control group for days 10-14. SELP-mediated delivery reduced this effect to only a single day (day 11) on which weight gain was significantly reduced compared to control.

Figure 4.5 represents the white blood cell count data gathered for animals at the 2-week time point. While the primary mechanism of toxicity in the free virus delivery case at 1 week appeared to be immune-response-related based on significantly elevated lymphocytes, monocytes, and granulocytes, at 2 weeks, this response appears to have resolved as levels returned comparable to control. In contrast, at 2 weeks, there was a significant elevation in total white cell and lymphocyte counts in the SELP-mediated delivery case compared to both control and free viral delivery. However, in both cases, the levels were less than those at 1 week in the free virus group. These results suggest that delivering the virus in SELP delays the onset of an immune response, and possibly reduces its magnitude.

The results of blood chemistry analysis at the 2-week time point are displayed in Figure 4.6. The elevated ALT and AST levels in the two treatment groups as compared to control suggest that liver damage is occurring. Hepatotoxicity is indicated most readily by AST, with statistically significant elevations in both treatment groups compared to

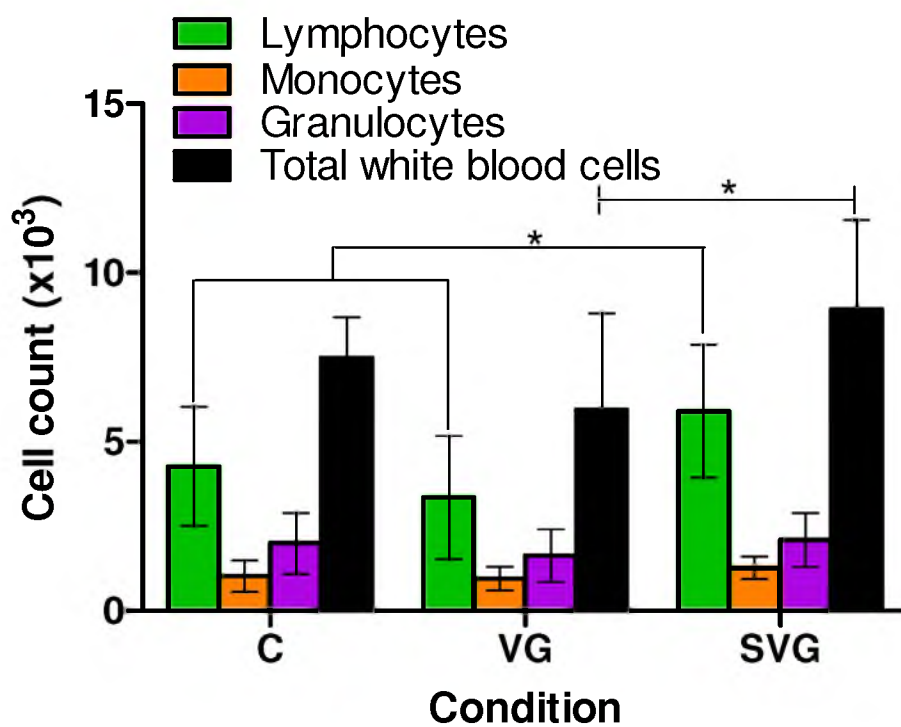


Figure 4.5: Differential white blood cell count at week 2 for SELP-mediated GDEPT toxicity study. C: Control (saline only injection), VG: Ad.HSVtk administered in saline with daily GCV injections, SVG: Ad.HSVtk administered in SELP-815K 4% with daily GCV injections

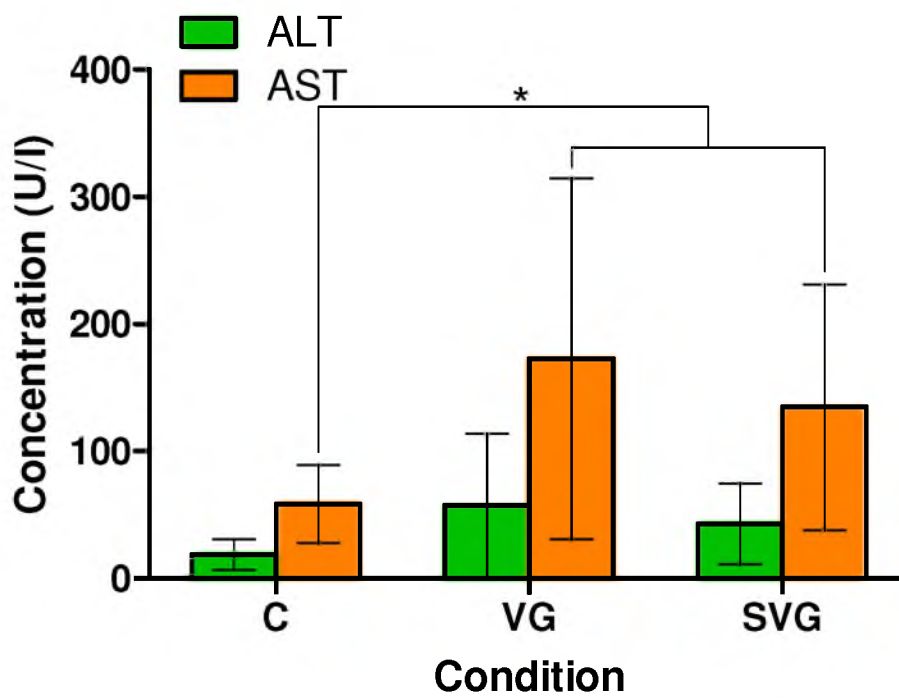


Figure 4.6: Liver enzyme levels at week 2 for SELP-mediated GDEPT toxicity study. C: Control (saline only injection), VG: Ad.HSVtk administered in saline with daily GCV injections, SVG: Ad.HSVtk administered in SELP-815K 4% with daily GCV injections

control. This evidence is supported by ALT levels, which were also elevated for several animals in the virus treatment groups. While not statistically significant, the AST and ALT levels were reduced in the SELP-mediated delivery group versus free virus. This damage is likely caused by transfection of the cells of the liver and subsequent cell death due to sensitivity to the prodrug and the bystander effect,<sup>9</sup> as opposed to an immune reaction to the viral constructs themselves.

#### 4.3.3 Subacute toxicity – 4-week time point

The next time point considered was 4 weeks after the initial injection of virus, chosen based on results discussed in Chapter 3<sup>11</sup> indicating that viral load is essentially completely released by the end of 4 weeks, making this a likely “turning point” after which toxicity should resolve. Between 2 weeks and 4 weeks, all groups displayed weight gain; however, the order of weight gain between the groups established early in the study remained. Based on the animal weight data (Figure 4.1) at 4 weeks (28 days), the free virus group appeared to be delayed in growth by 7-14 days as compared to the control group, while the SELP-mediated group appears to be delayed by less than 7 days. This demonstrates an advantage of SELP-mediated delivery over free viral injection in terms of general health as measured by body weight increase.

White blood cell counts, shown in Figure 4.7, did not indicate any significant differences in immune state of the mice at 4 weeks postinjection, possibly due to complete or near-complete clearance of the virus. There was a minor elevation, although not statistically significant, of the mean values for all three differential counts and in the total white cell count in the free virus group, suggesting a possible low-level immune

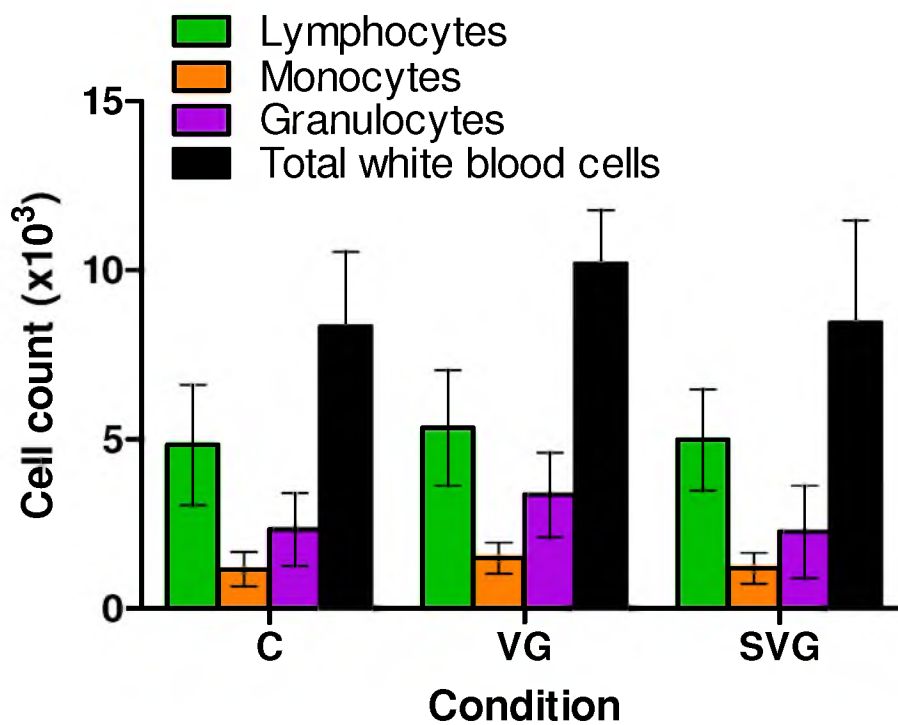


Figure 4.7: Differential white blood cell count at week 4 for SELP-mediated GDEPT toxicity study. C: Control (saline only injection), VG: Ad.HSVtk administered in saline with daily GCV injections, SVG: Ad.HSVtk administered in SELP-815K 4% with daily GCV injections



activation. Further evidence of SELP's utility in improving the safety of this treatment is shown in Figure 4.8. It is apparent from these data that at 4 weeks, the uncontrolled delivery of virus in combination with prodrug was still causing hepatotoxicity, as evidenced by AST elevation in the free virus group compared to the control and the SELP-mediated conditions. The significance of this effect suggests that there was some lingering toxicity of the initial free viral delivery.

#### 4.3.4 Recovery study

A 12-week time point served as an indication of how well animals are able to recover from the effects of the treatment previously observed. Animal weight is the primary indicator of recovery at this point, as CBC and blood chemistry evidenced toxicity is very likely to be resolved, particularly considering the rapid metabolism and healing capability of mice. As shown in Figure 4.1, between 4 and 12 weeks following viral injection, signs of toxicity had generally resolved and except for two instances, animals in all groups gained weight at a steady rate. However, between days 36 and 44 and between days 72 and 86, the mean weight gains for the free virus group decreased; the only weight losses recorded throughout the entire study. In contrast, the weight gains of the SELP-mediated group actually surpassed the control group from day 36 through the end of the study. CBC analysis of the animals at 12 weeks, shown in Figure 4.9, reveals no overt evidence of toxicity, although mononuclear leukocytes appear to be depressed slightly in the two treatment groups compared to control. These low values are not particularly of concern as their quantity can fluctuate significantly for any number of reasons, and there was no other independent evidence of an issue related to this analyte.

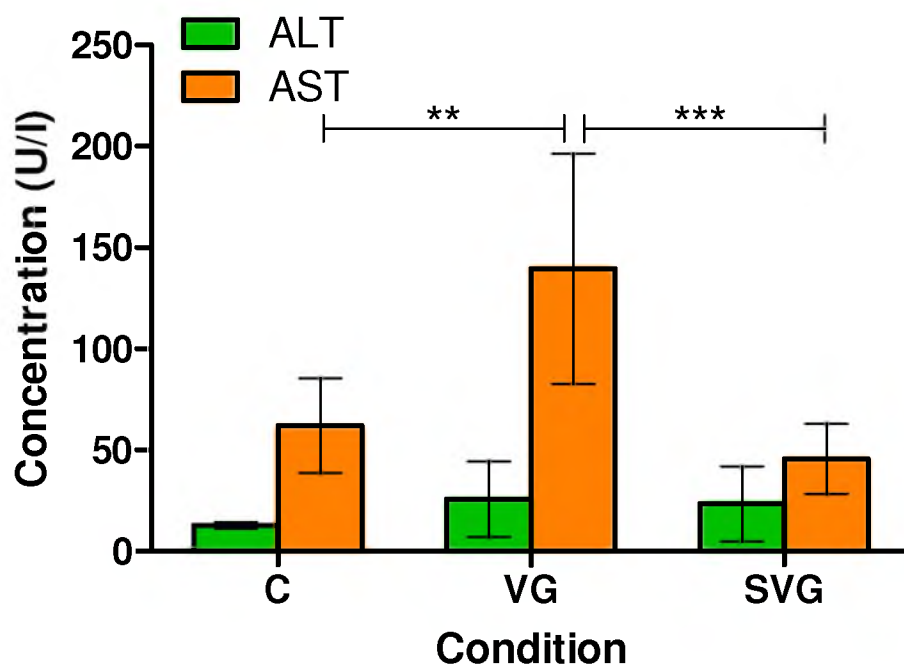


Figure 4.8: Liver enzyme levels at week 4 for SELP-mediated GDEPT toxicity study. C: Control (saline only injection), VG: Ad.HSVtk administered in saline with daily GCV injections, SVG: Ad.HSVtk administered in SELP-815K 4% with daily GCV injections

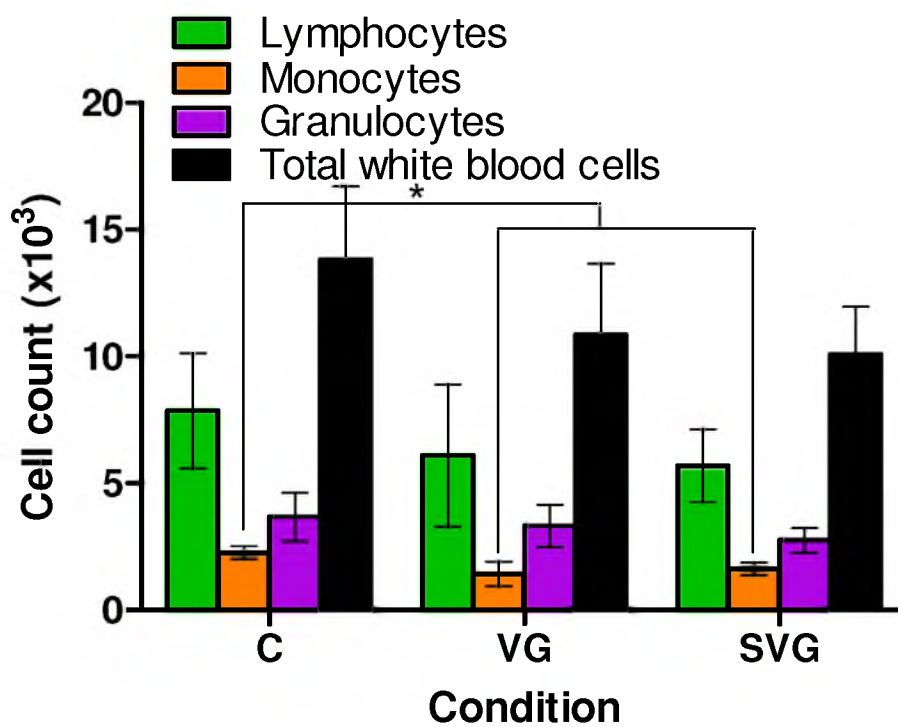


Figure 4.9: Differential white blood cell count at week 12 for SELP-mediated GDEPT toxicity study. C: Control (saline only injection), VG: Ad.HSVtk administered in saline with daily GCV injections, SVG: Ad.HSVtk administered in SELP-815K 4% with daily GCV injections

These data indicate that animals were able to completely recover from the toxic effects previously observed in the treatment time points.

#### **4.4 Conclusions**

Administration of Ad.HSVtk in SELP-815K 4 wt% hydrogel was shown to reduce the systemic toxicity of gene-directed enzyme-prodrug therapy compared to free viral injection. This reduction in toxicity in conjunction with previously collected data showing improved efficacy in a nude mouse/human xenograft HNSCC model<sup>12</sup> makes SELP-mediated delivery a promising approach for viral cancer gene therapy.

Supporting this conclusion is a set of unpublished data described in the Appendix, which investigated the efficacy of SELP-mediated delivery compared to aqueous viral injection in a short pilot study in immunocompetent mice. This brief experiment illustrated a significant reduction in tumor growth rate in an aggressive fibrosarcoma and further serves to illustrate the utility of this delivery system for matrix-mediated gene-directed enzyme-prodrug therapy.

#### 4.5 References

1. Sims, K.; Ahmed, Z.; Read, M. L.; Cooper-Charles, L.; Gonzalez, A. M.; Fisher, K. D.; Berry, M.; Seymour, L. W.; Logan, A., In vitro evaluation of a 'stealth' adenoviral vector for targeted gene delivery to adult mammalian neurones. *J Gene Med* **2009**, *11*, (4), 335-344.
2. Mok, H.; Palmer, D. J.; Ng, P.; Barry, M. A., Evaluation of polyethylene glycol modification of first-generation and helper-dependent adenoviral vectors to reduce innate immune responses. *Mol Ther* **2005**, *11*, (1), 66-79.
3. Hofherr, S. E.; Shashkova, E. V.; Weaver, E. A.; Khare, R.; Barry, M. A., Modification of adenoviral vectors with polyethylene glycol modulates in vivo tissue tropism and gene expression. *Mol Ther* **2008**, *16*, (7), 1276-1282.
4. Waddington, S. N.; McVey, J. H.; Bhella, D.; Parker, A. L.; Barker, K.; Atoda, H.; Pink, R.; Buckley, S. M.; Greig, J. A.; Denby, L.; Custers, J.; Morita, T.; Francischetti, I. M.; Monteiro, R. Q.; Barouch, D. H.; van Rooijen, N.; Napoli, C.; Havenga, M. J.; Nicklin, S. A.; Baker, A. H., Adenovirus serotype 5 hexon mediates liver gene transfer. *Cell* **2008**, *132*, (3), 397-409.
5. Kalyuzhniy, O.; Di Paolo, N. C.; Silvestry, M.; Hofherr, S. E.; Barry, M. A.; Stewart, P. L.; Shayakhmetov, D. M., Adenovirus serotype 5 hexon is critical for virus infection of hepatocytes in vivo. *Proc Natl Acad Sci U S A* **2008**, *105*, (14), 5483-5488.
6. Cheng, Y. C.; Grill, S. P.; Dutschman, G. E.; Nakayama, K.; Bastow, K. F., Metabolism of 9-(1,3-dihydroxy-2-propoxymethyl)guanine, a new anti-herpes virus compound, in herpes simplex virus-infected cells. *J Biol Chem* **1983**, *258*, (20), 12460-12464.
7. Hamel, W.; Magnelli, L.; Chiarugi, V. P.; Israel, M. A., Herpes simplex virus thymidine kinase/ganciclovir-mediated apoptotic death of bystander cells. *Cancer Res* **1996**, *56*, (12), 2697-2702.
8. Touraine, R. L.; Ishii-Morita, H.; Ramsey, W. J.; Blaese, R. M., The bystander effect in the HSVtk/ganciclovir system and its relationship to gap junctional communication. *Gene Ther* **1998**, *5*, (12), 1705-1711.
9. Mesnil, M.; Yamasaki, H., Bystander effect in herpes simplex virus-thymidine kinase/ganciclovir cancer gene therapy: role of gap-junctional intercellular communication. *Cancer Res* **2000**, *60*, (15), 3989-3999.
10. Dandu, R.; Cresce, A. V.; Briber, R.; Dowell, P.; Cappello, J.; Ghandehari, H., Silk-elastinlike protein polymer hydrogels: Influence of monomer sequence on physicochemical properties. *Polymer* **2009**, *50*, (2), 366-374.

11. Gustafson, J.; Greish, K.; Frandsen, J.; Cappello, J.; Ghandehari, H., Silk-elastinlike recombinant polymers for gene therapy of head and neck cancer: from molecular definition to controlled gene expression. *J Control Release* **2009**, *140*, (3), 256-261.
12. Greish, K.; Frandsen, J.; Scharff, S.; Gustafson, J.; Cappello, J.; Li, D.; O'Malley, B. W., Jr.; Ghandehari, H., Silk-elastinlike protein polymers improve the efficacy of adenovirus thymidine kinase enzyme prodrug therapy of head and neck tumors. *J Gene Med* **2010**, *12*, (7), 572-579.
13. Sen, L.; Hong, Y. S.; Luo, H.; Cui, G.; Laks, H., Efficiency, efficacy, and adverse effects of adenovirus vs. liposome-mediated gene therapy in cardiac allografts. *Am J Physiol Heart Circ Physiol* **2001**, *281*, (3), H1433-1441.

## CHAPTER 5

### SYNTHESIS AND CHARACTERIZATION OF A MATRIX- METALLOPROTEINASE RESPONSIVE SILK- ELASTINLIKE PROTEIN POLYMER

#### **5.1 Introduction**

The field of genetically engineered polymers has grown steadily over the last several decades such that current research has expanded into using this powerful polymer design and production platform to produce materials with highly specific properties. Silk-elastinlike protein polymer (SELP) is one of these materials which is composed of repeating units of silkworm silk fibroin domains (GAGAGS) interspersed with repeating units derived from mammalian elastin (GVGVP). Monomer units of SELP are composed of several silk units in a diblock arrangement with elastin units.

Previous work has demonstrated that modifying the number of silk and elastin units in a monomer can have very specific effects on the properties of the polymers and hydrogels assembled from them.<sup>1-5</sup> One specific structure of SELP, namely SELP-815K, was identified as an effective material for improving the safety, efficacy, and biodistribution of adenoviral delivery for the treatment of head and neck squamous cell carcinoma (HNSCC). In an effort to further improve the viral gene delivery capability of SELP-815K, work described in this chapter investigates the effects of adding a matrix-

metalloproteinase (MMP)-responsive peptide sequence to the monomer unit. MMP-degradable sequences in hydrogels have been used successfully for growth factor delivery,<sup>6</sup> tissue ingrowth scaffolds,<sup>6-8</sup> and drug delivery.<sup>9</sup> Several products incorporating this technology have reached the clinical research stage, and have garnered significant attention from large biosurgery companies for licensing agreements.<sup>10</sup>

The amino acid sequence GPQGIFGQ has been shown to be highly degradable by both MMP-2 and MMP-9, and is derived from a sequence ubiquitously found in collagen to promote its ability to be degraded and remodeled.<sup>11</sup> This sequence is intended to provide a similar property to SELP-815K by allowing it to respond to local intratumoral changes in MMP levels to affect increased release rate in response to the increased aggression and invasiveness of the disease state. Here, the biosynthesis, scale up, and *in vitro* characterization of SELP-815K containing an MMP-responsive sequence is described. The effects of degradation on the mechanical properties of these hydrogels and the release of 100 nm polystyrene particles from them are evaluated. The goal of this work is to demonstrate that adding the MMP-responsive sequence to SELP will allow it to increase release rate of nanoparticulates in the size range of viruses in the presence of MMP-2 and MMP-9, which would impart the capability of this delivery system to respond to disease state with increased delivery of therapeutic adenovirus.

## 5.2 Materials and methods

### 5.2.1 Materials

Restriction enzyme XagI, T4 DNA ligase, and shrimp alkaline phosphatase were purchased from Fermentas (Glen Burnie, MD). Restriction enzymes BanI, AvaII, NcoI,



and XcmI, 1 kilobase TriDye DNA marker, and Orange G loading buffer were purchased from New England Biolabs (Ipswich, MA). DNA miniprep and maxiprep kits and Qiaquick gel extraction kit were purchased from Qiagen (Valencia, CA). MAXEfficiency Dh5 $\alpha$  *E.coli* and 100nm fluorescent spheres were purchased from Invitrogen (Carlsbad, CA). Active matrix-metalloproteinase 2 and 9 and Terrific Broth powder were purchased from EMD (Gibbstown, NJ). BupH borate buffer packs, Lowry assay kit, and GelCode Blue staining reagent (colloidal Coomassie formulation) were purchased from Thermo Pierce (Rockford, IL). Lysogeny broth agar was purchased from BD Biosciences (Franklin Lakes, NJ). 4-15% Bis-Tris precast PAGE gels and Kaleidoscope protein standard were purchased from BioRad (Hercules, CA). Antifoam 204 was purchased from Sigma Aldrich (St.Louis, MO). All oligonucleotides were purchased from Integrated DNA Technologies, Inc. (Coralville, IA). Plasmids pSY1378 (parental) and pPT317 encoding for SELP-815K dimer were provided by Protein Polymer Technologies, Inc. (San Diego, CA). Polyhistidine protein purification was carried out using a Maxwell 16 system equipped with the Polyhistidine Protein Purification Kit purchased from Promega (Madison, WI)

## 5.2.2 Methods

### 5.2.2.1 Construction of the monomer gene segment

Monomer gene segment construction is summarized in Figure 5.1. Plasmid pSY1378 (cloning vector) was digested with BanI and dephosphorylated with shrimp alkaline phosphatase (SAP). Plasmid pPT317 containing two copies of SELP-815K monomer gene segment were digested with BanI and separated on a 1% agarose gel. The

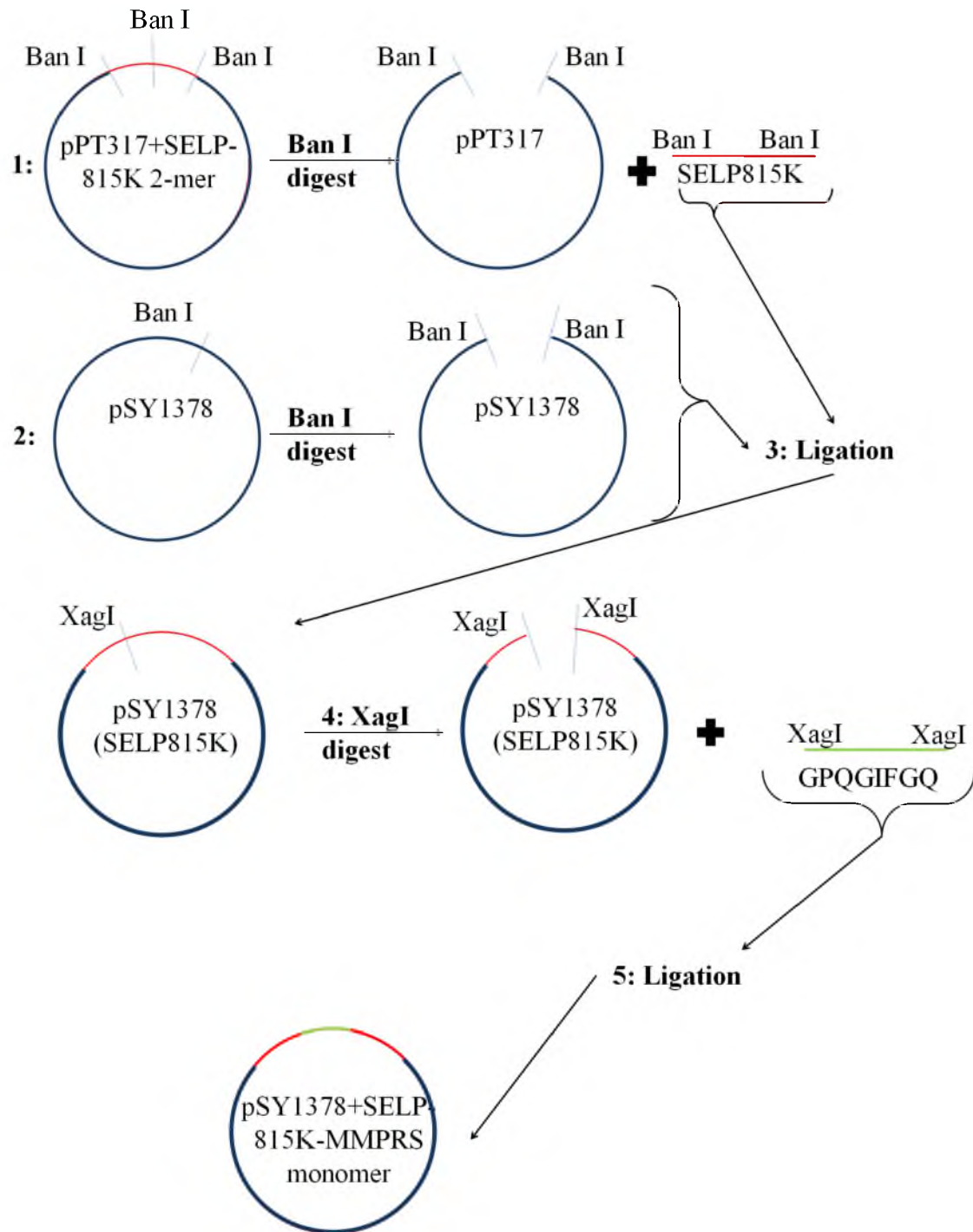


Figure 5.1: Synthesis of SELP-815K-MMPRS monomer gene segment.

~400bp fragment corresponding to SELP-815K monomer gene was purified using the Qiaquick Gel Extraction Kit. SELP-815K monomer gene segments were ligated with linearized, dephosphorylated pSY1378 in a 3:1 ratio overnight at room temperature. The ligation mixture was used to transform MAXefficiency Dh5 $\alpha$  *E. coli* and the transformation was plated on chloramphenicol-selective LB agar plates. Cultures were grown overnight and colonies were selected and grown in 4 ml starter cultures in chloramphenicol-selective Terrific Broth overnight at 37°C in a shaking incubator at 240 RPM. DNA was isolated from cultures by Qiaprep Spin Miniprep kit, and screened by digestion with BanI. A positive colony was then grown overnight in a 200 ml chloramphenicol-selective Terrific Broth culture and DNA was then extracted using a Qiagen Maxiprep kit.

Custom oligonucleotides encoding for the matrix-metalloproteinase responsive sequence GPQGIFGQ in addition to XagI-compatible overhangs and 5' phosphorylation were solubilized in annealing buffer composed of 10mM Tris, 50mM NaCl, and 1mM EDTA in 18M $\Omega$  deionized water to a concentration of 1mM. The sequence of the oligos is shown in Table 5.1. Oligos were mixed in a 1:1 ratio and 50 $\mu$ l of oligo mixture was annealed by heating to 95°C in an aluminum heating block, then allowed to cool to room temperature gradually by switching off the heating block.

Plasmid pSY1378 containing SELP-815K monomer gene segment was digested with XagI and dephosphorylated using SAP. Annealed oligos were ligated with the linearized pSY1378+SELP-815K monomer gene segment in a 5:1 molar ratio overnight at room temperature. This ligation mixture was used to transform MAXefficiency Dh5 $\alpha$  *E. coli* and the transformation was plated on chloramphenicol-selective LB agar plates

Table 5.1

Oligonucleotide sequences for SELP-815K-MMPRS monomer gene synthesis

---

Forward	5'AGG ACC GCA AGG AAT TTT TGG ACA GCC TGG 3' (5' Phosphorylated)
Reverse	5'TCC AGG CTG TCC AAA AAT TCC TTG CGG TCC 3' (5' Phosphorylated)

and grown overnight at 37°C. Colonies were grown in 4 ml chloramphenicol-selective overnight Terrific Broth cultures, DNA extracted, and digested with *Ava*II to identify colonies containing the MMP-responsive insert, which appear as a 311bp fragment in Figure 5.2. DNA sequencing was used to confirm correct insertion, after which 200 ml terrific broth cultures were grown and pSY1378 containing SELP-815K-MMPRS monomer gene segment was isolated using a Qiagen Maxiprep kit.

#### **5.2.2.2 Construction of the polymer gene segment**

Construction of the polymer gene segment for SELP-815K-MMPRS is shown in Figure 5.3. Plasmid pPT317 (expression plasmid) containing SELP-815K dimer was digested with *Ban*I and dephosphorylated using SAP. pSY1378 containing SELP-815K-MMPRS monomer gene segment was digested with *Ban*I. Both digests were separated on a 1% agarose gel. The bands corresponding to the 4000 bp linearized and dephosphorylated pPT317 parental vector and the ~400 bp band corresponding to SELP-815K-MMPRS monomer gene segment were purified. Monomer gene segments and linearized dephosphorylated pPT317 were ligated overnight at room temperature at a 42.5:1 molar ratio, with total DNA content of ~650 ng. The ligation mixture was used to transform MAXefficiency Dh5 $\alpha$  *E. coli* and the transformation was plated on kanamycin-selective LB agar plates and grown overnight at 30°C. Colonies were grown in kanamycin-selective Terrific Broth, DNA extracted with Qiagen Minipreps, and screened with a double digest with *Nco*I and *Xcm*I. Screening digests were run on 1% agarose and colonies displaying a band at ~2400 bp, corresponding to SELP-815K-MMPRS 6-mer were stocked in 50% glycerol and analyzed for protein production. Figure 5.4 shows an

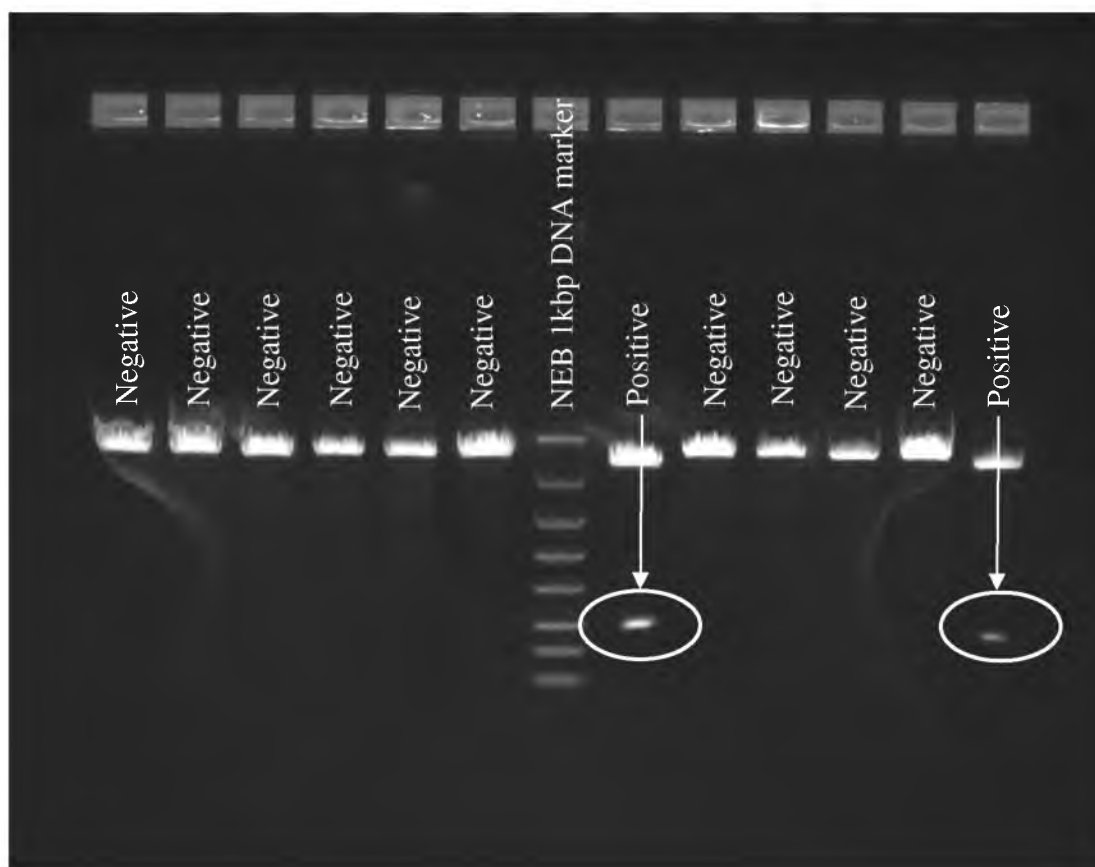


Figure 5.2: Agarose gel showing SELP-815K-MMPRS colony screening for monomer gene segment. Colonies 7 and 12 are positive for insertion.

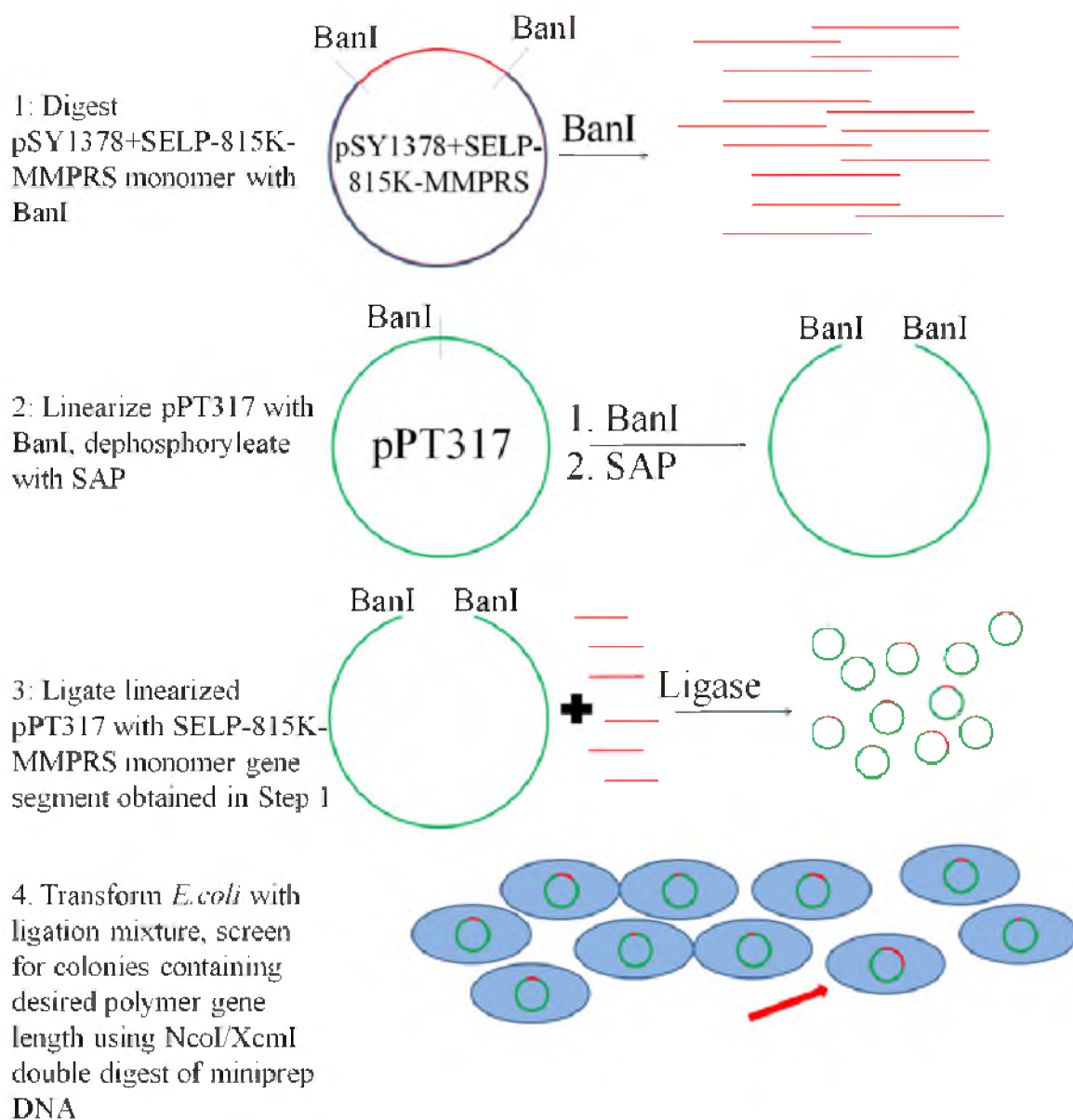


Figure 5.3: Multimerization of SELP-815K-MMPRS gene segments

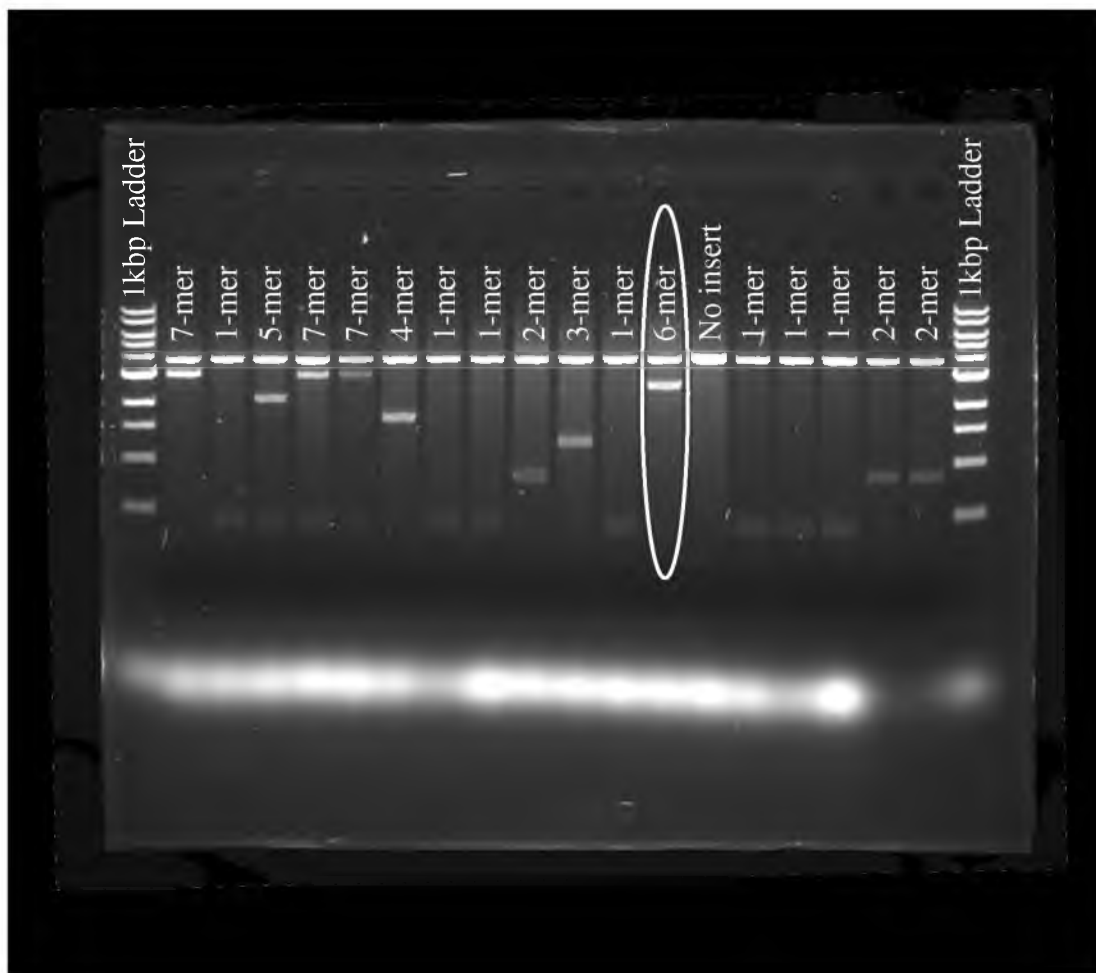


Figure 5.4: Agarose gel showing SELP-815K-MMPRS polymer gene segments. Colony 12 contains a 6-mer polymer gene segment.



example of the result of a typical multimerization reaction.

### 5.2.2.3 Small-scale protein production

The ability of the newly constructed polymer gene containing plasmid pPT317 to induce protein production was confirmed by transforming the genetically engineered EC3R *E. coli* with pPT317 encoding SELP-815K-MMPRS 6-mer. 6-mer was chosen specifically because it most accurately mimics the molecular weight of previous SELP constructs for hydrogel formation, including SELP-815K.<sup>2, 5, 12</sup> EC3R was derived from a postfermentation cell culture of pPT317+SELP-815K 6-mer by defrosting a small chip of postfermentation cell mass which was grown using the production cell line EC3 from Protein Polymer Technologies, Inc. (San Diego, CA). Approximately 25 subculture/replica plate cycles were performed on cells from this culture until a viable kanamycin-sensitive *E. coli* colony was identified, indicating that the plasmid encoding SELP-815K 6-mer had been purged. Following transformation, colony screening, and identification of a positive colony, a 4 ml kanamycin-selective MM50 culture was inoculated, grown to slightly turbid culture and then divided into two subcultures and diluted to 4 ml each with additional MM50 (Protein Polymer Technologies, Inc. San Diego, CA). One of these cultures was intended for protein production, while the other was earmarked for inoculum development. These cultures were grown at 30°C at 240 RPM agitation until OD600 indicated that the cells were approaching stationary phase. At this point, the inoculum development culture was divided and added to each of two 0.4L MM50 cultures and grown at 30°C and 240 RPM, while the culture for protein production capacity was heat shocked and outgrown for analysis. Specifically, the culture

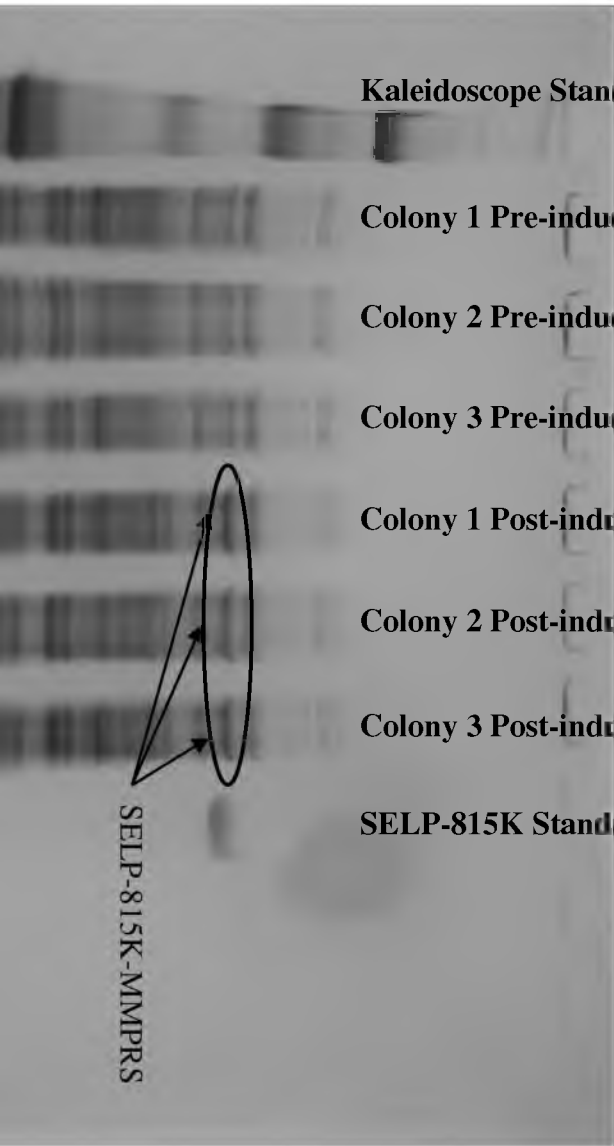
was immersed in 60°C water and culture temperature was monitored until it reached 42°C, at which point it was transferred to a 42°C water bath for 5 minutes. Following induction, the culture was grown at 40°C and 240 RPM for 2 hours, at which point protein production was evaluated by SDS-PAGE by comparing the induced culture to a pre-induction sample and a known SELP-815K 6-mer sample (Figure 5.5). Inoculum OD600 was monitored hourly until an OD greater than 4.0 was measured (10mm path length, Eppendorf BioPhotometer) at which point it was used to inoculate the fermenter.

#### **5.2.2.4 Large-scale polymer production**

SELP-815K-MMPRS was produced in gram quantities by fermentation in a 14 liter New Brunswick Scientific BioFlo 115 fermenter (Eppendorf, Enfield, CT) with a 10 liter working volume. An initial volume of 6 liters of MM50 was added sterile to the autoclaved fermenter, followed by the 0.8 liter inoculum. Fermentation was initiated at 30°C and 1000 RPM agitation, with 8-10 liters/minute airflow, pH 6.8. Foam was controlled by addition of Antifoam 204 (Sigma Aldrich, St.Louis, MO), and was controlled by a foam level probe placed approximately 2 inches above the culture level. pH control was done by addition of ammonium hydroxide via the fermenter pH control loop. When dissolved oxygen decreased below 60%, agitation was increased to 1200 RPM. Dissolved oxygen was monitored constantly until it was observed to show a sharp drop followed by recovery to nearly 90%, indicating a switch of the bacteria from anabolic to catabolic metabolism (depletion of initial glucose charge), at which point glucose feed was initiated at 150 ml/min. Culture OD600 was measured every 2 hours until OD600 reached 100, at which point protein production was induced by heat shock.



Figure 5.5: PAGE gel showing small-scale SELP-815K-MMPRS production.



**Kaleidoscope Standard**

**Colony 1 Pre-induction**

**Colony 2 Pre-induction**

**Colony 3 Pre-induction**

**Colony 1 Post-induction**

**Colony 2 Post-induction**

**Colony 3 Post-induction**

**SELP-815K Standard**

SELP-815K-MMPPRS

In order to heat shock the culture, the fermenter heating blanket was adjusted to maximum output, and water heated to 80°C was rapidly pumped through the cooling loop by a peristaltic pump. When temperature reached 41°C, the heating blanket was removed and cold tap water (approximately 10-15°C) was pumped through the cooling loop briefly to purge the hot water from the system. Temperature reached 42°C between 3 and 4 minutes, with one degree of overshoot. The heating blanket was then replaced, and temperature was allowed to gradually decrease to 40°C, approximately 45 minutes. At this point, the cooling system was reconnected, and the temperature setpoint was adjusted to 40°C.

OD600 was continually monitored following induction, until it was observed to decrease, at which point harvest was initiated. Final culture OD600 was 154, with a maximum of 180. Harvest began by removing the heating blanket, stopping glucose feed, and reducing agitation to 300 RPM. Ice-cold water was pumped through the cooling loop until culture temperature reached 10°C, at which point the culture was pumped into 1 liter centrifuge bottles and pelleted at 6000 x g for 30 minutes at 4°C. Wet cell paste was stocked in plastic bags, weighed, and frozen at -80°C to aid in cell lysis for SELP purification. Approximately 2.2kg of wet cell paste was yielded from fermentation of SELP-815K-MMPRS 6-mer.

#### **5.2.2.5 Purification of SELP-815K-MMPRS**

Approximately 1.1kg of frozen cell paste from fermentation was defrosted and lysed via high-pressure mechanical extrusion using a Microfluidics Microfluidizer 110M set to 10,000 psi. The lysed cell solution was then centrifuged at 4°C for 30 minutes to

remove cell debris, and PEI was used to precipitate nucleic acids and other negatively charged contaminants. The PEI-treated supernatant was then centrifuged at 4°C, after which the supernatant was subjected to ammonium sulfate precipitation. The precipitated protein was solubilized and then further purified by both cation and anion exchange chromatography, and tangential flow filtration. Following chromatography and filtration steps, the polymer solution was lyophilized in depyrogenated flasks, transferred to depyrogenated Teflon jars, and stored at -80°C. Yield from a single SELP-815K-MMPRS purification batch was approximately 2.5g.

#### **5.2.2.6 Polymer characterization**

Characterization of SELP-815K-MMPRS polymers was performed by MALDI-TOF mass spectrometry, amino acid composition analysis, SDS-PAGE, and enzymatic digest analysis via HPLC for MMP-2 and MMP-9. MALDI-TOF was performed by the University of Utah Mass Spectrometry and Proteomics core facility, while amino acid analysis was performed by Alphalyse, Inc. (Palo Alto, CA).

For SDS-PAGE, samples of lyophilized SELP-815K and SELP-815K-MMPRS were solubilized in “Reaction Buffer” (RB) containing 50mM Tris-HCl, 150mM NaCl, 5mM CaCl<sub>2</sub>, and 0.2mM NaN<sub>3</sub>, pH 7.6 at a concentration of 1 mg/ml. This buffer recipe is sourced from the Molecular Probes EnzChek Gelatinase/Collagenase Assay Kit (Invitrogen, Carlsbad, CA), which was used to confirm the activity of MMP-2 and MMP-9 prior to use. 2x Laemmli Buffer was supplemented with 5% β-mercaptoethanol and added 1:1 by volume to the polymer solutions, which were then placed in a PCR thermal cycler and heated to 95°C for 5 minutes to denature the protein. 25μl of each sample was

added to 4-15% Bis-Tris precast PAGE gel and electrophoresis was performed at 200V until the dye front reached the bottom of the gel, approximately 30 minutes. Kaleidoscope protein standard was used as a molecular weight marker. Following electrophoresis, gels were stained with GelCode Blue (colloidal Coomassie formulation) following manufacturer's instructions for staining and destaining.

Enzymatic digest was performed by solubilizing SELP-815K and SELP-815K-MMPRS in RB at 1 mg/ml. 100  $\mu$ l samples of each polymer were digested with a final concentration of 10nM and 40nM MMP-2 or MMP-9. MMP samples were incubated at room temperature for 2, 4, 12, 24, 36, and 48 hours and samples were run on PAGE gels and stained with GelCode Blue to visualize band patterns corresponding to protein degradation.

#### **5.2.2.7 Hydrogel characterization**

The properties of hydrogels formed from SELPs are strongly dependent on the shear applied to liquid solutions of polymer prior to gelation. SELPs solubilized in phosphate buffered saline were loaded into a 1 ml luer-lock syringe connected at the hub to another 1 ml luer-lock syringe via two 27G needles, joined by a section of .0155" HPLC tubing. The SELP solution was passed through this device at maximum hand pressure for five full bidirectional cycles, at which point it was used for studies. Polymers used for previous studies provided by PPTI were sheared by 15,000 psi pressure through a series of micron-scale meshes. This shearing method is not considered to be identical to the shearing method used for previously published polymers, and therefore, the

characteristics of hydrogels studied in this work are expected to differ from those of previously published works.

Hydrogels were characterized for their sensitivity to MMP degradation in the context of protein loss from the gel, changes in mechanical properties, and release of model 100nm fluorescent nanoparticles. Previous applications of SELP-815K have investigated its utility as a viral delivery material, and this particle size was chosen as a model for the adenoviruses. One limitation of this model of viral release is related to size, as adenoviruses are typically 70-90nm. Another limitation is the differences in surface chemistry between the beads and viruses which can influence bead-polymer interaction and release. For the protein release and mechanical properties, 10 wt% solutions of SELP-815K and SELP-815K-MMPRS were sheared according to the above protocol, and then loaded into 1 ml tuberculin slip-tip syringe. Syringes were sealed with Parafilm and allowed to gel upright overnight at 37°C. Following gelation, the end of the syringe was cut off with an autoclaved razor blade and individual 50 µl test samples were cut off of the gel cylinder using a new autoclaved razor blade. Gel samples were placed in round bottom 1.8 ml cryovials with gasket-sealed screw caps, and 250µl of test solution consisting of RB alone, RB + MMP-2, or RB + MMP-9 was added to each tube. Samples were agitated at 180 RPM at room temperature. Test solution was completely withdrawn every 32-40 hours and frozen at -20°C, rinsed with RB, and replaced. For the release study, gels were formed and treated as above except that when the SELP solutions were being made, 6.6 µl of 0.2% fluorescent bead suspension was added per ml of SELP solution, and all agitation and sample manipulation was performed with minimal light to avoid photobleaching.



Protein loss was quantified using a Modified Lowry Assay Kit, and using known SELP solutions for the standard curve instead of the supplied bovine serum albumin, as SELP contains few Lowry-reactive amino acids. The mechanical properties of SELPs were evaluated in cyclic compression at 1Hz and 1% strain, with ~10 grams of preloading applied for 10 minutes to eliminate stress relaxation. Stress was measured using a 2 lb load cell. Release was quantified by measuring the fluorescence of release samples with an excitation/emission of 260/515.

#### **5.2.2.8 Statistical analysis**

All statistical analyses were performed using GraphPad Prism software. One way ANOVA was used to determine statistical significance, with Tukey's post test for all pairs of samples within a hydrogel group. For data reported as additive over time, standard deviations for each time point were added to the geometric mean of all previous time points to calculate the propagation of error. All error bars report standard deviation.

### **5.3 Results**

#### **5.3.1 Synthesis of monomer and polymer gene segments**

The synthesis of the SELP-815K-MMPRS monomer gene segment was successfully confirmed by restriction digest with *AvaII*, which produces a cut within the insert encoding for the GPQGIFGQ sequence, and another 14 base pairs 3' of the *BanI* site marking the end of the monomer gene, forming a fragment of 311 bp (Figure 5.2). Monomer gene segment generation was additionally confirmed by DNA sequencing.

The synthesis of the polymer gene segment was confirmed by simultaneous double digest with restriction enzymes NcoI and XcmI, which cut 4 base pairs past the 3' end of the polymer gene, and 8 base pairs prior to the 5' end of the polymer gene, respectively. An example of an agarose gel image showing SELP-815K-MMPRS polymer gene analysis including monomer through 7-mer is shown in Figure 5.4. Optimization of ligation conditions (data not shown) revealed that increasing molar ratio combined with increasing total DNA content led to longer polymer gene lengths.

### 5.3.2 Polymer production and purification

The small-scale protein production capability of pPT317+SELP-815K-MMPRS 6-mer was confirmed by SDS-PAGE (Figure 5.5). The SELP-815K standard, shown in lane 8, indicates the approximate position of the band corresponding to SELP production among the native *E. coli* proteins. The postinduction samples for representative colonies 1, 2, and 3 (lanes 5-7, respectively) illustrate an increased band density corresponding to SELP-815K as compared to the pre-induction sample for these colonies (lanes 2-4), confirming production of SELP-815K-MMPRS. It is important to note in these images and all PAGE gels analyzing SELP that, due to a lack of charged residues, SDS binding to SELP is significantly lower compared to standard proteins. As a consequence, SELP regularly appears to be of higher molecular weight than expected on PAGE gels.

Large-scale fermentation was performed with a wet cell paste yield of 2.2 kg. Purification of SELP-815K-MMPRS yielded 2.5 grams of material.

### 5.3.3 Polymer characterization

The newly synthesized SELP-815K-MMPRS was initially characterized by MALDI-TOF mass spectrometry, which predicted the molecular weight of SELP-815K-MMPRS to be 70,645 Da. While this value does differ from the expected molecular weight of 70,510 Da, this is within reasonable instrument error for proteins of this size.

Amino acid composition analysis confirmed the addition of the expected quantities of amino acids unique to the MMP-responsive insert. Specifically, isoleucine and phenylalanine were not detected in the SELP-815K sample, but were detected in approximate quantities of 6 and 7 amino acids, respectively, in SELP-815K-MMPRS, while 14 additional glutamic acid residues were detected in the responsive sequence, approximately equal to expected values for these key indicators (I=6, F=6, Q=12 expected).

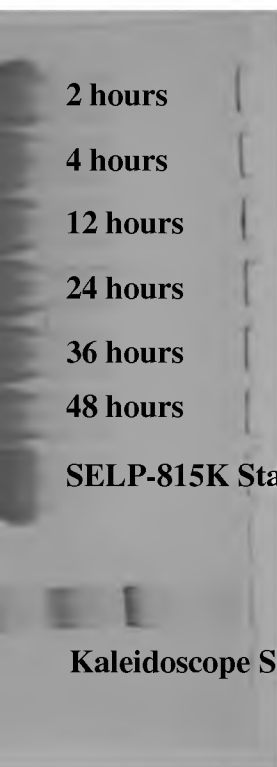
SDS-PAGE analysis of enzymatic digestion of these polymers is shown in Figures 5.6-5.13. It is clear that SELP-815K-MMPRS is digested by MMP-2 and MMP-9, and SELP-815K without the responsive sequence is not. Additionally, this digestion is dependent on both time of exposure and concentration of MMP.

### 5.3.4 Hydrogel characterization

Characteristics of hydrogels formed from SELP-815K-MMPRS were compared to SELP-815K in the context of MMP-sensitivity. Initial analysis consisted of comparing the loss of protein from each hydrogel in the presence and absence of MMPs as an indicator of the sensitivity of the hydrogel to degradation. The degradation and release of total soluble protein from these hydrogels following 2 weeks of treatment is shown in



Figure 5.6: SDS-PAGE analysis of 10 nM MMP-2 digest of SELP-815K over time.



**2 hours**

**4 hours**

**12 hours**

**24 hours**

**36 hours**

**48 hours**

**SELP-815K Standard**

**Kaleidoscope Standard**



Figure 5.7: SDS-PAGE analysis of 10 nM MMP-2 digest of SELP-815K-MMPRS over time.

**2 hours**

**4 hours**

**12 hours**

**24 hours**

**36 hours**

**48 hours**

**SELP-815K-MMPRS**

**Standard**

**Kaleidoscope Standard**



Figure 5.8: SDS-PAGE analysis of 40 nM MMP-2 digest of SELP-815K over time.



**2 hours**

**4 hours**

**12 hours**

**24 hours**

**36 hours**

**48 hours**

**SELP-815K Standard**

**Kaleidoscope Standard**

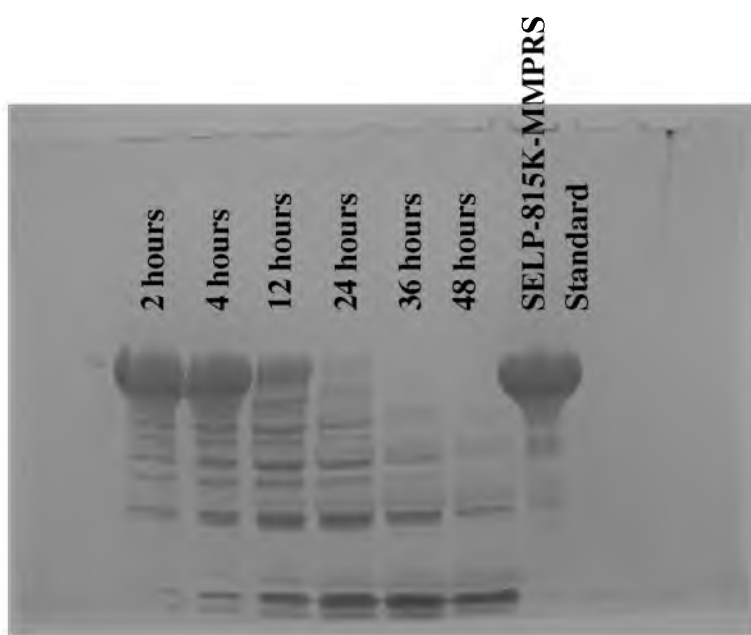


Figure 5.9: SDS-PAGE analysis of 40 nM MMP-2 digest of SELP-815K-MMPRS over time.

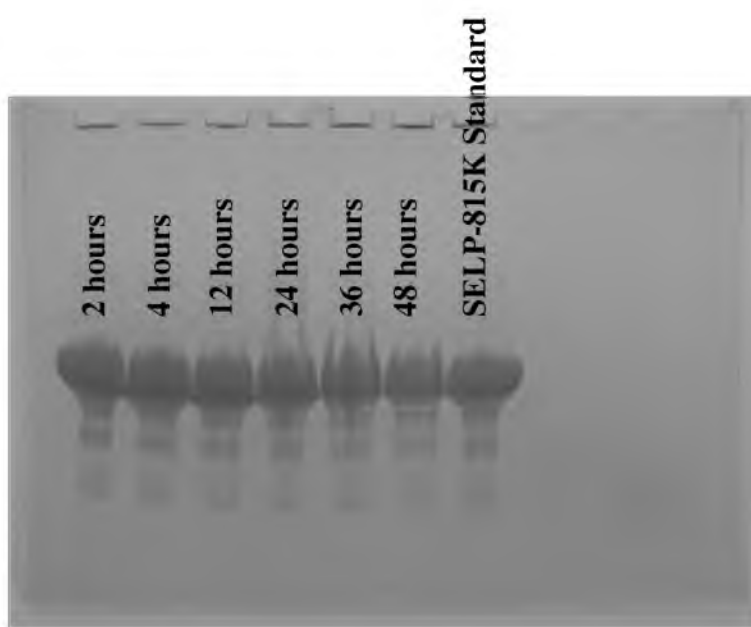


Figure 5.10: SDS-PAGE analysis of 10 nM MMP-9 digest of SELP-815K over time.



Figure 5.11: SDS-PAGE analysis of 10 nM MMP-9 digest of SELP-815K-MMP9 over time.

**2 hours**

**4 hours**

**12 hours**

**24 hours**

**36 hours**

**48 hours**

**SELP-815K-MMPRS**

**Standard**

**Kaleidoscope Standard**

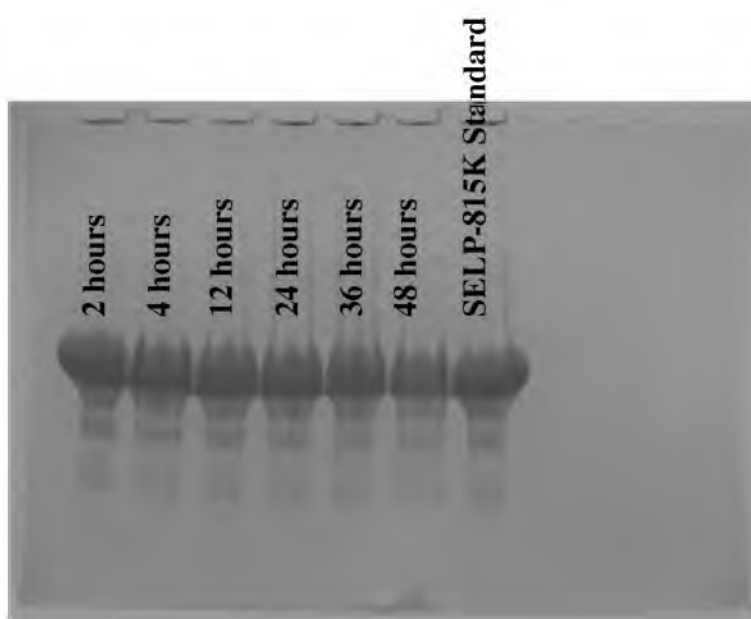


Figure 5.12: SDS-PAGE analysis of 40 nM MMP-9 digest of SELP-815K over time.



Figure 5.13: SDS-PAGE analysis of 40 nM MMP-9 digest of SELP-815K-MMPRS over time.

**2 hours**

**4 hours**

**12 hours**

**24 hours**

**36 hours**

**48 hours**

**SELP-815K-MMPRS  
Standard**

**Kaleidoscope Standard**



Figure 5.14, while Figures 5.15 and 5.16 display these results over time for SELP-815K and SELP-815K-MMPRS, respectively. SELP-815K displayed statistically insignificant levels of increased protein loss in the presence of MMPs, with only minor elevations compared to the control soluble fraction. Exposure of hydrogels composed of SELP-815K-MMPRS to MMP-2 and MMP-9 resulted in 63% and 44% higher protein loss compared to control. Protein loss from control is attributed to soluble polymer chains which do not participate in crosslinking. As a percentage of total protein in each gel, assuming precise 50  $\mu$ l gels at 10 wt% would contain 5 mg of polymer, approximately 24% of the polymer per hydrogel was lost as soluble fraction, with enzymatic digestion increasing this percentage to 39% and 35% for MMP-2 and MMP-9-induced degradation, respectively. These results were found to be statistically significant by Tukey's post test of all pairs of values, which revealed a statistical difference between both MMP-2 and MMP-9 and control, and no significance between each other. Results demonstrate that hydrogels composed of SELP-815K-MMPRS are degraded by MMP-2 and MMP-9 due to the inclusion of the MMP-responsive sequence GPQGIFGQ.

The effects of enzymatic treatment on the mechanical properties of SELP hydrogels were examined. Cyclic loading at 1 Hz was chosen as a method to simultaneously derive the Young's modulus and investigate viscoelasticity of these hydrogels with and without enzymatic degradation. Figure 5.17 shows the differences in Young's modulus for SELP-815K and SELP-815K-MMPRS. Treatment with either MMP-2 or MMP-9 significantly affected the modulus of the MMP-responsive hydrogels, while there was no significant effect present in the standard SELP-815K polymer. In the case of SELP-815K-MMPRS, there was a 41% loss in Young's modulus due to MMP-2

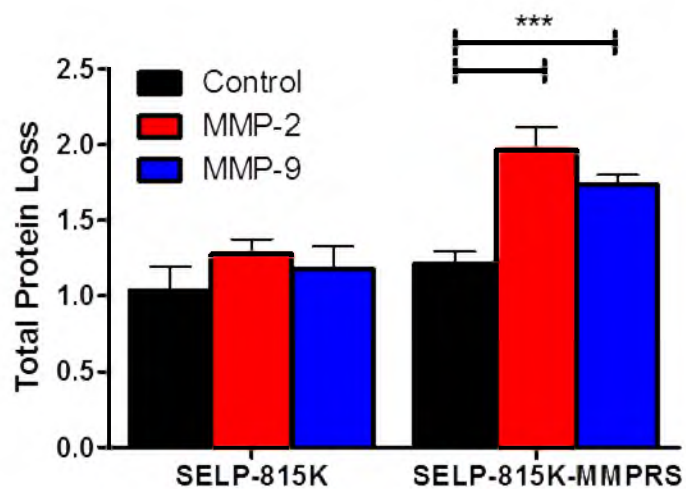


Figure 5.14: Total degradation at 2 weeks for SELP-815K±MMPRS hydrogels. Control: Agitation in RB in the absence of MMP. MMP-2: Agitation in RB containing 10nM activated MMP-2. MMP-9: Agitation in RB containing 10nM activated MMP-9.

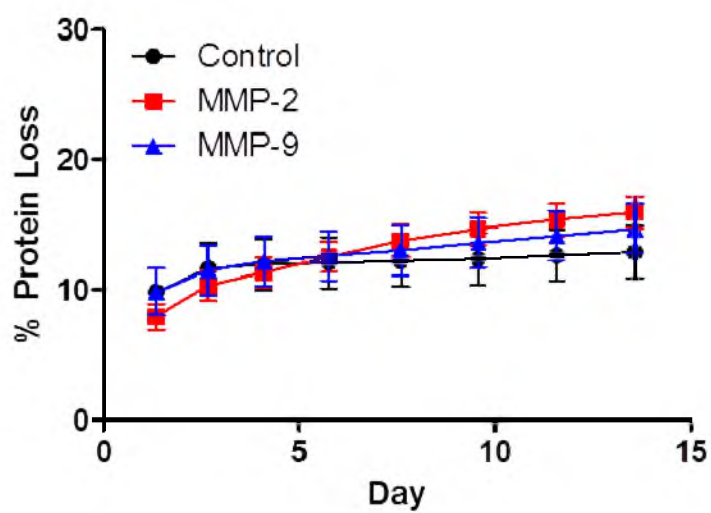


Figure 5.15: Protein loss over time for SELP-815K hydrogels. Control: Agitation in RB in the absence of MMP. MMP-2: Agitation in RB containing 10nM activated MMP-2. MMP-9: Agitation in RB containing 10nM activated MMP-9.

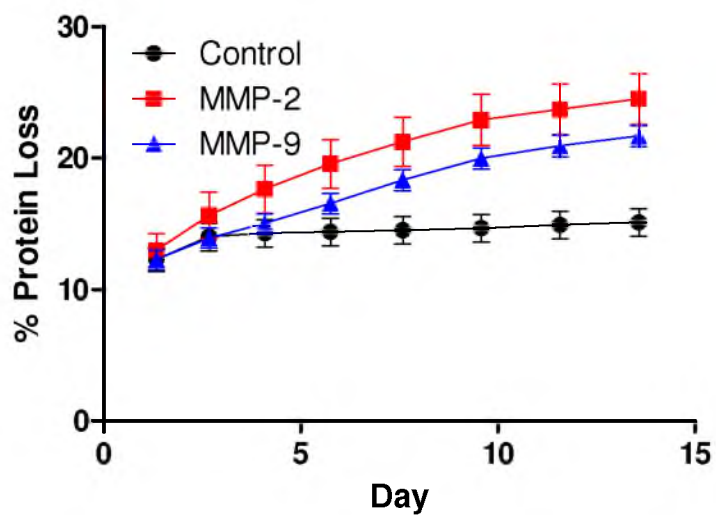


Figure 5.16: Protein loss over time for SELP-815K-MMPRS hydrogels. Control: Agitation in RB in the absence of MMP. MMP-2: Agitation in RB containing 10nM activated MMP-2. MMP-9: Agitation in RB containing 10nM activated MMP-9.

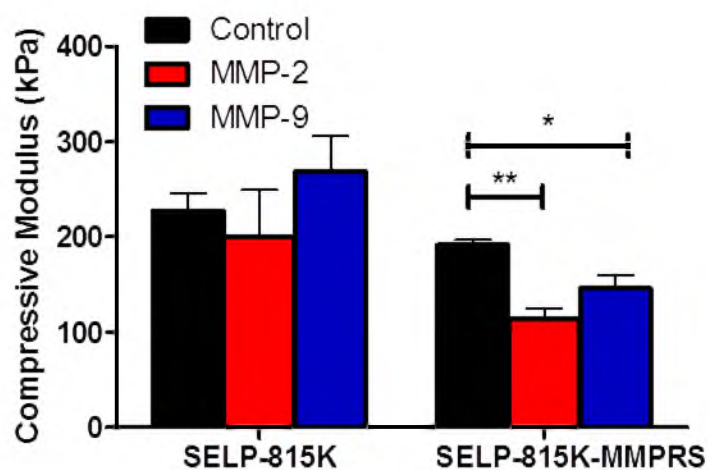


Figure 5.17: Compressive modulus of hydrogels in the presence and absence of MMPs. Control: Agitation in RB in the absence of MMP. MMP-2: Agitation in RB containing 10nM activated MMP-2. MMP-9: Agitation in RB containing 10nM activated MMP-9.

treatment, while MMP-9 affected a 24% loss. As a basic model comparison of nanoparticulate release between these two hydrogels, the release of 100 nm fluorescent polystyrene spheres was monitored over time for hydrogels in the presence and absence of MMP-2 and MMP-9. The total fluorescence release at the end of the 2-week study is shown in Figure 5.18, and the release over time for this study is shown in Figures 5.19 and 5.20 for SELP-815K and SELP-815K-MPRS2, respectively. These data show that following initial burst release, the release rates between the two polymers are similar until Day 8, at which point the release rates for SELP-815K-MMPRS with enzymatic treatment begin to increase. The total release at the end of the study for SELP-815K with no treatment was 9.3%, while MMP-2 and MMP-9 treatment conditions yielded release of 12.1% and 9.4%, respectively. SELP-815K-MMPRS without treatment released 8.2% at the end of 2 weeks; however, in contrast to the nonresponsive polymer, treatment with MMP-2 and MMP-9 caused release of 13.5% and 16%, respectively, or increases of 65% and 95% compared to control. This effect was observed to be statistically significant by ANOVA, with paired analysis via Tukey's post test revealing significance between either of the two MMP treatments and control, but not between the two treatments.

#### 5.4 Discussion

The results presented in this chapter show progress towards the development of bioactive genetically engineered biomaterials. This is shown both in the context of single polymer chains and in hydrogels self-assembled from these polymers. Studies characterizing SELP-815K-MMPRS in comparison to SELP-815K showed all expected hallmarks of having successfully added the MMP-responsive sequence to the polymer at

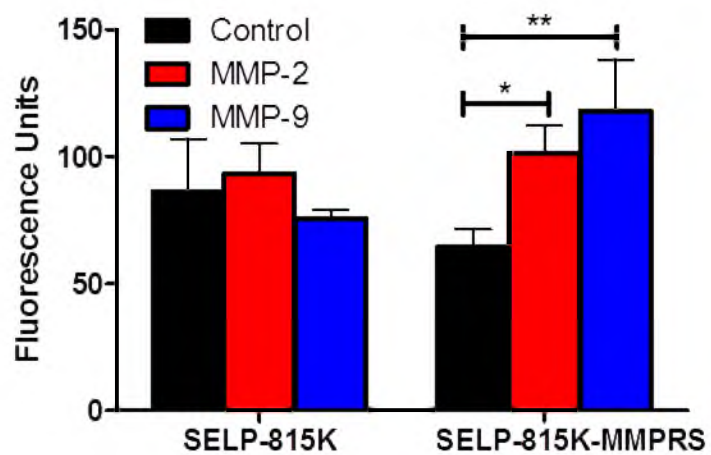


Figure 5.18: Total release of 100nm nanoparticles from SELP-815K $\pm$ MMPRS hydrogels in the presence and absence of MMPs. Control: Agitation in RB in the absence of MMP. MMP-2: Agitation in RB containing 10nM activated MMP-2. MMP-9: Agitation in RB containing 10nM activated MMP-9.

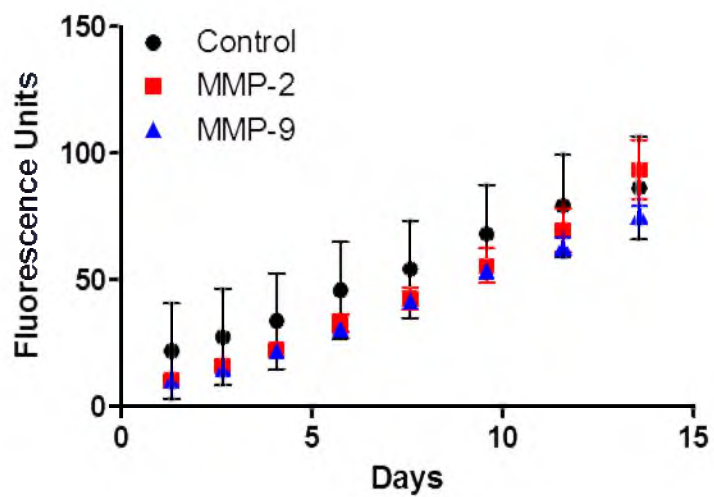


Figure 5.19: Nanoparticle release over time for SELP-815K hydrogels. Control: Agitation in RB in the absence of MMP. MMP-2: Agitation in RB containing 10nM activated MMP-2. MMP-9: Agitation in RB containing 10nM activated MMP-9.



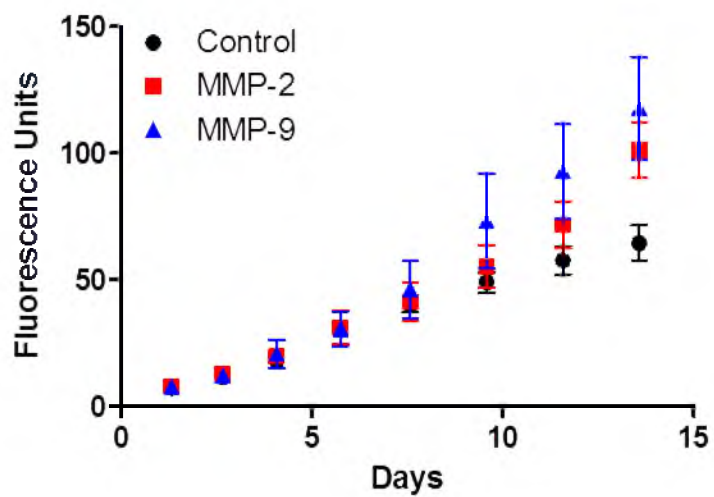


Figure 5.20: Nanoparticle release over time for SELP-815K-MMPRS hydrogels.

Control: Agitation in RB in the absence of MMP. MMP-2: Agitation in RB containing 10nM activated MMP-2. MMP-9: Agitation in RB containing 10nM activated MMP-9.

six evenly spaced locations, and the confirmation of correct sequence placement in the monomer gene ensures that the location of the responsive sequence along the monomer is correct. MALDI-TOF mass spectrometry results show an increase in molecular weight from SELP-815K 6-mer to SELP-815K-MMPRS 6-mer which corresponds to the insertion of six copies of GGPQGIFGQP within reasonable instrument error. These results combined with the appearance of characteristic amino acids on the amino acid analysis results confirm the identity of SELP-815K-MMPRS 6-mer.

The sensitivity of SELP-815K-MMPRS to MMP-2 and MMP-9 was confirmed by SDS-PAGE. Degradation appears to proceed by random cutting of the GPQGIFGQ sequence, evidenced by evenly spaced bands for all conditions of SELP-815K-MMPRS digestion (Figures 5.7, 9, 11, and 13) which correspond to various lengths of cleaved polymer. The appearance of double bands is likely due to the generation of fragments of SELP which include the head or tail sequences, which are produced in lower abundance than multimers of the repeat unit but still occur in appreciable quantities. In conditions using 40nM MMP for digestion, all full-length polymer has been cleaved by 36 hours, and at these later time points, the increasing intensity of low molecular weight bands indicates increasingly complete digestion of SELP at the GPQGIFGQ sequence (Figures 5.9 and 5.13). From an individual polymer, one fragment would be generated corresponding to the head sequence and the first half of the first monomer, five identical fragments corresponding to monomer repeats being separated at the GPQGIFGQ site, and one fragment corresponding to half of the last monomer repeat and the tail sequence. This analysis confirms the apparent specificity of digestion by MMPs to only the degradable

sequence, as no condition of MMP digestion of SELP indicated any signs of digestion (Figures 5.6, 5.8, 5.10, and 5.12).

Hydrogel degradation studies illustrate the utility of this material as a bioactive controlled delivery system. The insertion of the MMP-responsive sequence caused significant levels of degradation of the hydrogel to occur in the presence of MMP-2 and MMP-9, which are found at high levels in the tumor microenvironment and are associated with increased invasiveness and metastasis formation in HNSCC and other cancers.<sup>13-15</sup> Studies focusing on the degradability of the polymer suggest that following administration of a therapeutic in this material, it may have the capability to biodegrade and be completely removed from the administration site. This presents a significant advantage over standard SELP-815K, which was observed to last up to at least 12 weeks *in vivo* in an immunocompetent mouse model. In addition to the implications of degradation on the potential performance of this material in viral gene delivery, the manner in which the degradation occurs yields interesting information regarding the mechanism of self-assembly of the hydrogel. The release of significant quantities of protein following specific cleavage of elastin units supports recent conclusions published by Kaplan et al.,<sup>16</sup> suggesting that the structure of SELP in a hydrogel is dominated by aggregates of silk units interconnected with elastin units in an arrangement similar to a micelle. Cleavage of a sufficient number of elastin units interconnecting the nodes of silk eventually lead to liberation of these particle-like agglomerates, which appear as released protein from the hydrogel. This hypothesis is supported by both the decrease in mechanical properties observed, and the increased release rate. The loss of the primary intercrosslink material would naturally cause both of these observed effects, as existing

pores would be enlarged and possibly new pores would be formed by this type of degradation. Additionally, the trends indicating increased viscoelastic character of the enzymatically treated SELP-815K-MMPRS as well as decreased modulus support this type of degradation, as the increased void volume of the hydrogel would cause larger amounts of liquid to enter the gel, as well as a breakdown of the crystalline-dominated domain structure of SELP.

The increased release of the 100 nm polystyrene beads in the presence of MMP degradation suggests that when applied *in vivo*, this material could provide disease-state responsive delivery of nanoparticulate therapeutics. When combined with codelivery of nanoscale and/or microscale drug carriers of variable size, this could provide very long-term delivery with tunable administration of various drugs when certain microenvironmental conditions are present. Interestingly, while protein loss from SELP-815K-MMPRS appears to occur at a steady rate over the course of the study (Figure 5.16), the release appears to be slow and constant until between days 8 and 10 for MMP-9, and 10 and 12 for MMP-2, at which point the release rate increases significantly. This type of release profile could be caused by the opening and enlargement of existing pores causing more rapid release of particles from the hydrogel void space, or the liberation of particles which were entrapped within the hydrogel network. The effect is likely a combination of both of these, and indicates that future application of these polymers as viral delivery materials could be accomplished by using higher weight percentages than previous studies to further extend the duration of release of adenovirus from these hydrogels. The mechanism of degradation of these polymers is likely to be surface degradation from the interior surface area of the pores of the hydrogel, which would

result in enlargement of the pores. This type of degradation would occur without demonstrating the traditional signs of surface degradation, as much more of the surface of the hydrogel is contained within the pore structure than is exposed on the outside of the gel. Mechanistic studies for evaluating the pattern of degradation of these hydrogels need further investigation. This material can have utility for application as a postsurgery treatment to target tumor margins, as it would likely remain in place for a long period of time while delivering adenovirus to the surrounding tissue in a slow, constant dose.

### 5.5 Conclusions

This work illustrates an important step forward in the development of genetically engineered silk-elastinlike biomaterials. The ability to precisely insert a bioactive sequence into a highly tunable and specifically modified polymer has the potential to have significant impact in many areas of research, including applications as therapeutic drug delivery materials, *in vitro* or *in vivo* diagnostics, or as research tools. The advantage to producing polymers in this manner is the control over sequence and length, leading to a significant ability to impart very specific properties on the linear polymers. Adding to this distinct capability the ability to insert bioactive sites at specific locations along the polymer backbone increases the possible applications for such materials, as the sites inserted can be selected to respond to specific environmental conditions or cell types. The release results indicate that SELP-815K-MMPRS could potentially improve current virus-mediated gene therapy approaches by responding to the local environment and increasing release rate when the delivery of therapeutics is most needed. Given the observations made in this work, it is likely that increasing the number of bioactive sites

per monomer unit or blending responsive polymers with nonresponsive polymers can increase or decrease the release rate, respectively, in a very specific and finely adjustable manner. Additionally, the location and specificity of the bioresponsive sequence can be modified in order to impart bioactive properties to these polymers and hydrogels.

## 5.6 References

1. Cresce, A. W.; Dandu, R.; Burger, A.; Cappello, J.; Ghandehari, H., Characterization and real-time imaging of gene expression of adenovirus embedded silk-elastinlike protein polymer hydrogels. *Mol Pharm* **2008**, *5*, (5), 891-897.
2. Dandu, R.; Cresce, A. V.; Briber, R.; Dowell, P.; Cappello, J.; Ghandehari, H., Silk-elastinlike protein polymer hydrogels: Influence of monomer sequence on physicochemical properties. *Polymer* **2009**, *50*, (2), 366-374.
3. Dandu, R.; Ghandehari, H.; Cappello, J., Characterization of structurally related adenovirus-laden silk-elastinlike hydrogels. *J Bioact Compat Pol* **2008**, *23*, (1), 5-19.
4. Gustafson, J.; Greish, K.; Frandsen, J.; Cappello, J.; Ghandehari, H., Silk-elastinlike recombinant polymers for gene therapy of head and neck cancer: from molecular definition to controlled gene expression. *J Control Release* **2009**, *140*, (3), 256-261.
5. Haider, M.; Leung, V.; Ferrari, F.; Crissman, J.; Powell, J.; Cappello, J.; Ghandehari, H., Molecular engineering of silk-elastinlike polymers for matrix-mediated gene delivery: biosynthesis and characterization. *Mol Pharm* **2005**, *2*, (2), 139-150.
6. Zisch, A. H.; Lutolf, M. P.; Ehrbar, M.; Raeber, G. P.; Rizzi, S. C.; Davies, N.; Schmokel, H.; Bezuidenhout, D.; Djonov, V.; Zilla, P.; Hubbell, J. A., Cell-demanded release of VEGF from synthetic, biointeractive cell ingrowth matrices for vascularized tissue growth. *FASEB J* **2003**, *17*, (15), 2260-2262.
7. Park, Y.; Lutolf, M. P.; Hubbell, J. A.; Hunziker, E. B.; Wong, M., Bovine primary chondrocyte culture in synthetic matrix metalloproteinase-sensitive poly(ethylene glycol)-based hydrogels as a scaffold for cartilage repair. *Tissue Eng* **2004**, *10*, (3-4), 515-522.
8. Lutolf, M. P.; Lauer-Fields, J. L.; Schmoekel, H. G.; Metters, A. T.; Weber, F. E.; Fields, G. B.; Hubbell, J. A., Synthetic matrix metalloproteinase-sensitive hydrogels for the conduction of tissue regeneration: engineering cell-invasion characteristics. *Proc Natl Acad Sci U S A* **2003**, *100*, (9), 5413-5418.
9. Tauro, J. R.; Lee, B. S.; Lateef, S. S.; Gemeinhart, R. A., Matrix metalloprotease selective peptide substrates cleavage within hydrogel matrices for cancer chemotherapy activation. *Peptides* **2008**, *29*, (11), 1965-1973.
10. Kuros News. [http://www.kuros.ch/cms/front\\_content.php?idcat=35](http://www.kuros.ch/cms/front_content.php?idcat=35) (March 26, 2012),
11. Nagase, H.; Fields, G. B., Human matrix metalloproteinase specificity studies using collagen sequence-based synthetic peptides. *Biopolymers* **1996**, *40*, (4), 399-416.

12. Cappello, J.; Crissman, J. W.; Crissman, M.; Ferrari, F. A.; Textor, G.; Wallis, O.; Whitley, J. R.; Zhou, X.; Burman, D.; Aukerman, L.; Stedronsky, E. R., In-situ self-assembling protein polymer gel systems for administration, delivery, and release of drugs. *J Control Release* **1998**, *53*, (1-3), 105-117.
13. Fingleton, B., Matrix metalloproteinases: roles in cancer and metastasis. *Front Biosci* **2006**, *11*, 479-491.
14. John, A.; Tuszynski, G., The role of matrix metalloproteinases in tumor angiogenesis and tumor metastasis. *Pathol Oncol Res* **2001**, *7*, (1), 14-23.
15. Rosenthal, E. L.; Matrisian, L. M., Matrix metalloproteases in head and neck cancer. *Head Neck* **2006**, *28*, (7), 639-648.
16. Xia, X. X.; Xu, Q.; Hu, X.; Qin, G.; Kaplan, D. L., Tunable self-assembly of genetically engineered silk--elastin-like protein polymers. *Biomacromolecules* **2011**, *12*, (11), 3844-3850.



## CHAPTER 6

### CONCLUSIONS AND FUTURE DIRECTIONS

#### 6.1 Conclusions

The results presented in this work, taken as a whole, demonstrate the potential of the genetically engineered polymer platform as a powerful method for producing very specific polymers with well-defined properties. In addition to this concept, this work demonstrates for the first time a sensitive, enzymatically degradable structure of SELP which has the potential to lead to a real-time disease state responsive localized drug delivery system. Chapter 3 demonstrates the high degree of control over viral gene expression magnitude, extent, and location which can be affected by modifying the structure of SELP, and the weight percentage of SELP solution injected to form the hydrogel.<sup>1</sup> Chapter 4 expands on this work by showing that delivery of adenovirus in SELP-815K at 4 wt%, which showed the most promising results from the studies in Chapter 3, significantly reduces key markers of toxicity associated with viral delivery, most importantly acute immune response.<sup>2</sup> In Chapter 5, SELP-815K is modified with a MMP-degradable sequence along the polymer chain, which caused hydrogels formed from this material to be degradable as well as imparting MMP-specific responses in terms of release rate of model nanoparticles and mechanical properties.<sup>3</sup>

The systematic variation of SELP sequence and its ability to affect function of these polymers *in vivo* was demonstrated in Chapter 3. It was shown that the biodistribution of adenoviruses delivered in SELP is directly influenced by polymer sequence and composition, and that by making small changes to the polymer structure, significant changes can be made to viral delivery. Specifically, the increase in length in both silk and elastin units from SELP-47K to SELP-815K yielded increased localized gene expression from adenovirus.<sup>1</sup> Increasing only the elastin unit length, as going from SELP-47K to SELP-415K, affected a significant decrease in local magnitude of gene expression. The reason behind this pattern is likely related to the release rates of adenoviruses from these hydrogels. A very fast release rate, which is the case in SELP-415K and saline-administered virus, would produce very high transfection levels very early on in the study, with levels potentially diminishing even as early as 1 week. A more constant release scenario, as is likely the case in SELP-815K and has been shown for SELP-47K, would keep expression rates at an elevated level throughout the early period of constant or near-constant release. The observation of decreased expression following 2 weeks of treatment indicates that the “releasable” quantity of adenovirus is being diminished, and by 3 weeks, gene expression levels appear to be at or near background. Of note is that, in the case of SELP-47K, substantial fractions of adenovirus are never released from the hydrogel *in vitro*,<sup>4</sup> and the *in vivo* scenario likely mimics this pattern. This highlights the need for a degradable system to allow full release of the injected adenovirus dose. Further, it is demonstrated that the structure of SELP has a significant effect on its degradation properties by elastin, which is not necessarily dependent on the

elastin content of monomer chains but instead appears to depend more on the length of silk units in the monomer.

Chapter 4 demonstrates the ability of a specific SELP hydrogel, SELP-815K at 4 wt%, to improve the safety of adenoviral gene-directed enzyme-prodrug therapy in an immunocompetent animal model.<sup>2</sup> Notably, while viral administration without controlled delivery by SELP did not appear to cause significant toxicity in this mouse model, it did produce signs of a strong acute systemic immune response, which were eliminated when the same viral titer was administered using SELP as a controlled release material. This is a significant result as the acute immune response to adenoviral vectors has long been an important barrier to entry into the clinic for this otherwise safe and effective vector, as discussed in Chapter 2. Work performed concurrently in our lab on this same SELP hydrogel demonstrated its efficacy against a human xenograft HNSCC tumor model in nude mice,<sup>5</sup> which when combined with the results observed in Chapter 4 are encouraging for the use of SELP as a viable controlled and localized delivery matrix for adenoviral gene therapy, and possibly other types of agents at similar size scale.

The work demonstrated in Chapter 5 further illustrates the possibilities which become available when precise control over polymer sequence is achievable. In the presence of MMP-2, the amount of 100 nm polystyrene beads released from SELP-815K-MMPRS after 2 weeks was nearly double that of the same polymer without MMP-2 exposure. Further, the degradation rate of this hydrogel in the presence of MMP-2 and MMP-9 was significantly accelerated compared to hydrogel in the absence of MMP-2 and MMP-9, suggesting that as the therapeutic payload of the injection is continuing to be released, the hydrogel is gradually degrading and could potentially be completely

eliminated over time. The addition of these capabilities only further enhances the utility of SELPs as adenoviral delivery materials in addition to serving as an example of the design possibilities available with the genetically engineered polymer platform. In the context of HNSCC treatment, the addition of the MMP-degradable sequence can be used to fine-tune the release rate of adenovirus from SELP-815K hydrogel by either introducing the sequence multiple times or in multiple locations to increase the degradation rate, or by blending MMP-responsive SELP-815K-MMPRS with the nonMMP-responsive SELP-815K to decrease the degradation rate. Further, different sequences could be used which exhibit different MMP-specificities or levels of sensitivity to MMPs to further tune the response of these materials.

## **6.2 Future directions**

The development of SELPs for adenoviral delivery for the treatment of head and neck cancer has been underway for nearly a decade, and a significant quantity of data has been gathered to suggest that this is a promising approach to the treatment of this disease. Future work on the development of this material will be to examine carefully the effects of fibrous capsule formation on adenovirus release kinetics and the ability of the MMP-responsive sequence to affect removal of the hydrogel mass from the injection site. This potentially important factor has not been considered to this point and could be helpful for controlling adenoviral delivery. The presence of a fibrous capsule is likely to slow down the transport of adenoviruses to the intratumoral space, while additionally slowing down the transport of MMPs into the hydrogel and degradation products out of it. Further, the effect of MMP-responsive sequence location and specificity on the biodistribution,

efficacy, and toxicity of viral delivery in an *in vivo* tumor model needs to be evaluated. It is important particularly in the efficacy study that this treatment be compared to the currently employed treatment for head and neck cancer in a relevant and meaningful animal model. Translation of this approach will be difficult due to its focus on using adenovirus in humans, which even 13 years removed from the most recent adenovirus-related fatality still holds a stigma with investors who would be necessary to fund the development of such a treatment. Further, the challenges associated with having a novel biomaterial approved for use in humans, in this case SELP, should not be understated or ignored. It is important that data made available be strong, but more importantly, accurately representative. In other words, to truly pursue translation of this treatment, the difficult studies must be done first, meaning the “litmus test” type of studies which may provide results catastrophic to the translatability of this treatment approach.

In addition to the application of SELP-mediated adenoviral delivery for the treatment of HNSCC, there are several other avenues of research which may benefit from the high level of control over release, mechanical properties, and degradation offered by SELP. One very good opportunity for expanding this work is to create materials with very specific degradable sequences which are sensitive to specific cell types. One could easily imagine that this could somehow be applied in a tissue engineering application where the invasion of only one cell type would be preferable, and applying lithography or other patterning methods to scaffold production using various types of these materials could lead to a very advanced and potentially viable product. Another area of future expansion which would be easily tested and likely to be successful is the application of this material as an intra-articular drug delivery material for the management of arthritis.

The arthritis market is immense and there is a large quantity of public and private funding available. The ability to finely tune an injectable biomaterial to have degradation-sensitive release of, for example, anti-inflammatory medication, which is triggered by the very factors causing the inflammatory and degradative state, could potentially be very significant. Further, due to the ability of the material to degrade and eventually disappear, the delivery system could be administered on a set timetable based on the disease state of the patient, and the release rate in response to disease state could be matched to the patient's specific needs by either using polymers with more rapidly degraded sequences, more occurrences of the degradable sequence, or by blending various responsive and nonresponsive polymers to form interpenetrating networks with "averaged" properties. There are many more possible directions in which to expand the application of specifically bioactive hydrogels; the difficult part is going to be choosing which ones to prioritize.

### 6.3 References

1. Gustafson, J.; Greish, K.; Frandsen, J.; Cappello, J.; Ghandehari, H., Silk-elastinlike recombinant polymers for gene therapy of head and neck cancer: from molecular definition to controlled gene expression. *J Control Release* **2009**, *140*, (3), 256-261.
2. Gustafson, J. A.; Price, R. A.; Greish, K.; Cappello, J.; Ghandehari, H., Silk-elastin-like hydrogel improves the safety of adenovirus-mediated gene-directed enzyme-prodrug therapy. *Mol Pharm* **2010**, *7*, (4), 1050-1056.
3. Gustafson, J. A.; Price, R. A.; Frandsen, J.; Henak, C.; Cappello, J.; Ghandehari, H., Synthesis and characterization of a matrix-metalloproteinase responsive silk-elastinlike protein polymer. *Biomacromolecules* **2012**, *To be submitted*.
4. Dandu, R.; Ghandehari, H.; Cappello, J., Characterization of structurally related adenovirus-laden silk-elastinlike hydrogels. *J Bioact Compat Pol* **2008**, *23*, (1), 5-19.
5. Greish, K.; Frandsen, J.; Scharff, S.; Gustafson, J.; Cappello, J.; Li, D.; O'Malley, B. W., Jr.; Ghandehari, H., Silk-elastinlike protein polymers improve the efficacy of adenovirus thymidine kinase enzyme prodrug therapy of head and neck tumors. *J Gene Med* **2010**, *12*, (7), 572-579.

## APPENDIX

### PILOT DATA FOR EFFICACY OF CONTROLLED DELIVERY OF ADENOVIRUS IN IMMUNOCOMPETENT MICE

#### **A.1 Introduction**

As was discussed in Section 2.2.2.2.1, the acute immune response to adenoviral vectors is the most significant safety and efficacy concern associated with this type of vector.<sup>1-3</sup> Chapter 4 discussed work performed to illustrate the ability of silk-elastinlike protein polymers to reduce the severity of this response with the overall goal being to improve the safety of cancer treatment using adenoviruses.<sup>4</sup> One aspect of this treatment that had not been explored to this point was the ability of SELP-mediated delivery to improve the efficacy of this treatment in the presence of a fully competent immune system. Previous efficacy work had been performed in athymic nude mice bearing human patient-derived xenograft tumors, which essentially handicap the cancer due to the lack of T-cell responses which have been shown to reduce the efficiency of adenoviral gene delivery both in terms of extent and duration.<sup>5,6</sup>

In order to investigate this important question, a small pilot study was undertaken to compare SELP-mediated adenoviral delivery to aqueous intratumoral injection in the context of efficacy in an immunocompetent tumor model. The model



which was chosen for this study was sarcoma-180 (S-180). This model was chosen due to its ability to rapidly induce tumors in standard CD-1, noninbred, fully immunocompetent mice. It is acknowledged that this sarcoma cell line is not a suitable replacement for a squamous cell carcinoma model; however, there is a lack of available HNSCC tumor models which can be used in immunocompetent mice. Tumors were treated with high-titer adenovirus encoding herpes simplex virus thymidine kinase (Ad.HSVtk) as in the safety studies; however, the dosing schedule of ganciclovir (GCV) was conservatively designed to protect the mice following a large adenoviral administration. The study produced results which confirmed that administration of the adenovirus in SELP does, in fact, improve efficacy in immunocompetent tumor models; however, the duration of the study was reduced due to unacceptably large tumors, and GCV dosing was not as aggressive as later efficacy studies; therefore, this study did not provide publishable data and the following should be regarded as preliminary.

## **A.2 Materials and methods**

### A.2.1 Materials

Animals used in this study were 4-6-week-old female albino standard CD-1 mice (Charles River Labs, Cambridge, MA). Custom adenovirus encoding HSVtk and luciferase was purchased from Vector Biolabs (Philadelphia, PA). 1cc and 20cc syringes, 26G 5/8, 25G 5/8, and 18G 1 1/2 needles were purchased from Becton Dickinson (Franklin Lakes, NJ). Cell culture ware including centrifuge tubes was purchased from ISC Bioexpress (Kaysville, UT). Sterile 0.9% saline for injection was

purchased from Baxter, Deerfield, IL. GCV was purchased from Sigma-Aldrich (St. Louis, MO).

## A.2.2 Methods

### A.2.2.1 Expansion of S-180 fibrosarcoma cells

Frozen stocks of S-180 fibrosarcoma, a generous gift from Dr. Hiroshi Maeda, were defrosted at room temperature. CD-1 mice were weighed and prepared for injection by swabbing the right lateral, ventral, posterior region with 60% isopropanol. Mice were injected intraperitoneally with 1ml of S-180 stock through a 25G 5/8 needle slowly to avoid cell lysis. Following injection, mice were inverted for 10-12s to reduce injection site leakage. Mice were monitored daily for weight, behavior, and apparent increase in girth due to intraperitoneal cell growth. Following weight gain of no more than 5 grams, animals were sacrificed by CO<sub>2</sub> asphyxiation, placed on their side, and an 18G 1 ½ needle on a 20cc syringe was inserted below the midline to draw cells. Slow drawing of cell suspension from the peritoneum continued until no further cell suspension was removed, at which point the peritoneum was opened and the remaining cell suspension was removed by aspiration with or without the needle. Cell suspensions were pooled and washed with sterile phosphate buffered saline twice, and adjusted to 10 million cells/ml.

### A.2.2.2 Induction of S-180 tumors

Mice were prepared for tumor inoculation by isofluorane anesthesia followed by shaving of the medial dorsal flanks and swabbing with 60% isopropanol. 200 µl of

injection stock (10 million S-180 cells/ml) was administered subcutaneously into each flank using a 25G 5/8 needle, for a total of 2 tumors per mouse. The needle entry wound was held shut with forceps for 10-12s to reduce backflow of cell suspension from the injection site. Tumors were observed approximately 5 days following injection, and were measured with calipers every other day until the average size was observed to be approximately 7 mm x 7 mm, which occurred 9 days following initial inoculation.

#### **A.2.2.3 Virus administration, treatment, and tumor monitoring**

Viral stocks containing Ad.HSVtk.Luc were defrosted and mixed appropriately with 0.9% injection saline or SELP-815K+injection saline to result in a final viral titer of  $4.3 \times 10^9$  plaque-forming units (PFU) per 50  $\mu$ l injection volume. The final concentration of SELP-815K was 4 wt% in the SELP-mediated condition. Intratumoral injections of virus were performed by inserting a 26G 5/8 needle attached to a 250  $\mu$ l Hamilton glass syringe into the approximate center of each tumor, and injecting 50  $\mu$ l of each condition. Control mice received only 50  $\mu$ l saline. The day of virus injection was considered Day 0.

GCV was dissolved in 0.9% injection saline at a final concentration of 1mg/ml. Mice were weighed individually and dosed at 25mg/kg, with a typical dose being 0.6 ml. The dosing schedule for this initial study was 5 consecutive daily injections followed by an “off” day. The dosing schedule was intentionally conservative, as it was unknown how the mouse would tolerate such a viral dose in combination with daily GCV administration. Tumors were measured every third day with calipers, and

tumor volumes were calculated by multiplying the longer dimension by the square of the shorter dimension, and dividing by two. Animals were sacrificed if either tumor reached a volume greater than 2000 mm<sup>3</sup>, the animal exhibited any signs of pain and distress, or if extensive necrosis occurred resulting in skin breakage at the tumor exterior.

### **A.3 Results and discussion**

The results of this study are shown in Figure A.1. Due to rapid growth of tumors in the control condition and a lack of an approved IACUC protocol to perform a survival study, it became necessary to end the study on Day 12 following the initiation of treatment. While brief, the results of this study revealed that intratumoral delivery of adenovirus without a controlled delivery system is not efficacious in the presence of a fully competent immune system. Controlled delivery mediated by SELP-815K 4 wt%, however, showed significantly reduced tumor growth over the study period, as shown in Figure A.1. These results compared to previous efficacy data in an immunocompromised nude mouse model bearing human HNSCC tumors<sup>6</sup> suggest some interesting conclusions which warrant further work. In the previous study comparing delivery methods in immunocompromised mice, the virus administered in saline alone exhibited nearly the same efficacy as virus delivered in SELP-815K 4 wt%. This discrepancy between the two studies in the context of controlled delivery could be caused by several different factors:

1. The SELP-815K 4 wt% used for controlled delivery offers an immunoprotective effect by sequestering virus in pores too small to be accessed by T-cells capable of neutralizing them. The distribution pattern of

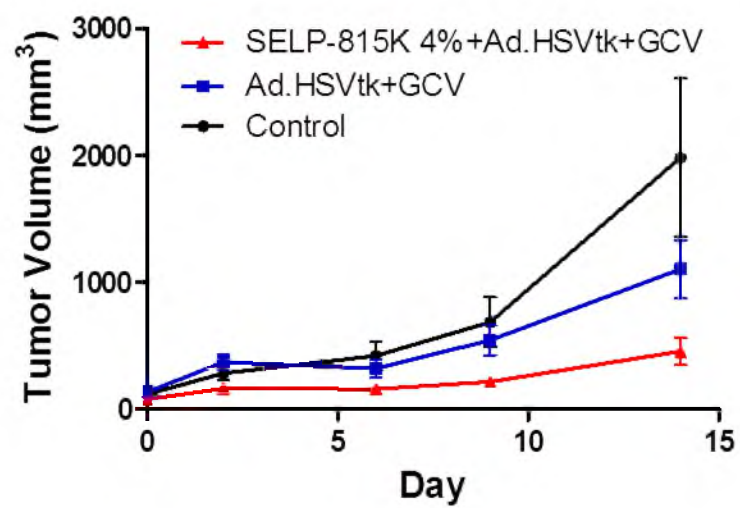


Figure A.1: Efficacy of SELP-mediated GDEPT in immunocompetent mice. Control: saline injection with no virus or SELP.

SELP in the tumor resulted in a large surface area of virus-releasing hydrogel in intimate contact with cells of the tumor, facilitating rapid killing of cells in direct contact while additionally distributing the tumor mass affected by the bystander effect over a larger area than the single bolus dose of virus.

2. There is no immunoprotective effect, but the slow release of the virus and therefore constant reduced level of virus contacting the tumor is more effective than a larger bolus dose, of which the same or lower percentage is likely neutralized by the immune system.
3. There is a cell-line-dependent difference in susceptibility to initial viral transfection, the bystander effect, or both which somehow accounts for the discrepancy.
4. The physical presence of the hydrogel inside the tumor caused an appreciable reduction in growth rate, and the viruses were not at all involved in this result. This conclusion may be corroborated by data collected in the aforementioned immunocompromised efficacy study,<sup>6</sup> which showed that the presence of a SELP hydrogel inside a tumor slightly inhibited growth, although the magnitude of the effect observed in the previous study is much less significant than the effect observed in the current study.

It is most likely that the efficacy is primarily related to point number 1, with a likely small contribution of points 3 and 4. Point 2, while not completely invalid, does not apply in this case due to the short duration of the study; i.e., if this hypothesis is true, the current study period is insufficient in length to make such a conclusion due to the time necessary for this effect to be observed. Point 3 is also a possibility, as in this

case, the primary mechanism of adenoviral transfection would be CAR-receptor mediated, and CAR receptor densities can vary widely among cell lines, even from anatomically similar locations.<sup>7</sup> If this is the case, however, it is to be expected that the relative difference in effect between the two treatment modalities would mirror that of the immunocompromised study. Point 1 additionally is supported by the toxicity data presented in Chapter 4, as this study suggested that delivery in SELP-815K 4 wt% almost completely knocks down the acute immune response to the large administered viral dose.<sup>4</sup> Therefore, with limited data, controls, and follow-up, it can be tentatively stated that delivery of adenovirus in SELP-815K 4 wt% mediates enhanced therapeutic efficacy by protecting the delivered viral dose from clearance by the immune system while simultaneously increasing the surface area of tumor exposed to the therapeutic virus.

#### **A.4 Conclusion**

While insufficient in length and breadth to draw definitive conclusions regarding the efficacy of this treatment in an immunocompetent scenario, the study does provide some promising data as to the potential clinical viability of this treatment approach. The combination of the results of this study with the toxicity data reported in Chapter 4 and the previously published efficacy results in immunocompromised mice<sup>6</sup> supports the conclusion that SELP-815K 4 wt% offers an immunoprotective environment for co-injected adenovirus. This in turn increases the efficacy of adenoviral treatment while simultaneously making the administration of large adenoviral doses safer.

### A.5 References

1. Yang, Y.; Li, Q.; Ertl, H. C.; Wilson, J. M., Cellular and humoral immune responses to viral antigens create barriers to lung-directed gene therapy with recombinant adenoviruses. *J Virol* **1995**, *69*, (4), 2004-2015.
2. Yang, Y.; Nunes, F. A.; Berencsi, K.; Furth, E. E.; Gonczol, E.; Wilson, J. M., Cellular immunity to viral antigens limits E1-deleted adenoviruses for gene therapy. *Proc Natl Acad Sci U S A* **1994**, *91*, (10), 4407-4411.
3. Tripathy, S. K.; Black, H. B.; Goldwasser, E.; Leiden, J. M., Immune responses to transgene-encoded proteins limit the stability of gene expression after injection of replication-defective adenovirus vectors. *Nat Med* **1996**, *2*, (5), 545-550.
4. Gustafson, J. A.; Price, R. A.; Greish, K.; Cappello, J.; Ghandehari, H., Silk-elastin-like hydrogel improves the safety of adenovirus-mediated gene-directed enzyme-prodrug therapy. *Mol Pharm* **2010**, *7*, (4), 1050-1056.
5. Worgall, S.; Wolff, G.; Falck-Pedersen, E.; Crystal, R. G., Innate immune mechanisms dominate elimination of adenoviral vectors following in vivo administration. *Hum Gene Ther* **1997**, *8*, (1), 37-44.
6. Greish, K.; Frandsen, J.; Scharff, S.; Gustafson, J.; Cappello, J.; Li, D.; O'Malley, B. W., Jr.; Ghandehari, H., Silk-elastinlike protein polymers improve the efficacy of adenovirus thymidine kinase enzyme prodrug therapy of head and neck tumors. *J Gene Med* **2010**, *12*, (7), 572-579.
7. Li, D.; Duan, L.; Freimuth, P.; O'Malley, B. W., Jr., Variability of adenovirus receptor density influences gene transfer efficiency and therapeutic response in head and neck cancer. *Clin Cancer Res* **1999**, *5*, (12), 4175-4181.